Title	Studies on Nonbonded Interactions in Organic Selenium Compounds : Based on 1,8-Disubstituted Naphthalene Systems
Author(s)	Hayashi, Satoko
Citation	大阪大学, 2000, 博士論文
Version Type	VoR
URL	https://doi.org/10.11501/3178726
rights	
Note	

Studies on Nonbonded Interactions in Organic Selenium Compounds: Based on 1,8-Disubstituted Naphthalene Systems

2000

Satoko Hayashi

Department of Material Science and Chemistry
Faculty of Systems Engineering, Wakayama University

# Studies on Nonbonded Interactions
in Organic Selenium Compounds:
Based on 1,8-Disubstituted Naphthalene Systems

2000

Satoko Hayashi

Department of Material Science and Chemistry
*Faculty of Systems Engineering, Wakayama University*

Contents

Chapter 1

General Introduction

Organic chalcogen compounds are well known to show versatile reactivities and they afford many structurally interesting compounds.[1] For example, organic chalcogenides (RZR) react with halogens (X–X) to give adducts (R_2ZX_2). The adducts will be molecular complexes (MC) when the magnitude of the charge transfer (CT) is not so large.[2,3] The halogen can no longer exist as a halogen molecule if the magnitude becomes larger. Trigonal biphyramidal adducts (TB) will form with highly polar three center-four electron bonds[4] ($X^{\delta-}$–$Z^{\delta+}$–$X^{\delta-}$: 3c-4e) in this case. The adducts should be TB if the electronegativity[5] of X (χ_X) is larger than that of Z (χ_Z) in R_2ZX_2, and they are MC if χ_X is not larger than χ_Z.[2a,3a,b]

$$RZR' \;+\; X_2 \longrightarrow \quad\quad \longrightarrow \quad\quad \tag{1}$$

MC ($\chi_X > \chi_Z$)   TB ($\chi_X < \chi_Z$)
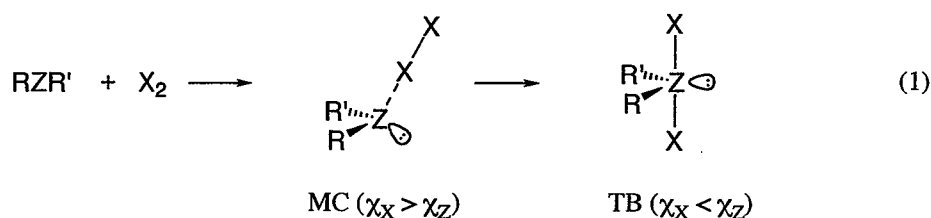
Mulliken has proposed a theory for MC based on quantum mechanics.[6] The driving force for the association of the components is CT where electrons move from electron donors to acceptors in the complexes. A theory for TB has also been proposed by Pimentel and Musher.[4a] The linear σ(p) orbitals construct the hypervalent 3c-4e in TB. The 3c-4e description of the X–Z–X bond in R_2ZX_2 (TB) was further developed by the preparation and characterization of variety of new compounds with TB structure[2] and by theoretical calculations.[4] Thus the character of the X–Z–X bond in TB is well understood by the 3c-4e description of this bond.[2,4]
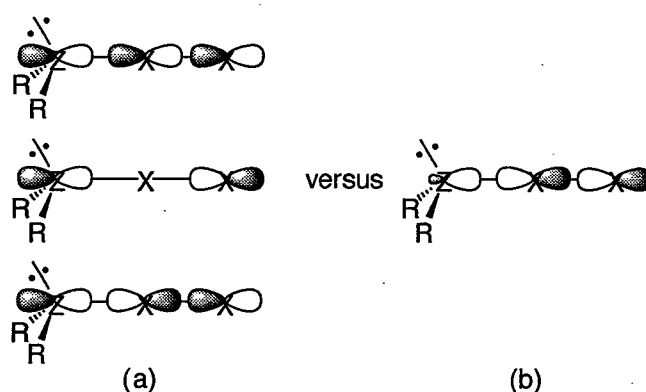
Scheme 1. Bonding Models for R_2ZX_2 (MC): (a) 3c-4e versus (b) n→σ* Descriptions

1

However, I sometimes worry about the character of the Z–X–X bond in R_2Z–X–X (MC) which cannot be so easily imagined by a weak n$\rightarrow\sigma^*$ CT description. I decided to improve the bonding model of the Z–X–X bond in R_2Z–X–X (MC): The 3c-4e model must be a most attractive candidate for the Z–X–X bond in R_2ZX_2 (MC) (Scheme 1). It must also be useful to clarify the bonding scheme to investigate organic selenium compounds containing novel chemical bondings. MO calculations were performed on H_2ZX_2 (TB) and H_2ZX_2 (MC) for Z = S, Se and X = Cl, Br, together with the related compounds with the 6-311G++(3df,2pd) basis sets at the MP2 level of the Gaussian 94 program.[7] Molecular orbitals of the Se–Br–Br bond (ψ_1, ψ_2, and ψ_3) in H_2SeBr_2 (MC) are depicted with the 3-21G* basis sets of the McSpartan program[8] employing the structure optimized for the adduct with B3LYP/6-311G++(3df,2pd) method. Molecular orbitals ψ_1, ψ_2, and ψ_3 are shown in Figure 1. Completing the results, I come to the conclusion that the $Z-^1X-^2X$ bonds in the MC (Z = S, Se and X = Cl, Br) can be analyzed by the 3c-4e model.

ψ_1 ψ_2 ψ_3
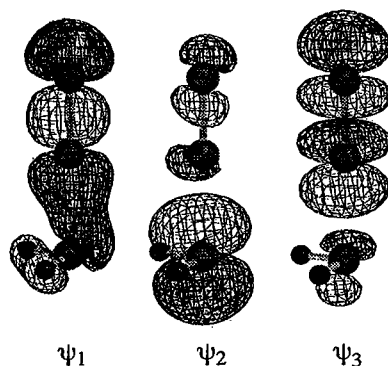
Figure 1. 3c-4e Type Molecular Orbitals in H_2SeBr_2 (MC)

I also applied the Pauling's equation (eq 2)[9] on the reported bond lengths in TB and MC in the literature to demonstrate the 3c-4e characters of Z–X–X in MC. D(n) and D(1) represent the bond distances where the bond orders are n (< 1) and 1, respectively. The bond orders between the adjacent atoms in the 3c-4e bond are expected to be ca. 0.5 since the ψ_2 orbital is usually nonbonding. The Z–X–X bond can be substantially described by the 3c-4e model since the two bond orders in Z–X–X are close with each other.[10]

$$D(n) \quad = \quad D(1) - 0.60 \log n \tag{2}$$

The 3c-4e description was proposed for Z–X–X in R_2ZX_2 (MC) based on the results of the calculations. The 3c-4e description of the Z–X–X bond in MC enables easily to understand the characters of the bond based on those of the X–Z–X bond in TB, which are extensively investigated and well characterized so far. It can be achieved by changing the central atom Z in X–Z–X with the terminal atom X in Z–X–X, although the electronegativity of Z and X must be carefully taken into

account. The results are shown in Chapter 2.

The lone pair–lone pair interaction[11] is one of the important factors to determine the structure and the reactivity of organic compounds containing heteroatoms bearing lone pairs such as organic chalcogen compounds. After the establishment of the 3c-4e characters of the Z–X–X bonds in MC, I started my project to elucidate the role of nonbonding interactions containing lone pairs of Se atoms on the structure and the reactivity of organic selenium compounds. Scheme 2 shows the types of nonbonded interactions investigated (**D** – **G**), together with the representations of lone pairs (**A** and **B**) and the p-π interaction between a p-type lone pair and adjacent π-orbitals (**C**).
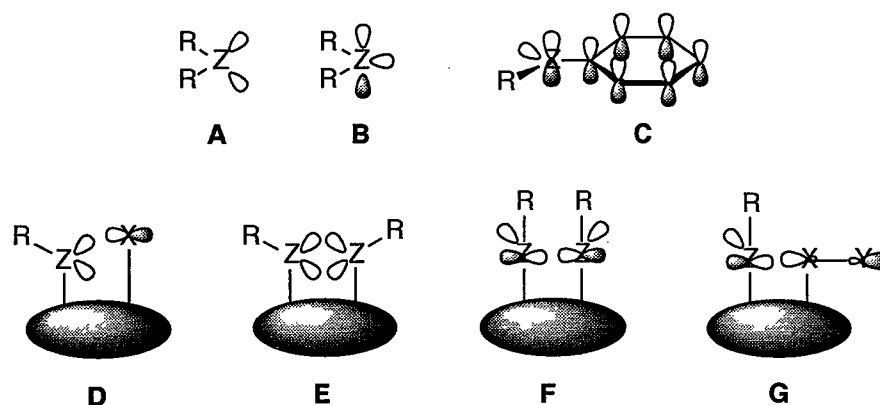
Scheme 2. Intramolecular Interactions between Lone Pairs.

Lone pairs of chalcogens have been represented by two types of orbitals: the one is depicted by the two sp^3–hybrid orbitals as shown in **A** and the other is based on the p- and s-type orbitals or p- and sp^2–hybrid orbitals as shown in **B**. The sp^3–hybrid orbital model is convenient when one discusses the collective properties of chalcogenides such as the electron densities or the total energies of lone pairs. The p- and s-type orbitals must be employed if the one-electron properties such as the energy of each molecular orbital are discussed.[12] Since the p-type orbital of a lone pair has a C_s symmetry, it interacts with π-orbitals of aryl groups to which the lone pair orbital is attached if the orientation is suitable[13] (**C**). Lone pair orbitals interact with orbitals of other atoms or groups (**D**) and with other lone pairs (**E**), of which lone pairs are exemplified by sp^3–hybrid orbitals. The interaction between lone pairs will construct the σ bond(s) when two or more p-type orbitals of lone pairs align linearly (**F**), and the p-type orbitals are expected to interact with σ-bonds if the energy
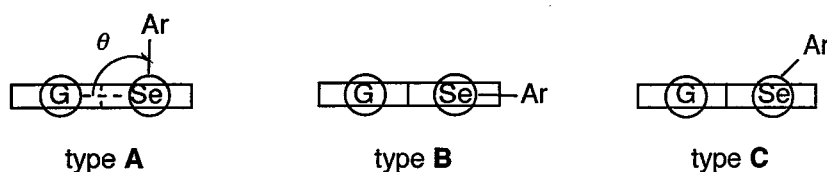

Scheme 3. Three Types of Conformation in 8-G-1-(ArSe)$C_{10}H_6$

levels of the σ*-orbitals are low enough for the interaction (**G**).

I have been interested in the nature of nonbonded interactions between chalcogen and halogen atoms. The interaction containing lone pairs must play an important role in the construction of the linear long bonds. I am much interested in the intramolecular interaction containing group 16 elements, especially that in selenium atoms. I prepared such organoselenium compounds that could be the typical examples of lone pair–lone pair interactions shown in **D** – **G** and examined the novel properties brought into the compounds by the interactions.

A naphthalene system is employed since the naphthalene 1,8-positions are expected to serve as a good geometrical system to study the nonbonded interactions between heteroatoms and/or groups. There must be three types of conformations of the naphthalene system such as 8-G-1-(ArSe)$C_{10}H_6$: type **A**, if θ is ca. 90° or less, of which θ is shown in this type, type **B** when θ is ca 180°, and type **C** with θ = ca. 135°. The conformations are shown in Scheme 3, for the convenience of the discussion.
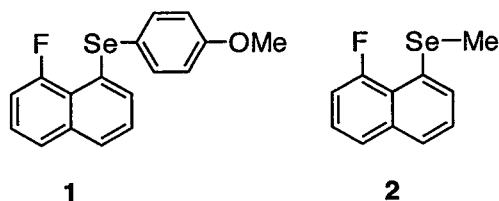
I have been interested in the nonbonded interaction between a fluorine atom with a small size of the valence orbitals and other hetero atoms in proximity in space, such as a selenium atom. The nonbonded Se---F interaction, where Z = Se and X = F in Scheme **2D**, was investigated as the first step to study such interactions. Lone pair–lone pair interactions have been elucidated to play an important role in the nonbonded spin–spin couplings between fluorine–fluorine,[14] fluorine–nitrogen,[15] and selenium–selenium[16,17] atoms. Electrostatic[18a] and charge-transfer[18b] mechanisms were proposed to explain the attractive interactions between oxygen and selenium atoms in close proximity, together with the downfield shifts of the ^{77}Se NMR chemical shifts by the neighboring oxygen, but there are controversy.
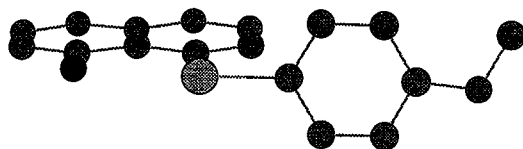

Figure 2. Structure of 1

The ^{77}Se NMR chemical shifts of 8-fluoro-1-(p-anisylselanyl)naphthalene (**1**) and 8-fluoro-1-

4

(methylselanyl)naphthalene (**2**) were observed at much downfield (ca. 90 ppm) relative to those of 1-(*p*-anisylselanyl)naphthalene and 1-(methylselanyl)naphthalene, respectively. It is puzzling how the fluorine atom at the 8-position in **1** and **2** causes such large downfield shifts. The selenium atom in **1** is expected to be electron rich due to the *p*-methoxyl group, which would be disadvantageous for the electrostatic mechanism, since the mechanism requires the positive charge development at the Se atom.[18a] It must be very interesting if the fluorine atom interacts attractively with the selenium atom or the Se–C(An) bond (the bond between the selenium atom and the *ipso*-carbon atom of the *p*-anisyl group) in **1** by the through-space mechanism irrespective of its small size of the valence orbitals. The structure of **1** studied by the X-ray crystallographic analysis and by the ab initio MO calculations exhibits the linear alignment of the F---Se–C(An) atoms with the analysis of the charge-transfer[18b] mechanism for the interaction. The results are discussed in Chapter 3.

3   4
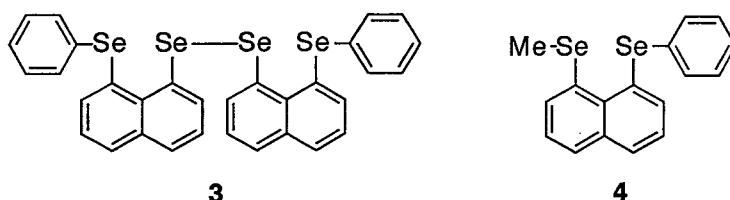
The nonbonded interactions between selenium atoms containing linear long bonds higher than 3c-4e were studied next. The nonbonded Se---Se interactions correspond to those in Scheme **2D**, where Z = Se and X = F, [8-(Phenylselanyl)naphthyl]-1,1'-diselenide (**3**) and 1-(methylselanyl)-8-(phenylselayl)naphthalene (**4**) were prepared. The structure of **3** was examined by the X-ray crystallographic analysis and revealed that the four selenium atoms in the compound align linearly. The structure of **4** was also investigated by the X-ray crystallographic analysis. The lone pair–lone pair repulsive interaction of the 2c-4e type plays an important role to determine the structure. The 4c-6e in **3** and 2c-4e in **4** are classified as the double type **A**-type **B** pairing and the type **C** pairing, respectively.

3   4

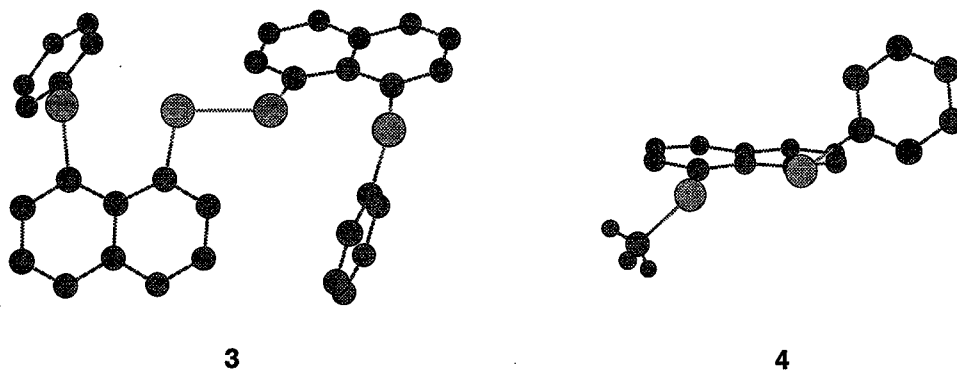**Figure 3. Structure of 3 and 4**

5

Ab initio MO calculations revealed the character of its structure. The linear bond constructed by the four Se atoms is shown to be analyzed by the four center-six electron model (4c-6e). The interaction in **4** constructs π and π^* molecular orbitals, which distort the Se-Me and Se-Ph groups from the naphthyl plane to some extent to avoid large exchange repulsive interaction brought about by the two center-four electron (2c-4e) interaction based on the ab initio MO calculations. The results are shown in Chapter 4.
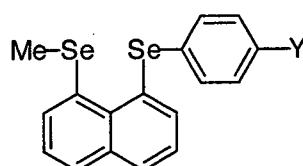
5 (Y = OMe), **6** (Y = Cl)

The type **C** pairing demonstrated in **4** is stabilized by the distorted π type 2c-4e interaction although the nonbonded 2c-4e interaction itself must be repulsive. As an extension of the structural study on the distorted π 2c-4e type interaction in **4**, I looked for such nonbonded Se---Se interaction that is the attractive in nature. The structure of 1-(methylselanyl)-8-(p-anisylselanyl)naphthalene (**5**) and 1-(methylselanyl)-8-(p-chlorophenylselanyl)naphthalene (**6**) is examined by the X-ray crystallographic analysis. The results show that the structure of **5** can be described as the pseudo type **A**-type **B** pairing around the Se–Me and Se–C_6H_4OMe-p (Se–C_{An}) groups, respectively, and that of **6** is the pure type **A**-type **B** pairing around the Se–C_6H_4Cl-p (Se–C_{Ar}) and Se–Me groups, respectively.

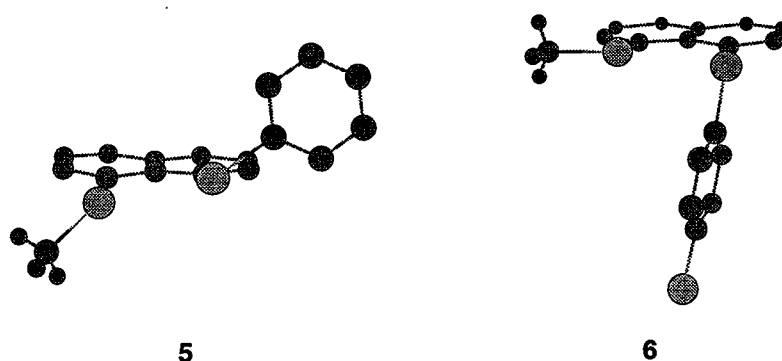**5**   **6**

Figure 4. Structure of 5 and 6

This finding led me to examine the nonbonded Se---Se interaction in the naphthalene system in more detail. The type **A**-type **B** pairing in **6** strongly suggest that the nonbonded Se---Se interaction should be characterized by the n(Se_{Ar})---σ^*(Se–C_{Me}) 3c-4e interaction. The pseudo-type **A**-type **B**

pairing in **2** also suggests the contribution of the $n(Se_{Me})$---$\sigma^*(Se-C_{An})$ 3c-4e interaction. The $\sigma^*(Se-C)$ bonds in **5** and **6** need to act as the electron acceptors. The nature of the $n(Se)$---$n(Se)$ interaction in 1,8-bis(selanyl)naphthalenes are also elucidated by the MO calculations performed on the models of **5** and **6**. The whole nature of the nonbonded $n(Se)$---$n(Se)$ 2c-4e interaction is elucidated by the MO calculations. The results are shown in Chapter 5.

The ^{77}Se NMR spectroscopy, as well as the ^1H and ^{13}C NMR spectroscopy, plays an important role in the study of the organic selenium chemistry.[19] The $\delta(Se)$ values are much reflected by the structural change of the selenium compounds. Therefore, it must be very useful not only in the structural study of the selenium compounds but also in the preparation of new compounds, if the calculated ^{77}Se NMR chemical shifts ($\delta_{calcd}(Se)$) can well explain the $\delta_{obsd}(Se)$ values. Recently the magnetic shielding tensor is shown to be reliable for some nuclei containing carbon, oxygen, and hydrogen, calculated with the gauge-including atomic orbitals (GIAO) theory.[20] Efforts have also been made to calculate the magnetic shielding tensor for the ^{77}Se nucleus on the theoretical background, and the reliability has been essentially established so far.[21,22]

$$Y-\!\!\left\langle\bigcirc\right\rangle\!\!-Se-R$$

7
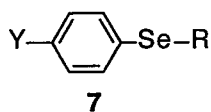
	a	b	c	d	e	f	g	h	i	j	k	l
Y =	H	OR	Me	Cl	Br	CO_2R	NO_2	NH_2	F	CF_3	CHO	CN

This encouraged me to interpret uniformly the $\delta_{obsd}(Se)$ values of p-substituted phenyl selenides, p-YC$_6$H$_4$SeR (ArSeR), in relation with their structures in solutions, based on the $\delta_{calcd}(Se)$ values. Before discussion of the $\delta(Se)$ values of p-YC$_6$H$_4$SeR (**7**), the GIAO magnetic shielding tensor for the ^{77}Se nucleus ($\sigma(Se)$) in selenium compounds of versatile structures was calculated and/or recalculated using Gaussian 94 program[7] with some basis sets. The calculations showed which method (basis sets and the level) is practically suitable for my purpose to calculate the $\delta_{calcd}(Se)$ values of p-YC$_6$H$_4$SeR. The results are shown in Chapter 6.

In Chapters 3 and 4, the characteristic structures were revealed for **3 – 6**. As the next extension of the study, I looked for novel properties which arose from the 4c-6e type interaction constructed by the 4c-6e in **3** in connection with the properties of the π type 2c-4e in **4** and the linear 3c-4e in **5** and **6**. The p-substituted derivatives of **3** and **4** were prepared and the ^1H, ^{13}C, and ^{77}Se NMR spectra were measured for **3** and **4**, together with their p-substituted derivatives.

Di[(p-substituted phenylselanyl)naphthyl] diselenides (1-[8-(p-YC$_6$H$_4$Se)C$_{10}$H$_6$]Se-Se[C$_{10}$H$_6$(SeC$_6$H$_4$Y-p)-8']-1' (**8**: **8a – 8g** for Y = H, OMe, Me, Cl, Br, COOEt, NO$_2$, respectively) were prepared. 1-(Methylselanyl)-8-(p-substituted phenylselanyl)naphthalenes **9** (**9a – 9g**) were

also prepared by the addition of methyl iodide to aqueous THF solutions of the corresponding 8-(p-substituted phenylselanyl)-1-naphthaleneselenates from **8a** – **8g**, respectively.

	a	b	c	d	e	f	g
Y =	H	OR	Me	Cl	Br	CO$_2$R	NO$_2$
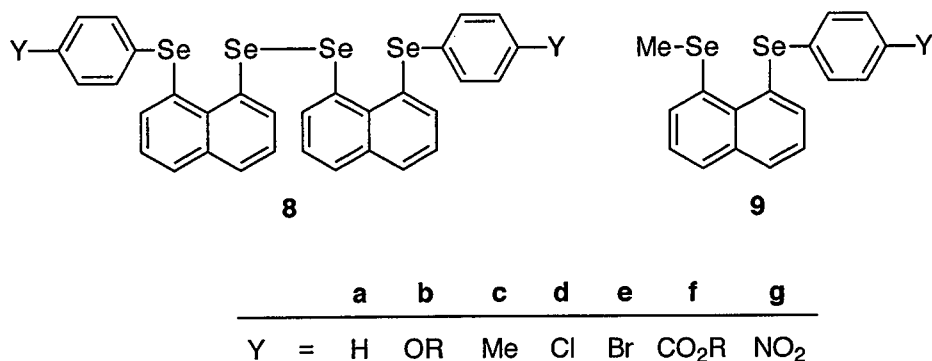
The $\delta(^8Se)$ values for 1-[8-(p-YC$_6$H$_4$Se)C$_{10}$H$_6$]SeSe[C$_{10}$H$_6$(SeC$_6$H$_4$Y-p)-8']-1' (**1** : Y = OMe, Me, H, Cl, Br, COOEt, and NO$_2$) showed a good correlation with those of 1-(MeSe)-8-(p-YC$_6$H$_4$Se)C$_{10}$H$_6$ (**2**). While the $\delta(^1Se)$ values correlated well with $\delta(^8Se)$ in **2** with a positive proportionality constant of 0.252 (regular correlation), a similar correlation for **1** gave a negative proportionality constant of –0.282 (inverse correlation).

Ab initio MO calculations, containing the GIAO magnetic shielding tensor of the selenium nucleus ($\sigma(Se)$), were performed on the model adducts **10** – **12**, which are the diselenides and the bis-selenides, to elucidate the nature of the nonbonded interactions characteristic of the 4c-6e, 2c-4e, and 3c-4e types. I present the results of investigations exhibiting the characteristic substituent effect on the Se atoms in **8**, in contrast to that of 2c-4e and/or 3c-4e in **8**. The interpretation of the nonbonded interactions in **8**, **9**, and their derivatives based on the MO calculations are further examined.
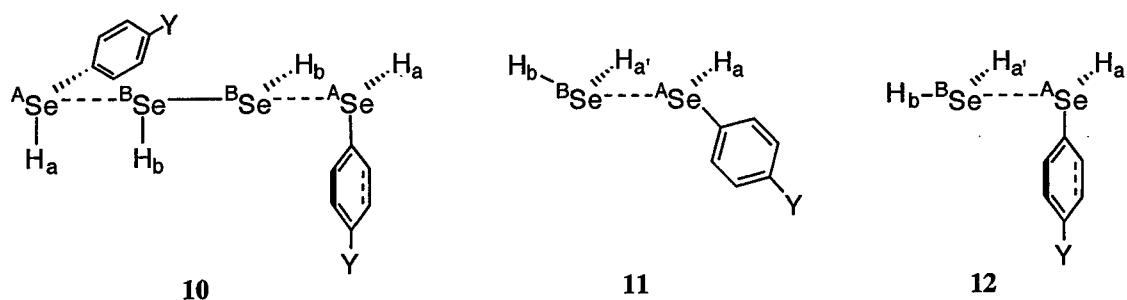
Scheme 4. Structures of Models 10 - 12.

The characters in the substituent effect on the atomic charges and the $\delta(Se)$ values of **8** are shown in eqs 3 and 4, respectively, assuming Y is electron-withdrawing. The superscript up (or down) in eq 4 shows upfield (or downfield) shifts in the $\delta(Se)$ values. The results explain the $\delta(Se)$ values of

8. The mechanism of the substituent effect on $\delta(^{B}Se)$ in **9** would be through-bond by way of the naphthylidene π-system. The results of the calculations on **9** are in accordance with the expectation. Nevertheless the $^{B}Se-H_b$ polarization mechanism is predicted to operate in **9**.

$$Y^{\delta-}\leftarrow C_6H_4-Se^{\delta+}---Se^{\delta+}-Se^{\delta+}---Se^{\delta+}-C_6H_4\rightarrow Y^{\delta-} \tag{3}$$

$$Y^{\delta-}\leftarrow C_6H_4-Se^{down}---Se^{up}-Se^{up}---Se^{down}-C_6H_4\rightarrow Y^{\delta-} \tag{4}$$

$$Y^{\delta-}\leftarrow C_6H_4-Se^{\delta+}---Se^{\delta-}-H_b^{\delta+} \tag{5}$$

$$Y^{\delta-}\leftarrow C_6H_4-Se^{down}---Se^{down}-H_b^{down} \tag{6}$$
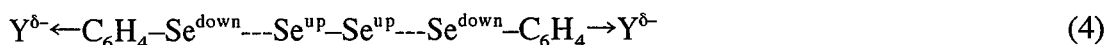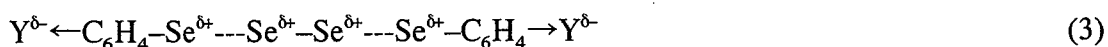
The observed $\delta(Se)$ values of **9** can be well explained by the results of the calculations on **12** at least in a qualitative sense. The nature of the substituent effect on the atomic charges and the $\delta(Se)$ values are shown in eqs 5 and 6, respectively, exemplified by the electron-withdrawing group of Y. The $\delta(C_{Me})$ values in **9** go upfield when Y = electron-withdrawing which is just the opposite of that predicted for H_b shown in eq 5. The discrepancy may arise from the difference between H in **12** and CH_3 in p-substituted derivatives of **4**: the C–H bond in **4** can also be polarized. The results are shown in Chapter 7.

References and Notes

(1) (a) S. Patai (ed), "The Chemistry of the Ether Linkage," Wiley, New York (1967). S. Patai (ed), "The Chemistry of the Thiol Group," Wiley, New York (1974), Part 1, Part 2. S. Patai (ed), "Supplement E The Chemistry of Ethers, Crown Ethers, Hydroxy Groups and Their Sulphur Analogues," Wiley, New York (1980), Part 1, Part 2. S. Patai and Z. Rappoport (eds), "The Chemistry of Organic Selenium and Tellurium Compounds," Wiley, New York (1986), Vol. 1 (1986), Vol. 2 (1987). (b) S. Oae (ed), "Organic Chemistry oh Sulfur," Plenum Press, New York (1977). (c) Bernardi, F.; Csizmadia, I. G.; Mangini, A. (eds), *"Organic Sulfur Chemistry: Theoretical and Experimental Advances,"* Elsevier, Amsterdam, 1985. (d) Klayman, D. L.; Günther, W. H. H. (Eds.), *Organic Selenium Compounds: Their Chemistry and Biology*, Wiley, New York, 1973. (e) D. Liotta (ed), "Organic Selenium Chemistry," Wiley-Interscience, New York (1987). K. J. Irgolic (ed), "The Organic Chemistry of Tellurium," Gordan and Breach Science Publishers, New York (1974).

(2) (a) Baenziger, M. C.; Buckles, R. E.; Maner, R. J.; Simpson, T. D. *J. Am. Chem. Soc.*, **1969**, *91*, 5749. (b) Chapter XV in ref 1d. (c) Hayes, R. A.; Martin, J. C. *Sulfurane Chemistry*, in ref 1c. See also refs cited therein.

(3) (a) Nakanishi, W.; Hayashi, S.; Tukada, H.; Iwamura, H. *J. Phys. Org. Chem.*, **1990**, *3*, 358. (b) Nakanishi, W.; Yamamoto, Y.; Hayashi, S.; Tukada, H.; Iwamura, H. *J. Phys. Org. Chem.*, **1990**, *3*, 369. (c) Nakanishi, W.; Hayashi, S.; Nakamura, Y.; Iwamura, H. *Chem. Lett.*, **1992**, 735; Nakanishi, W.; Sakamoto, K.; Isaka, K.; Hayashi, S. *Phosphorus, Sulfur, and Silicon*, **1992**, *67*, 79. (d) Nakanishi, W.; Hayashi, S. *Chem. Lett.*, **1995**, 75.

(4) (a) Pimentel, G. C. *J. Chem. Phys.* **1951**, *19*, 446. Musher, J. I. *Angew. Chem., Int. Ed. Engl.* **1969**, *8*, 54. (b) Chen, M. M. L.; Hoffmann, R. *J. Am. Chem. Soc.* **1976**, *98*, 1647. (c) Cahill, P. A.; Dykstra, C. E.; Martin, J. C. *J. Am. Chem. Soc.* **1985**, *107*, 6359.

(5) The electronegativity proposed by Allred-Rochow was employed to discuss the structure of the adducts. See, Allred, A. L.; Rochow, E. G. *J. Inorg. Nucl. Chem.* **1958**, *5*, 264; Allred, A. L.; Rochow, E. G. *J. Inorg. Nucl. Chem.* **1958**, *5*, 269.

(6) Mulliken, R. S. *J. Am. Chem. Soc.* **1950**, *72*, 600; Mulliken, R. S. *J. Am. Chem. Soc.* **1952**, *74*, 811.

(7) *Gaussian 94, Revision D.4*; Frisch, M. J.; Trucks, G. W.; Schlegel, H. B.; Gill, P. M. W.; Johnson, B. G.; Robb, M. A.; Cheeseman, J. R.; Keith, T.; Petersson, G. A.; Montgomery, J. A.; Raghavachari, K.; Al-Laham, M. A.; Zakrzewski, V. G.; Ortiz, J. V.; Foresman, J. B.; Cioslowski, J.; Stefanov, B. B.; Nanayakkara, A.; Challacombe, M.; Peng, C. Y.; Ayala, P. Y.; Chen, W.; Wong, M. W.; Andres, J. L.; Replogle, E. S.; Gomperts, R.; Martin, R. L.; Fox, D. J.; Binkley, J. S.; Defrees, D. J.; Baker, J.; Stewart, J. P.; Head-Gordon, M.; Gonzalez, C.; Pople, J. A. *Gaussian, Inc.*, Pittsburgh, PA, 1995.

(8) MacSpartan Plus Ver. 1.0, Hehre, H.J. *Wavefunction Inc.*

(9) (a) Pauling, L. *J. Am. Chem. Soc.*, **1947**, *69*, 542. (b) Pauling, L. *The Nature of the Chemical Bond*, 3rd ed.; Cornell University Press: Ithaca, New York, 1960; Chapter 7.

(10) The bond orders n(Se–I) and n(I–I) of Se–I–I bond in $(CH_2)_4$Se–I–I are 0.37 and 0.38, respectively, which are very close to 0.40 of n(Se–Br) for Br–Se–Br bond in $(p$-$MeC_6H_4)_2SeBr_2$.

(11) (a) Asmus, K.-D. *Acc. Chem. Res.*, **1979**, *12*, 436; Musker, W. K. *Acc. Chem. Res.*, **1980**, *13*, 200; (b) Fujihara, H.; Furukawa, N. *J. Mol. Struct. (Theochem)*, **1989**, *186*, 261.

(12) Albright, T. A.; Burdett, J. K.; Whangbo, M.-H. *Orbital Interactions in Chemistry*, Wiley-Interscience, New York, 1985.

(13) Topson, R. D. *The Nature and Analysis of Substituent Electronic Effects*, in *Progress in Physical Organic Chemistry*, ed by Taft, R. W. John Wiley & Sons, Vol. 12, New York, 1976. See also refs cited therein.

(14) (a) Mallory, F. B. *J. Am. Chem. Soc.* **1973**, *95*, 7747. (b) Mallory, F. B.; Mallory, C. W.; Fedarko, M.-C. *J. Am. Chem. Soc.* **1974**, *96*, 3536. (c) Mallory, F. B.; Mallory, C. W.; Ricker, W. M. *J. Am. Chem. Soc.* **1975**, *97*, 4770. Mallory, F. B.; Mallory, C. W.; Ricker, W. M.

J. Org. Chem. **1985**, *50*, 457. Mallory, F. B.; Mallory, C. W.; Baker, M. B. *J. Am. Chem. Soc.* **1990**, *112*, 2577. (d) Ernst, L.; Ibrom, K. *Angew. Chem. Int. Ed. Engl.* **1995**, *34*, 1881. Ernst, L.; Ibrom, K.; Marat, K.; Mitchell, R. H.; Bodwell, G. J.; Bushnell, G. W. *Chem. Ber.* **1994**, *127*, 1119.

(15) Mallory, F. B.; Luzik, Jr., E. D.; Mallory, C. W.; Carroll, P. J. *J. Org. Chem.* **1992**, *57*, 366. Mallory, F. B.; Mallory, C. W. *J. Am. Chem. Soc.* **1985**, *107*, 4816.

(16) (a) Fujihara, H.; Saito, R.; Yabe, M.; Furukawa, N. *Chem. Lett.* **1992**, 1437. (b) Nakanishi, W.; Hayashi, S.; Yamaguchi, H. *Chem. Lett.* **1996**, 947.

(17) Johannsen, I.; Eggert, H. *J. Am. Chem. Soc.* **1984**, *106*, 1240. Johannsen, I.; Eggert, H.; Gronowitz, S.; Hörnfeldt, A.-B. *Chem. Scr.* **1987**, *27*, 359. Fujihara, H.; Mima, H.; Erata, T.; Furukawa, N. *J. Am. Chem. Soc.* **1992**, *114*, 3117.

(18) (a) Goldstein, B. M.; Kennedy, S. D.; Hennen, W. J. *J. Am. Chem. Soc.* **1990**, *112*, 8265. (b) Barton, D. H. R.; Hall, M. B.; Lin, Z.; Parekh, S. I.; Reibenspies, J. *J. Am. Chem. Soc.* **1993**, *115*, 5056.

(19) (a) McFarlane, W.; Wood, R. J. *J. Chem. Soc. Dalton Trans.* **1972**, 1397. (b) Iwamura, H.; Nakanishi, W. *J. Syn. Org. Chem. Jpn.* **1981**, *39*, 795; Patai, S.; Rappoport, Z. (eds), *The Chemistry of Organic Selenium and Tellurium Compounds*, Wiley, New York, 1986, Chap. 6 (Vol. 1); Klapötke, T. M.; Broschag, M. *Compilation of Reported ^{77}Se NMR Chemical Shifts*, Wiley, New York, 1996.

(20) Cheeseman, J. R.; Trucks, G. W.; Keith, T. A.; Frisch, M. J. *J. Chem. Phys.* **1996**, *104*, 5497. Pulay, P.; Hinton, J. F. in *Encyclopedia of Nuclear Magnetic Resonance*, Eds. Grant, D. M.; Harris, R. K. John Wiley & Sons, New York, p. 4434 (Vol. 7), 1996. See also, Forsyth, D. A.; Sebag, A. B. *J. Am. Chem. Soc.* **1997**, *119*, 9483; Olah, G. A.; Shamma, T.; Burrichter, A.; Rasul, G.; Prakash, G. K. S. *J. Am. Chem. Soc.* **1997**, *119*, 12923, 12929.

(21) (a) Nakatsuji, H.; Higashioji, T.; Sugimoto, M. *Bull. Chem. Soc. Jpn.* **1993**, *66*, 3235. (b) Magyarfalvi, G.; Pulay, P. *Chem. Phys. Lett.* **1994**, *225*, 280. (c) Bühl, M.; Gauss, J.; Stanton, J. F. *Chem. Phys. Lett.* **1995**, *241*, 248. (d) Bühl, M.; Thiel, W.; Fleischer, U.; Kutzelnigg, W. *J. Phys. Chem.* **1995**, *99*, 4000. (e) Malkin, V. G.; Malkina, O. L.; Casida, M. E.; Salahub, D. R. *J. Am. Chem. Soc.* **1994**, *116*, 5898. (f) Schreckenbach, G.; Ruiz-Morales, Y.; Ziegler, T. *J. Chem. Phys.* **1996**, 104, 8605. (g) Ellis, P. D.; Odom, J. D.; Lipton, A. S.; Chen, Q.; Gulick, J. M. in *Nuclear Magnetic Shieldings and Molecular Structure*; NATO ASI Series; Tossel, J. A. Ed.; Kluwer Academic Publishers; Dordrecht, 1993, p. 539. See also refs cited therein.

(22) Although the contribution of relativistic terms has been pointed out for heavier atoms, the perturbation is expected to be small for the selenium nucleus. Tanaka, S.; Sugimoto, M.; Takashima,

H.; Hada, M.; Nakatsuji, H. *Bull. Chem. Soc. Jpn.* **1996**, *69*, 953; Ballard, C. C.; Hada, M.; Kaneko, H.; Nakatsuji, H. *Chem. Phys. Lett.* **1996**, *254*, 170; Nakatsuji, H.; Hada, M.; Kaneko, H.; Ballard, C. C. *Chem. Phys. Lett.* **1996**, *255*, 195; Hada, M.; Kaneko, H.; Nakatsuji, H. *Chem. Phys. Lett.* **1996**, *261*, 7. See also refs cited therein.

Chapter 2

On the Stability and the Bonding Model of n→σ* Type Molecular Complexes, R_2Z-X-X: Proposal of 3c-4e Description for Z–X–X in the Adducts

Abstract

The stability of the $Z-{}^1X-{}^2X$ bonds in $R_2Z-{}^1X-{}^2X$ molecular complexes (MC) was examined for $O(CH_2CH_2)_2Se-I-X$, $PhMeSe-I-X$ (X = Cl, Br), and $Se(C_6H_4)_2Se-Br-Br$. The MC adducts were shown to be comparably stable or more stable than the corresponding trigonal bipyramidal adducts (TB) which equilibrate with the MC in some cases. In order to clarify the reason for the stability of the MC, the model adducts of $H_2Z^1X^2X$ (MC and TB) (Z = O, S, Se and X = Cl, Br), together with the related species (H_2Z, X_2, H_2ZX^+, and $H_2ZX\bullet$), were optimized with the 6-311++G(3df,2pd) basis sets at the MP2 and/or B3LYP levels. Calculations were also performed with different distances between ${}^1Cl$ and ${}^2Cl$ ($r({}^1Cl,{}^2Cl)$) in $H_2S-{}^1Cl-{}^2Cl$ (MC) and $r(S,{}^2Cl)$ in $H_2S^1Cl^2Cl$ (TB), where $r = r_0 + 0.1m$ Å (r_0: the optimized distance and m = –1, (0), 1, 2, and 3). A charge transfer (CT) occurs from S to ${}^2Cl$ in the $S-{}^1Cl-{}^2Cl$ bond of the MC as $r({}^1Cl,{}^2Cl)$ becomes larger, assuming a singlet multiplicity in the calculations. The situation is equal to that of ${}^1Cl-S-{}^2Cl$ in the TB, for which CT occurs from ${}^1Cl$ to ${}^2Cl$. A 3c-4e description of the $Z-{}^1X-{}^2X$ bond in $R_2Z-{}^1X-{}^2X$ (MC) is proposed based on the ab initio MO calculations by exhibiting the 10-${}^1X$-2 character, the N–X–L cording system for hypervalent bonds proposed by Martin, for $R_2Z-{}^1X-{}^2X$ (MC) practically. Bond orders for typical TB and MC were calculated from literature data according to Pauling's equation. The bond orders agree with the proposed 3c-4e model for the MC.

Introduction

The concept of molecular compounds or molecular complexes (MC) has been developed for a loose reversible association of the original molecules in a well-defined ratio, mostly 1 : 1. Mulliken has proposed a theory for MC based on quantum mechanics.[1] The driving force for the association is a charge transfer (CT) where electrons move from electron donors to acceptors in the complexes. On the other hand, a theory for complexes with trigonal bipyramidal structure has been proposed by Pimentel and Musher.[2a] Such trigonal bipyramidal adducts (TB) contain hypervalent three center-four electron bonds (3c-4e) composed of linear $\sigma(p)$ orbitals. The 3c-4e description of the X–Z–X bond in TB, such as halogen adducts of chalcogenides (R_2ZX_2 (TB)), was further developed by the preparation and characterization of variety of new compounds with TB structure[3] and by theoretical calculations.[2] Thus the character of the X–Z–X bond in TB is easily understood by the 3c-4e description of this bond.[2,3] However, the character of the Z–X–X bond in R_2Z–X–X (MC) cannot be so easily imagined by a weak $n{\rightarrow}\sigma^*$ CT description in some cases. The 3c-4e model is an attractive description for the Z–X–X bond in R_2Z–X–X (MC) (Scheme 1).
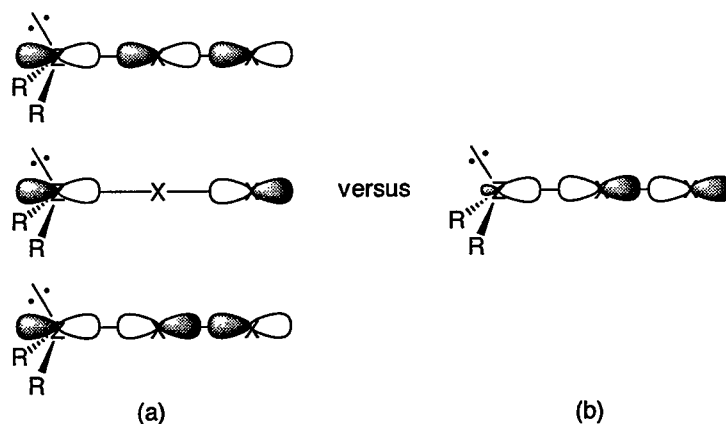
Scheme 1. Bonding Models for R_2ZX_2 (MC): (a) 3c-4e versus (b) $n{\rightarrow}\sigma^*$ Descriptions

The R_2Z–X–X (MC) are stabilized by CT from $n(Z)$ to $\sigma^*(X$–X) orbitals of the components. The linear alignment of the three atoms, Z–X–X, must be superior to the bent structure for the CT. If the magnitude of the CT is small, the adduct will be an MC with a longer X–X bond. If the magnitude of the CT becomes large enough, the halogen can no longer exist as a halogen molecule, which leads to the formation of a TB with a hypervalent 3c-4e bond.[3,4] The adduct should be a TB

$$RZR' \ + \ X_2 \ \rightleftharpoons \ \text{MC} \ (\chi_X < \chi_Z) \ \rightleftharpoons \ \text{TB} \ (\chi_X > \chi_Z) \tag{1}$$

14
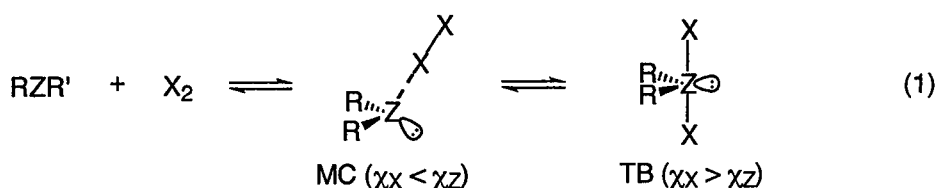
if the electronegativity[5] of X (χ_X) is larger than that of Z (χ_Z) in R_2ZX_2, and an MC if χ_X is not larger than χ_Z (general rule).[3a,4a,4b] On the basis of this rule, the structure of bromine adducts of selenides is expected to be a TB, but the difference of the electronegativity between Br and Se is small, which in some cases can lead to an equilibrium between TB and MC (eq 1).

Recently, the MC structure became popular in addition to the TB structure and/or ionic ones, since X-ray crystallographic studies increased the number of examples with an MC structure in the solid state, such as Ph_3P-X-X' (X–X' = Br_2, I_2, and IBr).[6] I encountered the formation of a mixture of a chlorine adduct (TB) and an iodine adduct (MC) of 1-selena-4-oxane when iodine monochloride is allowed to react with the selenide in solutions. The structure of the iodine monochloride adduct of 1-selena-4-oxane has been demonstrated to be $O(CH_2CH_2)_2Se-I-Cl$ by X-ray crystallographic analysis (see eqs 2 and 3).[7] The MC structure of selenanthrene with bromine was established in solutions (cf: eq 4).[4b] An equilibrium between MC and TB was also reported for $ArAr'Se \cdot Br_2$.[8] These findings show that the stability of MC and TB must be comparable in some cases, which means that the stability of the Z–X–X bond in the MC should be comparable to the stability of the X–Z–X bond in the TB in such a case.

Martin and his coworkers redefined the bonding scheme for hypervalent species with a 3c-4e bond based on detailed ab initio MO calculations performed for the trifluoride ion.[2c] The unique characteristic of all hypervalent molecules is redefined as follows: (1) the presence of at least one occupied high-energy molecular orbital which is s rather than p in symmetry with respect to a central atom to ligand bond and (2) which has virtually no overlap with the valence orbitals on a central atom.[2c] The trifluoride ion is a typical TB with the typical 3c-4e bond. However, the definition (2) would be difficult to apply to hypervalent molecules with unsymmetrical 3c-4e bonds, as they appear in an MC.

A general systematic classification scheme has been proposed, which is practically useful for molecules with electron-rich multi-center (hypervalent) bonding.[3c,d] The N–X–L cording system starts from a resonance structure that has only single bonds to X, and it designates the bonding around an atom X in terms of the number of valence shell electrons N formally associated directly with X and ligands L directly bonded to it. The R_2ZX_2 (TB) adduct and the trifluoride ion are classified as the 10–Z–4 and 10–F–2 species, respectively. The bonding scheme of $R_2Z-^1X-^2X$ (MC) is formally represented as 10–^{1}X–2. The atoms X in R_2ZX_2 (TB), ^{2}X in $R_2Z-^1X-^2X$ (MC), and Z in R_2ZX_2 (MC) are formally classified as 8–X–1, 8–^{2}X–1, and 8–Z–3, respectively. We would like to represent the situation as follows: $R_2Z-^1X-^2X$ (MC) is an MC for Z, but the central ^{1}X is recognized as a TB. Correspondingly, R_2ZX_2 (TB) is a TB for Z, but for X it can be viewed as an MC. This consideration led me to the working hypothesis that the bonding scheme in $R_2Z-^1X-^2X$ (MC) can be described by the 3c-4e hypervalent model, if the 10–^{1}X–2 character is

proven for $R_2Z-^1X-^2X$ (MC).

Much attention has been paid to the bonding and the nonbonded interactions between heteroatoms containing 2c-2e,[9] 2c-3e,[9] 3c-4e,[10] 4c-6e,[11] and other bonds.[12] Ab initio MO calculations were recently performed on H_2O-X-X'[13] and H_3N-X-X'[14] (X-X' = F_2, Cl_2, and Cl-F), which also encouraged me to further investigate the character of the Z-X-X bond in MC. Here I would like to present the results of my recent investigations, which confirmed my working hypothesis of a 3c-4e description of the bonding in some $n\rightarrow\sigma^*$ type R_2Z-X-X (MC) systems.

Results and Discussion

Stability of MC versus TB in RR'SeXY. The ^{13}C NMR spectra were measured for 1-selena-4-oxane (**1**) in chloroform-d with and without addition of iodine monochloride, iodine monobromide, chlorine, bromine, or iodine (eq 2). Table 1 shows the results. The ^{1}H, ^{13}C, and ^{77}Se NMR chemical shifts ($\delta(^1H)$, $\delta(^{13}C)$, and $\delta(^{77}Se)$, respectively) were also measured for selenoanisole (**2**) in the presence or absence of the halogens and interhalogens (eq 3). Table 2 collects the results, which include the half widths ($v_{1/2}$) and the integrals of the methyl proton signals. Table 3 exhibits selected $\delta(^1H)$ values of selenanthrene (**3**) and p-nitrophenyl phenyl selenide (**4**), together with those of the mixtures with bromine (eq 4).
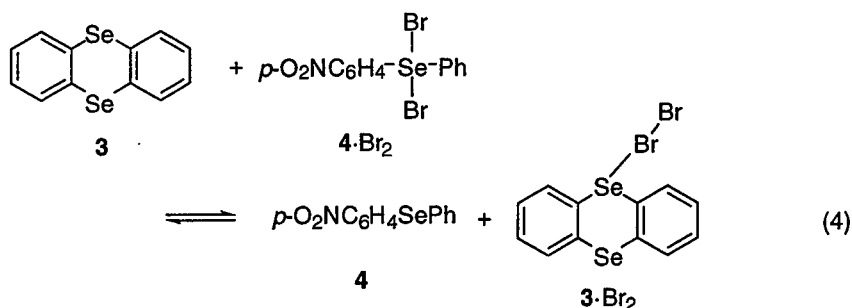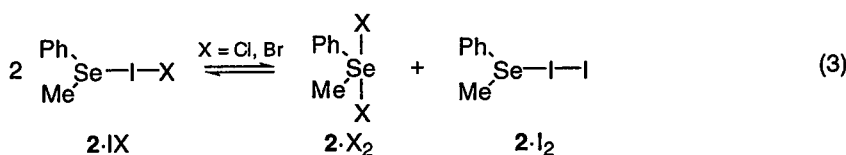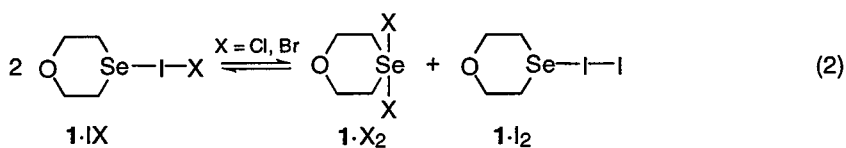
The formation of the 1 : 1 mixture of $1\cdot Cl_2$ (TB) and $1\cdot I_2$ (MC) from $1\cdot ICl$ (MC) in the solution is demonstrated by the $\delta(^{13}C)$ values (Table 1). Such a mixture was not observed in the solid state. In solution, the bonding energy of the hypervalent Cl-Se-Cl bond (and of the $n\rightarrow\sigma^*$

type Se–I–I bond) must be larger than two equivalents of the n→σ* type Se–I–Cl bond. On the other hand, an equilibrium between $1 \cdot Br_2$ and $1 \cdot I_2$ and $1 \cdot IBr$ is indicated by the $\delta(^{13}C)$ values for the $1 \cdot IBr$ solution. In order to clarify this point, the NMR chemical shifts of the adducts with selenoanisole (2) were examined.

Table 1. ^{13}C NMR Chemical Shifts of $O\,(^2CH_2{}^1CH_2)_2Se \cdot XY^a$

XY	$\delta(^1C)$	$\delta(^2C)$	XY	$\delta(^1C)$	$\delta(^2C)$
null[b]	17.2	69.5	null[b]	17.2	69.5
ICl[c]	31.3	–7.1	$Cl_2{}^c$	31.2	–7.2
	3.5	–1.7	$Br_2{}^c$	28.1	–6.6
IBr[c]	27.9	–6.1	$I_2{}^c$	3.1	–1.4
	0.8	–0.9			

[a] In $CDCl_3$. [b] From TMS. [c] From the parent selenide.

The $\delta(^1H)$, $\delta(^{13}C)$, and $\delta(^{77}Se)$ values of $2 \cdot ICl$ shown in Table 2 consist of two sets of chemical shifts similar to the case of $1 \cdot ICl$. The chemical shifts for one set were the same as those of $2 \cdot Cl_2$ and those for the second set were slightly different from those of $2 \cdot I_2$. The molar fraction of $2 \cdot Cl_2$ in the $2 \cdot ICl$ solution was estimated to be 0.42 based on the integral of the methyl protons, which yields fractions of 0.42 and 0.16 for $2 \cdot I_2$ and $2 \cdot ICl$, respectively, although the MC adducts were in equilibrium with the components. The larger $v_{1/2}$ values for the latter set are consistent with the presence of the equilibrium.

Table 2. ^1H, ^{13}C, and ^{77}Se NMR Chemical Shifts of the MeSe Groups in $2 \cdot XY^a$

XY	$\delta(^1H)$	$\Delta v_{1/2}{}^b$	Content[c]	$\delta(^{13}C)$	$\Delta v_{1/2}{}^b$	$\delta(^{77}Se)$	$\Delta v_{1/2}{}^b$
null[d]	2.35	1.0	1.00	7.2	1.0	206.9	4.0
ICl[e]	1.55	8.8	0.42	39	f	286.0	16.6
	0.38	11.4	0.58	8	f	53.3	25.1
IBr[e]	0.61	2.0	1.00	11.8	5.5	77	f
$Cl_2{}^e$	1.56	1.0	1.00	38.7	1.0	285.0	4.9
$Br_2{}^e$	1.55	1.0	1.00	36.5	1.0	227.1	4.9
$I_2{}^e$	0.33	1.0	1.00	5.6	3.3	44.9	7.7

[a] In $CDCl_3$. [b] In hertz. [c] Relative integrals of the signal(s). [d] From TMS for $\delta(^1H)$ and $\delta(^{13}C)$ and from MeSeMe for $\delta(^{77}Se)$. [e] From the parent selenide. [f] Very broad.

Only one set of signals was observed for $2 \cdot IBr$. It must be due to a relatively fast equilibrium between the adducts. The $\delta(^1H)$, $\delta(^{13}C)$, and $\delta(^{77}Se)$ values of MeSe group in $2 \cdot IBr$ were much smaller than those of the average of $2 \cdot Br_2$ and $2 \cdot I_2$. The molar fraction of $2 \cdot Br_2$ was estimated to be ca. 0.2 assuming that the chemical shifts of $2 \cdot IBr$ are equal to those of $2 \cdot I_2$. The fractions of $2 \cdot I_2$ and $2 \cdot IBr$ were estimated to be about 0.2 and 0.6, respectively. These results show that the stability of $2 \cdot ICl$ is comparable to that of $2 \cdot Cl_2$ and that the two equimolar $2 \cdot IBr$ are more stable than the mixture of $2 \cdot Br_2$ and $2 \cdot I_2$. The stability of the $n \rightarrow \sigma^*$ type Se–I–X (X = Cl, Br) bonds suggested to be comparable to that of the hypervalent 3c-4e X–Se–X (X = Cl, Br) bonds.[15]

The stability of the MC adduct of $3 \cdot Br_2$ relative to that of the TB adduct of $4 \cdot Br_2$ was examined by analyzing the $\delta(^1H)$ values of 3, 4, their bromine adducts, and the mixtures. Table 3 shows the results.[15] The molar ratios of 3, $3 \cdot Br_2$, 4, and $4 \cdot Br_2$ were calculated to be 0.36, 0.64, 0.64, and 0.36, respectively, when one equimolar amount of 3 was added to a solution of $4 \cdot Br_2$ in chloroform-d. The K value (K = $[3 \cdot Br_2][4]/[3][4 \cdot Br_2]$) of eq 4 was estimated to be 3.2. The ratios became 1.18, 0.82, 0.81, and 0.19, respectively, when an additional 1 equiv of 3 was added to the solution (K = 3.0). These results clearly show that $3 \cdot Br_2$ (MC) is more stable than $4 \cdot Br_2$ (TB), which in turn exhibits that the $n \rightarrow \sigma^*$ type Se-Br-Br bond in the former must be more stable than the 3c-4e hypervalent Br-Se-Br bond in the latter.

We wondered why some Se–X–Y bonds in the MC were more stable than those expected from the $n \rightarrow \sigma^*$ type CT model. The $n \rightarrow \sigma^*$ type Se–X–X bonds in the MC were therefore examined on the basis of ab initio MO calculations.

Table 3. ^{1}H NMR Chemical Shifts of 3 and 4 with and without Bromine, Together with Their Mixtures[a]

Condition	3	4	
	$\delta(^1H(o))$	$\delta(^1H(o))$	$\delta(^1H(2))$
3[b]	7.700		
3 + Br$_2$[c]	0.124		
4[b]		7.616	7.337
4 + Br$_2$[c]		0.392	0.788
4 + 2Br$_2$[c]		0.392	0.788
4 + 3Br$_2$[c]		0.393	0.788
3 + 4 + Br$_2$[c]	0.079	0.141	0.283
2·3 + 4 + Br$_2$[c]	0.051	0.075	0.150

[a] In CDCl$_3$. [b] From TMS. [c] From the parent selenide.

Molecular Orbital Calculations for H_2ZX_2. Ab initio MO calculations were performed on the TB and MC adducts (H_2ZX_2) using Gaussian 94 program,[16] together with the related species (H_2Z, X_2, H_2ZX^+, and $H_2ZX\bullet$[17]). The optimized TB and MC structures are indicated by H_2ZX_2 (TB) and H_2ZX_2 (MC) (sometimes H_2ZXX (TB) and H_2Z-X-X (MC)), respectively. Table 4 shows the results of calculations on H_2ZX_2 (TB) and H_2ZX_2 (MC), where (Z,X) = (O,Cl), (S,Cl), and (S,Br), with the 6-311+G(d,p), 6-311+G(2d,p), and 6-311++G(3df,2pd) basis sets at the MP2 and/or DFT (B3LYP) levels.[18] The Z–X–X bonds in MC were calculated to be almost linear, which is in accordance with the observations. The TB adduct of H_2SCl_2 was found to be more stable than the MC when 6-311+G(2d,p) and 6-311++G(3df,2pd) basis sets at the MP2 level and 6-311++G(3df,2pd) basis sets at the B3LYP level were applied. However, the application of the 6-311+G(d,p) basis sets at the MP2 level lead to the prediction that the TB is less stable than the MC, which is not in accordance with the experimental findings on diorganyl sulfide dichlorides.[3a,d]

The optimized r(O–Cl)) and r(Cl–Cl) values in H_2O–Cl–Cl (MC) were 2.738 and 1.995 Å, respectively, with the 6-311++G(3df,2pd) basis sets at the MP2 level and 2.710 and 2.028 Å, respectively, with the same basis sets at the B3LYP level.[13] The calculated values reproduce the bond lengths observed for $O(CH_2CH_2)_2OCl_2$ (2.67 and 2.02 Å, respectively),[19] fairly well. The (r(S–Br), r(Br–Br)) distances in H_2S–Br–Br (MC) were calculated to be (3.146, 2.303 Å) and (3.033, 2.361 Å) at the MP2 and the B3LYP levels, respectively, applying the 6-311++G(3df,2pd) basis sets. The observed values for a 1 : 2 adduct of 1,2,4,5-tetrakis(ethylthio)benzene with bromine are (2.81, 2.41 Å).[20] The calculated r(S-Br) and r(Br-Br) distances are 0.22 – 0.34 Å longer and 0.11 – 0.05 Å shorter than the observed ones, respectively. The observed values for $(CH_2)_4S$–Br–Br are (2.321, 2.724 Å).[21] The differences between the observed and calculated values are very large in this case. This discrepancy must be due to the ionic nature of $(CH_2)_4S$–Br–Br (such as $(CH_2)_4S^+$–Br---Br$^-$) in the solid state. The calculated r(S,[1]Br) in H_2S[1]Br$^+$ is 2.152 Å (see Table 5), which is slightly shorter than the observed value in $(CH_2)_4S$–Br–Br.

Z = O, S, Se and X = Cl, Br
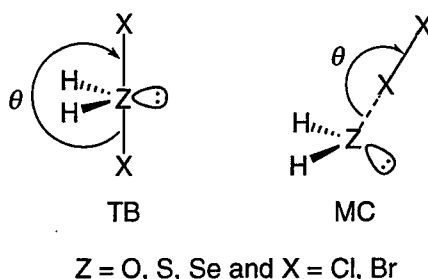
Table 4. Results of Ab initio MO Calculations for H_2ZX_n with Various Basis Sets at MP2 and/or DFT (B3LYP) Levels

	Energy (E) (au)	r(Z–H) (Å)	r(Z–X) (Å)	r(X–X) (Å)	∠HZH (deg)	∠HZX (deg)	∠ZXX[a] (deg)
H_2O–Cl–Cl (MC)							
MP2/6-311++G(3df,2pd)	-995.6872	0.9596	2.7380	1.9946	104.31	112.96	180.06
B3LYP/6-311++G(3df,2pd)	-996.8936	0.9619	2.7098	2.0279	105.31	104.70	180.90
H_2SCl_2(TB)							
MP2/6-311+G(d,p)	-1318.0824	1.3308	2.2907		96.14	86.76	170.29
MP2/6-311+G(2d,p)	-1318.1655	1.3305	2.2673		96.17	87.06	171.19
MP2/6-311++G(3df,2pd)	-1318.2683	1.3304	2.2313		96.39	87.00	171.01
B3LYP/6-311++G(3df,2pd)	-1319.8662	1.3382	2.2763		95.65	87.19	171.63
H_2S–Cl–Cl (MC)							
MP2/6-311+G(d,p)	-1318.0925	1.3338	3.3151	2.0333	92.25	110.70	176.80
MP2/6-311+G(2d,p)	-1318.1580	1.3337	3.1304	2.0450	92.88	97.41	179.62
MP2/6-311++G(3df,2pd)	-1318.2623	1.3331	3.1053	2.0011	92.19	93.94	180.69
B3LYP/6-311++G(3df,2pd)	-1319.8593	1.3424	2.9650	2.0551	92.57	93.04	180.47
H_2S–Br–Br (MC)							
MP2/6-311++G(3df,2pd)	-5543.9692	1.3336	3.1456	2.3027	92.27	92.59	181.03
B3LYP/6-311++G(3df,2pd)	-5547.7293	1.3427	3.0332	2.3607	92.61	93.51	180.71

[a] ∠ClSCl for TB.

Table 5. Results of Ab initio MO Calculations for H_2SX_n (X = Cl, Br) with 6-311++G(3df,2pd) Basis Sets at the MP2 Level

	H_2S	$H_2S^1Cl\bullet^a$	$H_2S^1Cl^+$	H_2SCl_2(TB)	$H_2S^1Cl^2Cl$ (MC)	$H_2S^1Br\bullet^b$	$H_2S^1Br^+$	H_2SBr_2(TB)	$H_2S^1Br^2Br$ (MC)
E (au)	-398.8986	-858.5500	-858.2595	-1318.2683	-1318.2623	-2971.4031	-2971.1101	-5543.9556	-5543.9692
r(S–H) (Å)	1.3324	1.3332	1.3496	1.3304	1.3331	1.3339	1.3487	1.3320	1.3336
r(S-^{1}X) (Å)		2.5540	1.9719	2.2313	3.1053	2.7991	2.1522	2.4232	3.1456
r(^{1}X–^{2}X) (Å)					2.0011				2.3027
∠HSH (deg)	92.15	92.66	93.37	96.39	92.19	92.42	93.35	95.23	92.27
∠HS^{1}X (deg)		88.48	100.03	87.00	93.94	89.38	99.66	87.19	92.59
∠S^{1}X^{2}X (deg)				171.01^c	180.69			171.66^c	181.03
Qn(S)	-0.2158	0.0336	0.6110	0.6296	-0.1988	-0.0645	0.4687	0.5055	-0.1881
Qn(H)	0.1079	0.1240	0.1798	0.1494	0.1136	0.1226	0.1852	0.1577	0.1162
Qn(H_2S)		0.2815	0.9706	0.9283	0.0284	0.1807	0.8390	0.8208	0.0443
Qn(^{1}X)		-0.2815	0.0294	-0.4642	0.0080	-0.1807	0.1610	-0.4104	0.0110
Qn(^{2}X)				-0.4642	-0.0364			-0.4104	-0.0553

^{a} Spin densities: S(S) 0.3174, S(H) -0.0142, S(^{1}Cl) 0.7110. ^{b} Spin densities: S(S) 0.2035, S(H) -0.0102, S(^{1}Br) 0.8168. ^{c} ∠^{1}XS^{2}X for TB.

After the comparison of the observed structure for some MC with that calculated for some models, calculations on H_2ZX_2 (TB) and H_2ZX_2 (MC) were performed in more detail for $Z = S$, Se and $X = Cl$, Br, together with the related species (H_2Z, X_2, H_2ZX^+, and $H_2ZX\bullet$), applying the 6-311++G(3df,2pd) basis sets at the MP2 level. Tables 5 and 6 exhibit the energies (E), optimized structures, and natural charges (Qn), obtained from a natural population analysis,[22] for the sulfur and the selenium compounds. The TB adducts were found to be more stable than the corresponding MC for H_2SCl_2, H_2SeCl_2, and H_2SeBr_2, whereas H_2SBr_2 (TB) was calculated to be less stable than H_2SBr_2 (MC), which was in accordance with the observations. The energy difference between H_2SeBr_2 (TB) and H_2SeBr_2 (MC) was only 0.0019 au (5.0 kJ mol^{-1}), which indicated the possible existence of an equilibrium between TB and MC in ArAr'Se·Br$_2$.

Large positive and negative charges were predicted on the central and the terminal atoms of the TB adducts, which are well explained by the 3c-4e model for the bond.[3] On the other hand, the predicted Qn values on Z (and H_2Z), ^1X, and ^2X in $H_2Z-^1X-^2X$ (MC) were negative, positive, and negative, respectively. The development of a positive charge on the central atom ^1X in the MC, as well as the negative charge predicted on the terminal atom ^2X, are in agreement with the 3c-4e model of the $Z-^1X-^2X$ bond. The development of negative charge on the terminal atom, Z, also seems to agree with that model. But one has to be careful. The charge on Z of H_2Z-X-X (MC) has to be compared with that of free H_2Z, since the MC is formed by the reaction of H_2Z with X_2. The Qn values on Z in H_2Z-X-X (MC) (Z = S, Se and X = Cl, Br) were predicted to be slightly more positive than those on the corresponding atoms of H_2Z. The magnitude of the positive charge at the Z atoms as well as the H_2Z components were larger for X = Br than for X = Cl in the MC,[23] irrespective of the electronegativity[5] of the elements.

Let me compare the charges on Z in H_2ZX_2 (MC) with those of the atoms in H_2ZX^+, which corresponds to the charge transfer in the reaction of H_2ZX^+ with X$^-$ to form H_2Z-X-X (MC). The most typical example is found for (Z,X) = (Se,Cl). The charges at Se and ^1Cl in $H_2Se^1Cl^+$ were 0.830 and –0.073, respectively. They became -0.084 and 0.004 in $H_2Se-^1Cl-^2Cl$ (MC), after reaction with $^2Cl^-$. The positive charge development at ^1Cl in the MC is interesting. The negative charge at $^2Cl^-$ decreases to –0.039 in $H_2Se-^1Cl-^2Cl$ (MC): the negative charge does not accumulate on ^1Cl, but is transferred to Se in $H_2Se-^1Cl-^2Cl$ (MC). A negative charge of ca. 0.96 passes through ^1Cl to Se or H_2Se. Some negative charge also moves from ^1Cl to Se or H_2Se during this process. Similar amounts of CT are also predicted for other MC adducts where the charge at ^1X in $H_2Z^1X^+$ is determined by the relative electronegativity of X and Z. A similar picture for the character of the CT is obtained if one considers the formation of H_2Z-X-X (MC) from $H_2Z^1X\bullet$ and $^2X\bullet$ (see Tables 5 and 6).
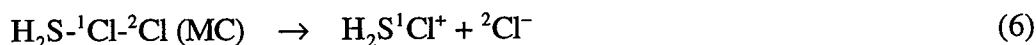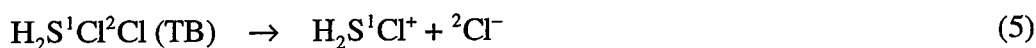
Table 6. Results of Ab initio MO Calculations for H_2SeX_n (X = Cl, Br) with 6-311++G(3df,2pd) Basis Sets at the MP2 Level

|	H_2Se	$H_2Se^1Cl•^a$	$H_2Se^1Cl^+$	$H_2SeCl_2(TB)$	$H_2Se^1Cl^2Cl$ (MC)	$H_2Se^1Br•^b$	$H_2Se^1Br^+$	$H_2SeBr_2(TB)$	$H_2Se^1Br^2Br$ (MC)
E (au)	-2401.1385	-2860.7964	-2860.5145	-3320.5261	-3320.5023	-4973.6472	-4973.3643	-7546.2113	-7546.2094
r(Se–H) (Å)	1.4591	1.4595	1.4758	1.4580	1.4598	1.4601	1.4749	1.4592	1.4603
r(Se–^{1}X) (Å)		2.5956	2.1049	2.3337	3.1784	2.8139	2.2744	2.5159	3.1908
r(^{1}X–^{2}X) (Å)					2.0052				2.3102
∠HSeH (deg)	91.27	91.91	92.10	95.16	91.30	91.63	92.02	94.24	91.36
∠HSe^{1}X (deg)		88.01	97.65	86.51	92.10	89.21	97.52	86.79	92.56
∠Se^{1}X^{2}X (deg)				169.65^c	180.80			170.56^c	180.65
Qn(Se)	-0.1072	0.2366	0.8296	0.8483	-0.0843	0.1280	0.6849	0.7185	-0.0666
Qn(H)	0.0536	0.0691	0.1219	0.0927	0.0594	0.0693	0.1271	0.1008	0.0627
Qn(H$_2$Se)		0.3748	1.0733	1.0338	0.0588	0.2666	0.9390	0.9200	0.0587
Qn(^{1}X)		-0.3748	-0.0733	-0.5169	0.0042	-0.2666	0.0610	-0.4600	0.0048
Qn(^{2}X)				-0.5169	-0.0388			-0.4600	-0.0635

[a] Spin densities: S(Se) 0.4563, S(H) -0.0268, S(^{1}Cl) 0.5973. [b] Spin densities: S(Se) 0.3219, S(H) -0.0241, S(^{1}Br) 0.7263. [c] ∠^{1}ClSe^{2}Cl for TB.

The above results are well explained by assuming that the $Z-^1X-^2X$ bonds in $H_2Z-^1X-^2X$ (MC) (Z = S, Se and X = Cl, Br) can be discussed by a 3c-4e model. The slightly less negative charge predicted on Z of H_2Z-X-X (MC), relative to that of H_2Z, is also explained by the 3c-4e hypervalent character of the $Z-^1X-^2X$ bonds, since the formation of the bonds is connected with an unavoidable CT from H_2Z to X_2 in the initial stage of the MC formation. The two electrons in one of the lone pair orbitals of Z extend over the $\sigma^*(^1X-^2X)$ orbital of the newly formed 3c-4e $Z-^1X-^2X$ bond. The expected development of negative charge on Z in the formation of H_2Z-X-X (MC) is canceled by the CT from Z to X_2 in the initial stage of the interaction. The 3c-4e character of the $Z-X-X$ bond in the MC was further examined through the investigation of some distance dependences.

Characters of CT in the Formation of H_2SCl_2 (TB and MC). Ab initio MO calculations were performed on $H_2S^1Cl^2Cl$ (TB) and $H_2S-^1Cl-^2Cl$ (MC) with different $r(S-^2Cl)$ and $r(^1Cl-^2Cl)$ values: $r(S-^2Cl) = r_o(S-^2Cl) + 0.1m$ Å and $r(^1Cl-^2Cl) = r_o(^1Cl-^2Cl) + 0.1m$ Å, where $r_o(S-^2Cl)$ and $r_o(^1Cl-^2Cl)$ are the optimized values for the TB and MC and $m = -1$, (0), 1, 2, 3.

$$H_2S^1Cl^2Cl \text{ (TB)} \rightarrow H_2S^1Cl^+ + {}^2Cl^- \qquad (5)$$
$$H_2S-^1Cl-^2Cl \text{ (MC)} \rightarrow H_2S^1Cl^+ + {}^2Cl^- \qquad (6)$$

From these calculations I obtain the character of the CT for the initial stage of the dissociation processes for the TB and MC, which corresponds to eqs 5 and 6, respectively. The process will produce $H_2S^1Cl^+$ and $^2Cl^-$, if it is assumed that the singlet multiplicity is conserved during the reaction. Figures 1 and 2 show the plots of Qn versus the bond lengths in the TB and MC, together with those for $H_2S^1Cl^+$ and $^2Cl^-$ (A). As seen from Figure 1, the Qn values of ^1Cl and ^2Cl in $H_2S^1Cl^2Cl$ (TB) are increased and decreased, respectively, whereas the values for S, H, and H_2S change only little with increasing $r(S-^2Cl)$. The main result in the case of the TB is a CT from ^1Cl to ^2Cl.[24]
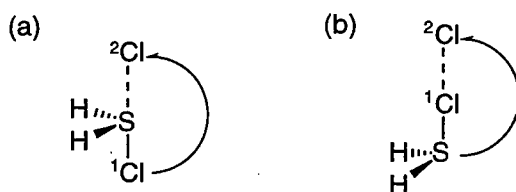
**Scheme 2. Characters of CT in the Heterolytic Dissociation of H_2SCl_2: (a) for TB and (b) for MC**

In the case of the MC (Figure 2), the Qn values of S and H_2S in $H_2S-^1Cl-^2Cl$ (MC) increase with increasing $r(^1Cl-^2Cl)$. The Qn value of ^2Cl decreases and that of ^1Cl is almost unchanged.

The ionic species, $H_2S^1Cl^+$ and $^2Cl^-$, are again produced at the end of this process if it is assumed that the singlet multiplicity is conserved during the reaction. The results demonstrate that the $S^{-1}Cl^{-2}Cl$ bond in $H_2S^{-1}Cl^{-2}Cl$ (MC) can be indeed analyzed by the 3c-4e model. The CT must be examined not by the nature of elements but by their positions (Scheme 2). The character of the CT in $H_2Se^{-1}Br^{-2}Br$ (MC) was found to be essentially the same as the one discussed for $H_2S^{-1}Cl^{-2}Cl$ (MC).
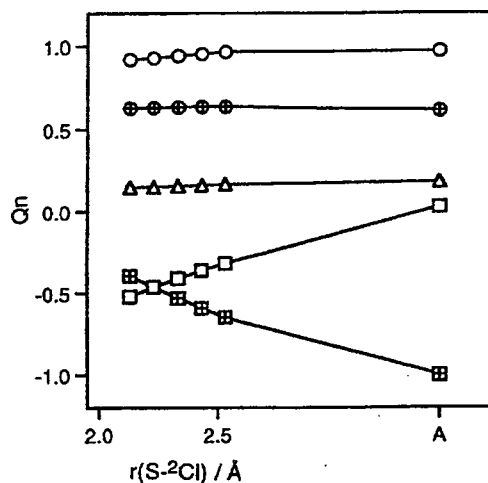
Figure 1. Plots of Qn in $H_2S^1Cl^2Cl$ (TB) against $r(S-^2Cl)$, together with those for $H_2S^1Cl^+$ and $^2Cl^-$ (A); $r_o(S-^2Cl) = 2.231$ Å; $\oplus$ stands for $Qn(S)$, O for $Qn(H_2S)$, $\triangle$ for $Qn(H)$, $\square$ for $Qn(^1Cl)$, and $\boxplus$ for $Qn(^2Cl)$.
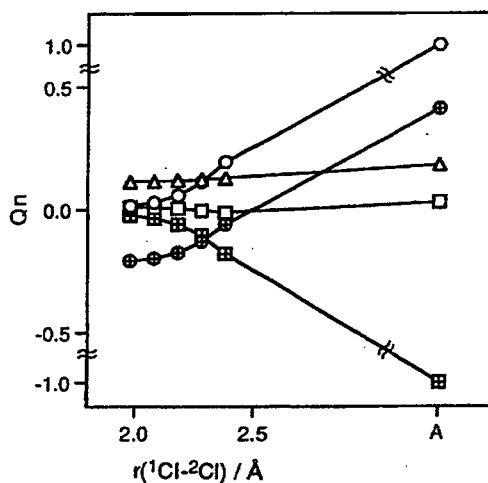
Figure 2. Plots of Qn in $H_2S-^1Cl-^2Cl$ (MC) against $r(^1Cl-^2Cl)$, together with those for $H_2S^1Cl^+$ and $^2Cl^-$ (A); $r_o(^1Cl-^2Cl)$ = 2.001 Å; $\oplus$ stands for $Qn(S)$, O for $Qn(H_2S)$, $\triangle$ for $Qn(H)$, $\square$ for $Qn(^1Cl)$, and $\boxplus$ for $Qn(^2Cl)$.

Molecular Orbitals Constructing the 3c-4e Bond of Z–X–X in MC. Molecular orbitals were calculated for H_2SeBr_2 (MC) with the 3-21G$^{(*)}$ basis sets of the MacSpartan program,[25] using the structure optimized with the 6-311++G(3df,2pd) basis sets at the B3LYP level. The overlap between the $\sigma^*(Br-Br)$ and the $n(p_z)$ of H_2Se decreases dramatically as $r(Se,Br)$

becomes larger, which affects significantly the shapes of ψ_2 and ψ_3. Since the shortest r(Se,Br) value was predicted at the B#LYP level (Table 4), this structure was employed to depict the orbitals, although the real value might be even shorter than the predicted one. Figure 3 shows the energy diagram for the formation of H_2SeBr_2 (MC), together with the molecular orbitals ψ_1, ψ_1', ψ_2, and ψ_3 in H_2SeBr_2 (MC), the $n(p_z)$ and ψ_a of H_2Se, and the σ and σ^* of Br_2. The orbitals ψ_1, ψ_2, and ψ_3, result mainly from the $n(p_z)$ of H_2Se and the σ and σ^* of Br_2 while the contribution from ψ_a is large in ψ_1'. The orbitals ψ_2 and ψ_3 of H_2SeBr_2 (MC) are HOMO and LUMO which again supports the 3c-4e interpretation of the Se-Br-Br bond, according to the redefinition proposed by Martin et al.[2c]
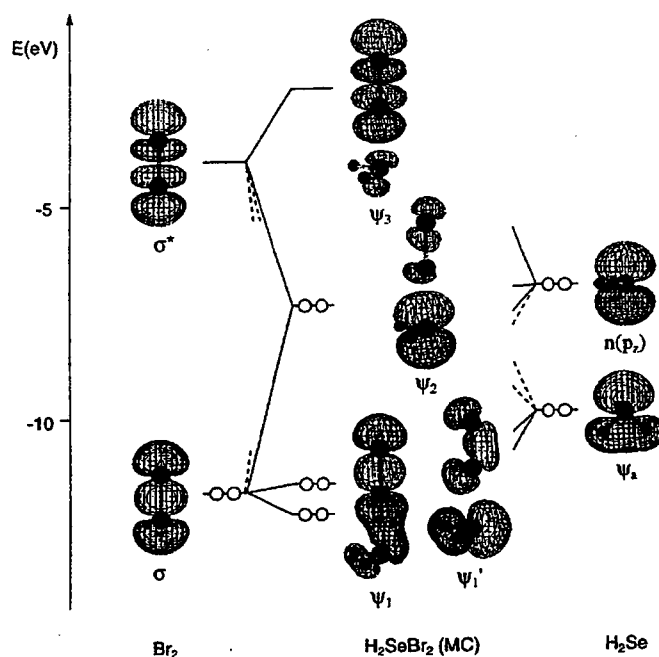
Figure 3. Energy diagram in the formation of the 3c-4e bond (ψ_1, ψ_1', ψ_2, and ψ_3) in H_2SeBr_2 (MC) from the $n(p_z)$ and ψ_a of H_2Se and the σ and σ^* of Br_2.

Bond Orders for Z–X–X in MC and for X–Z–X in TB. The 3c-4e character of the bonding in the investigated MC was further examined by calculating bond orders from observed bond lengths of TB and MC adducts using Pauling's equation[26] (eq 7). $D(n)$ and $D(1)$ represent the bond distances where the bond orders are n (< 1) and 1, respectively. Table 7 shows the results. The bond orders between the adjacent atoms in the 3c-4e bond are expected to be in the order of 0.5 because the ψ_2 orbital is usually nonbonding. The Z–X–X bond is well described by the 3c-4e model if the two bond orders in Z–X–X are close to each other.

$$D(n) = D(1) - 0.60 \log n \qquad (7)$$

Table 7. Bond Lengths and Bond Orders in Some TB and MC[a]

Compound	TB/MC	∠XZX (deg) ∠ZXX' (deg)	$r(Z–X)$ (Å) $r(X–X')$ (Å)	Σr_{co} (Å) Σr_{co} (Å)	$r_{obs} - \Sigma r_{co}$ (Å) $r_{obs} - \Sigma r_{co}$ (Å)	n n	ref
F_2SF_2	TB	186.9	1.646	1.68	-0.034	1.14	b
$(CF_3)_2SF_2$	TB	186.1	1.681	1.68	0.001	1.00	c
$(Me_2N)_2SF_2$	TB	174.7	1.770	1.68	0.09	0.71	d
$(4\text{-}ClC_6H_4)_2SCl_2$	TB	174.5	2.259	2.03	0.229	0.42	e
			2.323	2.03	0.293	0.32 (av.0.37)	
Ph_2SeCl_2	TB	180	2.30	2.16	0.14	0.58	f
$(4\text{-}MeC_6H_4)_2SeCl_2$	TB	177.5	2.38	2.16	0.22	0.43	g
$S(CH_2CH_2)_2SeBr_2$	TB	184.9	2.547	2.31	0.237	0.40	h
Ph_2SeBr_2	TB	180	2.52	2.31	0.21	0.45	f
$(4\text{-}MeC_6H_4)_2SeBr_2$	TB	177	2.55	2.31	0.24	0.40	g
Me_2TeCl_2	TB	172.44	2.488	2.36	0.128	0.61	i
			2.541	2.36	0.181	0.50 (av.0.56)	
Ph_2TeBr_2	TB	178	2.682	2.51	0.172	0.52	j
$(4\text{-}ClC_6H_4)_2TeI_2$	TB	173.5	2.922	2.70	0.222	0.43	k
			2.947	2.70	0.247	0.39 (av.0.41)	
$1,2\text{-}C_6H_4(CH_2)_2TeI_2$	TB	176.53	2.900	2.70	0.200	0.46	k
			2.928	2.70	0.228	0.42 (av.0.44)	
$C_4H_8O_2Cl_2$	MC		2.67	1.65	1.02	0.02	l
		178	*2.02*	*1.98*	*0.04*	*0.86*	
$C_4H_4O_2Br_2$	MC		2.71	1.80	0.91	0.03	m
		180	*2.31*	*2.28*	*0.03*	*0.89*	
ArEtSBr_2	MC	2.81	2.18	0.63	0.09	n	
		m	*2.41*	*2.28*	*0.13*	*0.61*	
$(CH_2)_4SBr_2$	MC		2.321	2.18	0.141	0.58	o
		182	*2.724*	*2.28*	*0.444*	*0.18*	
$I_2S(CH_2CH_2)_2SI_2$	MC		2.867	2.37	0.497	0.15	p
		177.9	*2.787*	*2.66*	*0.127*	*0.61*	
$(PhCH_2)_2SI_2$	MC		2.78	2.37	0.41	0.21	q
		179	*2.819*	*2.66*	*0.159*	*0.54*	
$BrIS(CH_2CH_2)_2SIBr$	MC		2.687	2.37	0.317	0.30	r
		178.2	*2.646*	*2.47*	*0.176*	*0.51*	
$(CH_2)_4SeI_2$	MC		2.762	2.50	0.262	0.37	s

		180.6	*2.914*	*2.66*	*0.254*	*0.38*
O(CH$_2$CH$_2$)$_2$SeI$_2$	MC		2.755	2.50	0.255	0.38	*t*
		185.2	*2.956*	*2.66*	*0.296*	*0.32*
I$_2$Se(CH$_2$CH$_2$)$_2$SeI$_2$	MC		2.829	2.50	0.329	0.28	*u*
		180.0	*2.870*	*2.66*	*0.21*	*0.45*
O(CH$_2$CH$_2$)$_2$SeICl	MC		2.63	2.50	0.13	0.61	*v*
		184.2	*2.73*	*2.32*	*0.41*	*0.21*
Me$_3$NI$_2$	MC		2.27	2.03	0.24	0.40	*w*
		179	*2.83*	*2.66*	*0.17*	*0.52*
Me$_3$NICl	MC		2.30	2.03	0.27	0.35	*x*
		180	*2.52*	*2.32*	*0.20*	*0.46*
Ph$_3$PI$_2$	MC		2.481	2.43	0.051	0.82	*y*
		178.22	*3.161*	*2.66*	*0.501*	*0.15*

[a] Italic number shows data around the X–X' bond in MC. [b] Ref. 28. [c] Ref. 29. [d] Ref. 30. [e] Ref. 3a. [f] Ref. 31. [g] Ref. 32. [h] Ref. 33. [i] Ref. 34. [j] Ref. 35. [k] Ref. 36. [l] Ref. 19. [m] Ref. 37. [n] Ref. 20: ∠SBrBr being not given. [o] Ref. 21. [p] Ref. 38. [q] Ref. 39. [r] Ref. 40. [s] Ref. 41. [t] Ref. 42. [u] Ref. 43. [v] Ref. 7. [w] Ref. 44. [x] Ref. 45. [y] Ref. 6b.

Before I discuss the bond orders of Z–X–X in the MC, I first deal with those in the TB. The bond orders between S and F (n(S,F))[27] in R$_2$SF$_2$ (TB)[28-30] were found to be 1.14 – 0.71, depending on the electronegativity of the equatorial ligands. The value of n(S,Cl) for (4-ClC$_6$H$_4$)$_2$SCl$_2$[3a] is 0.37 on the average. The n(Se,X) values for R$_2$SeX$_2$ (X=Cl, Br)[31-33] are in the range 0.58 - 0.40 and n(Te,X) for R$_2$TeX$_2$ (X=Cl, Br, I)[34-36] lie between 0.61 and 0.39. The two bond orders for the essentially symmetric X–Z–X group differ up to 0.1, which is attributed to the crystal packing effect.

The n(O,X) and n(X,X) values in O(CH$_2$CH$_2$)$_2$OX$_2$ (X = Cl,[19] Br[37]) are in the ranges 0.02 - 0.03 and 0.86 – 0.89, respectively. The n(S,I) values of sulfide diiodides[38,39] lie between 0.15 – 0.21, and their n(I,I)) values between 0.54 – 0.61 and the (n(S,I), n(I,Br)) for BrIS(CH$_2$CH$_2$)$_2$SIBr[40] is (0.30, 0.51). The values for n(Se,I) and n(I,I)) of selenide diiodides[41-43] are in the ranges 0.28 – 0.38 and 0.37 – 0.45, respectively. The bond orders for the selenide diiodides are in the same range as for other TB adducts of selenides and tellurides and the n(Se,I) and n(I,I) values are close with each other. Therefore, the selenide diiodides are well described by the 3c-4e model. The bonds in sulfide diiodides have to be described by a somewhat unsymmetric 3c-4e model, due to the substantially smaller n(S,I) values compared to those of n(I,I). The S–I–Br bond in BrIS(CH$_2$CH$_2$)$_2$SIBr is understood in a similar way. The chlorine and bromine

adducts of the ether are described by the weak n→σ* CT model. Nevertheless, I prefer to describe the O---X–X bonds by the unsymmetrical 3c-4e model, too.

The S–Br–Br bonds in 1,2,4,5-tetrakis(ethylthio)benzene tetrabromide[20] and in $(CH_2)_4SBr_2$[21] are also described as the unsymmetrical 3c-4e model, with an ionic character of S^+–Br---Br⁻ for the latter. The Se–I–Cl bonds in $O(CH_2CH_2)_2SeICl$[7] and the P–I–I bond in Ph_3PI_2[6b] can also be viewed as the unsymmetrical 3c-4e bonds with a stronger Z–¹X bond. The N–I–I bond in Me_3NI_2[44] and the N–I–Cl bond in Me_3NICl[45] are typical 3c-4e bonds judging from the calculated bond orders.

Conclusion

It is proposed that the Z–X–X bond in R_2Z–X–X (MC), such as halogen adducts of selenides or sulfides, can be described by the 3c-4e model. The 3c-4e description of the Z–X–X bonds in MC makes it easier to understand the character of the bonding in these systems by comparison with the X–Z–X bonds in TB, which has been extensively investigated and well characterized so far. The comparison is achieved by changing the central atom Z in X–Z–X with the terminal atom X in Z–X–X, although the electronegativity of Z and X must be carefully taken into account.

Experimental Section

Chemicals were used without further purification unless otherwise noted. Solvents were purified by standard methods. Boiling points were uncorrected. ¹H, ¹³C, and ⁷⁷Se NMR spectra were measured at 400, 100, and 76 MHz, respectively. The ¹H, ¹³C, and ⁷⁷Se chemical shifts are given in ppm relative to those of internal $CHCl_3$ slightly contaminated in the solution (or TMS), $CDCl_3$ as the solvent, and external MeSeMe, respectively. Column chromatography was performed on silica gel (Fujidebison BW-300). Acidic alumina and basic alumina (E. Merck) were also used on silica gel, if necessary.

1-Selena-4-oxane (1) was prepared according to the literature.[7,46] The crude product after a usual workup was distilled to give **1** in 55 % yield as a colorless oil, bp 167.5 – 168.0 °C. lit.[46] bp 167.5 – 168.5 °C. ¹H NMR ($CDCl_3$, 400 MHz) 2.55 – 2.80 (m, 4H), 3.92 – 4.17 (m, 4H); ¹³C NMR ($CDCl_3$, 100 MHz) 17.18, 69.54.

Iodine monochloride was prepared by distillation under reduced pressure after stirring the mixture of iodine and chlorine. It gave 72 % yield as a black oil, bp 98.0 – 99.5 °C. lit.[47] bp 94.7 –102 °C. Iodine monobromide was used as the equimolar mixture of bromine and iodine in carbon tetrachloride.

MO Calculations. Ab initio MO calculations were performed on a Power Challenge L computer with the Gaussian 94 program.[16] The 6-311++G(3df,2pd) basis sets at the MP2 level were mainly applied on the TB and MC structures of H_2ZX_2, H_2Z, and H_2ZX^+ (Z = S, Se and X =

Cl, Br) and the UMP2 formalism with the 6-311++G(3df,2pd) basis sets was used for the corresponding radicals, $H_2ZX\bullet$,[17] supposing doublet spin multiplicity. Calculations were also carried out for $H_2O–Cl–Cl$ (MC), H_2SCl_2 (TB and MC), and $H_2S–Br–Br$ (MC) using various basis sets with or without application of MP2 and/or DFT (B3LYP) methods. The molecular orbitals shown in Figure 3 were obtained with the MacSpartan program[25] and the 3-21G$^{(*)}$ basis sets using the optimized geometry from the B3LYP/6-311++G(3df,2pd) calculations.

References and Notes

(1) Mulliken, R. S. *J. Am. Chem. Soc.* **1950**, *72*, 600; Mulliken, R. S. *J. Am. Chem. Soc.* **1952**, *74*, 811.

(2) (a) Pimentel, G. C. *J. Chem. Phys.* **1951**, *19*, 446. Musher, J. I. *Angew. Chem., Int. Ed. Engl.* **1969**, *8*, 54. (b) Chen, M. M. L.; Hoffmann, R. *J. Am. Chem. Soc.* **1976**, *98*, 1647. (c) Cahill, P. A.; Dykstra, C. E.; Martin, J. C. *J. Am. Chem. Soc.* **1985**, *107*, 6359.

(3) (a) Baenziger, M. C.; Buckles, R. E.; Maner, R. J.; Simpson, T. D. *J. Am. Chem. Soc.* **1969**, *91*, 5749. (b) Klayman, D. L.; Günther, W. H. H. *Organic Selenium Compounds: Their Chemistry and Biology*; Wiley: New York, 1973; Chapter XV. (c) Perkins, C. W.; Martin, J. C.; Arduengo, A. J.; Lau, W.; Alegria, A.; Kochi, J. K. *J. Am. Chem. Soc.* **1980**, *102*, 7753. (d) Hayes, R. A.; Martin, J. C. *Sulfurane Chemistry* in *Organic Sulfur Chemistry: Theoretical and Experimental Advances*; Bernardi, F., Csizmadia, I. G., Mangini, A., Eds.; Elsevier: Amsterdam, 1985. See also refs cited therein.

(4) (a) Nakanishi, W.; Hayashi, S.; Tukada, H.; Iwamura, H. *J. Phys. Org. Chem.* **1990**, *3*, 358. (b) Nakanishi, W.; Yamamoto, Y.; Hayashi, S.; Tukada, H.; Iwamura, H. *J. Phys. Org. Chem.* **1990**, *3*, 369. (c) Nakanishi, W.; Hayashi, S.; Nakamura, Y.; Iwamura, H. *Chem. Lett.* **1992**, 735; Nakanishi, W.; Sakamoto, K.; Isaka, K.; Hayashi, S. *Phosphorus, Sulfur, and Silicon* **1992**, *67*, 79.

(5) The electronegativity proposed by Allred-Rochow was employed to discuss the structure of the adducts. See, Allred, A. L.; Rochow, E. G. *J. Inorg. Nucl. Chem.* **1958**, *5*, 264. Allred, A. L.; Rochow, E. G. *J. Inorg. Nucl. Chem.* **1958**, *5*, 269.

(6) (a) Bricklebank, N.; Godfrey, S. M.; McAuliffe, C. A.; Mackie, A. G.; Pritchard, R. G. *J. Chem. Soc., Chem. Commun.* **1992**, 355. (b) Godfrey, S. M.; Kelly, D. G.; McAuliffe, C. A.; Mackie, A. G.; Pritchard, R. G.; Watson, S. M. *J. Chem. Soc., Chem. Commun.* **1991**, 1163. (c) Bricklebank, N.; Godfrey, S. M.; McAuliffe, C. A.; Pritchard, R. G. *J. Chem. Soc., Dalton*

Trans. **1993**, 2261. See also, Bricklebank, N.; Godfrey, S. M.; Mackie, A. G.; McAuliffe, C. A.; R. G.; Pritchard, Kobryn, P. J. *J. Chem. Soc., Dalton Trans.* **1993**, 101.

(7) Knobler, C.; McCullough, J. D. *Inorg. Chem.* **1968**, *7*, 365.

(8) Nakanishi, W.; Hayashi, S. *Chem. Lett.* **1995**, 75.

(9) (a) Asmus, K.-D. *Acc. Chem. Res.* **1979**, *12*, 436. Musker, W. K. *Acc. Chem. Res.* **1980**, *13*, 200. (b) Fujihara, H.; Furukawa, N. *J. Mol. Struct. (THEOCHEM)* **1989**, *186*, 261.

(10) Yamamoto, Y.; Chen, X.; Kojima, S.; Ohdoi, K.; Kitano, M.; Doi, Y.; Akiba, K.-y. *J. Am. Chem. Soc.* **1995**, *117*, 3922. Fujihara, H.; Mima, H.; Erata, T.; Furukawa, N. *J. Am. Chem. Soc.* **1993**, *115*, 9826. Fujihara, H.; Chiu, J.-J.; Furukawa, N. *J. Am. Chem. Soc.* **1988**, *110*, 1280.

(11) Nakanishi, W.; Hayashi, S.; Toyota, S. *J. Chem. Soc., Chem. Comm.* **1996**, 371. Alvarez, S.; Mota, F.; Novoa, J. *J. Am. Chem. Soc.* **1987**, *109*, 6586.

(12) Dixon, D. A.; Arduengo, A. J. III, *Inorg. Chem.* **1990**, *29*, 970; Blake, A. J.; Lippolis, V.; Parsons, S.; Schröder, M. *J. Chem. Soc., Chem. Comm.* **1996**, 2207; Cotton, F. A.; Kibala, P. A. *J. Am. Chem. Soc.* **1987**, *109*, 3308.

(13) Dahl, T.; Røeggen, I. *J. Am. Chem. Soc.* **1996**, *118*, 4152. The calculated r(O–Cl) distance of H_2O–Cl–Cl (MC) was reported to be 0.15 Å longer than that observed in a chlorine adduct of dioxane.[19]

(14) Røeggen, I.; Dahl, T. *J. Am. Chem. Soc.* **1992**, *114*, 511.

(15) Further investigations were carried out on the selenides with and without the halogens (and/or interhalogens) in various ratios. Details will be reported elsewhere.

(16) *Gaussian 94, Revision D.4*; Frisch, M. J.; Trucks, G. W.; Schlegel, H. B.; Gill, P. M. W.; Johnson, B. G.; Robb, M. A.; Cheeseman, J. R.; Keith, T.; Petersson, G. A.; Montgomery, J. A.; Raghavachari, K.; Al-Laham, M. A.; Zakrzewski, V. G.; Ortiz, J. V.; Foresman, J. B.; Cioslowski, J.; Stefanov, B. B.; Nanayakkara, A.; Challacombe, M.; Peng, C. Y.; Ayala, P. Y.; Chen, W.; Wong, M. W.; Andres, J. L.; Replogle, E. S.; Gomperts, R.; Martin, R. L.; Fox, D. J.; Binkley, J. S.; Defrees, D. J.; Baker, J.; Stewart, J. P.; Head-Gordon, M.; Gonzalez, C.; Pople, J. A. Gaussian, Inc., Pittsburgh, PA, 1995.

(17) Calculations for radical species see, (a) Kobayashi, T.; Matsuzawa, H.; Iwata, S. *Bull. Chem. Soc. Jpn.* **1994**, *67*, 3172. (b) Takane, S.; Fueno, T. *Bull. Chem. Soc. Jpn.* **1993**, *66*, 3633.

(18) Ab initio MO calculations, that take into account electron correlation by using MP2 and DFT (B3LYP) methods, predicted much shorter distances between S and Cl (r(S–Cl)) for H_2S–Cl–Cl (MC), relative to the HF level, which reflects the complex interaction between S and

Cl atoms in the MC. The r(S–Cl) for H_2S–Cl–Cl (MC) with the 6-311++G(3df,2pd) basis sets at the HF level was predicted to be 3.7538 Å, for example.

(19) Hassel, O.; Stroϕmme, K. O. *Acta Chem. Scand.* **1959**, *13*, 1775.

(20) Bock, H.; Havlas, Z.; Rauschenbach, A.; Näther, C.; Kleine, M. *Chem. Commun.* **1996**, 1529.

(21) Allegra, G.; Wilson, Jr., G. E.; Benedetti, E.; Pedone, C.; Allbert, R. *J. Am. Chem. Soc.* **1970**, *92*, 4002.

(22) NBO Ver. 3.1, Glendening, E. D.; Reed, A. E.; Carpenter, J. E.; Weinhold, F.

(23) The reason must be very complex. The character of CT in the 3c-4e bond seems to be more typical for X = Cl than for X = Br. Further investigations are necessary as the predicted charges also depend on the optimized structures (see also Figure 2).

(24) The (Qn(C), Qn(H), Qn(Cl)) values for CH_3Cl and CH_2Cl_2 were calculated to be (–0.4538, 0.1816, –0.0910) and (–0.3093, 0.1890, –0.0344), respectively, with the MP2/6-311++G(3df,2pd) method. The values for CH_3^+ and CH_2Cl^+ were calculated to be (0.4205, 0.1932, no Cl atom) and (0.1644, 0.2283, 0.3792), respectively, based on the same method. The (Qn(C), Qn(H), Qn(^{1}Cl), Qn(^{2}Cl)) values were found to be (–0.2747, 0.1901, –0.0207, –0.0846) for $CH_2^1Cl^2Cl$, if the calculations were performed with a C–Cl bond length 0.1 Å longer than the optimized value. The calculated CT mainly occurs from C to Cl, if the dissociation proceeds from CH_2XCl to CH_2X^+ (X = H or Cl) and Cl. In this case the character of CT corresponds to the 2c-2e model.

(25) MacSpartan Plus Ver. 1.0, Hehre, H.J. *Wavefunction Inc.*

(26) (a) Pauling, L. *J. Am. Chem. Soc.* **1947**, *69*, 542. (b) Pauling, L. *The Nature of the Chemical Bond*, 3rd ed.; Cornell University Press: Ithaca, New York, 1960; Chapter 7.

(27) Although some r(S–F) values for R_2SF_2 are not larger than the sum of covalent radii of S and F, eq 7 is applied to evaluate the bond orders.

(28) Stone, R. G.; Tigelaar, H. L.; Flygare, W. H.; *J. Chem. Phys.* **1970**, *53*, 3947.

(29) Oberhammer, H.; Kumar, R. C.; Knerr, G. D.; Shreeve, J. M. *Inorg. Chem.* **1981**, *20*, 3871.

(30) Cowley, A. H.; Riley, P. E.; Szobota, J. S.; Walker, M. L. *J. Am. Chem. Soc.* **1979**, *101*, 5620.

(31) McCullough, J. D.; Hamburger, G. *J. Am. Chem. Soc.* **1942**, *64*, 508; McCullough, J. D.; Hamburger, G. *J. Am. Chem. Soc.* **1941**, *63*, 803.

(32) McCullough, J. D.; Marsh, R. E. *Acta Cryst.* **1950**, *3*, 41.

(33) Battelle, L.; Knobler, C.; McCullough, J. D. *Inorg. Chem.* **1967**, *6*, 958.

(34) Ziolo, R. F.; Troup, J. M. *J. Am. Chem. Soc.* **1983**, *105*, 229.

(35) Christofferson, G. D.; McCullough, J. D. *Acta Cryst.* **1958**, *11*, 239.

(36) Chao, G. Y.; McCullough, J. D. *Acta Cryst.* **1962**, *15*, 887; Knobler, C.; Ziolo, R. F. *J. Organomet. Chem.* **1979**, *178*, 423.

(37) Hassel, O.; Hvoslef, J. *Acta Chem. Scand.* **1954**, *8*, 873.

(38) Chao, G. Y.; McCullough, J. D. *Acta Cryst.* **1960**, *13*, 727.

(39) Rømming, C. *Acta Chem. Scand.* **1960**, *14*, 2145.

(40) Knobler, C.; Baker, C; Hope, H.; McCullough, J. D. *Inorg. Chem.* **1971**, *10*, 697.

(41) Hope, H.; McCullough, J. D. *Acta Cryst.* **1964**, *17*, 712.

(42) Maddox, H.; McCullough, J. D. *Inorg. Chem.* **1966**, *5*, 522.

(43) Chao, G. Y.; McCullough, J. D. *Acta Cryst.* **1961**, *14*, 940.

(44) Strømme, K. O. *Acta Chem. Scand.* **1959**, *13*, 268.

(45) Hassel, O.; Hope, H. *Acta Chem. Scand.* **1960**, *14*, 391.

(46) Gibson, C. S.; Johnson, J. D.A. *J. Chem. Soc.* **1931**, 266.

(47) Buckles, R. E.; Bader, J. M. *Inorg. Syntheses* **1967**, *9*, 130.

Chapter 3.

Attractive Interaction Caused by the Linear F---Se–C Alignment in Naphthalene Peri Positions

Abstract:

The X-ray crystallographic analysis of 8-fluoro-1-(p-anisylselanyl)naphthalene (**1**) revealed that the F and Se atoms and the *ipso*-carbon of the *p*-anisyl group (C(An)) aligned linearly. The F atom and the Se–C(An) bond lay on the naphthyl plane: the nonbonded distance between F and Se atoms was 2.753(3) Å and the FSeC(An) angle was 175.0(1)°. Ab initio MO calculations with the 6-311++G(3df,2pd) basis sets performed on the model compound of **1**, HF---SeH$_2$, where the aryl groups of **1** are replaced by hydrogens. The calculations exhibit that the energy minimum is achieved when the F, Se, and C(An) atoms aligne linearly. Charge transfer in the formation of HF---SeH$_2$ was suggested to occur from F to SeH$_2$ on the basis of the natural population analysis, which supported the np$_x$(F)–σ*(Se–C(An)) interaction.

Introduction

Nonbonded interactions between heteroatoms containing group 16 elements in naphthalene-1,8-positions are of current interest.[1] We have also been interested in the nonbonded interaction between a fluorine atom with a small size of the valence orbitals and other hetero atoms in proximity in space, such as a selenium atom. Lone pair-lone pair interactions have been elucidated to play an important role in the nonbonded spin–spin couplings between fluorine–fluorine,[2] fluorine–nitrogen,[3] and selenium–selenium[1d,g,4] atoms. Electrostatic[5a] and charge-transfer[5b] mechanisms were proposed to explain the attractive interactions between oxygen and selenium atoms in close proximity, together with the downfield shifts of the ^{77}Se NMR chemical shifts by the neighboring oxygen, but they are controversial.


1 (X = F)
3 (X = H)

2 (X = F)
4 (X = H)
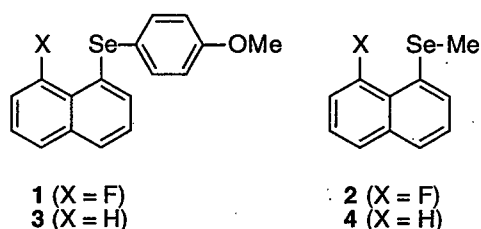
In the course of our investigation on the intramolecular interactions between naphthalene peri positions containing the selenium atom(s) were prepared 8-fluoro-1-(p-anisylselanyl)naphthalene (1) and 8-fluoro-1-(methylselanyl)naphthalene (2). The ^{77}Se NMR chemical shifts of 1 and 2 were observed at much downfield (ca. 90 ppm) relative to those of 1-(p-anisylselanyl)naphthalene (3) and 1-(methylselanyl)naphthalene (4), respectively.[6] It is puzzling how the fluorine atom at the 8-position in 1 and 2 causes such large downfield shifts. The selenium atom in 1 is expected to be electron-rich due to the p-methoxyl group, which would be disadvantageous for the electrostatic mechanism, since the mechanism requires the positive charge development at the Se atom.[5a] It is very interesting if the fluorine atom interacts attractively with the selenium atom or the Se–C(An) bond (the bond between the selenium atom and the ipso-carbon atom of the p-anisyl group) in 1 by the through-space mechanism irrespective of its small size of the valence orbitals. In this chapter, I report the structure of 1 studied by the X-ray crystallographic analysis and by the ab initio molecular orbital calculations, exhibiting the linear alignment of the F---Se–C(An) atoms with the analysis of the charge-transfer[5b] mechanism for the interaction.

Results and Discussion

Single crystals of 1 were obtained via slow evaporation of a hexane solution and one of suitable crystals was subjected to X-ray crystallographic analysis. The crystallographic data are collected in Table 1. There are two types of structures of 1 in the crystal (structure A and structure

B). The selected interatomic distances, angles, and torsional angles of structure **A** and structure **B** are shown in Table 2. One of the structures of **1** (structure **A**) is shown in Figure 1.[7] For structure **A**, the planarity of the naphthyl and anisyl planes was very good. The anisyl plane was perpendicular to the naphthyl plane (the torsional angle C(1)SeC(11)C(16) being 89.0(4)°). The fluorine atom and the Se–C(An) bond lay on the naphthyl plane: the torsional angles of FC(9)C(10)C(1), SeC(1)C(10)C(9), and C(11)SeC(1)C(10) were 1.2(6)°, -0.1(5)°, and -179.2(3)°, respectively. The FSeC(An) angle in the naphthyl plane ($\angle$FSeC(An)) was 175.0(1)°. The nonbonded distance between F and Se atoms (r(F,Se)) was 2.753(3) Å, which was shorter than the sum of the van der Waals radii[8] of F and Se atoms (3.35 Å) by 0.60 Å.
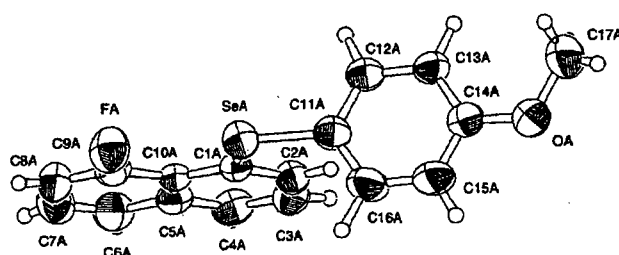
Figure 1. ORTEP drawing of **1** (structure **A**).

Table 1. Selected Crystal Data and Structure Refinement for **1**

formula	$C_{17}H_{13}FOSe$
fw, g mol^{-1}	331.25
cryst syst	triclinic
space group	*P-1(#2)*
color	colorless
a, Å	13.649(7)
b, Å	14.068(8)
c, Å	8.184(5)
α, deg	93.06(5)
β, deg	100.20(5)
γ, deg	68.21(4)
V, Å^3	1436(1)
D_{calcd}, g cm^{-3}	1.532
Z	4
θ range for data collected, deg	2.0 – 27.5
data	4292
parameter	362
R	0.045
Rw	0.044
GOF	1.4291

**Table 2. Selected Interatomic Distances (Å), Angles (deg), and Torsional Angles (deg) of 1**

structure A		structure B	
Interatomic Distances			
SeA–C1A	1.928(4)	SeB–C1B	1.932(4)
SeA–C11A	1.918(4)	SeB–C11B	1.906(4)
FA–C9A	1.352(5)	FB–C9B	1.346(6)
SeA–FA	2.753(3)	SeB–FB	2.744(3)
C1A–C10A	1.422(5)	C1B–C10B	1.427(5)
C9A–C10A	1.412(5)	C9B–C10B	1.409(6)
Angles			
C1A–SeA–C11A	100.8(2)	C1B–SeB–C11B	99.6(2)
SeA–C1A–C10A	120.5(3)	SeB–C1B–C10B	120.7(3)
FA–C9A–C10A	119.1(3)	FB–C9B–C10B	118.7(4)
C1A–C10A–C9A	125.9(3)	C1B–C10B–C9B	125.6(4)
FA–SeA–C11A	175.0(1)	FB–SeB–C11B	164.3(1)
Torsional Angles			
C11A–SeA–C1A–C10A	-179.2(3)	C11B–SeB–C1B–C10B	-162.8(3)
C1A–SeA–C11A–C16A	89.0(4)	C1B–SeB–C11B–C16B	-110.5(4)
SeA–C1A–C10A–C9A	-0.1(5)	SeB–C1B–C10B–C9B	-0.9(6)
FA–C9A–C10A–C1A	1.2(6)	FB–C9B–C10B–C1B	-3.7(6)

Why do the fluorine, selenium, and carbon atoms align linearly? Since the π-orbitals in naphthalene ring, together with p-type lone pairs of F and Se atoms, are perpendicular to those of the anisyl ring, the interaction between the two π-systems would be negligible. Two types of interactions are possible: one is the interaction of the π-framework of naphthalene ring cooperated by the p-type orbitals of fluorine and selenium atoms and the other is the n(F)–σ*(Se–C(An)) type interaction, which is strongly suggested by the linear alignment of the F---Se–C(An) atoms in 1.[9,10]

The n(F)–σ*(Se–C(An)) type interaction is examined first. Ab initio molecular orbital calculations were performed on the model compound of 1, HF---SeH$_a$H$_b$, to elucidate the nature of the nonbonded interaction between the atoms: the aryl groups in 1 are replaced by hydrogens in the model compound and H$_a$ and H$_b$ denote the hydrogens near HF and far from HF, respectively (Scheme 1). The 6-311++G(3df,2pd) basis sets of the Gaussian 94[11] program at HF and MP2 levels were employed for the calculations. Calculations were carried out for the two structures. For structure a: all atoms are placed on the xz-plane and the Se atom is placed at the origin. The angle

θ_1 is defined as the sum of the angles between F–Se bond and the y-axis and between y-axis and Se–H$_b$ bond (namely, θ_1 is equal to the torsional angle HH$_a$SeH$_b$), which is therefore fixed at 180.0°. The $\angle$HFSe, $\angle$FSeHb (θ_2; θ_2 is defined as 360.0 - ($\angle$FSeH$_a$ + $\angle$H$_a$SeH$_b$)° when θ_1 is not 180.0°), and $\angle$H$_a$SeH$_b$ in HF---SeH$_a$H$_b$ are fixed at 100.0°, 185.0°, and 100.8°, respectively. The r(F,Se) value is fixed at 2.753 Å and r(F,H), r(Se,H$_a$), and r(Se,H$_b$) are optimized (Scheme 1a). For structure **b**: all atoms are placed on the xz-plane except for H$_b$ and the Se atom is placed at the origin. The $\angle$HFSe, $\angle$FSeH$_a$, and the torsional angle HFSeH$_a$ in HF---SeH$_a$H$_b$ are fixed at 90.0°, 90.0°, and 0.0°, respectively, while θ_1 and θ_2 (and therefore $\angle$H$_a$SeH$_b$) are optimized. The r(F,Se) value is fixed at 2.753 Å, and r(F,H), r(Se,H$_a$), and r(Se,H$_b$) are optimized (Scheme 1b). Calculations on HF and SeH$_2$ were also performed similarly for convenience of comparison.

Scheme 1
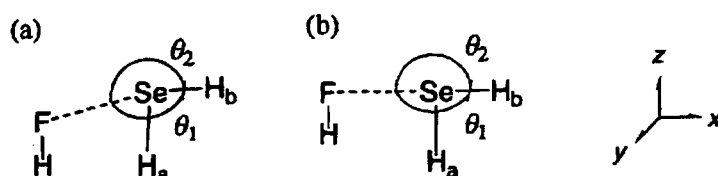
The results of the MO calculations on structure **a** at the HF and MP2 levels with the 6-311++G(3df,2pd) basis sets are shown in Table 3. The MO calculations were performed with variously fixed θ_1 for structure **b** at the MP2/6-311++G(3df,2pd) level, and two energy minima existed. The one corresponds to structure **b** with $\theta_1 = 180.0°$[12,13] and the other to structure **b** with $\theta_1 = 65.4°$. The energy of the adduct was plotted against θ_1 and the results are shown in Figure 2. Structure **b** with $\theta_1 = 180.0°$ was shown to be more stable than structure **b** with $\theta_1 = 65.4°$ by 0.0073 au (19 kJ mol⁻¹). The results, together with those at the HF level, are also shown in Table 3. Structure **b** with $\theta_1 = 65.4°$ brought out the importance of the linear F---Se–H$_b$ interaction in structure **b** with $\theta_1 = 180.0°$. The bond distances, especially r(Se,H$_b$), of structure **b** with $\theta_1 = 180.0°$ became longer and the bond angle of the adduct became smaller relative to the corresponding values of the free components whereas those of structure **b** with $\theta_1 = 65.4°$ were close to those of the components. Both of the r(Se,H$_a$) and r(Se,H$_b$) values of structure **b** with $\theta_1 = 180.0°$ increased, whereas only r(Se,H$_b$) was increased in structure **a** in the formation of the adduct. The results of MO calculations support that the linear alignment of F---Se–C(An) atoms is not due to the crystal-packing effect but the results of the energy lowering effect caused by the linear alignment of the F atom and the Se–C(An) bond.

Table 3. Structures, Energies, and Natural Charges (Qn) in HF---SeH$_2$, HF, and SeH$_2$ Calculated with the 6-311++G(3df,2pd) Basis Sets[a]

	Level	E (au)	r(F,H) (Å)	r(Se,H$_a$) (Å)	r(Se,H$_b$) (Å)	θ_l (deg)	∠H$_a$SeH$_b$ (deg)	Qn(F)	Qn(H)	Qn(Se)	Qn(H$_a$)	Qn(H$_b$)
structure a												
HF---SeH$_2$[b,c]	HF	-2501.0175	0.8979	1.4509	1.4559	180.0[d]	100.8[d]	-0.5517	0.5581	-0.0772	0.0346	0.0361
HF	HF	-100.0577	0.8973					-0.5581	0.5581			
SeH$_2$	HF	-2400.9668		1.4515	1.4515		100.8[d]			-0.1144	0.0572	0.0572
Δ		0.0070	0.0006	-0.0006	0.0044		0.0	0.0064	0.0000	0.0372	-0.0226	-0.0211
HF---SeH$_2$[b,c]	MP2	-2501.4645	0.9184	1.4562	1.4617	180.0[d]	100.8[d]	-0.5556	0.5620	-0.0781	0.0350	0.0367
HF	MP2	-100.3321	0.9172					-0.5617	0.5617			
SeH$_2$	MP2	-2401.1363		1.4568	1.4568		100.8[d]			-0.1161	0.0580	0.0580
Δ		0.0039	0.0012	-0.0006	0.0049		0.0	0.0061	0.0003	0.0380	-0.0230	-0.0213
structure b												
HF---SeH$_2$[e]	HF	-2501.0177	0.8979	1.4563	1.4577	180.0[f]	90.8[g,h]	-0.5507	0.5573	-0.0784	0.0364	0.0355
HF	HF	-100.0577	0.8973					-0.5581	0.5581			
SeH$_2$	HF	-2400.9684		1.4530	1.4530		93.2[g]			-0.1064	0.0532	0.0532
Δ		0.0084	0.0006	0.0033	0.0047		-2.4	0.0074	-0.0008	0.0280	-0.0168	-0.0177
HF---SeH$_2$[e]	MP2	-2501.4658	0.9184	1.4622	1.4643	180.0[f]	88.9[g,i]	-0.5547	0.5614	-0.0787	0.0366	0.0354
HF	MP2	-100.3321	0.9172					-0.5617	0.5617			
SeH$_2$	MP2	-2401.1385		1.4591	1.4591		91.3[g]			-0.1072	0.0536	0.0536
Δ		0.0048	0.0012	0.0031	0.0052		-2.4	0.0070	-0.0003	0.0285	-0.0170	-0.0182
HF---SeH$_2$[e]	MP2	-2501.4585	0.9176	1.4604	1.4559	65.4[g]	91.7[g]	-0.5610	0.5606	-0.0843	0.0354	0.0493
Δ		0.0121	0.0004	0.0013	0.0008		0.4	0.0007	-0.0011	0.0229	-0.0182	-0.0043

[a] r(F,Se) fixed at 2.753 Å. [b] θ_2 fixed at 185.0°. [c] ∠HFSe fixed at 100.0°. [d] Fixed value. [e] ∠HFSe fixed at 90.0°. [f] See ref 12. [g] Optimized value. [h] θ_2 optimized to be 179.2°. [i] θ_2 optimized to be 181.1°.

39
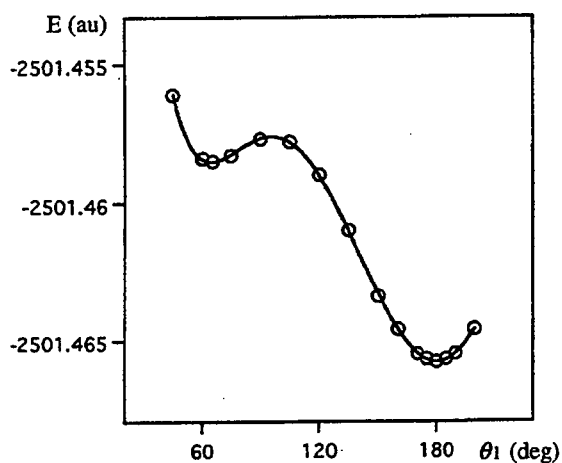
Figure 2. Plot of energy against θ_1 in structure b.

Molecular orbitals were drawn using the MacSpartan Plus program[14] with the 3-21G$^{(*)}$ basis sets for structure **a** and the corresponding structures of HF and SeH_2: the single point calculations were performed on the structures that were partially optimized at the MP2/6-311++G(3df,2pd) level, as shown in Table 3. Figure 3 shows the diagram in the formation of HF---SeH_2,

Figure 3. Diagram in the formation of HF···SeH_2 from HF and SeH_2 (see text).

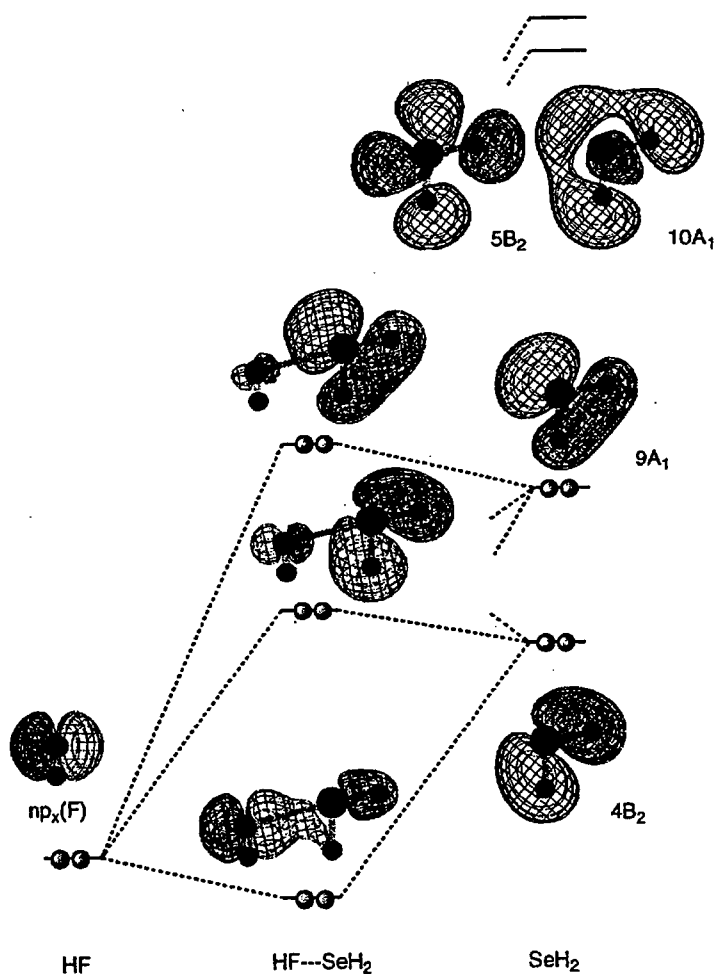exemplified by structure **a**, together with the $np_x(F)$ orbital of HF and the $4B_2$, $9A_1$, $10A_1$, and $5B_2$ orbitals of SeH_2. The $4B_1$ orbital of SeH_2, which is HOMO consisted of the $4p_z$ orbital of the Se atom, is not shown in Figure 3, since the orbital does not interact with the $np_x(F)$ due to its symmetry.[15]

Although the molecular orbitals of SeH_2 do not interact with each other due to the orthogonality, if the molecule is far from others, they begin to interact with each other, as well as with the $np_x(F)$ orbital when HF comes close to SeH_2.[16] While the energy levels of $4B_2$ and $9A_1$ orbitals of SeH_2 must be considerably higher than that of the $np_x(F)$ of HF, the three orbitals become to interact to make new molecular orbitals in the formation of HF---SeH_2. The $np_x(F)$ orbital also interacts with the unoccupied orbitals such as $10A_1$ and $5B_2$ of SeH_2 by the same reason. The interaction with the unoccupied orbitals must be important since it stabilizes the bond of the adduct and modifies the new orbitals of the adduct to some extent. Such orbital interaction in HF---SeH_2 results in the contribution of the $np_x(F)$-$\sigma^*(Se-H_b)$ interaction[16] as well as the charge transfer from HF to SeH_2.

Natural charges (Qn) were computed by natural population analysis[17] for structure **a** and structure **b** and the corresponding structures of SeH_2 and HF with the 6-311++G(3df,2pd) basis sets of both the HF and MP2 levels. The results are collected in Table 3. The fluorine atom became substantially more positive when the adducts of structure **a** and structure **b** with $\theta_1 = 180.0°$ were formed, which showed that the fluorine atom acted as an electron donor in this interaction. The change transfer shown in the Qn can be explained by assuming the two processes: (i) the charge transfer from F to SeH_2 and (ii) the charge transfer from $np_x(F)$ to $\sigma^*(Se-H_b)$ resulting from the linear F---$Se-H_b$ interaction. If the linear F---$Se-H_b$ interaction can be recognized as the unsymmetrical three center-four electron (3c-4e) F---$Se-H_b$ interaction, the F, Se, and H_b atoms are expected to be more negative, positive, and negative, respectively.[18] The positive and negative charge developed on the Se and H_b atoms in the formation of the adduct are well explained by the 3c-4e model. The positive and negative charge development at the F and H_a atoms must show the contribution of the charge transfer from F to SeH_2 (see also Figure 3). On the other hand, the electrons at the F and Se atoms of structure **b** with $\theta_1 = 65.4°$ moved to hydrogens. The lone pair-lone pair repulsive interaction of the F and Se atoms must expel electrons to hydrogens, mainly to H_a. The $Se-H_b$ bond no longer play an important role, and the HF molecule does not act as an electron donor in the adduct.

Parthasarathy et al. have suggested that there are two types of directional preferences of nonbonded atomic contacts with divalent sulfur, Y–S–Z.[9] Type I contacts with electrophiles which have S---X directions in YZS---X where n-electrons of sulfides are located and type II contacts with nucleophiles tending to lie along the extension of one of sulfur's bond. Electrophiles should

41

interact preferentially with HOMO of the sulfur lone pair and nucleophiles with LUMO of the σ^*(S–Y) or σ^*(S–Z) orbital. Similar directional preferences of nonbonded atomic contacts have also shown with divalent selenium.[10] The linear alignment of F, Se, and C(An) atoms in **1** apparently belongs to type II with the central atom of Se. The F atom as the type II in F--- Se–C(An) linear alignment should be recognized as a nucleophile and must act as an electron donor accompanied by the σ^*(Se–C(An)) orbital as an acceptor in the close proximity. The MO calculations, containing the natural population analysis, support the n(F)---σ^*(Se–C(An)) interaction in **1**.

5　　　　**6**　　　　**7**
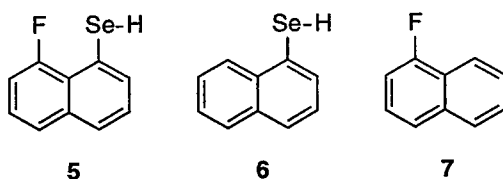
Contributions of π-orbitals were also examined. 8-Fluoro-1-naphthaleneselenole (**5**), together with 1-naphthaleneselenole (**6**) and 1-fluoronaphthalene (**7**), was calculated with the 6-311+G(d,p) basis sets at the HF level. The fluorine atom and the Se–H bond were optimized to be placed on the plane of the naphthalene ring. The $\angle$CSeH, $\angle$FSeH, and r(F,Se) values in **5** were estimated to be 93.7°, 166.4°, and 2.779 Å, respectively. Natural charges (Qn) were also computed, and the results are shown in Table 4. The Qn values of F, Se, and H(Se) became more positive, positive, and negative, respectively, relative to those of the corresponding atoms in **6** and **7**, which was the same trend calculated on the models shown in Table 3. The structure of **5** was also optimized using the MacSpartan Plus program with the 3-21G$^{(*)}$ basis sets. The HOMO of **5** is shown in Figure 4. The p-orbitals of F and Se atoms contribute to the π-type HOMO. The np_x(F)-σ^*(Se–H_b) type interaction was shown to contribute to the lower energy orbitals.

Table 4.　Natural Charges (Qn) in 5 - 7 Calculated with 6-311+G (d,p) Basis Sets at the HF Level

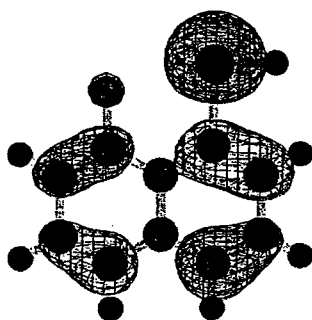| compd	Qn(F)	Qn(Se)	Qn(H)
5	-0.3922	0.2086	0.0252
6		0.1560	0.0489
7	-0.3950		
ΔQn	0.0028	0.0526	-0.0237

Figure 4. HOMO of 8-fluoro-1-naphthaleneselenole (5).

The nonbonded r(F,Se) of 2.753(3) Å was shorter than the sum of the van der Waals radii[8] of F and Se atoms by 0.60 Å (Δr_v(F,Se) = 0.60 Å). The nonbonded Se---Se distances in 1-(methylselanyl)-8-(phenylselanyl)naphthalene (**8**)[19] and bis[8-(phenylselanyl)naphthyl] diselenide (**9**)[1f] are 3.070(1) and 3.053(1) Å, respectively, on the average. Since the sum of the van der Waals radii of the two Se atoms is 4.00 Å, the nonbonded Se---Se distances in **8** and **9** are shorter than the value by 0.93 - 0.95 Å (Δr_v(Se,Se) = 0.93 - 0.95 Å). Indeed, the r(F,Se) must be mostly determined by the peri positions where the two atoms are joined, but the fluorine atom in **1** might contribute to decrease the distance to some extent since the Δ r_v(F,Se) in **1** is larger than a half of the Δ r_v(Se,Se) in **8** and **9**. The observed r(F,Se) value would be consistent with the attractive interaction of the linear n(F)-σ*(Se–C(An)) alignment in **1**, although the energy of structure **b** with θ_1 = 180.0° is evaluated to be higher than the free components by 0.0048 au (13 kJ mol⁻¹) at the MP2/6-311++G(3df,2pd) level.[13]

8   **9**
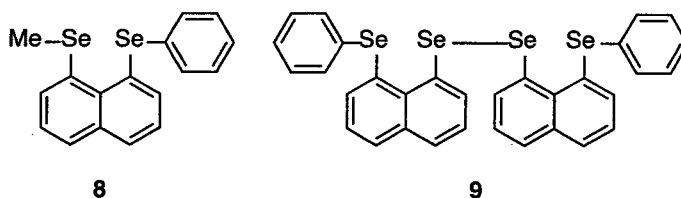
Four bond couplings between F and Se atoms (^4J(F,Se)) of **1** and **2** were observed to be 285.0 and 276.7 Hz, respectively, while ^4J(F,F) in 1,8-difluoronaphthalene[2b] and ^4J(Se,Se) in 1-(methylselanyl)-8-(phenylselanyl)naphthalene[1g] were reported to be 58.8 and 322.4 Hz, respectively. The ^5J(F,C) values in F---Se–C bonds of **1** and **2** were detected to be 18.2 and 14.9 Hz, respectively. The role of the linear F---Se–C alignment on the downfield shifts of the ^{77}Se NMR chemical shifts and the large J values containing the Se nucleus in **1** and **2**, together with some novel reactions[20] correlated with the formation of the compounds, is in progress.

Experimental Section

Chemicals were used without further purification unless otherwise noted. Solvents were purified by standard methods. Melting points were recorded on a YANAKO Model MP and uncorrected. ^{1}H, ^{13}C, and ^{77}Se NMR spectra were recorded on a JEOL Lambda 400 spectrometer operating at 399.7, 100.4, and 76.2 MHz, respectively. Coupling constants (J) are given in hertz. 1-(Methylselanyl)naphthalene (**4**) was prepared according to the method in the literature.[1c]

8-Fluoro-1-(p-anisylselanyl)naphthalene (1). To an ethereal solution of 8-(fluoronaphthyl)magnesium bromide, resulting from 8-bromo-1-fluoronaphthalene[21,22] and magnesium, was added an ethereal solution of di(p-anisyl) diselenide under argon atmosphere. After a usual workup, was obtained **1**. Recrystallization from hexane gave colorless prisms: yield 67 %; mp 83-84.5 °C; ^{1}H NMR (399.65 MHz, CDCl$_3$) δ 3.86 (s, 3H), 6.89 (dd, J = 1.0, 7.8, 1H), 6.96 (d, J = 9.4, 2H), 7.15 (t, J = 7.8, 1H), 7.17 (ddd, J = 1.0, 7.8, 13.2, 1H), 7.37 (dt, J = 5.4, 8.1, 1H), 7.56 (dd, J = 1.0, 7.8, 1H), 7.58 (dd, J = 1.0, 7.8, 1H), 7.64 (d, J = 9.4, 2H). Anal. Calcd for C$_{17}$H$_{13}$FOSe: C, 62.00; H, 3.96. Found: C, 62.21; H, 4.05.

8-Fluoro-1-(methylselanyl)naphthalene (2). Sodium 8-fluoro-1-naphthaleneselenate was allowed to react with methyl iodide in a THF–water mixed solvent under argon atmosphere to give **2**. After chromatography on silica gel with hexane as an eluent, recrystallization from hexane gave colorless prisms: yield 93 %; mp 59-60 °C; ^{1}H NMR (399.65 MHz, CDCl$_3$) δ 2.38 (s, 3H), 7.14 (ddd, J = 1.2, 7.8, 13.2, 1H), 7.30 (br d, J = 7.3, 1H), 7.36 (t, J = 7.8, 1H), 7.36 (dt, J = 4.8, 7.8, 1H), 7.59 (dd, J = 0.9, 8.3, 1H), 7.62 (dd, J = 1.0, 8.3, 1H). Anal. Calcd for C$_{11}$H$_9$FSe: C, 55.25; H, 3.79. Found: C, 55.48; H, 3.99.

Sodium 8-fluoro-1-naphthaleneselenate was prepared from bis(8-fluoronaphthyl)-1,1'-diselenide.[23] The diselenide was obtained in the reaction of 8-bromo-1-fluoronaphthalene,[21,22] magnesium, and selenium powder in diethyl ether under argon atmosphere followed by oxidation with air and recrystallized from hexane.

1-(p-Anisylselanyl)naphthalene (3). To an ethereal solution of naphthylmagnesium bromide, resulting from 1-bromonaphthalene and magnesium, was added an ethereal solution of di(p-anisyl) diselenide under argon atmosphere. After a usual workup, was obtained **3**. Recrystallization from hexane gave colorless prisms: yield 62 %; mp 100.0-101.0 °C; ^{1}H NMR (399.65 MHz, CDCl$_3$) δ 3.78 (s, 3H), 6.82 (d, J = 8.9, 2H), 7.30 (dd, J = 7.3, 8.2, 1H), 7.45 (d, J = 8.9, 2H), 7.46 - 7.55 (m, 3H), 7.75 (d, J = 8.2, 1H), 7.83 (dd, J = 2.2, 7.2, 1H), 8.28 (ddd, J = 0.9, 2.0, 7.6, 1H). Anal. Calcd for C$_{17}$H$_{14}$OSe: C, 65.18; H, 4.50. Found: C, 65.23; H, 4.46.

X-ray Structural Determination of 1. The colorless single crystals of **1** were grown by slow evaporation of a hexane solution at room temperature. A crystal of dimensions 0.60 × 0.30 ×

0.30 mm^3 was measured on a Rigaku AFC7R diffractometer with graphite monochromated Mo Kα radiation (λ = 0.710 69 Å). The structure was solved by direct methods using *SHELXS-86*[24] and was refined by block diagonal least-squares using *UNICS III.*[25] The function minimized was $\Sigma\ w\ (|F_o| - |F_c|)^2$, where $w\ =\ 1/[\sigma^2(|F_o|)\ +\ 0.001|F_o|^2]$. The non-hydrogen atoms were refined anisotropically. All hydrogen atoms were located on a Fourier difference map and not refined. The final cycle of block diagonal least-squares refinement was based on 4292 observed reflections (I > 3.00σ(F)) and 362 variable parameters and converged with unweighted and weighed agreement factors to give R = 0.045 and Rw = 0.044 for independent observed reflections.

MO Calculations. Ab initio molecular orbital calculations were performed on a Power Challenge L computer using the Gaussian 94 program with the 6-311++G(3df,2pd) and 6-311+G(d,p) basis sets at the HF and/or MP2 levels. The molecular orbitals in Figures 3 and 4 were drawn by a Power Macintosh 8500/180 personal computer using MacSpartan Plus program (Ver. 1.0) with 3-21G$^{(*)}$ basis sets.

References and Notes

(1) (a) Glass, R. S.; Andruski, S. W.; Broeker, J. L. *Rev. Heteroatom Chem.* **1988**, *1*, 31. Glass, R. S.; Andruski, S. W.; Broeker, J. L.; Firouzabadi, H.; Steffen, L. K.; Wilson, G. S. *J. Am. Chem. Soc.* **1989**, *111*, 4036. Glass, R. S.; Adamowicz, L.; Broeker, J. L. *J. Am. Chem. Soc.* **1991**, *113*, 1065. (b) Fujihara, H.; Ishitani, H.; Takaguchi, Y.; Furukawa, N. *Chem. Lett.* **1995**, 571. (c) Fujihara, H.; Yabe, M.; Chiu, J.-J.; Furukawa, N. *Tetrahedron Lett.* **1991**, *32*, 4345. Furukawa, N.; Fujii, T.; Kimura, T.; Fujihara, H. *Chem. Lett.* **1994**, 1007. (d) Fujihara, H.; Saito, R.; Yabe, M.; Furukawa, N. *Chem. Lett.* **1992**, 1437. (e) Nakanishi, W. *Chem. Lett.* **1993**, 2121. (f) Nakanishi, W.; Hayashi, S.; Toyota, S. *J. Chem. Soc., Chem. Comm.* **1996**, 371. (g) Nakanishi, W.; Hayashi, S.; Yamaguchi, H. *Chem. Lett.* **1996**, 947.

(2) (a) Mallory, F. B. *J. Am. Chem. Soc.* **1973**, *95*, 7747. (b) Mallory, F. B.; Mallory, C. W.; Fedarko, M.-C. *J. Am. Chem. Soc.* **1974**, *96*, 3536. (c) Mallory, F. B.; Mallory, C. W.; Ricker, W. M. *J. Am. Chem. Soc.* **1975**, *97*, 4770. Mallory, F. B.; Mallory, C. W.; Ricker, W. M. *J. Org. Chem.* **1985**, *50*, 457. Mallory, F. B.; Mallory, C. W.; Baker, M. B. *J. Am. Chem. Soc.* **1990**, *112*, 2577. (d) Ernst, L.; Ibrom, K. *Angew. Chem. Int. Ed. Engl.* **1995**, *34*, 1881. Ernst, L.; Ibrom, K.; Marat, K.; Mitchell, R. H.; Bodwell, G. J.; Bushnell, G. W. *Chem. Ber.* **1994**, *127*, 1119.

(3) Mallory, F. B.; Luzik, E. D., Jr.; Mallory, C. W.; Carroll, P. J. *J. Org. Chem.* **1992**, *57*, 366. Mallory, F. B.; Mallory, C. W. *J. Am. Chem. Soc.* **1985**, *107*, 4816.

(4) Johannsen, I.; Eggert, H. *J. Am. Chem. Soc.* **1984**, *106*, 1240. Johannsen, I.; Eggert, H.; Gronowitz, S.; Hörnfeldt, A.-B. *Chem. Scr.* **1987**, *27*, 359. Fujihara, H.; Mima, H.; Erata, T.; Furukawa, N. *J. Am. Chem. Soc.* **1992**, *114*, 3117.

(5) (a) Goldstein, B. M.; Kennedy, S. D.; Hennen, W. J. *J. Am. Chem. Soc.* **1990**, *112*, 8265. (b) Barton, D. H. R.; Hall, M. B.; Lin, Z.; Parekh, S. I.; Reibenspies, J. *J. Am. Chem. Soc.* **1993**, *115*, 5056.

(6) The ^{77}Se chemical shifts of **1**, **2**, **3**, and **4** were δ 440.9, 250.4, 354.2, and 159.0, respectively.

(7) Although the discussion is focused on structure **A**, it is also valid on structure **B**.

(8) Pauling, L. *The Nature of the Chemical Bond*, 3rd ed.; Cornell University Press: Ithaca, New York, 1960; Chap. 7. See also: Bondi, A. *J. Phys. Chem.* **1964**, *68*, 441.

(9) Rosenfield, R. E., Jr.; Parthasarathy, R.; Dunitz, J. D. *J. Am. Chem. Soc.* **1977**, *99*, 4860.

(10) Ramasubbu, N.; Parthasarathy, R. *Phosphorus Sulfur* **1987**, *31*, 221.

(11) *Gaussian 94, Revision D.4*; Frisch, M. J.; Trucks, G. W.; Schlegel, H. B.; Gill, P. M. W.; Johnson, B. G.; Robb, M. A.; Cheeseman, J. R.; Keith, T.; Petersson, G. A.; Montgomery, J. A.; Raghavachari, K.; Al-Laham, M. A.; Zakrzewski, V. G.; Ortiz, J. V.; Foresman, J. B.; Cioslowski, J.; Stefanov, B. B.; Nanayakkara, A.; Challacombe, M.; Peng, C. Y.; Ayala, P. Y.; Chen, W.; Wong, M. W.; Andres, J. L.; Replogle, E. S.; Gomperts, R.; Martin, R. L.; Fox, D. J.; Binkley, J. S.; Defrees, D. J.; Baker, J.; Stewart, J. P.; Head-Gordon, M.; Gonzalez, C.; Pople, J. A. Gaussian, Inc., Pittsburgh PA, 1995.

(12) In the actual calculations on structure **b**, the angles θ_1 and θ_2 were optimized to be 180.11° and 179.16°, respectively, at the HF level and 180.03° and 181.12°, respectively, at the MP2 level. However, precisely the same results such as bond lengths and angles and energies were obtained at both levels when the calculations were performed with θ_1 of structure **b** fixed at 180.00°. The potential surface must be almost flat near $\theta_1 = 180°$.

(13) The energy of the adduct was evaluated to be larger than the sum of those for HF and H_2Se. The results exhibit that the adduct is destabilized relative to the free components. The fluoro and selanyl groups can not exist so close if the two groups are not joined by the naphthalene 1,8-positions.

(14) MacSpartan Plus Ver. 1.0, Hehre, H.J. Wavefunction Inc.

(15) The results for structure **b** with $\theta_1 = 180.0°$ and the corresponding molecules were essentially the same as those exhibited in Figure 3.

(16) Inagaki, S.; Fujimoto, H.; Fukui, K. *J. Am. Chem. Soc.*, **1976**, *98*, 4054.

(17) NBO Ver. 3.1, Glendening, E. D.; Reed, A. E.; Carpenter, J. E.; Weinhold, F.

(18) (a) Pimentel, G. C. *J. Chem. Phys.* **1951**, *19*, 446. Musher, J. I. *Angew. Chem., Int. Ed. Engl.* **1969**, *8*, 54. (b) Chen, M. M. L.; Hoffmann, R. *J. Am. Chem. Soc.* **1976**, *98*, 1647. (c) Cahill, P. A.; Dykstra, C. E.; Martin, J. C. *J. Am. Chem. Soc.* **1985**, *107*, 6359. See also, Hayes, R. A.; Martin, J. C. *Sulfurane Chemistry In Organic Sulfur Chemistry: Theoretical and Experimental Advances*; Bernardi, F. Csizmadia, I. G. Mangini, A., Eds,; Elsevier: Amsterdam, 1985; Chap. 8.

(19) Nakanishi, W.; Hayashi, S.; Toyota, S. *J. Org. Chem.* **1998**, *63*, 8790.

(20) We have encountered a facile reductive C–F bond cleavage in the reaction of sodium 8-fluoro-1-naphthaleneselenate with *p*-(methoxybenzene)diazonium chloride, which yields not **1** but **3**. The C–F bond cleavage must be, I believe, the reflection of the nonbonded interaction between F and Se atoms.

(21) Adcock, W.; Matthews, D. G.; Rizvi, S. Q. A. *Aust. J. Chem.* **1971**, *24*, 1829.

(22) The compound was prepared according the literature and obtained the same results for elemental analyses:[21] The observed value for carbon was ca. 1 % larger than that of the calculated one while that for hydrogen was satisfactory.

(23) It was also difficult to purify the compound similarly to the case of ref 22. Further investigation containing the C–F bond cleavage[20] is in progress, and the results will be reported elsewhere.

(24) Sheldrick, G. M. *Acta Crystallogr. Sect. A* **1990**, *A46*, 467.

(25) Sakurai, T.; Kobayashi, K. *Rep. Inst. Phys. Chem. Res.* **1979**, *55*, 69.

Chapter 4

Four-Center Six-Electron Interaction versus Lone Pair–Lone Pair Interaction between Selenium Atoms in Naphthalene Peri Positions

Abstract

The X-ray crystallographic analysis of bis[8-(phenylselanyl)naphthyl]-1,1'-diselenide (1) and 1-(methylselanyl)-8-(phenylselanyl)naphthalene (2) showed that the four selenium atoms in 1 aligned linearly, while the Se–C(Me) and Se–C(Ph) bond in 2 declined by about 50° and 40° from the naphthyl plane, respectively. Ab initio molecular orbital calculations were performed on the models of 1 and 2, model a ($H_bH_c{}^2Se$---$H_a{}^1Se^3SeH_a$---$^4SeH_bH_c$) and model b ($H_aH_b{}^1Se$---$^2SeH_aH_{b'}$), respectively, with the 6-311++G(3df,2pd) basis sets at the HF and MP2 levels, and the calculations were reproduced well the observed structures and revealed the nature of the bonds constructed by the selenium atoms containing nonbonded interactions. The bond with four linearly aligned selenium atoms in model a can be analyzed with the 4c-6e model constructed with the nonbonded interaction between the two p-type lone pairs at the outside selenium atoms and the σ*(Se–Se) orbital of the inside Se–Se bond, which results in the charge transfer from the outside Se atoms to the inside Se atoms. The nonbonded interaction between the two p-type lone pairs at the Se atoms in model b is analyzed as a π-type 2c-4e bond. The bent structure in H_b--^1Se---^2Se–$H_{b'}$ was demonstrated to be the results of the requirement to avoid the severe exchange repulsion between the filled p-type lone pairs at the two selenium atoms. The calculations on the other models, PhSeH---HSeSeH---HSePh and PhSeH---HSeMe, with the 6-311+G(d,p) basis sets at the DFT (B3LYP) level showed that the π-orbitals of the phenyl groups of the former interacted effectively with the 4c-6e orbitals but the π-orbitals of the latter did little with the 2c-4e orbitals due to the orthogonality of the two systems.

Introduction

Lone pairs of heteroatoms bound to π-systems will interact with them if the orientation of the two orbitals is suitable for the interaction.[1] The lone pairs of heteroatoms often encounter such orbitals that may interact with the lone pairs, extending over the electron deficient atoms or groups in cationic species, partially positive centers of polar bonds, and radical centers, together with low lying antibonding orbitals.[2] The interaction of the lone pairs occurs not only by the through-bond mechanism but also by the through-space mechanism in such cases. The naphthalene peri positions supply a suitable system for the lone pairs to interact by the through-space mechanism, which is of current interest.[3-6] The lone pair–lone pair interactions have been demonstrated to play an important role in the nonbonded spin–spin couplings between fluorine–fluorine,[7] fluorine–nitrogen,[8] fluorine–selenium,[6d] and selenium–selenium.[4,6c,9]
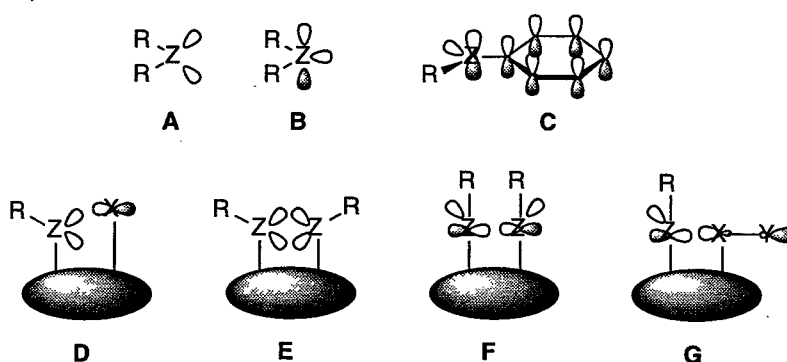
A   B   C

D   E   F   G

Lone pairs of chalcogens have been represented by two types of orbitals; the one is depicted by the two sp^3-hybrid orbitals as shown in **A**, and the other is based on the p- and s-type orbitals or p- and sp^2-hybrid orbitals as shown in **B**.[5] The sp^3-hybrid orbital model is convenient when one discusses the collective properties of chalcogenides such as the electron densities or the total energies of lone pairs. The p- and s-type orbitals must be employed if the one-electron properties such as the energy of each molecular orbital are discussed containing the lone pair orbital(s).[10] Since the p-type orbital of a lone pair has a C_s symmetry, it interacts with π-orbitals of aryl groups to which the lone pair orbital is attached if the orientation is suitable (**C**), as mentioned above. Lone pair orbitals interact with orbitals of other atoms or groups (**D**) and with other lone pairs (**E**), of which lone pairs are exemplified by sp^3-hybrid orbitals. The interaction between lone pairs will construct the σ bond(s) when two or more p-type orbitals of lone pairs align linearly (**F**), and the p-type orbitals are expected to interact with σ-bonds if the energy levels of the σ^*-orbitals are low enough for the interaction (**G**).
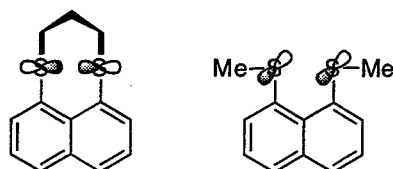
Parthasarathy et al. have suggested that there are two types of directional preferences of nonbonded atomic contacts with divalent chalcogens such as sulfur[11] and selenium,[12] R–Z–R' (Z = S and Se). Type I contacts are with electrophiles which have Z---X directions in RR'Z---X where n-electrons of sulfides or selenides are located (D), and type II contacts are with nucleophiles tending to lie along the extension of one of sulfur's or selenium's bond (G for X = S, Se). Electrophiles and nucleophiles should interact preferentially with the HOMO of the lone pair of Z and with the LUMO of the σ*(Z–R) or σ*(Z–R') orbital, respectively. Glass and his coworkers have shown that the lone pairs of sulfur atoms in naphtho[1,8-b,c]-1,5-dithiocin interact directly with each other, since the two orbitals lay on the naphthyl plane, while those in 1,8-bis(methylthio)naphthalene mainly interact with its π-system.[5] The former is an example of the interaction shown by F, and the latter like that in C.
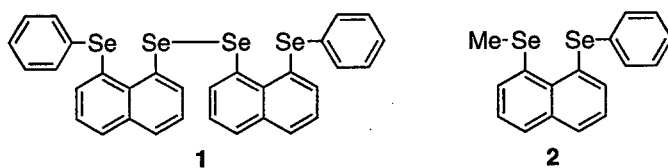

We have been interested in the intramolecular interaction containing in group 16 elements, especially that in selenium atoms.[6] We started my project to prepare such organoselenium compounds that are the typical examples of the lone pair–lone pair interactions shown in D – G and to examine the novel properties brought into the compounds by the interaction. Bis[8-(phenylselanyl)naphthyl]-1,1'-diselenide (1) and 1-(methylselanyl)-8-(phenylselanyl)naphthalene (2) were prepared as the first step of my investigations. The X-ray crystallographic analyses of 1 and 2 reveal that the four selenium atoms in 1 align linearly while the Se–C(Me) and Se–C(Ph) bonds in 2 decline by about 50° and 40° from the naphthyl plane, respectively. Ab initio MO calculations exhibit that the linear bond formed by the four selenium atoms in 1 can be analyzed by the four-center six-electron bond (4c-6e) model and the interaction between the lone pairs in 2 is characterized by the π-type two-center four-electron (2c-4e) interaction. We would like to present the results of the investigation of 1 and 2 based on the X-ray crystallographic analysis and ab initio MO calculations.

Results and Discussion

Structure of 1 and 2. The reaction between the dianion of naphto[1,8-c,d]-1,2-diselenol and 2 or more equiv of benzenediazonium ion at low temperature, followed by a usual workup, gave bis[8-(phenylselanyl)naphthyl]-1,1'-diselenide (1).[6b] Reduction of 1 with sodium borohydride followed by the reaction with methyl iodide gave 1-(methylselanyl)-8-(phenylselanyl)naphthalene (2).[6c]

Single crystals of **1** and **2** were obtained *via* slow evaporation of hexane solutions, and each of the suitable crystals was subjected to X-ray crystallographic analysis. The crystallographic data are collected in Table 1. The selected interatomic distances, angles, and torsional angles of **1** and **2** are shown in Tables 2 and 3, respectively. Two independent molecules (structure **A** and structure **B**) were found in an asymmetric unit of the crystal of **2** (see Table 3). Figures 1 and 2 depict the structure of **1** and structure **A** of **2**, respectively.[13]
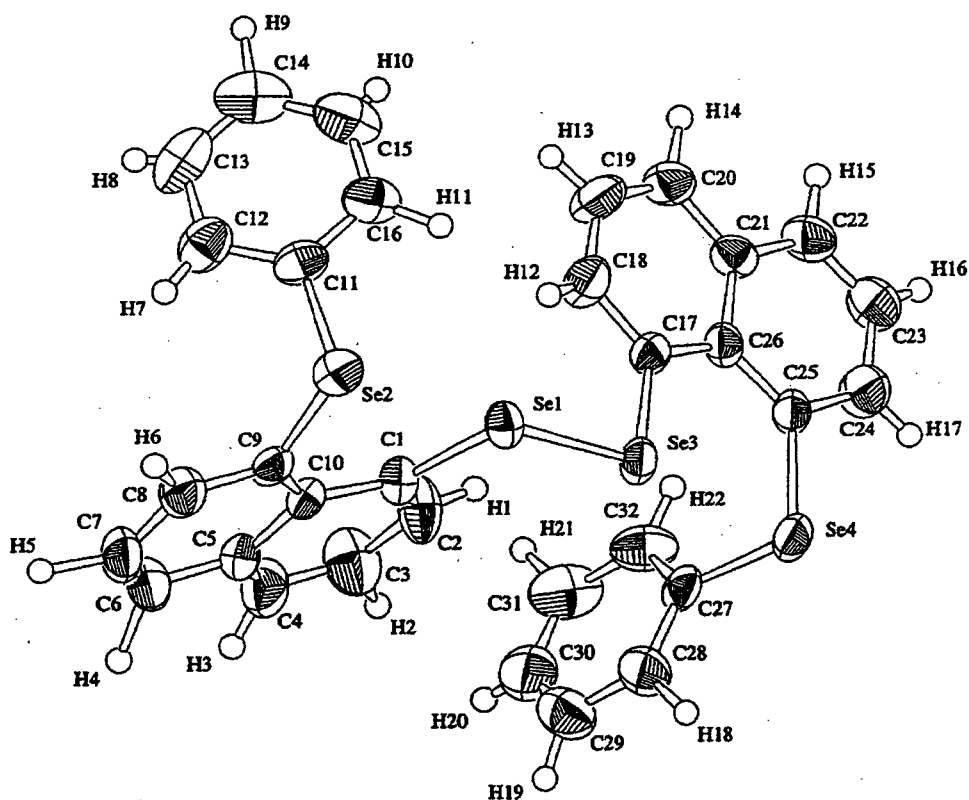
Figure 1. ORTEP drawing of **1**.
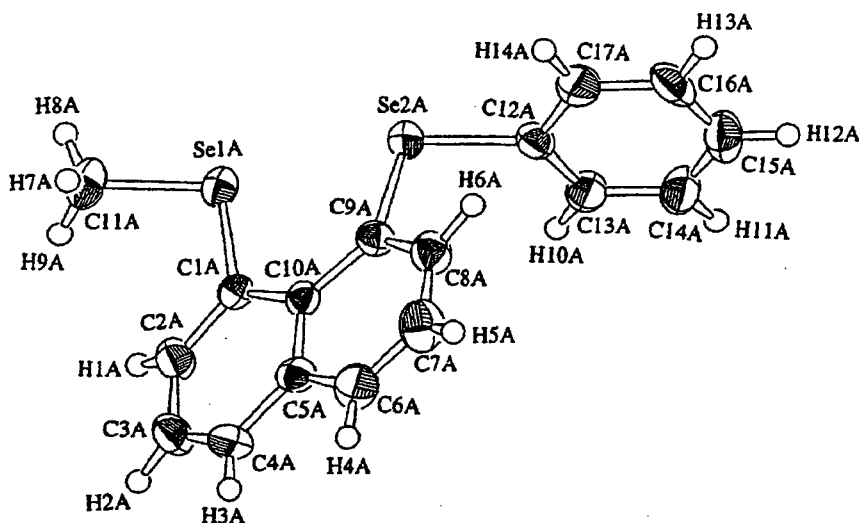
Figure 2. ORTEP drawing of **2** (structure **A**).

Table 1. Selected Crystal Data and Structure Refinement for 1 and 2

	1	2
formula	$C_{32}H_{22}Se_4$	$2 \times C_{17}H_{14}Se_2$
fw, g mol^{-1}	722.37	2×376.22
cryst syst	triclinic	triclinic
space group	*P-1(#2)*	*P-1(#2)*
color	yellow	colorless
a, Å	12.2175(8)	10.660(2)
b, Å	12.3430(8)	11.509(3)
c, Å	9.7474(8)	12.021(3)
α, °	103.038(6)	90.40(2)
β, °	110.715(5)	96.29(2)
γ, °	91.791(6)	92.75(2)
V, Å^3	1329.5(2)	1464.0(6)
D_{calcd}, g cm^{-3}	1.804	1.707
Z	2	4
Scan Width, °	$1.73 + 0.30 \tan\theta$	$0.96 + 0.35 \tan\theta$
$2\theta_{max,}$ °	120.1	55.0
no. of observations	3669	3700
no. of variables	414	412
R	0.055	0.043
R_w	0.065	0.050
goodness-of-fit	3.89	2.32

Table 2. Selected Interatomic Distances, Angles, and Torsional Angles of **1**

Interatomic Distances, Å

Se(1)–Se(2)	3.018(1)	Se(1)–Se(3)	2.365(1)
Se(3)–Se(4)	3.087(1)	Se(1)–C(1)	1.957(9)
Se(2)–C(9)	1.915(9)	Se(3)–C(17)	1.959(8)
Se(4)–C(25)	1.909(9)	C(1)–C(10)	1.42(1)
C(9)–C(10)	1.41(1)	C(17)–C(26)	1.42(1)
C(25)–C(26)	1.42(1)		

Angles, °

Se(2)–Se(1)–Se(3)	177.10(5)	Se(1)–Se(3)–Se(4)	170.45(5)
Se(3)–Se(1)–C(1)	101.8(3)	Se(1)–Se(3)–C(17)	103.1(3)
Se(1)–C(1)–C(10)	122.6(7)	C(1)–C(10)–C(9)	126.0(8)
Se(2)–C(9)–C(10)	123.2(6)	C(9)–Se(2)–C(11)	99.7(4)
Se(3)–C(17)–C(26)	122.8(6)	C(17)–C(26)–C(25)	127.5(8)
Se(4)–C(25)–C(26)	124.7(6)	C(25)–Se(4)–C(27)	100.6(4)

Torsional Angles, °

Se(2)–Se(1)–Se(3)–Se(4)	157.3(8)	Se(1)–C(1)–C(10)–C(9)	10(1)
C(1)–Se(1)–Se(3)–C(17)	91.4(4)	Se(3)–Se(1)–C(1)–C(10)	163.0(7)
Se(2)–C(9)–C(10)–C(1)	12(1)	C(10)–C(9)–Se(2)–C(11)	76.2(7)
Se(3)–C(17)–C(26)–C(25)	6(1)	Se(1)–Se(3)–C(17)–C(26)	179.0(7)
Se(4)–C(25)–C(26)–C(17)	6(1)	C(26)–C(25)–Se(4)–C(27)	70.0(8)
C(9)–Se(2)–C(11)–C(12)	51.4(9)	C(25)–Se(4)–C(27)–C(28)	-162.0(7)
C(5)–C(10)–C(1)–C(2)	-7(1)	C(5)–C(10)–C(9)–C(8)	2(1)

Table 3. Selected Interatomic Distances, Angles, and Torsional Angles of 2

structure A		structure B	
Interatomic Distances, Å			
Se(1A)–C(1A)	1.931(8)	Se(1B)–C(1B)	1.923(8)
Se(1A)–C(11A)	1.936(9)	Se(1B)–C(11B)	1.938(9)
Se(2A)–C(9A)	1.937(8)	Se(2B)–C(9B)	1.947(8)
Se(2A)–C(12A)	1.933(8)	Se(2B)–C(12B)	1.936(7)
Se(1A)–Se(2A)	3.048(1)	Se(1B)–Se(2B)	3.091(1)
C(1A)–C(10A)	1.43(1)	C(1B)–C(10B)	1.41(1)
C(9A)–C(10A)	1.44(1)	C(9B)–C(10B)	1.458(10)
Angles, °			
C(1A)–Se(1A)–C(11A)	97.8(4)	C(1B)–Se(1B)–C(11B)	98.2(4)
Se(1A)–C(1A)–C(10A)	122.9(6)	Se(1B)–C(1B)–C(10B)	125.6(5)
C(9A)–Se(2A)–C(12A)	98.4(3)	C(9B)–Se(2B)–C(12B)	98.1(3)
Se(2A)–C(9A)–C(10A)	123.1(6)	Se(2B)–C(9B)–C(10B)	122.3(6)
C(1A)–C(10A)–C(9A)	126.4(7)	C(1B)–C(10B)–C(9B)	125.5(7)
Se(1A)–Se(2A)–C(12A)	157.6(2)	Se(1B)–Se(2B)–C(12B)	156.5(3)
Se(2A)–Se(1A)–C(11A)	148.6(4)	Se(2B)–Se(1B)–C(11B)	140.2(3)
Torsional Angles, °			
C(11A)–Se(1A)–C(1A)–C(10A)	133.0(7)	C(11B)–Se(1B)–C(1B)–C(10B)	-122.4(7)
Se(1A)–C(1A)–C(10A)–C(9A)	-10(1)	Se(1B)–C(1B)–C(10B)–C(9B)	13(1)
C(2A)–C(1A)–Se(1A)–C(11A)	43.1(7)	C(2B)–C(1B)–Se(1B)–C(11B)	-52.3(7)
C(12A)–Se(2A)–C(9A)–C(10A)	143.2(6)	C(12B)–Se(2B)–C(9B)–C(10B)	-141.8(6)
Se(2A)–C(9A)–C(10A)–C(1A)	-8(1)	Se(2B)–C(9B)–C(10B)–C(1B)	7(1)
C(9A)–Se(2A)–C(12A)–C(13A)	87.7(7)	C(9B)–Se(2B)–C(12B)–C(13B)	97.5(7)
C(9A)–Se(2A)–C(12A)–C(17A)	-97.8(7)	C(9B)–Se(2B)–C(12B)–C(17B)	-87.8(7)
C(8A)–C(9A)–Se(2A)–C(12A)	31.3(7)	C(8B)–C(9B)–Se(2B)–C(12B)	-33.1(7)
C(11A)–Se(1A)–Se(2A)–C(12A)	170.9(9)	C(11B)–Se(1B)–Se(2B)–C(12B)	-169.0(8)
C(5A)–C(10A)–C(1A)–C(2A)	6(1)	C(5B)–C(10B)–C(1B)–C(2B)	-6(1)
C(5A)–C(10A)–C(9A)–C(8A)	-3(1)	C(5B)–C(10B)–C(9B)–C(8B)	4(1)

As shown in Figure 1, the two naphthyl planes in **1** are almost perpendicular with each other, which must be a reflection of those in ArSeSeAr.[14] The planarity of the naphthyl planes was good; the torsional angles of C(5)C(10)C(1)C(2) and C(5)C(10)C(9)C(8) were -7(1) and 2(1)°, respectively. The four selenium atoms in **1** lay almost on the planes; the torsional angles of Se(1)C(1)C(10)C(9), Se(2)C(9)C(10)C(1), Se(3)Se(1)C(1)C(10), Se(3)C(17)C(26)C(25), Se(4)C(25)C(26)C(17), and Se(1)Se(3)C(17)C(26) were 10(1), 12(1), 163.0(7), 6(1), 6(1), and 179.0(7)°, respectively. The C(1)Se(1)Se(3) and Se(1)Se(3)C(17) angles and the torsional angle C(1)Se(1)Se(3)C(17) around the diselenide moiety were 101.8(3), 103.1(3), and 91.4(4)°, respectively. The angles for Se(3)Se(1)Se(2) and Se(1)Se(3)Se(4) and the torsional angle for Se(2)Se(1)Se(3)Se(4) were 177.10(5), 170.45(5), and 157.3(8)°, respectively. Each phenyl group is located near the naphthyl group to which the phenyl group is not bonded (roof structure). The C(Nap)–Se(Se) bonds of **1** may rotate freely, which results in the zigzag alignment for the four Se atoms of **1** (cf Scheme 1d), however, the two C(Nap)–Se(Se) bonds rotate for the naphthyl planes to be perpendicular with each other. The fact that the two naphthyl planes meet at about a right angle is also an important factor for the linear alignment of the four Se atoms, which must be the reflection of the torsional angles of two Se–C bonds in usual diaryl diselenides being about 90°.[14] The linear alignment of the four selenium atoms detected in **1** is the first observation of this to the best of my knowledge.

1   **2**   **3**   **4**   **5**   **6**
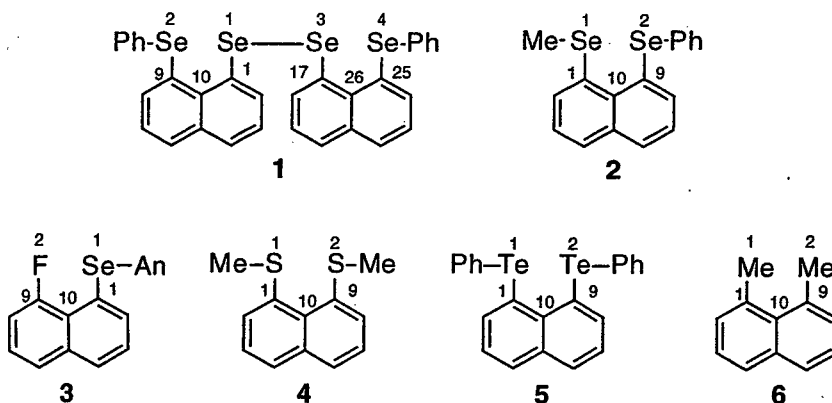
As shown in Figure 2, the planarity of the naphthyl planes of the bis-selenide **2** (structure **A**) was also good; the torsional angles of C(5A)C(10A)C(1A)C(2A) and C(5A)C(10A)C(9A)C(8A) were 6(1) and -3(1)°, respectively. The two selenium atoms slightly deviated from the plane; the torsional angles of Se(1A)C(1A)C(10A)C(9A) and Se(2A)C(9A)C(10A)C(1A) were -10(1)° and -8(1)°, respectively. The Se–C(Me) and Se–C(Ph) bonds of structure **A** and structure **B** in **2** decline by about 50° and 40° from the naphthyl plane, respectively: the torsional angles of C(11A)Se(1A)C(1A)C(10A) and C(12A)Se(2A)C(9A)C(10A) of structure **A** were 133.0(7)° and 143.2(6)°, respectively, and those of C(11B)Se(1B)C(1B)C(10B) and C(12B)Se(2B)C(9B)C(10B) of structure **B** were -122.4(7)° and -141.8(6)°, respectively.

Table 4. Nonbonded Distances, Angles, and Torsional Angles of Some Peri Substituted Naphthalenes

compd	r(Z1,Z2) (r(Z3,Z4)	∠Z1C1C10 ∠Z3C17C26	∠Z2C9C10 ∠Z4C25C26	∠C1C10C9 ∠C17C26C25	∠Z1C1C10C9 ∠Z3C17C26C25	∠Z2C9C10C1 ∠Z4C25C26C17	∠C10C1Z1M ∠C26C17Z3M	∠C10C9Z2C ∠C26C25Z4C)
1	3.018(1)	122.6(7)	123.2(6)	126.0(8)	10(1)	12(1)	-163.0(7)	76.2(7)
	(3.087(1)	122.8(6)	124.7(6)	127.5(8)	6(1)	6(1)	-179.0(7)	70.0(8))
2[a]	3.048(1)	122.9(6)	123.1(6)	126.4(7)	-10(1)	-8(1)	-133.0(7)	-143.2(6)
2[b]	3.091(1)	125.6(5)	122.3(6)	125.5(7)	13(1)	7(1)	122.4(7)	141.8(6)
3[c]	2.753(3)	120.5(3)	119.1(3)	125.9(3)	-0.1(5)	1.2(6)	179.2(3)	
3[d]	2.744(3)	120.7(3)	118.7(4)	125.6(4)	-0.9(6)	-3.7(6)	162.8(3)	
4[e]	2.918(2)	122.5(3)	121.1(3)	126.3(4)	-8.3	-8.9	143.2	158.3
4[f]	2.934(2)	122.1(3)	123.5(3)	125.4(4)	-6.4	-7.6	142.0	153.0
5	3.29	123(1)	124(1)	128(1)	-12.0	-16.2	g	g
6	2.932	124.8(1)	124.7(1)	125.2(1)	-0.015	0.001		

[a] For structure A. [b] For structure B. [c] For structure A in ref. 1. [d] For structure B in ref. 1. [e] For structure 1 in ref. 5c. [f] For structure 2 in ref. 5c. [g] Structure of type C for both the Te atoms being suggested in the figure, although the values were not specified.

Table 4 collects the nonbonded distances between atoms at the peri positions and the selected angles and torsional angles of the naphthalenes, 1 – 6.[4a,5c,6d,15] The nonbonded Se---Se distances in 1 were 3.018(1) and 3.087(1) Å for Se(1)---Se(2) and Se(3)---Se(4), respectively (3.053 Å on the average). That for Se(1)---Se(2) in structure A of 2 was 3.048(1) Å and the corresponding value for structure B was 3.091(1) Å, which is shown in Table 4 (3.070 Å on average). Since the sum of the van der Waals radii[16] of the two Se atoms is 4.00 Å, the nonbonded Se---Se distances in 1 and 2 are shorter than the van der Waals value by 0.95 and 0.93 Å, respectively (Δr_v(Se,Se) = 0.95 Å for 1 and Δr_v(Se,Se) = 0.93 Å for 2). The Δr_v(F,Se) in 3,[6d] Δr_v(S,S) in 4,[5c] Δr_v(Te,Te) in 5,[4a] and Δr_v(C(Me),C(Me)) in 6[15] were 0.60, 0.77, 1.11, and 1.07 Å, respectively. The Δr_v value becomes large as the sum of the van der Waals radii increase. The Δr_v values must be strongly controlled by the intrinsic distance of the peri positions where the two atoms are bonded, the chalcogen–carbon bond distances, and their van der Waals values.

Three types of directional preferences are found around the divalent selenium atoms drawn in the perspective view of 1 and 2 (7 and 8, respectively). Such a view is also shown for 3 (9). The types can be classified by the perspective angle θ shown in 10; I call the direction type A if θ is ca. 90° or less, type B when θ is ca. 180°, and type C with θ = ca. 135°. The structure of 1 consists of type A for the two outside phenylselanyl groups and type B for the central Se–Se group. The methylselanyl and phenylselanyl groups in 2 belong to type C. The chalcogen atoms in methylthio and phenyltelluro groups in 4 and 5 also belong to type C. The p-anisylselanyl group in 3 is one of the typical examples that belongs to type B.
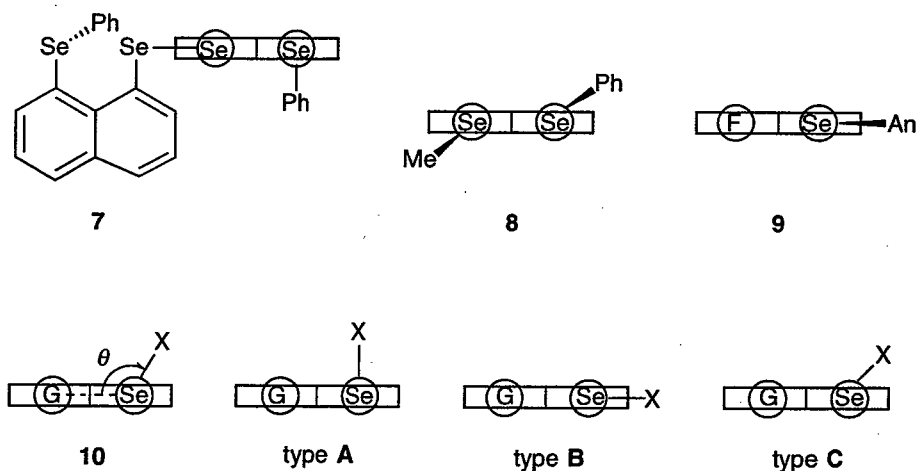
7   8   9

10   type A   type B   type C

Parthasarathy et al. have suggested that there are two types of directional preferences of nonbonded atomic contacts with divalent sulfur, R–S–R'.[11] Type I contacts have S---X directions in RR'S---X where n-electrons of sulfides are located, and type II contacts tend to lie along the extension of one of sulfur's bond. Nearly all type I contacts are with electrophiles, while nearly all type II contacts are with nucleophiles. Electrophiles should interact preferentially with the HOMO and nucleophiles with the LUMO. The type I pattern suggests that the HOMO is essentially sulfur

lone pair extending nearly perpendicular to the R–S–R' plane, while the type II pattern indicates the LUMO of a σ*(S–R) or σ*(S–R') orbital. Similar directional preferences of nonbonded atomic contacts have also been seenshown with divalent selenium.[12] Type A and type **B** of my case belong to type I and type II of Parthasarathy's definitions, respectively, if one recognizes G in **1 0** to be the nucleophile or electrophile. Type **C** is the intermediate between type I and type II or the edge of the type II.

When two divalent selenium atoms are placed in close proximity in space, two types of pairings are suggested to play an important role among a lot of possibilities.[12] The one is the type I and type II pairing, and the other is type III, where the θ values of the paired selenides are almost equal.[17] The structure of **1** is recognized to consist of two sets of the type I and type II pairing with the linear alignment of the four selenium atoms. The type I and type II pairing must be stabilized by the electron donor-acceptor interaction. The p-type lone pairs at the two selenium atoms of the phenylselanyl groups must act as electron donors while the σ*(Se–Se) bond must accept the electrons from the phenylselanyl groups. Since the two 4p-type lone pairs and the σ*(Se–Se) bonds of the 4p atomic orbitals in **1** interact linearly, the interaction should be analyzed by the 4c-6e model of which the four electrons come from the two lone pair orbitals and the two from the σ(Se–Se) bond. The structure of **2**, as well as those of **4** and **5**, belongs to the type III pairing. No special stabilizing factors can be found for the type III pairing in **2**,[12] at first glance. The steric or static repulsion of the selanyl groups may be reduced in the type III pairing. Ab initio MO calculations were performed to elucidate the nature of the 4c-6e bond in **1** and to clarify the stabilizing factors of the type III pairing in **2**.

Scheme 1

(a)   (b)   (c)

model a   model b

(d)

model a

$(\theta_1 = \theta_2 = 90°)$ $(\theta_1 = \theta_2 = 270°)$

58
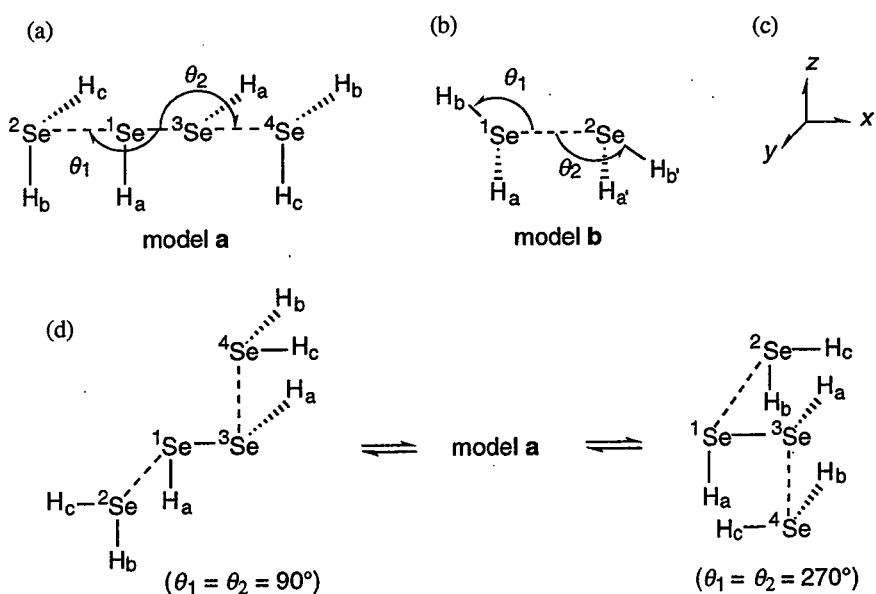
Molecular Orbital Calculations on the Model Compounds of 1 and 2. Why is the linear alignment of the four selenium atoms more stable than the bent forms usually observed in polyselenides?[18] The effective interaction of the 4p-type lone pair orbitals of the outside Se atoms with the 4p-4p σ^* orbital of the Se(1)–Se(3) bond is suggested by the structure of **1**. The factor that stabilizes the structure of **2** is also interesting. Ab initio MO calculations were performed with the 6-311++G(3df,2pd) basis sets of the Gaussian 94 program[19] on the models of **1** and **2** at the HF and MP2 levels. The simplified models, $H_bH_c{}^2Se\text{---}H_a{}^1Se^3SeH_a\text{---}{}^4SeH_bH_c$ (model **a**) and $H_aH_b{}^1Se\text{---}{}^2SeH_aH_b$, (model **b**), are shown in Scheme 1. The rotation around the Se–Ha bonds in model **a** would produce the zigzag alignment of the four selenium atoms; some possibilities are shown in Scheme 1d.

For model **a**, the two 1,8-naphthylidene groups in **1** are replaced by two sets of H_a and H_b; two H_c's stand for phenyl groups. The atomic distances of $r({}^1Se–{}^2Se)$ and $r({}^3Se–{}^4Se)$ were fixed at the averaged value of the corresponding values observed in **1** (3.053 Å). The $\angle{}^1Se^2SeH_b$ and $\angle{}^3Se^4SeH_b$ values and the torsional angle of $H_a{}^1Se^3SeH_a$ were fixed at 90.00°. The torsional angles of $H_b{}^2Se^1SeH_a$ and $H_b{}^4Se^3SeH_a$ were fixed at 0.00°. While the $\angle{}^1Se^3SeH_a$ and $\angle{}^3Se^1SeH_a$ values were fixed at 90.00° for the calculations at the HF level, they were optimized at the MP2 level. Ab initio MO calculations were performed assuming the C_2 symmetry. The $r({}^1Se–{}^3Se)$ and all $r(Se–H)$ values were optimized. The angles θ_1 (and θ_2) and $\angle H_b{}^1SeH_c$ (and $\angle H_b{}^4SeH_c$), were also optimized. The calculations were carried out with or without fixing the torsional angles $H_aH_b{}^2SeH_c$ and $H_aH_b{}^4SeH_c$ at 90.00°, together with fixed at 180.00°. The results are given in Table 5 with the optimized structures shown by **11a**, **11b**, and **11b'**, respectively. Table 5 also contains the results of calculations for the corresponding structures of H_2Se and H_2Se_2. Natural charges of the H and Se atoms of the model and the components were calculated with the natural population analysis.[20] The results are also shown in Table 5.

11a

11b

11b'
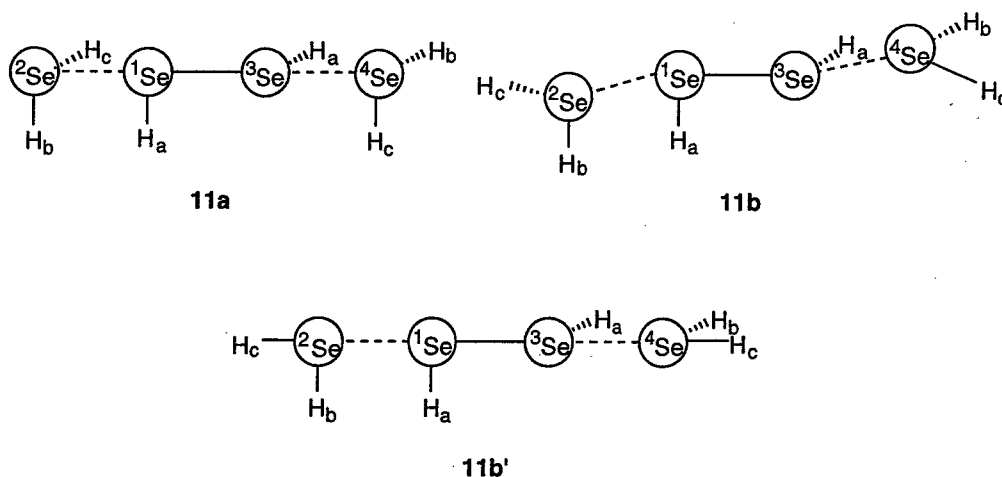
Table 5. Results of the MO Calculations for $H_cH_b{}^2Se$---$^1SeH_a{}^3SeH_a$---$^4SeH_bH_c$ (Model a),[a] SeH_2, and Se_2H_2

	E (au)	r(Se,Se) (Å)	r(Se,H_a) (Å)	r(Se,H_b) (Å)	r(Se,H_c) (Å)	∠SeSeH_a (°)	$\theta_1(=\theta_2)$ (°)	∠SeSeH_c (°)	∠H_bSeH_c (°)	Qn(^{1}Se)	Qn(H_a)	Qn(^{2}Se)	Qn(H_b)	Qn(H_c)
HF/6-311++G(3df,2pd)														
11a[b]	-9602.6928	2.4030	1.4525	1.4533	1.4523	90.00[c]	181.40	90.00[c]	93.17	-0.0988	0.0392	-0.0551	0.0557	0.0590
Δ[d]	0.0307	0.0496	-0.0008	0.0003	-0.0007	0.00[c]		0.00[c]	-0.05	-0.0519	-0.0077	0.0513	0.0025	0.0058
11b[b]	-9602.6966	2.3774	1.4545	1.4538	1.4584	90.00[c]	161.73	151.88	91.91	-0.0606	0.0442	-0.0887	0.0545	0.0506
Δ[d]	0.0269	0.0240	0.0012	0.0008	0.0054	0.00[c]			-1.31	-0.0137	-0.0027	0.0177	0.0013	-0.0028
11b'[b]	-9602.6936	2.3644	1.4544	1.4547	1.4572	90.00[c]	180.00[c]	180.00[c]	90.00[c]	-0.0515	0.0453	-0.1085	0.0542	0.0605
Δ[d]	0.0293	0.0110	0.0011	0.0005	0.0030	0.00[c]			0.00[c]	-0.0046	-0.0016	-0.0034	0.0016	0.0079
Se_2H_2[b]	-4800.7867	2.3534	1.4533			90.00[c]				-0.0469	0.0469			
SeH_2	-2400.9684			1.4530	1.4530	0.00[c]			93.22			-0.1064	0.0532	0.0532
SeH_2	-2400.9681			1.4542	1.4542				90.00[c]			-0.1051	0.0526	0.0526
MP2/6-311++G(3df,2pd)														
11a[b]	-9603.3758	2.3915	1.4637	1.4604	1.4596	96.59	178.68	90.00	91.20	-0.0965	0.0373	-0.0557	0.0551	0.0598
Δ[d]	0.0071	0.0607	-0.0004	0.0013	0.0005	0.48			-0.07	-0.0504	-0.0088	0.0515	0.0015	0.0062
11b[b]	-9603.3771	2.3679	1.4654	1.4607	1.4656	96.00	161.14	144.08	90.23	-0.0656	0.0419	-0.0831	0.0546	0.0522
Δ[d]	0.0058	0.0371	0.0013	0.0016	0.0065	-0.11			-1.04	-0.0195	-0.0042	0.0241	0.0010	-0.0014
11b'[b]	-9603.3721	2.3710	1.4646	1.4609	1.4649	90.00[c]	180.00[c]	180.00[c]	90.00[c]	-0.0536	0.0474	-0.1109	0.0553	0.0619
Δ[d]	0.0088	0.0163	0.0025	0.0053	0.0053	0.00[c]			0.00[c]	-0.0051	-0.0011	-0.0041	0.0019	0.0085
Se_2H_2	-4801.1059	2.3308	1.4640			96.11				-0.0461	0.0461			
Se_2H_2[b]	-4801.1059	2.3308	1.4641			96.11				-0.0461	0.0461			
Se_2H_2[b]	-4801.1041	2.3547	1.4621			90.00[c]				-0.0485	0.0485			
SeH_2	-2401.1385			1.4591	1.4591				91.27			-0.1072	0.0536	0.0536
SeH_2	-2401.1384			1.4596	1.4596				90.00[c]			-0.1068	0.0534	0.0534

[a] r(^{2}Se,^{1}Se) and r(^{3}Se,^{4}Se) being fixed at 3.053 Å. [b] Torsional angle HSeSeH and ∠SeSeH of the Se_2H_2 moiety being fixed at 90.00°. [c] Fixed at the given value. [d] Values corresponding to the formation of the adduct from its components.

Table 6. Natural Charges (Qn) in $H_2{}^1Se\text{---}{}^2SeH_2$ (Model b) and SeH_2 Calculated with the 6-311++G(3df,2pd) Basis Sets[a]

	Level	E (au)	$r(Se,H_a)$ (Å)	$r(Se,H_b)$ (Å)	$\theta_1(=\theta_2)$ (°)	$\angle H_aSeH_b$ (°)	$Qn(^1Se)$	$Qn(H_a)$	$Qn(H_b)$
12a	HF	-4801.9013	1.4521	1.4467	74.18	93.65	-0.1000	0.0489	0.0511
Δ		0.0355	-0.0009	-0.0063		0.43	0.0064	-0.0043	-0.0021
12b	HF	-4801.9222	1.4542	1.4587	158.95	91.64	-0.0986	0.0511	0.0476
Δ		0.0146	0.0012	0.0057		-1.58	0.0078	-0.0021	-0.0056
SeH₂	HF	-2400.9684	1.4530	1.4530		93.22	-0.1064	0.0532	0.0532
12a	MP2	-4802.2516	1.4589	1.4536	72.72	91.63	-0.1012	0.0492	0.0520
Δ		0.0254	-0.0002	-0.0055		0.36	0.0060	-0.0044	-0.0016
12b	MP2	-4802.2714	1.4608	1.4665	157.43	89.77	-0.0995	0.0522	0.0474
Δ		0.0056	0.0017	0.0074		-1.50	0.0077	-0.0014	-0.0062
SeH₂	MP2	-2401.1385	1.4591	1.4591		91.27	-0.1072	0.0536	0.0536

[a] The C_2 symmetry was postulated and $r(^2Se,^1Se)$ being fixed at 3.070 Å.

The optimized structures of model **a** at the MP2 level are as follows. The θ_1 (= θ_2) was 178.68° (**11a**) when the calculations were performed with the torsional angles $H_aH_b^2SeHc$ and $H_aH_b^4SeH_c$ being fixed at 90.00°. Whereas the θ_1 (= θ_2) and the torsional angles $H_aH_b^2SeH_c$ and $H_aH_b^4SeH_c$ were evaluated to be 161.14° and 144.08°, respectively, if the torsional angles were not fixed (**11b**). The MO calculations were also carried out on model **a** with $\theta1$ (= $\theta2$) and the torsional angle $H_aH_b^2SeH_c$ (and $H_aH_b^4SeH_c$) being fixed at 180.00° (**11b'**).

The 1,8-naphthylidene group in **2** is replaced by H_a and $H_{a'}$ and the methyl and phenyl groups are by H_b and $H_{b'}$, respectively, in model **b**. The $\angle^2Se^1SeH_b$ and $\angle^1Se^2SeH_{b'}$ are shown by θ_1 and θ_2, respectively. The r(^1Se–^2Se) was fixed at the averaged value of the two structures observed in **2** (3.070 Å). The $\angle^1Se^2SeH_{a'}$, $\angle^2Se^1SeH_a$, and the torsional angle of $H_a^1Se^2SeH_{a'}$ were fixed at

12a   12b   12c
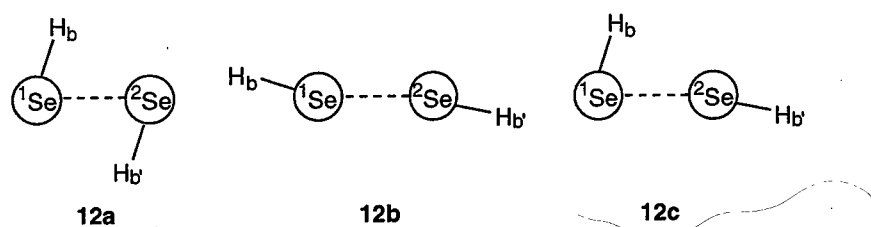
90.00°, 90.00°, and 0.00°, respectively. The angles, $\angle^2Se^1SeH_b$ (θ_1), $\angle^1Se^2SeH_{b'}$ (θ_2), $\angle H_a^1SeH_b$, and $\angle H_{a'}^2SeH_{b'}$, and the r(Se–H) values were optimized.

The results of the calculations are collected in Table 6. There were two energy minima for θ_1 (=θ_2) = 72.72° (**12a**) and θ_1 (= θ_2) = 157.43° (**12b**) if the calculations were performed with the 6-311++G(3df,2pd) basis sets at the MP2 level. The structure **12c**, for which θ_1 and θ_2 are close to 72° and 157°, respectively, might also be an energy minimum, since the adduct is expected to be the type I and type II pairing proposed by Parthasarathy and his coworkers,[12] which could be stabilized by the electron donor-acceptor interaction. However, the optimized structure was **12b** when the calculations were started from θ_1 =72.7° and θ_2 = 157.4° at the MP2 level. As shown in Table 6, calculations at the HF level gave essentially the same results. Natural charges of the H and Se atoms in **12a** and **12b** were also calculated with the natural population analysis,[20] which are also shown in Table 6.

Molecular orbitals were drawn using the MacSpartan program[21] with 3-21G[(*)] basis sets employing the structures calculated with the 6-311++G(3df,2pd) basis sets at the MP2 level in Table 5 (**11a** and **11b'**). Figures 3 and 4 depict the molecular orbitals of **11a** and **11b'**, respectively. The molecular orbitals of **11b** were essentially the same as those of **11b'**, although not shown. Figure 5 shows the energy diagram in the formation of **12a** and **12b** from $2H_2Se$, which also contains some molecular orbitals drawn using the program with 3-21G[(*)] basis sets for the structures calculated with the 6-311++G(3df,2pd) basis sets at the MP2 level shown in Table 6. Table 7 shows the
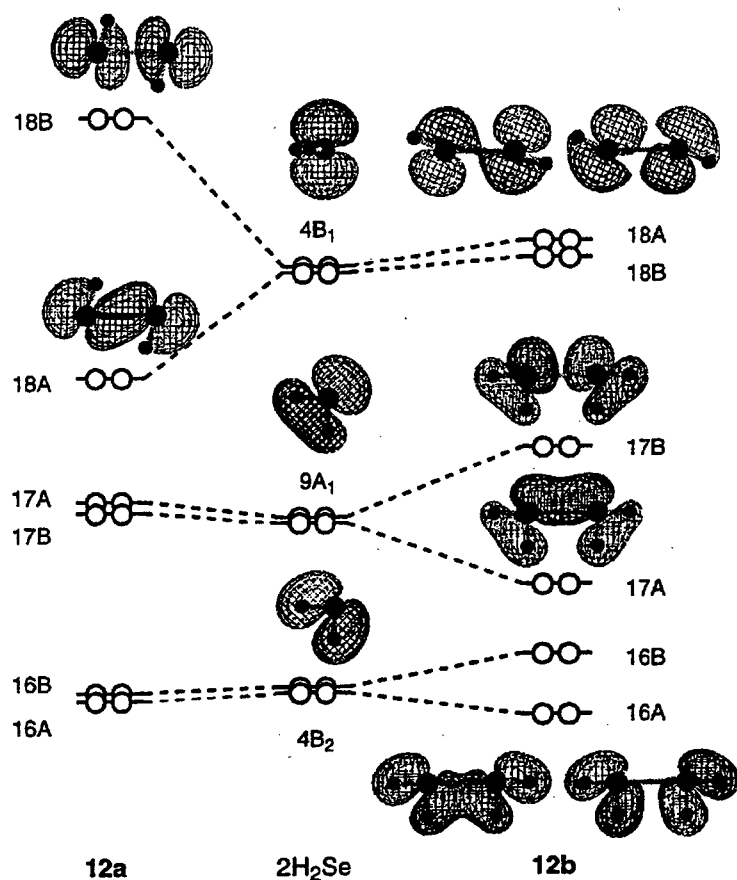
energies of some orbitals for **12a**, **12b**, and H_2Se calculated with the 6-311++G(3df,2pd) basis sets at the MP2 level.
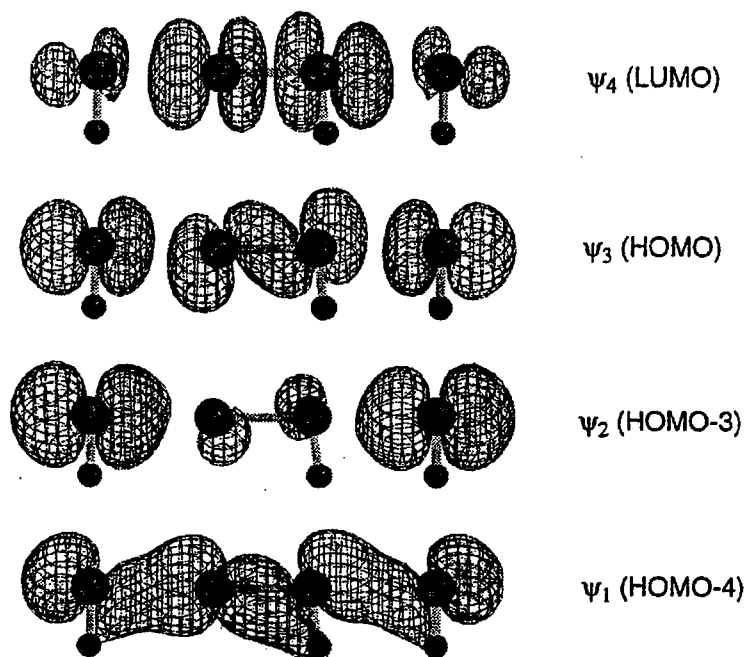
Figure 3. The 4c-6e model for the four linear Se atoms with molecular orbitals being drawn for **11a** (see Table 5).
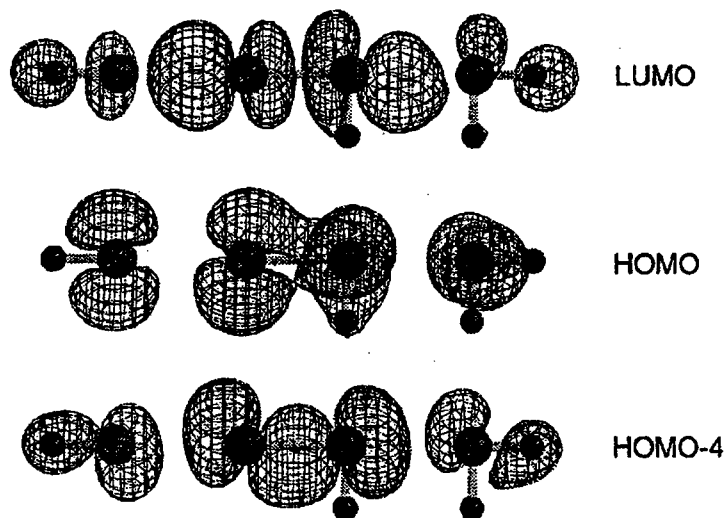
Figure 4. Molecular orbitals of linear H−Se⋯Se−Se⋯Se−H bond in **11b′**.

63

Figure 5. Energy diagram for the formation of **12a** and **12b** from 2H₂Se, together with some molecular orbitals of the species.

Table 7. Energies and Characters of Molecular Orbitals of H₂Se, 12a, and 12b Calculated with the 6-311++G(3df,2pd) Basis Sets at the MP2 Level[a]

H₂Se	12a	12b
-9.80 (4B1)	-8.00 (18B)	-9.57 (18A)
	-11.17 (18A)	-9.85 (18B)
	(-9.58 (av))	(-9.71 (av))
-13.03 (9A1)	-12.79 (17A)	-12.11 (17B)
	-12.95 (17B)	-13.92 (17A)
	(-12.87 (av))	(-13.01 (av))
-15.13 (4B2)	-15.13 (16B)	-14.85 (16B)
	-15.16 (16A)	-15.55 (16A)
	(-15.15 (av))	(-15.20 (av))

[a] In electronvolts.

Before discussion of the nature of the 4c-6e bond in **1**, I would like to discuss the case of **2** first. As shown in Table 6, two structures, **12a** and **12b**, were found to be the energy minima. The structure **12b** was more stable than **12a** by 0.0198 au (52.0 kJ mol^{-1}), and the former was less stable than two H_2Se molecules by 0.0056 au (14.7 kJ mol-1) at the MP2 level.[22] The natural charges at the Se, H_a, and H_b atoms (Qn(Se), Qn(H_a), and Qn(H_b), respectively) in **12a** became more positive, negative, and negative by 0.0060, 0.0044, and 0.0016, respectively, relative to those of the corresponding atoms of H_2Se at the MP2 level. On the other hand, the charges at the atoms in **12b** were estimated to be more positive, negative, and negative by 0.0077, 0.0014, and 0.0062, respectively, the similar calculations. These results suggest that the lone pair–lone pair interaction between selenium atoms in the almost linear alignment of H_b–Se---Se–H_b in **12b** expels electrons of the Se atoms to the H_b atoms while the H_a atoms accept electrons more effectively in **12a** than in **12b**. The results obtained at the HF level were almost the same as those obtained at the MP2 level.

As shown in Figure 5, the interaction between the p-type lone pairs (4B$_1$ of H_2Se) in **12a** forms σ- and σ*-type orbitals (18A and 18B, respectively) while that in **12b** gives π- and π*-type orbitals (18B and 18A, respectively). The interaction in **12a** is stronger than that in **12b**. The π-type orbitals extend more effectively on the H_b atoms than the σ-type orbitals in **12a**. The orbitals extend on the H_a atoms more effectively in **12a** than in **12b**, although not shown. This may be a reason that the H_a atoms in **12a** and the H_b atoms in **12b** accept electrons effectively. On the other hand, the 9A$_1$ (the σ-type lone pair) and 4B$_2$ orbitals of H_2Se interact more effectively in **12b** than in **12a** (17A,B and 16A,B, respectively). Such interactions in **12b** can be characterized by the σ-type 4p$_x$-4p$_x$ orbitals extending over the adduct containing the almost linear H_b–Se---Se–H_b framework. Molecular orbitals in **12a** are complex and difficult to be understand by a simple image, so they are not depicted except 18A and 18B.
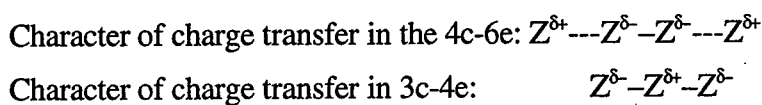
The energy difference between 18A and 18B and the averaged value for the two orbitals is larger in **12a** than in **12b**, as shown in Table 7. The interaction between the two 4B$_1$ orbitals of 2H$_2$Se should be larger in the σ-type overlap in **12a** than in the π-type overlap in **12b**, resulting in the larger energy difference in the former than in the latter.[23] The larger overlap integral in the σ-type interaction must cause the larger exchange repulsion[24] in **12a** relative to **12b**, since the two 4B$_1$ orbitals are filled with two electrons, which would be the reason why the averaged energy of 18A and 18B in **12a** is larger than that in **12b**, and that, in turn, would be the reason why **12a** is estimated to be less stable than **12b**. The severe exchange repulsion pointed out in the σ-type interaction in **12a**[25] must be avoided in the distorted π-type interaction in **12b**.

If the two orbitals, 18A and 18B, are filled only with only three electrons, the total energy of the σ- and σ*-orbitals in **12a** would significantly reduced and they would be more stable than the π- and π*-orbitals in **12b**. (The total energies of the two orbitals in **12a** and **12b** would be the same if 0.32

electrons were taken away from the orbitals of the model.) Such orbital interactions are predicted for 4c-6e in **11a**, which will be discussed later. Although the 17A,B and 16A,B in **12b** are constructed based on the typical σ-type interactions, the orbitals are evaluated to be not so destabilized, since the orbitals extend not only over the two Se atoms but also over the four hydrogens. The contribution of the vacant orbitals to the 17A,B and 16A,B in **12b** should also reduce their energies.

After establishment of the character of the lone pair–lone pair interaction in model **b**, I would like to examine the nature of the chemical bond in model **a**. As shown in Table 5, two energy minima, **11a** and **11b**, were found at the MP2 level.[26] Although **11a** was evaluated to be less stable than **11b** by 0.0013 au (3.4 kJ mol^{-1}), the structure **11a** reproduced well the observed X-ray crystallographic results of **1**. The two phenyl groups in **1** must play an important role for **1** to form a 4c-6e structure: the p-type lone pairs of the Se atoms of the phenylselanyl groups can interact with the π-orbitals of the phenyl group, and the interaction must be highly effective if the phenyl rings in **1** are perpendicular to the linear four Se atoms. The orientation of the phenyl groups in **1** satisfies the requirement of the orbital interaction in model **a**. The phenyl groups may also accept some electrons from the p-type lone pairs of the selenium atoms in **1**. The optimized structure of **11a** depicts that the linear alignment of the four Se atoms in **1** must be due to the energy-lowering effect of the linear alignment rather than the crystal-packing effect in the crystal. The role of the phenyl groups will be examined by the MO calculations on model **c**.

As shown in Table 5, the central Se–Se distance (r(^{2}Se,^{3}Se)) in **11a** becomes longer relative to that of Se$_2$H$_2$ by 0.06 Å, which strongly suggests that the charge transfer must take place from the outside Se atoms to the central σ*(Se–Se) bond. The natural population analysis revealed the character of the charge transfer in the adducts; the Qn(^{1}Se) and Qn(^{2}Se) values of **11a** become more negative and positive, respectively, relative to those of the Se$_2$H$_2$ and SeH$_2$ by ca 0.05. The Qn(H) values of Se$_2$H$_2$ and SeH$_2$ changed similarly to those of the Se atoms to which hydrogens were joined, although the magnitudes were smaller. These results strongly support the idea that the character of the charge transfer in **11a** is that from the two outside Se atoms (or SeH$_2$ molecules) to the central σ*(Se–Se) bond (or the central Se$_2$H$_2$). The bond constructed by the four Se atoms can be well described with the 4c-6e model. The character of the charge transfer in the 4c-6e model in **11a** is very different from that of the 3c-4e model.[27] The character in the 3c-4e model is that from the central atom to the outside ligands, which forms a highly polar hypervalent bond.

Character of charge transfer in the 4c-6e: $Z^{\delta+}$---$Z^{\delta-}$–$Z^{\delta-}$---$Z^{\delta+}$

Character of charge transfer in 3c-4e: $Z^{\delta-}$–$Z^{\delta+}$–$Z^{\delta-}$

The molecular orbitals constructed by the linearly aligned four Se atoms are depicted in Figure 3 exemplified by **11a**. The molecular orbitals are mainly constructed by the σ-type interactions

between two p_x-orbitals of the outside Se atoms (np_x(Se)) and the σ(Se–Se) and σ^*(Se–Se) orbitals of the central Se atoms, yielding four new molecular orbitals, ψ_1, ψ_2, ψ_3, and ψ_4. The ψ_1 orbital mainly consists of the $\sigma(^1Se-^3Se)$ orbital and the two np_x(Se) orbitals without any nodal plane between the Se atoms. The ψ_2 orbital extends over the two np_x orbitals of the outside Se atoms with smaller extension over the central Se atoms. The ψ_3 orbital, which is the HOMO, also mainly consists of the $\sigma(^1Se-^3Se)$ orbital and the two np_x(Se) orbitals with two nodal planes between the Se–Se bonds. The ψ_4 orbital (LUMO) has the contribution of the $\sigma^*(^1Se-^3Se)$ orbital with the smaller contributions of the two np_x(Se) orbitals. These results, containing the fact that the ψ_3 and ψ_4 are the HOMO and the LUMO, respectively, show that the bond should be analyzed by the 4c-6e model.[27]

The calculations on model **a** gave another minima, shown as **11b**. Some molecular orbitals of the linear H_c–Se---Se–Se---Se–H_c bond in **11b'** are shown in Figure 4, which are essentially the same as those of **11b**. The linear molecular orbitals are constructed by the interactions between the central σ(Se–Se) and σ^*(Se–Se) orbitals and the $9A_1$ and $4B_2$ orbitals of the outside H_2Se in **11b'**. Indeed, the LUMO and HOMO-4 orbitals extend mainly over the linear H_c–Se---Se–Se---Se–H_c atoms, but other orbitals are contributed by the atomic orbitals perpendicular to the line or on the H_a (and H_b) atoms. Therefore, it would not be suitable for the linear H_c–Se---Se–Se---Se–H_c bond to be analyzed by the 6c-6e model based on the MO calculations. The character of charge transfer in the formation of **11b'** is from the outside H_c to the four Se atoms, accompanied by the enlarged r(Se–H) and r(Se–Se) values, although the magnitudes are small. The character of the charge transfer in the formation of **11b** is similar to that in the case of **11a**, except for H_c. The interpretation based on the 4c-6e model may also be valid for the four Se atoms even in **11b**.

Scheme 2
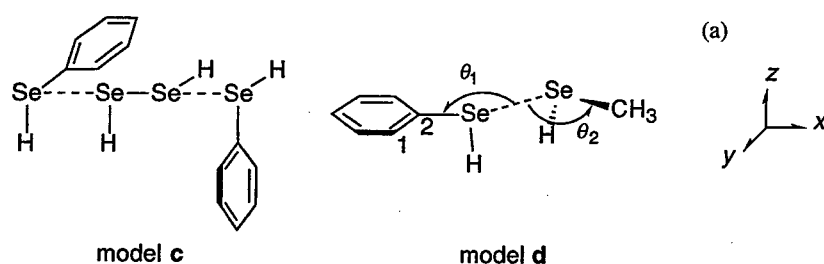
model c   model d

The effects of the π-orbitals of the phenyl groups on the 4c-6e bond in **1** and the 2c-4e bond in **2** were also examined. Ab initio MO calculations were performed on the adducts, PhSeH---HSeSeH---HSePh (model **c**) and PhSeH---HSeMe (model **d**), where naphthylidene groups in **1** and **2** were replaced by hydrogens, with the 6-311+G(d,p) basis sets at the DFT (B3LYP) level. Scheme 2 shows the structures of model **c** and model **d**, together with the axes (cf. Scheme 2a). The four Se atoms in model **c** were placed on the x-axis, its six Se-X (X = H and C) bonds were in the y-

or z-direction, and the two phenyl planes were on the yz-plane. The nonbonded r(Se,Se) values were fixed at 3.053 Å. Meanwhile, benzeneselenol was also calculated as the planar structure by the same method with the CSeH angle being fixed at 90.00°. The structure of the phenyl group was employed in the calculations of model **c** without further optimization. The six Se–X and the central Se–Se bond distances were optimized. While the r(Se,Se) value of the HSeSeH moiety in model **c** became larger than that of free HSeSeH, the r(Se,C) and r(Se,H) values of the PhSeH groups were coincidentally the same for both the adduct and the free compound. The C(1), C(2), Se(Ph), Se(Me), and C(Me) atoms in model **d** were placed on the xy plane with the Se---Se distance being fixed at 3.070 Å. The torsional angle between the Se–H and C(1)–C(2) bonds in PhSeH was assumed to be 90.00°. Other values containing the torsional angles in the phenyl plane were optimized. The θ_1 and θ_2 values in model **d** were optimized to be 153.80 and 153.82°, respectively, and the r(Se,C) values became larger relative to those of the free components. The slight deviation from the xy plane was also observed for the phenyl group. The results are summarized in Table 8.

The new molecular orbitals produced by the interaction between the 4c-6e orbitals (ψ_i) and the π-orbitals of the phenyl groups in **1** are shown by $\psi_{i'}$, named after ψ_i. The π-orbitals interact effectively with ψ_2 and ψ_3; they hardly interact with ψ_4 and interact a little with ψ_1, which also interacts with the Se–C σ-orbitals. Figure 6 shows $\psi_{1'}$, $\psi_{2'}$, $\psi_{3'}$, and $\psi_{4'}$ for model **c**. Figure 7 shows the HOMO and HOMO-1 for model **d**. The π-orbitals do not interact with the 2c-4e orbitals due to the orthogonality of the two systems. The p-type lone–pair orbitals in model **d** are estimated to interact only weakly with each other, which may be due to the energy difference caused by the methyl and phenyl groups compared with that of H_2Se. (The energies of p-type lone pairs in HSeH, MeSeH, and PhSeH are evaluated to be -0.2523, -0.2309, and -0.2391 au, respectively, with the 6-311+G(d,p) basis sets at the B3LYP level.) The structure of model **d** demonstrates that the type C structure of **2** must come from the 2c-4e interaction in the bis-selenide. The 2c-4e orbitals in **2** are thought again to interact more easily with the naphthyl π-system than with the phenyl π-system.
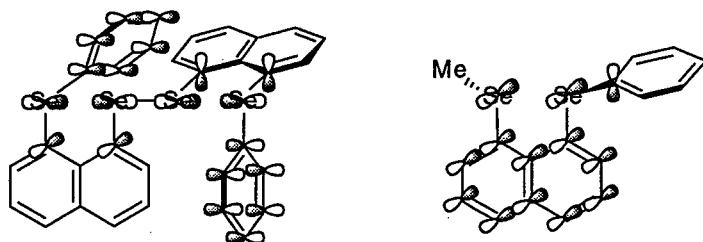
Table 8. Optimized Structures for PhSeH---HSeSeH---HSePh (Model c) and PhSeH---HSeMe (Model d) Calculated with the 6-311+G (d,p) Basis Sets at the B3LYP Level, Together with the Related Compounds

	E (au)	PhSeH			HSeSeH		MeSeH		
		r(Se,C) (Å)	r(Se,H) (Å)	∠CSeH (°)	r(Se,Se) (Å)	r(Se,H) (Å)	r(Se,C) (Å)	r(Se,H) (Å)	∠CSeH (°)
model c[a]	-10072.0134	1.9401	1.4707	90.00[b]	2.4827	1.4733			
PhSeH	-2633.8543	1.9401	1.4707	90.00[b]					
HSeSeH[c]	-4804.3167				2.3964	1.4743			
Δ	0.0123	0.0000	0.0000	0.00	0.0863	-0.0010			
model d[d]	-5075.9233	1.9616	1.4749	94.43			1.9889	1.4729	94.28
PhSeH	-2633.8550	1.9508	1.4753	95.20					
MeSeH	-2442.0760						1.9776	1.4732	95.19
Δ	0.0077	0.0108	-0.0004	-0.77			0.0133	-0.0003	-0.91

[a] The nonbonded r(Se,Se) value was fixed at 3.053 Å. [b] The ∠CSeH value was fixed at 90.00°. [c] The ∠SeSeH value and the torsional angle ∠HSeSeH were fixed at 90.00°. [d] The nonbonded r(Se,Se) value was fixed at 3.070 Å and the θ_1 and θ_2 values in Scheme 2 were optimized to be 153.80° and 153.82°, respectively.

ψ_4' (LUMO)

ψ_3'-2 (HOMO)

ψ_2'-2
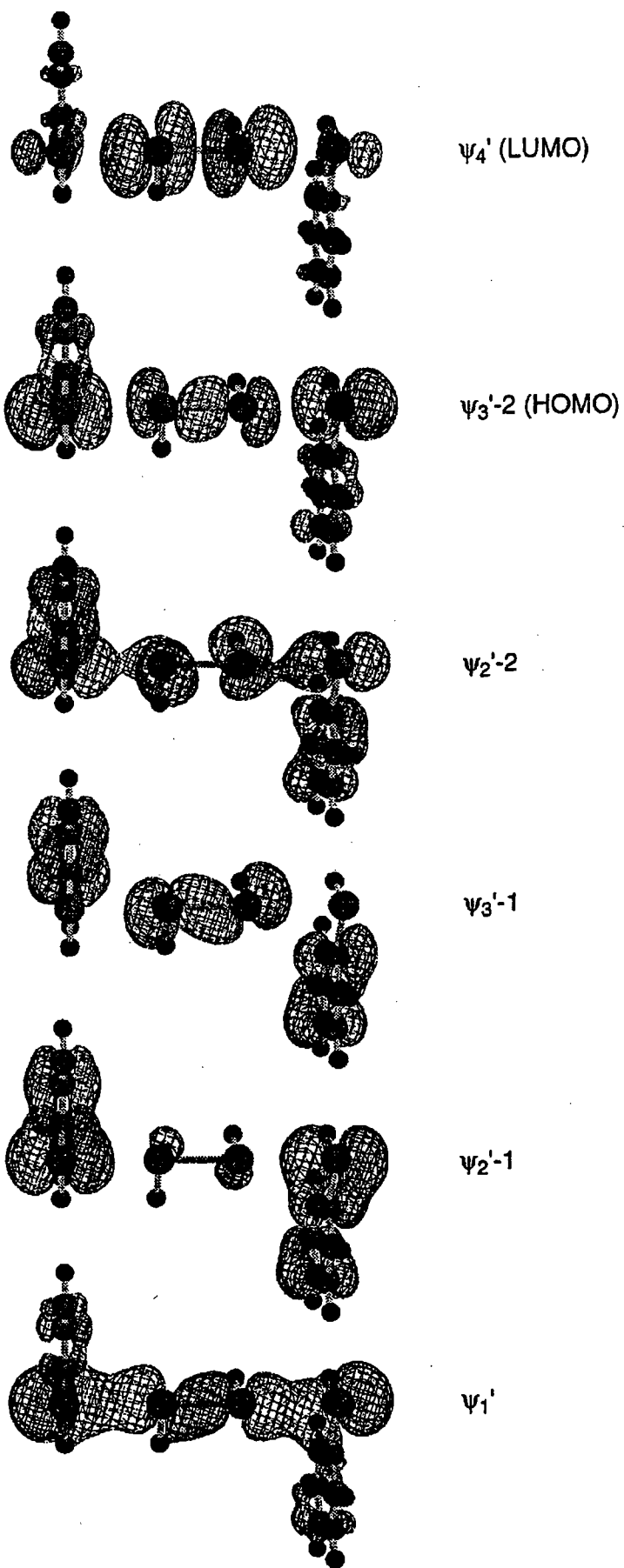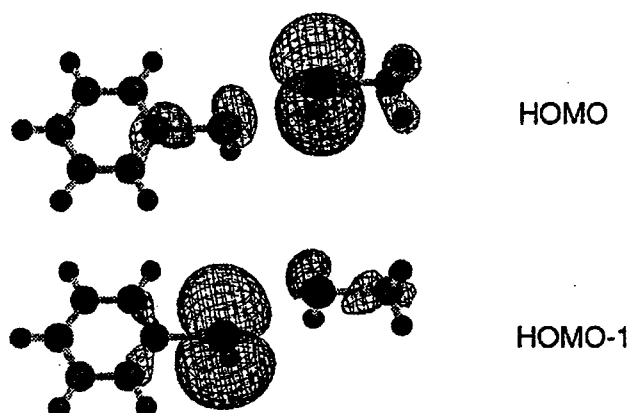
ψ_3'-1

ψ_2'-1

ψ_1'

Figure 6. Some molecular orbitals in model c.

Figure 7. HOMO and HOMO-1 in model d.

Alvarez et al. discussed the interaction of two bromine molecules to form a Br_2 dimer, which reacts with strong electron donors such as alkali metals to form the $Br_4{}^{2-}$ adduct.[28] If the four Br atoms in the Br_2 dimer align linearly, the linear bond can be analyzed by the 4c-4e model where the four Br atoms interact as Br–Br---Br–Br. On the other hand, for the four Br atoms in the $Br_4{}^{2-}$ adduct the linear bond constructed by the four Br atoms can be analyzed with the 4c-6e model, for which interaction must be [Br---Br–Br---Br]$^{2-}$. The bonding scheme of the 4c-6e model in the $Br_4{}^{2-}$ adduct is very similar to that constructed by the linear four Se atoms discussed above. The bonding scheme in $I_4{}^{2-}$ ion must also be analyzed by the 4c-6e model.[29] Furukawa and co-workers reported the structure of 1,5-dithioniabicyclo[3.3.0]octane bis(trifluoromethanesulfonate).[3b] In this structure, the two gegen anions located on the direction of the S^+--S^+ bond to form a linear CF_3SO_3---S^+--S^+---O_3SCF_3 bond. The linear alignment of the XO$^-$--S^+–S^+---O$^-$X bond shows that there are two energy minima for the two anionic species in the direction of the dicationic S–S bond, which may also be explained by the 4c-6e model. The X--Z--Z--X bonds constructed with chalcogens and halogens such as the I–Te–Te–I[30] bond might also be analyzed by the model if the bonds are linear. The linear bonds constructed by more than four atoms[31-33] and macro-cyclic frameworks34 are also reported.

Novel properties caused by the linear 4c-6e bond have been of interest. Such properties were looked for and I have examined the susceptibility of the substituent effect on ^{77}Se NMR chemical shifts of the atoms constructing the bond. Ab initio MO calculations containing nonbonded interactions are also in progress. The results will be presented elsewhere.

Experimental Section

Chemicals were used without further purification unless otherwise noted. Solvents were purified by standard methods. Melting points were uncorrected. ^{1}H, ^{13}C, and ^{77}Se NMR spectra were measured at 400, 100, and 76 MHz, respectively. The ^{1}H, ^{13}C, and ^{77}Se chemical shifts are

given in ppm relative to those of internal CHCl₃ slightly contaminated in the solution, CDCl₃ as the solvent, and external MeSeMe, in the three types of spectroscopy respectively. Column chromatography was performed on silica gel (Fujidebison BW-300) and acidic alumina (E. Merck).

Bis[8-(phenylselanyl)naphthyl]-1,1'-diselenide (1). To a solution of the dianion of naphto[1,8-*c,d*]-1,2-diselenol, which was prepared by reduction of the diselenol with $NaBH_4$ in an aqueous THF solution, was added benzenediazonium chloride at low temperature. After a usual workup, the solution was chromatographed on silica gel containing acidic alumina. Recrystallization of the chromatographed product from hexane gave **1** as a yellow solid in 66 % yield, mp 161-163 °C: ¹H NMR (CDCl₃, 400 MHz) 7.10-7.20 (m, 8H), 7.20-7.27 (m, 4H), 7.35 (t, 2H, $J = 7.6$ Hz), 7.66 (br.d, 2H, $J = 7.8$ Hz), 7.85 (br.d, 2H, $J = 7.3$ Hz), 7.96 (dd, 2H, $J = 7.4$ and 1.0 Hz), 8.08 (br.d, 2H, $J = 6.8$ Hz); ¹³C NMR (CDCl₃, 100 MHz) 125.87, 126.66, 126.69, 127.55, 128.17, 129.26, 130.31, 130.38, 130.99, 132.24, 135.54, 135.74, 136.25, 138.98; ⁷⁷Se NMR (CDCl₃, 76 MHz) 429.0, 534.2 (4*J*(Se,Se) = 341.4 Hz). Anal. Calcd for $C_{32}H_{22}Se_4$: C, 53.21; H, 3.07. Found: C, 53.12; H, 3.09.

1-(Methylselanyl)-8-(phenylselanyl)naphthalene (2). The diselenide **1** was reduced by $NaBH_4$ in an aqueous THF solution then allowed to react with methyl iodide giving **2** (Y=H) as a white solid in 87 % yield, mp 101.5 - 102.5 °C: ¹H NMR (CDCl₃: 400 MHz) δ 2.34 (s, 3H, J (Se,H) = 14.1Hz), 7.19-7.25 (m, 4H), 7.34 (t, 1H, $J = 7.8$ Hz), 7.37-7.42 (m, 2H), 7.63 (dd, 1H, $J = 7.3$ and 1.4 Hz), 7.70 (dd, 1H, $J = 8.0$ and 1.0 Hz), 7.71 (dd, 1H, $J = 8.0$ and 1.1 Hz), 7.73 (dd, 1H, $J = 6.8$ and 1.2 Hz); ¹³C NMR (CDCl₃, 100 MHz) 13.38 ($J = 72.8$ and 16.6 Hz), 125.86, 125.92, 127.29, 128.30, 129.22, 129.32, 131.21, 131.94, 132.37, 133.13 ($J = 11.5$ Hz), 135.29, 135.31, 135.54, 135.80; ⁷⁷Se NMR (CDCl₃, 76 MHz) 434.3, 235.4 (4*J*(Se,Se) = 322.4 Hz). Anal. Calcd for $C_{17}H_{14}Se_2$: C, 54.27; H, 3.75. Found: C, 54.33; H, 3.73.

X-ray Structural Determination. X-ray diffraction data were collected on a Rigaku AFC7R four circle diffractometer with graphic monochromated Cu Kα radiation (λ = 1.54178 Å) and a Mac Science MXC18 machine with graphic monochromated Mo Kα radiation (λ = 0.71069 Å) for **1** and **2**, respectively. The scan type was the *ω*–2θ method. The structure was solved by direct methods (SHELXS86[35]) and refined by the full-matrix least-squares method using the teXsan[36] program. Anisotropic thermal parameters were employed for non-hydrogen atoms and isotropic parameters were used for hydrogens. The positional and thermal parameters of some hydrogen atoms in the Fourier map in **2** were fixed during the refinement. The function minimized was $\Sigma[\omega(|F_o|-|F_c|)^2]$, where $\omega = (\sigma_c^2|F_o|)^{-1}$. Additional crystal and analysis data are listed in Table 1.

MO Calculations. Ab initio molecular orbital calculations were performed on a Power Challenge L computer using the Gaussian 94 program with the 6-311++G(3df,2pd) basis sets at the

72

HF and MP2 levels. The 6-311+G(d,p) basis sets at the DFT (B3LYP) level were also employed for the calculations of models containing the phenyl group(s) and the related compounds. The molecular orbitals in Figures 3 - 7 were drawn by a Power Macintosh 8500/180 personal computer using the MacSpartan Plus program (version 1.0) with 3-21G$^{(*)}$ basis sets.

References and Notes

(1) Topson, R. D. *The Nature and Analysis of Substituent Electronic Effects*, in *Progress in Physical Organic Chemistry*, ed by Taft, R. W. John Wiley & Sons, Vol. 12, New York, 1976. See also refs cited therein.

(2) Bernardi, F.; Csizmadia, I. G.; Mangini, A. (Eds.), *Organic Sulfur Chemistry: Theoretical and Experimental Advances*, Elsevier Scientific, Amsterdam, 1985. See also refs cited therein.

(3) (a) Asmus, K.-D. *Acc. Chem. Res.*, **1979**, *12*, 436; Musker, W. K. *Acc. Chem. Res.*, **1980**, *13*, 200; (b) Fujihara, H.; Furukawa, N. *J. Mol. Struct. (Theochem)*, **1989**, *186*, 261.

(4) (a) Fujihara, H.; Ishitani, H.; Takaguchi, Y.; Furukawa, N. *Chem. Lett.* **1995**, 571. (b) Fujihara, H.; Yabe, M.; Chiu, J.-J.; Furukawa, N. *Tetrahedron Lett.* **1991**, *32*, 4345. Furukawa, N.; Fujii, T.; Kimura, T.; Fujihara, H. *Chem. Lett.* **1994**, 1007. (c) Fujihara, H.; Saito, R.; Yabe, M.; Furukawa, N. *Chem. Lett.* **1992**, 1437.

(5) (a) Glass, R. S.; Andruski, S. W.; Broeker, J. L. *Rev. Heteroatom Chem.* **1988**, *1*, 31. (b) Glass, R. S.; Andruski, S. W.; Broeker, J. L.; Firouzabadi, H.; Steffen, L. K.; Wilson, G. S. *J. Am. Chem. Soc.* **1989**, *111*, 4036. (c) Glass, R. S.; Adamowicz, L.; Broeker, J. L. *J. Am. Chem. Soc.* **1991**, *113*, 1065.

(6) (a) Nakanishi, W. *Chem. Lett.* **1993**, 2121. (b) Nakanishi, W.; Hayashi, S.; Toyota, S. *J. Chem. Soc., Chem. Comm.* **1996**, 371. (c) Nakanishi, W.; Hayashi, S.; Yamaguchi, H. *Chem. Lett.* **1996**, 947. (d) Nakanishi, W.; Hayashi, S.; Sakaue, A.; Ono, G.; Kawada, Y. *J. Am. Chem. Soc.* **1998**, *120*, 3635.

(7) (a) Mallory, F. B. *J. Am. Chem. Soc.* **1973**, *95*, 7747. (b) Mallory, F. B.; Mallory, C. W.; Fedarko, M.-C. *J. Am. Chem. Soc.* **1974**, *96*, 3536. (c) Mallory, F. B.; Mallory, C. W.; Ricker, W. M. *J. Am. Chem. Soc.* **1975**, *97*, 4770. Mallory, F. B.; Mallory, C. W.; Ricker, W. M. *J. Org. Chem.* **1985**, *50*, 457. Mallory, F. B.; Mallory, C. W.; Baker, M. B. *J. Am. Chem. Soc.* **1990**, *112*, 2577. (d) Ernst, L.; Ibrom, K. *Angew. Chem. Int. Ed. Engl.* **1995**, *34*, 1881. Ernst, L.; Ibrom, K.; Marat, K.; Mitchell, R. H.; Bodwell, G. J.; Bushnell, G. W. *Chem. Ber.* **1994**, *127*, 1119.

(8) Mallory, F. B.; Luzik, Jr., E. D.; Mallory, C. W.; Carroll, P. J. *J. Org. Chem.* **1992**, *57*, 366. Mallory, F. B.; Mallory, C. W. *J. Am. Chem. Soc.* **1985**, *107*, 4816.

(9) Johannsen, I.; Eggert, H. *J. Am. Chem. Soc.* **1984**, *106*, 1240. Johannsen, I.; Eggert, H.; Gronowitz, S.; Hörnfeldt, A.-B. *Chem. Scr.* **1987**, *27*, 359. Fujihara, H.; Mima, H.; Erata, T.; Furukawa, N. *J. Am. Chem. Soc.* **1992**, *114*, 3117.

(10) Albright, T. A.; Burdett, J. K.; Whangbo, M.-H. *Orbital Interactions in Chemistry*, Wiley-Interscience, New York, 1985.

(11) Rosenfield, Jr., R. E.; Parthasarathy, R.; Dunitz, J. D. *J. Am. Chem. Soc.* **1977**, *99*, 4860.

(12) Ramasubbu, N.; Parthasarathy, R. *Phosphorus Sulfur* **1987**, *31*, 221.

(13) Although the discussion is focused on structure **A**, it is also valid on structure **B**.

(14) Marsh, R. E.; *Acta Cryst.*, **1952**, *5*, 458; Kruse, F. H.; Marsh, R. E.; McCullough, J. D. *Acta Cryst.*, **1957**, *10*, 201; Potrzebowski, M. J.; Michalska, M.; Blaszczyk, J.; Wieczorek, M. W.; Ciesielski, W.; Kazmierski, S.; Pluskowski, J. *J. Org. Chem.*, **1995**, *60*, 3139.

(15) Bright, D.; Maxwell, I. F.; de Boer, J. *J. Chem. Soc., Perkin Trans. 2*, **1973**, 2101.

(16) Pauling, L. *The Nature of the Chemical Bond*, 3rd ed.; Cornell University Press: Ithaca, New York, 1960; Chapter 7. See also, Bondi, A. *J. Phys. Chem.* **1964**, *68*, 441.

(17) Parthasarathy et al. defined θ from the normal to the selenide plane; see refs 11 and 12.

(18) (a) Takeda, N.; Tokitoh, N.; Imakubo, T.; Goto, M.; Okazaki, R. *Bull. Chem. Soc. Jpn.*, **1995**, *68*, 2757; Tokitoh, N. *J. Syn. Org. Chem. Jpn.*, **1994**, *52*, 136. (b) Klayman, D. L.; Günther, W. H. H. *Organic Selenium Compounds: Their Chemistry and Biology*, Wiley, New York, 1973; Chapter II.

(19) *Gaussian 94, Revision D.4*; Frisch, M. J.; Trucks, G. W.; Schlegel, H. B.; Gill, P. M. W.; Johnson, B. G.; Robb, M. A.; Cheeseman, J. R.; Keith, T.; Petersson, G. A.; Montgomery, J. A.; Raghavachari, K.; Al-Laham, M. A.; Zakrzewski, V. G.; Ortiz, J. V.; Foresman, J. B.; Cioslowski, J.; Stefanov, B. B.; Nanayakkara, A.; Challacombe, M.; Peng, C. Y.; Ayala, P. Y.; Chen, W.; Wong, M. W.; Andres, J. L.; Replogle, E. S.; Gomperts, R.; Martin, R. L.; Fox, D. J.; Binkley, J. S.; Defrees, D. J.; Baker, J.; Stewart, J. P.; Head-Gordon, M.; Gonzalez, C.; Pople, J. A. *Gaussian, Inc.*, Pittsburgh, PA, 1995.

(20) NBO Ver. 3.1, Glendening, E. D.; Reed, A. E.; Carpenter, J. E.; Weinhold, F.

(21) MacSpartan Plus Ver. 1.0, Hehre, H.J. *Wavefunction Inc.*

(22) The calculations exhibit that the adduct will form two in H_2Se molecules if there is no framework to join the two selenide molecules (or groups) such as the naphthylidene group.

(23) Hirschfelder, J. O.; Linnett, J. W. *J. Chem. Phys.*, **1950**, *18*, 130; Moore, N. *J. Chem. Phys.*, **1960**, *33*, 471.

(24) The energy levels of 18A and 18B are suggested to intersect as the θ value becomes larger from that in **12a** to that in **12b**.

(25) The results of the calculations explain well the UPS of 1,2-bis(methylthio)naphthalene and naphtho[1,8-*b*,*c*]-1,5-dithiocin,[5b] although the dithiocin is in a cisconformation around the thio groups, while **12a** is a transconformation.

(26) The results calculated at the HF level are adequately reliable, I believe, since those calculated on model **b** at the HF level are very similar to those at the MP2 level, as shown in Table 6. The fixing of the nonbonded Se---Se distances in model **a** and model **b** must also make the results at the HF level reliable.

(27) (a) Pimentel, G. C. *J. Chem. Phys.* **1951**, *19*, 446. Musher, J. I. *Angew. Chem., Int. Ed. Engl.* **1969**, *8*, 54. (b) Chen, M. M. L.; Hoffmann, R. *J. Am. Chem. Soc.* **1976**, *98*, 1647. (c) Cahill, P. A.; Dykstra, C. E.; Martin, J. C. *J. Am. Chem. Soc.* **1985**, *107*, 6359. See also, Hayes, R. A.; Martin, J. C. *Sulfurane Chemistry*, in ref. 2.

(28) Alvarez, S.; Mota, F.; Novoa, J. *J. Am. Chem. Soc.* **1987**, *109*, 6586.

(29) Siepmann, R.; von Schnering, H. G. *Z. Anorg. Allg. Chem.*, **1968**, *357*, 289.

(30) Fujihara, H.; Uehara, T.; Erata, T.; Furukawa, N. *Chem. Lett.*, **1993**, 263.

(31) Dixon, D. A.; Arduengo, III, A. J. *Inorg. Chem.*, **1990**, *29*, 970.

(32) Havinga, E. E.; Boswijk, K. H.; Wiebenga, E. H. *Acta Crystallogr.*, **1954**, *7*, 487; Dubler, E.; Linowsky, L. *Helv. Chim. Acta*, **1975**, *58*, 2604; Millan, A.; Bailey, P. M.; Maitlis, P. M. *Chem. Soc., Dalton Trans.*, **1982**, 73; Buse, K. D.; Keller, H. J.; Pritzkow, H. *Inorg. Chem.*, **1977**, *16*, 1072.

(33) Bock, H.; Havlas, Z.; Rauschenbach, A.; Nather, C.; Kleine, M. *Chem. Commun.*, **1966**, 1529.

(34) Blake, A. J.; Lippolis, V.; Parsons, S.; Schröder, M. *Chem. Commun.*, **1996**, 2207.

(35) Sheldrick, G. M. In Crystalographic Computing, 3; Ed. Sheldrick, G. M., Kruger, C., Doddard, R., Eds.; Oxford University Press: Oxford, England, 1985; p 175.

(36) TEXSAN: Single-crystal Structure Analysis Software, Version 5.0; Molecular Structure Corp.: The Woodlands, TX 77381, 1981.

Chapter 5

Successive Change in Conformation Caused by p-Y Groups in 1-(MeSe)-8-(p-YC$_6$H$_4$Se)C$_{10}$H$_6$: Role of Linear Se---Se–C 3c-4e versus n(Se)---n(Se) 2c-4e Nonbonded Interactions
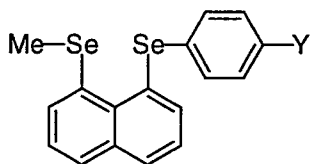
Abstract

The structure of 1-(methylselanyl)-8-(p-anisylselanyl)naphthalene (2) and 1-(methylselanyl)-8-(p-chlorophenylselanyl)naphthalene (3) was studied by the X-ray crystallographic analysis. The structures around the Se–Me and Se–C$_6$H$_4$OMe-p (Se–C$_{An}$) groups in 2 are close to type A and type B, respectively: type A if the Se–C bond being almost perpendicular to the naphthyl plane and type B when the Se–C bond being placed on the plane. Those around the Se–Me and Se–C$_6$H$_4$Cl-p (Se–C$_{Ar}$) groups in 3 are type B and type A, respectively. The nonbonded Se---Se distances of 2 and 3 are 3.0951(8) Å and 3.1239(7) Å, respectively. The structure of 3 is very different from that observed in 1-(methylselanyl)-8-(phenylselanyl)naphthalene (1), of which structure is type C where the two Se–C bonds decline by about 45° from the naphthyl plane. The structure of 3 strongly suggests the contribution of the nonbonded n(Se$_{Ar}$)---σ^*(Se–C$_{Me}$) 3c-4e type interaction. The nonbonded n(Se$_{Me}$)---σ^*(Se–C$_{An}$) 3c-4e type interaction must partly contribute to the structure of 2. To clarify the nature of the n(Se)---σ^*(Se–C) 3c-4e type interaction observed in 2 and 3, together with the π type 2c-4e interaction in 1, ab initio MO calculations with the B3LYP/6-311++G(3df,2pd) method were performed on model a, H$_a$H$_b$Se---SeH$_a$H$_{b'}$, where the naphthylidene group was replaced by H$_a$ and H$_{a'}$ and the Me and Ar groups by H$_b$ and H$_{b'}$. Two structures are optimized to be energy minima with $\angle$SeSeH$_b$ = $\angle$SeSeH$_{b'}$ = ca 74° and 155°. The latter corresponds to the conformation observed in 1, which is controlled by HOMO (π^*(Se---Se)): the former is HOMO-1 (σ(Se---Se))-controlled. On the contrary, similar calculations with the B3LYP/6-311+G(2d,p) method on naphthalene-1,8-diselenol show that the type A-type B pairing is evaluated to be most stable, which explains the conformations observed in 2 and 3: the n(Se)---σ^*(Se–C) 3c-4e interaction, as well as π-orbitals of the naphthyl group, play an important role to appear the pairing. The resonance effect of OMe and the inductive effect of Cl must also be important to determine the structures of 2 and 3, respectively. The character of CT calculated by the natural population analysis for the diselenol supports further the n(Se)---σ^*(Se–C) 3c-4e interaction.

Introduction

The lone pair–lone pair interaction[1] is one of the important factors to determine the structure and the reactivity of organic compounds containing heteroatoms bearing lone pairs such as organic chalcogen compounds. Such two center-four electron (2c-4e) interaction is demonstrated to play an important role in the nuclear spin–spin couplings between selenium–selenium[2,3] and selenium–fluorine[4] atoms, as well as those between fluorine–fluorine[5] and fluorine–nitrogen[6] atoms. Naphthalene 1,8-positions are expected to serve as a good system to study the nonbonded interactions between heteroatoms and/or groups containing 2c-4e.[2,3,7,8]

1 (Y = H), **2** (Y = OMe), **3** (Y = Cl)

We have recently reported the structure of 1-(methylselanyl)-8-(phenylselanyl)naphthalene (**1**)[8a] studied by the X-ray crystallographic analysis, together with the molecular orbital calculations performed on the models of **1**. The structure of **1** is demonstrated to decline by about 45° from the naphthyl plane, which is called type **C** for the two Se–C bonds (Scheme 1: θ is shown exemplified by type **A**).[8a] The nonbonded 2c-4e interaction itself must be repulsive but the type **C** pairing is stabilized by the distorted π type 2c-4e interaction. We looked for such nonbonded Se---Se interaction that is attractive in nature and examined the structure of p-substituted derivatives of **1**[9] such as 1-(methylselanyl)-8-(p-anisylselanyl)naphthalene (**2**) and 1-(methylselanyl)-8-(p-chlorophenylselanyl)naphthalene (**3**).

Scheme 1

type **A**: $\theta \le 90°$ type **B**: $\theta \approx 180°$ type **C**: $\theta \approx 135°$
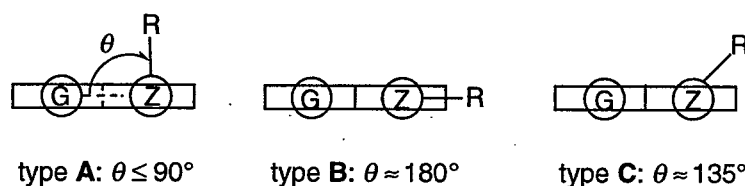
The type **C** pairing is usually found in 1,8-bis(chalcogena)naphthalenes such as **1**, 1,8-bis(methylsulfanyl)naphthalene (**4**),[7a] and 1,8-bis(phenyltelluro)naphthalene (**5**).[7b] On the other hand, the double type **A**-type **B** pairings are found around the Se–Ph and Se–Se moieties in bis[8-(phenylselanyl)naphthyl]-1,1'-diselenide (**6**).[8] The high electron accepting ability of the Se–Se bond due to the low lying σ^*(Se–Se) bond must be the driving force for the formation of the

pairings. Indeed the type **C** structure is stabilized by the distorted π type 2c-4e interaction as in **1**, but the type **A**-type **B** pairing must also be stabilized through the electron donor–acceptor interaction. The type **B** structure was also reported for 8-fluoro-1-(*p*-anisylselanyl)naphthalene (**7**).[4] However, such type **A**-type **B** pairing has not been reported in 1,8-bis(alkyl(or aryl)chalcogena)naphthalenes, yet. In the course of my investigation into the nonbonded Se---Se interaction, I encountered a pseudo type **A**-type **B** pairing around the Se–Me and Se–C$_6$H$_4$OMe-*p* (Se–C$_{An}$) groups in **2** and a pure type **A**-type **B** pairing around the Se–C$_6$H$_4$Cl-*p* (Se–C$_{Ar}$) and Se–Me groups in **3**. This finding led me to clarify the nature of the nonbonded Se---Se interaction in the naphthalene system in more detail.

4 (RZ = MeS)
5 (RZ = PhTe)

6

7
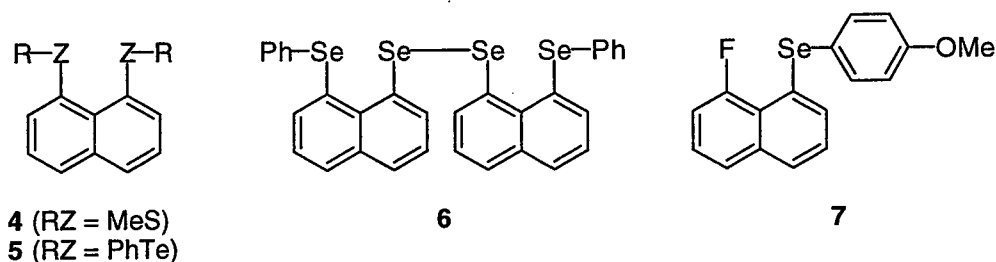
The type **A**-type **B** pairing in **3** strongly suggest that the nonbonded Se---Se interaction should be characterized by the n(Se$_{Ar}$)---σ*(Se–C$_{Me}$) 3c-4e interaction.[10,11] The pseudo type **A**-type **B** pairing in **2** also suggests the contribution of the n(Se$_{Me}$)---σ*(Se–C$_{An}$) 3c-4e interaction. The σ*(Se–C) bonds in **2** and **3** are to act as electron acceptors. We report the structures of **2** and **3** in crystals, together with the nature of the n(Se)---n(Se) interaction in the naphthalene system elucidated by the MO calculations performed on the models of **2** and **3**.

Results and Discussion

Structure of 1-(methylselanyl)-8-(arylselanyl)naphthalenes, 2 and 3. Single crystals of **2** and **3** were obtained via slow evaporation of hexane solutions, and each of the suitable crystals was subjected to X-ray crystallographic analysis. The crystallographic data are shown in Table 1. One type of structure corresponds to each crystal. Figures 1 and 2 predict the structures of **2** and **3**, respectively. Table 2 collects the selected interatomic distances, angles, and torsional angles for **2** and **3**.
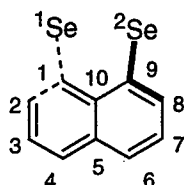

Deviations of atoms from the least-squares planes of C(3)C(4)C(5)C(6)C(7)C(10) in **2** and **3** are shown in Table 3, together with those of **1A** and **1B**.[8a] The planarity of the plane in **2** is good

and that in **3** is very good. The Se(1), C(1), and C(2) atoms deviate to a direction from the planes (minus direction) and the Se(2), C(8), and C(9) atoms to the opposite direction. Deviations of the Se atoms in **2** are in a range of 0.50 - 0.64 Å, while the atoms in **3** deviate only 0.20 ± 0.02 Å. The deviations of atoms are in an order of **3 < 1 < 2**.
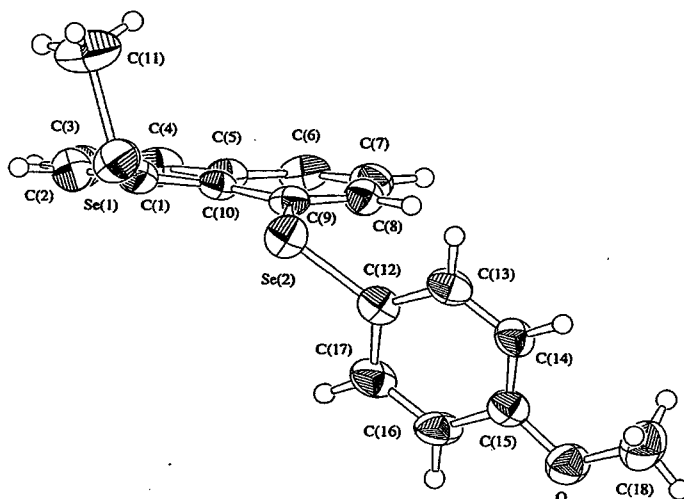
Figure 1. Structure of **2**.
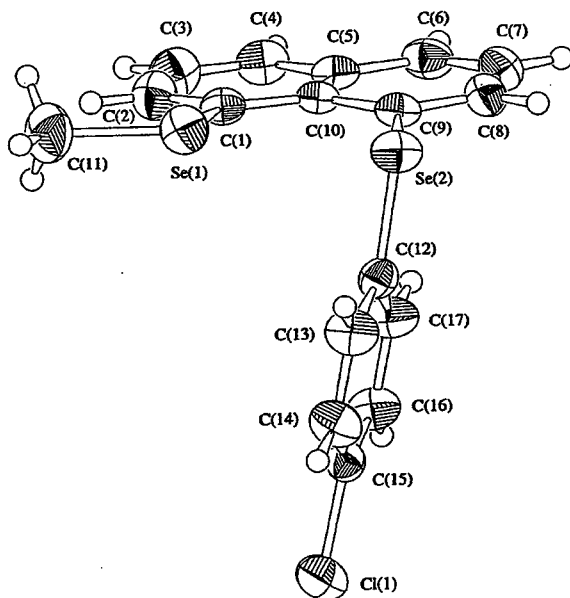
Figure 2. Structure of **3**.

Table 1. Selected Crystal Data and Structure Refinement for 2 and 3

	2	3
formula	$C_{18}H_{16}O_1Se_2$	$C_{17}H_{13}Cl_1Se_2$
fw [g mol^{-1}]	406.24	410.66
crystal color and habit	colorless, prismatic	pale yellow, cubic
crystal system	monoclinic	triclinic
space group	$P2_1/n$ (no. 14)	P1(no. 2)
unit cell dimens [Å, deg]	$a = 12.754(2)$	$a = 9.628(4)$
	$b = 9.804(1)$	$b = 10.901(3)$
	$c = 12.980(2)$	$c = 8.565(2)$
		$\alpha = 111.90(2)$
	$\beta = 96.68(1)$	$\beta = 96.55(3)$
		$\gamma = 109.99(3)$
Vol [Å^3]	1611.8(3)	753.1(5)
Z	4	2
density (calcd) [g cm^{-3}]	1.674	1.811
μ (Mo Kα) [cm^{-1}]	45.84	50.74
F(000)	800.00	400.00
Scan Width [deg]	$1.00 + 0.30 \tan\theta$	$1.20 + 0.30 \tan\theta$
$2\theta_{max}$ [deg]	55.0	55.0
no. of observations	2331	2754
no. of variables	191	182
R	0.042	0.030
R_ω	0.030	0.023
GOF	2.51	2.93

Table 2. Selected Interatomic Distances, Angles, and Torsional Angles of 2 and 3

	2	3
Interatomic Distances, Å		
Se(1)-C(1)	1.932(5)	1.926(3)
Se(1)-C(11)	1.931(5)	1.954(3)
Se(2)-C(9)	1.951(4)	1.924(3)
Se(2)-C(12)	1.928(5)	1.915(3)
Se(1)-Se(2)	3.0951(8)	3.1239(7)
C(1)-C(10)	1.422(6)	1.435(3)
C(9)-C(10)	1.432(6)	1.433(3)
Angles, deg		
C(1)-Se(1)-C(11)	53.8(2)	69.8(1)
Se(1)-C(1)-C(10)	122.6(4)	123.0(2)
C(9)-Se(2)-C(12)	98.2(2)	98.8(1)
Se(2)-C(9)-C(10)	121.8(3)	122.3(6)
C(1)-C(10)-C(9)	127.1(4)	125.3(2)
Se(1)-Se(2)-C(12)	81.4(1)	87.28(8)
Se(2)-Se(1)-C(11)	96.3(2)	172.2(1)
Torsional Angles, deg		
C(10)-C(1)-Se(1)-C(11)	107.1(4)	180.0(2)
Se(1)-C(1)-C(10)-C(9)	14.9(7)	4.8(4)
C(2)-C(1)-Se(1)-C(11)	−66.2(5)	1.7(2)
C(10)-C(9)-Se(2)-C(12)	145.7(4)	78.4(2)
Se(2)-C(9)-C(10)-C(1)	13.4(7)	5.0(4)
C(9)-Se(2)-C(12)-C(13)	110.1(4)	−165.5(2)
C(9)-Se(2)-C(12)-C(17)	−74.7(4)	14.8(3)
C(8)-C(9)-Se(2)-C(12)	−30.0(4)	−99.5(2)
C(11)-Se(1)-Se(2)-C(12)	38.6(2)	−23.8(7)
C(2)-C(1)-C(10)-C(5)	−9.2(7)	−2.6(4)
C(5)-C(10)-C(9)-C(8)	−7.6(6)	−3.2(4)

Table 3. Deviations of Atoms from Least-squares Planes of C(3)C(4)C(5)C(6)C(7)C(10)[a,b] in 1 - 3

Compd	Se(1)	Se(2)	C(1)	C(2)	C(8)	C(9)	C(3)	C(4)	C(5)	C(6)	C(7)	C(10)
2	−0.644	0.500	−0.134	−0.119	0.103	0.134	−0.007(5)	0.009(5)	0.001(5)	−0.011(5)	0.007(5)	−0.001(4)
3	−0.183	0.220	−0.050	−0.039	0.043	0.058	−0.003(3)	0.004(3)	0.000(3)	−0.004(3)	0.003(3)	0.000(2)
1A[c]	0.366	−0.372	0.075	0.019	−0.088	−0.088	−0.022(9)	0.010(9)	0.013(7)	0.006(9)	−0.02(1)	0.003(7)
1B[c]	0.398	−0.407	0.074	0.015	−0.112	−0.108	−0.025(9)	0.011(9)	0.012(8)	0.011(9)	−0.03(1)	0.004(7)

[a] In Å. [b] Conformations around MeSe and p-YC$_6$H$_4$Se groups in 2 and 3 are just the opposite of those in 1. [c] Based on the structures in reference 8a.

As shown in Figure 1 and Table 2, the Se–C_{Me} and Se–C_{An} bonds in **2** decline by about 73° and 34° from the naphthyl plane, respectively: the torsional angles of C(10)C(1)Se(1)C(11) and C(10)C(9)Se(2)C(12) were 107.1(4)° and 145.7(4)°, respectively. The *p*-anisyl plane was slightly declined from the naphthyl plane: the torsional angle of C(9)Se(2)C(12)C(13) were 110.1(4)°. The structures around the Se–C_{Me} and Se–C_{An} bonds in **2** were close to type **A** and type **B**, respectively, bearing some type **C** character. The nonbonded Se(1)---Se(2) distance was 3.0951(8) Å, which was almost equal to that in **1** (3.048(1) Å and 3.091(1) Å for the two structures).[8a] The type **A** and type **B** structures around the Se–C_{Ar} and Se–C_{Me} bonds were demonstrated for **3** (Figure 2 and Table 2). The Se–C_{Me} and Se–C_{Ar} bonds in **3** decline by about 0° and 78° from the naphthyl plane, respectively: the torsional angles of C(10)C(1)Se(1)C(11) and C(10)C(9)Se(2)C(12) were 180.0(2)° and 78.4(2)°, respectively. The *p*-chlorophenyl plane was almost perpendicular to the naphthyl plane: the torsional angle of C(9)Se(2)C(12)C(13) was –165.5(2)°. The nonbonded Se(1)---Se(2) distance was 3.1239(7) Å, which was somewhat longer than those of **1** (3.048(1) Å and 3.091(1) Å for the two structures)[8a] and **2** (3.0951(8) Å). It is worthwhile to note that the Se–Me groups in **2** and **3** are shown to be type **A** and type **B**, respectively. Their inverse contribution to the structures must be due to the difference in the electronic effect of the *p*-substituents in **2** and **3**.

Parthasarathy et al. have suggested that there are two types of directional preferences of nonbonded atomic contacts with divalent chalcogens such as sulfur[12] and selenium,[13] R–Z–R' (Z = S and Se). Type I contacts are with electrophiles which have Z---X directions in RR'Z---X where n-electrons of sulfides or selenides are located, and type II contacts are with nucleophiles tending to lie along the extension of one of sulfur's or selenium's bonds. Electrophiles and nucleophiles will interact preferentially with HOMO of the n(Z) and with LUMO of the σ*(Z–R) or σ*(Z–R'), respectively. Therefore, the type **A** and type **B** structures belong to type I and type II contacts in Parthasarathy's definition, respectively, if G in 8-G-1-(RZ)$C_{10}H_6$ is assumed to be electrophiles or nucleophiles (Scheme 1). The type **A**-type **B** pairing is equal to the type I-type II pairing, which is stabilized through the electron donor–acceptor interaction. The type **C** structure around the two chalcogen atoms must be equal to the type III pairing, of which θ values at the both sites should be almost equal.

The conformations around the Se–C_{Ar} and Se–C_{Me} bonds in **3** are demonstrated to be type **A** and type **B**, respectively, which is also recognized as the type I-type II pairing in Parthasarathy's classification. Since the type I and type II contacts are with LUMO and HOMO, respectively, the type I-type II pairing must be the HOMO-LUMO interaction. The pairing must be stabilized by the charge transfer (CT) from the electron donor to the acceptor. That is, the pairing in **3** strongly suggests that the interaction occurs between the n(Se) of the ArSe group and the σ*(Se–C) of the

MeSe group, which leads to the $n(Se_{Ar})$---$\sigma^*(Se-C_{Me})$ 3c-4e type interaction.[10,11] The pairing in **2** also suggests the contribution of the $n(Se_{Me})$---$\sigma^*(Se-C_{An})$ 3c-4e type, together with the contribution of the distorted π type 2c-4e interaction. The type **C** pairing of the distorted π type 2c-4e interaction is reported for **1**. The three structures show that the pairing changes successively with the substituent Y at the p-position in **1** - **3**.

2   **1**   **3**
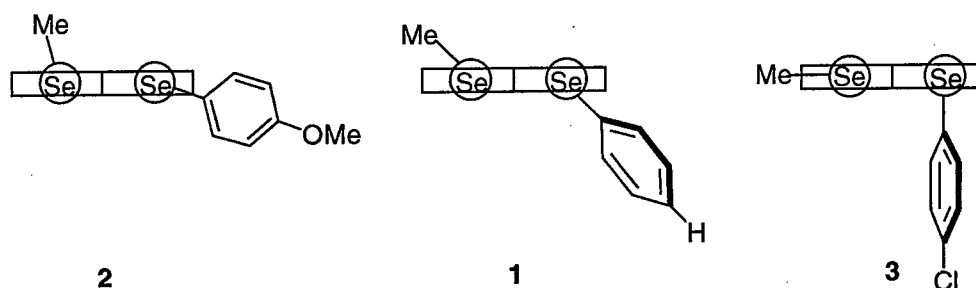
Why does the type **C** pairing in **1** change successively and/or dramatically to the type **A**-type **B** pairing in **2** and **3**, respectively? Three types of interactions between nonbonded Se---Se atoms in **1** - **3** should be considered for the successive change; i) pure $n(Se)$---$n(Se)$ 2c-4e interaction, ii) $n(Se)$---$\sigma^*(Se-C)$ 3c-4e interaction, and iii) contribution of the methyl and aryl groups, especially of π-orbitals of the naphthylidene group. The role of the substituents, OMe and Cl, at the phenyl *para* positions is also important. Ab initio MO calculations are performed on an adduct, H_2Se---SeH_2 (model **a**), to clarify the contributions of case i) and case ii), together with the whole nature of the nonbonded $n(Se)$---$n(Se)$ interaction. Calculations are also performed on naphthalene-1,8-diselenol (**8**) to elucidate the contributions of case ii) and case iii). The results are shown in the following sections.

Ab initio MO Calculations on model a. Scheme 2 shows model **a**, $H_aH_b{}^1Se$---${}^2SeH_aH_{b'}$, where aryl, methyl, and naphthylidene groups are replaced by hydrogens. The ^1Se atom of model **a** is placed at the origin and the ^2Se atom on the x-axis with the $^1Se,^2Se$ distance fixed at 3.124 Å and the $^1Se-H_a$ and $^2Se-H_{a'}$ bonds in the z-direction. Ab initio MO calculations were performed on model **a** using the Gaussian 94 program[14] with the 6-311++G(3df,2pd) basis sets at the B3LYP level. The results are shown in Table 4.
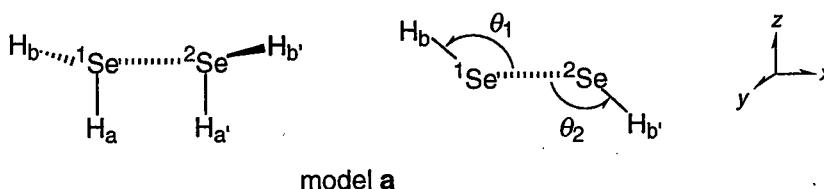
Scheme 2

model **a**

Table 4. Optimized Structures, Energies, and Natural Charges (Qn) for model a and 8

Compound	E (au)	Structure	r(Se,Se) (Å)	∠H$_a$H$_a$^{1}SeH$_b$ (deg)	∠H$_a$^{1}SeH$_b$ (deg)	Qn(^{1}Se)	Qn(H$_a$)	Qn(H$_b$)
B3LYP/6-311++G(3df,2pd)								
model a	−4805.4884	C_2	3.124^a	74.29	91.62	−0.1650	0.0812	0.0839
model a	−4805.5072	C_2	3.124^a	154.54	90.04	−0.1620	0.0837	0.0783
model a	−4805.5057	C_{2v}	3.124^a	180.00^b	90.44	−0.1752	0.0845	0.0908
model a	−4805.5052	C_1	3.124^a	90.00^a	91.24	−0.1229	0.0865	0.0905
				181.36^c	88.93^d	−0.1854^e	0.0789^f	0.0524^g
B3LYP/6-311+G(2d,p)								
8a^{h,i}	−5189.0663	C_2	3.5166	52.99	97.87	0.0993	−0.1829	0.0948
8b^{h,i}	−5189.0709	C_2	3.1173	143.11	92.44	0.1330	−0.1699	0.0696
8c^{h,j}	−5189.0684	C_{2v}	3.1047	180.00	93.13	0.1449	−0.1660	0.0768
8d^{h,i}	−5189.0714	C_1	3.1806	72.82	95.51	0.1310	−0.1871	0.0902
				172.84^k	91.14^l	0.1490^e	−0.1695^m	0.0398^g

^{a} Fixed value. ^{b} ∠H$_a$H$_a$^{2}SeH$_b'$ being optimized with ∠H$_a$H$_a$^{1}SeH$_b$ fixed at 180.00°. ^{c} ∠H$_a$H$_a$^{2}SeH$_b'$. ^{d} ∠H$_a$^{2}SeH$_b'$. ^{e} Qn(^{2}Se). ^{f} Qn(H$_a'$). ^{g} Qn(H$_b'$). ^{h} H$_a$ and H$_a'$ should be read C$_1$ and C$_9$, respectively. ^{i} All positive frequencies being predicted by the frequency analysis. ^{j} Three negative frequencies being predicted by the frequency analysis.
^{k} ∠C$_1$C$_9$^{2}SeH$_b'$. ^{l} ∠C$_9$^{2}SeH$_b'$. ^{m} Qn(C$_9$).

Two structures of the C_2 symmetry were optimized to be energy minima, of which the torsional angle $H_aH_a^1SeH_b$ (θ_1) were θ_1 (= θ_2) = 74.29° and 154.54°: the former (model a with θ = 74.3°) is less stable than the latter (model a with θ = 154.5°) by 0.0188 au (49.4 kJ mol^{-1}).[15] The former corresponds to the type A pairing with the nonbonded σ type 2c-4e interaction and the latter to type C pairing with the nonbonded π type 2c-4e interaction observed in 1.

To clarify the whole nature of the nonbonded interaction between Se atoms, the angular dependence of the energy of model a is calculated with variously fixed θ_1. The partial optimization of model a with a fixed value of θ_1 yields energies E (E_1 and E_2) and angles θ_2 (θ_{21} and θ_{22}). The energies E_1 and E_2 represent those obtained when θ_2 is started at near 154° and 74°, respectively, with a fixed θ_1. The values of E_1 and the corresponding θ_{21} are obtained for a trial range of 60° $\le$ θ_1 $\le$ 180°, while the E_2 value, together with θ_{22}, is found in a trial range of 60° $\le$ θ_1 < 120°. The energies E_1 and E_2 are on different energy curves, which cross at θ_2 = ca. 120°: E_2 is represented by E_1, if E_1 = E_2. For example, θ_{21} and θ_{22} are optimized to be 181.36° and 73.03°, respectively, when calculations are carried out with θ_1 fixed at 90.00°. In the case where θ_1 is fixed at 180.00°, two structures are optimized: the one is θ_{21} = 180.00° when calculations are started at θ_{21} = 180.0° and the other is θ_{21} = 155.33° starting with θ_{21} = 179.0°. The former may not be an energy minimum. Figures 3 and 4 show the plots of E and θ_2 versus θ_1, respectively.
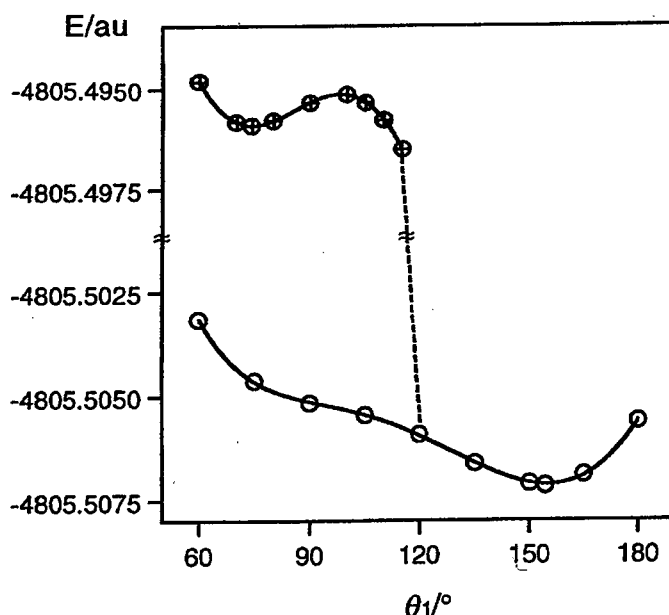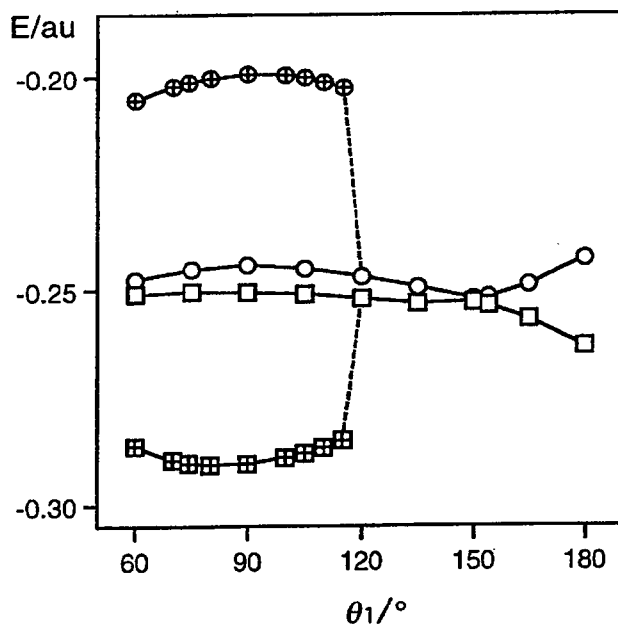

Figure 3. Plots of E_1 and E_2 of model a against θ_1: $\bigcirc$ and $\oplus$ stand for E_1 and E_2, respectively.

86
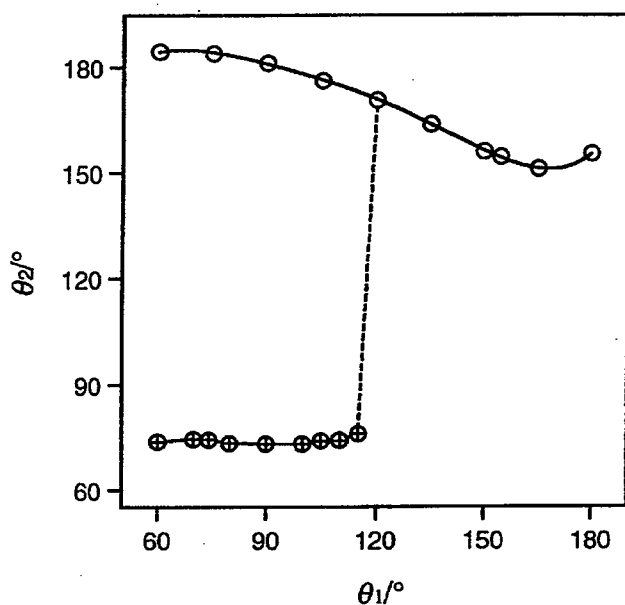
Figure 4. Plots of θ_{21} and θ_{22} of model **a** against θ_1: $\bigcirc$ and $\oplus$ stand for θ_{21} and θ_{22}, respectively.

Why do the E_1 and E_2 curves contain energy minima at $\theta_1 = \theta_2 = 154.54°$ and $74.29°$, respectively? The energies of HOMO and HOMO-1 are plotted against θ_1, which is shown in Figure 5. HOMO of E_1 shows a minimum at near $\theta_1 = \theta_{21} = 154.5°$, whereas its HOMO-1 changes rather monotonically with θ_1. On the other hand, HOMO and HOMO-1 of E_2 exhibit a maximum and a minimum at near $\theta_1 = \theta_{22} = 74.3°$, respectively. The HOMO curve is more flat than that of HOMO-1, in this case. These results show that the presence of minima on E_1 and E_2 is the reflection of the characters of HOMO of E_1 and HOMO-1 of E_2, respectively. Consequently, E_1 and E_2 are demonstrated to be HOMO- and HOMO-1-controlled,[16] respectively.

Molecular orbitals were depicted using MacSpartan program[17] with 3-21G$^{(*)}$ basis sets employing the structures given in Table 4. Figure 6 shows HOMO and HOMO-1 of model **a** with θ = 74.3° (a), 154.5° (b), 180.0° (c), and (θ_1, θ_2) = (90.0°, 181.4°) (d). Characters of the interactions are σ type 2c-4e (a), distorted π type 2c-4e (b), undistorted π type 2c-4e (c), and n(Se)---σ^*(Se–H) type 3c-4e interactions (d) between the nonbonded Se---Se atoms. Model **a** with (θ_1, θ_2) = (90.0°, 181.4°) (d) is less stable than that with θ = 154.5°(b) by 0.0020 au (5.3 kJ mol^{-1}) and slightly less stable than that with θ = 180.0° (c) by 0.0005 au (1.3 kJ mol^{-1}). The electron donor–acceptor interaction is not effectively contributed to the n(Se)---n(Se) interaction in model **a**, although that with (θ_1, θ_2) = (90.0°, 181.4°) (d) is more stable than that with θ = 74.3° (a) by 0.0168 au (44.1 kJ mol^{-1}).

87

**Figure 5.** Plots of the energies of HOMO and HOMO-1 for E_1 and E_2 of model **a** against θ_1: $\bigcirc$ and $\oplus$ stand for HOMO of E_1 and E_2, respectively, and $\square$ and $\boxplus$ for HOMO-1 of E_1 and E_2, respectively.
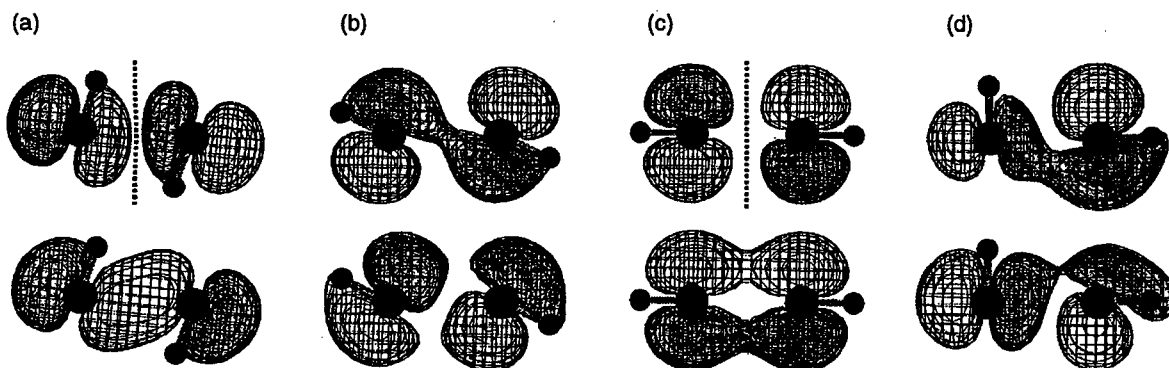
Figure 6. HOMO (upper) and HOMO-1 (lower) of model **a** with $\theta = 74.3°$ (a), with $\theta = 154.5°$ (b), with $\theta = 180.0°$ (c), and with $(\theta_1, \theta_2) = (90.0°, 181.4°)$ (d). The nodal planes are shown by dotted lines for (a) and (c).

It is worthwhile to note that the explicit nodal plane in the undistorted π^* orbital between the nonbonded Se---Se atoms disappears in the distorted π^* orbital (Figure 6). The disappearance of the nodal plane between the two Se atoms must stabilize model **a** with $\theta = 154.5°$, which may avoid the severe exchange repulsion of the π type 2c-4e interaction more effectively[8a] and be the driving force for the type **C** pairing in **1**, **4**, and **5**. The disappearance of the nodal plane in the distorted π type 2c-4e interaction may remember Möbius type interaction in cyclic π systems. We would like to call it "Möbius type stabilization in the distorted π type 2c-4e interaction", although the π type 2c-4e interaction does not form a ring.

Ab initio MO Calculations on 8. Table 4 collects the results of MO calculations performed on **8**[18] with the B3LYP/6-311+G(2d,p) method. The optimized structures of **8** are shown by **8a-d**, of which (θ_1, θ_2) = (52.99°, 52.99°), (143.11°, 143.11°), (180.00°, 180.00°), and (72.82°, 172.84°), respectively, where θ_1 and θ_2 are defined as torsional angles of $C_9C_1{}^1SeH_b$ and $C_1C_9{}^2SeH_{b'}$, respectively. Although all positive frequencies are predicted by the frequency analysis for **8a**, **8b**, and **8d**, three negative frequencies are predicted for **8c**, which is optimized when calculations are carried out assuming the C_{2v} symmetry. The conformer **8d** is most stable, which is a striking difference from the case of model **a**: **8d** is more stable than **8a** and **8b** by 0.0051 au (13.4 kJ mol⁻¹) and 0.0005 au (1.3 kJ mol⁻¹), respectively. HOMO and HOMO-1 of **8a-d** are essentially the same as those of model **a** shown by (a) - (d) in Figure 6, respectively.

8a   8b   8c   8d
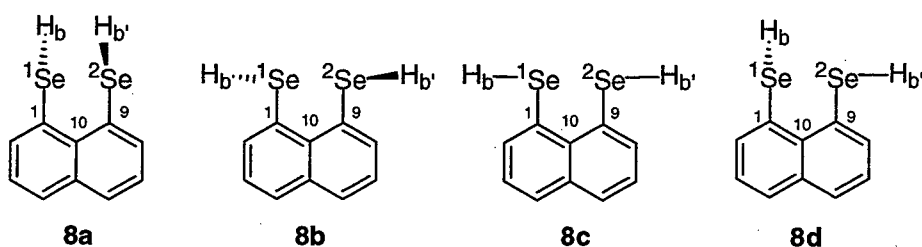
The most stable structure in model **a** with θ = 154.5° changes to **8d**. The large energy difference between model **a** with θ = 154.5° and that with θ = 74.3° (0.0188 au) decreases to 0.0046 au between **8b** and **8a**, which must be not only due to the interaction with the π orbitals of the naphthalene ring but also due to the increased Se---Se distance in **8a**. Model **a** with θ = 154.5°, together with **8b**, and **8d** correspond to those of **1** and **3**, respectively. The results show that the structures of **1** and **3** are mainly governed by the π type 2c-4e[8a] and the n(Se)---σ*(Se–C) 3c-4e interactions with the aid of the π orbitals of the naphthalene ring. The aryl and methyl groups in **1** - **3** must also play an important role to determine the structures since the energy difference between **8b** and **8d** is so small.

The magnitude of CT is a good measure to understand the nature of the nonbonded interaction between Se atoms. Natural charges (Qn) were calculated for the conformers of model **a** and **8**, applying the natural population analysis.[19] The results are also collected in Table 4. The Qn(^{1}Se), Qn(^{2}Se), and Qn(H_b) values in model **a** with (θ_1, θ_2) = (90.0°, 181.4°) were calculated to be more positive, negative, and negative, respectively, relative to corresponding values in model **a** with θ = 74.3° and that with 180.0°. The changes amount to 0.042 (= Qn(^{1}Se) of model **a** with (θ_1, θ_2) = (90.0°, 181.4°) – Qn(^{1}Se) of that with θ = 74.3°), –0.010, and –0.038, respectively. The total CT from an H_2Se molecule to another amounts to 0.054, which shows large contribution of the n(^{1}Se)---σ*(^{2}Se–H_b) 3c-4e type interaction in this structure. Similarly, changes in Qn(^{1}Se), Qn(^{2}Se), and Qn(H_b) in **8d** from the corresponding values in **8a** and **8c** are 0.032, 0.004, and –0.037,

respectively, whereas those for other atoms were less than 0.005. The results are in accordance with the large contribution of the $n(^1Se)$---$\sigma^*(^2Se-H_b)$ 3c-4e interaction also in **8d**.

The change in the structure of **1** to those of **2** and **3** in crystals must be accounted for based on electronic properties of MeO and Cl groups at the p-positions. Both substituents withdraw electrons inductively ($\sigma_I(OMe) = 0.27$ and $\sigma_I(Cl) = 0.46$) but they donate electrons by the resonance mechanism ($\sigma_R°(OMe) = -0.45$ and $\sigma_R°(Cl) = -0.23$).[20] Since the magnitude of the substituent effects is different for MeO and Cl groups, the observed effect on the structures can be inverse for the two groups if the resonance effect of OMe in **2** and the inductive effect of Cl in **3** are predominant in the structures. The electron donating ability of p-anisyl and p-chlorophenyl groups is expected to be larger and smaller than that of the methyl group in these cases, judging from their structures.

The characters of the structures of **1 - 3** are summarized as follows: (a) The contribution of the $n(Se)$---$n(Se)$ π type 2c-4e interaction is predominant in **1** and negligible in **3**.[21] (b) The $n(Se)$---$\sigma^*(Se-C)$ 3c-4e type interaction contributes to the structures of **2** and **3**. And (c) the interaction between Se and Y[22] through the π-orbitals of the SeC$_6$H$_4$Y group determines which Se atom (or Se-C bond) in **2** or **3** acts as an electron donor (or an acceptor) in the 3c-4e interaction.[23] The structures of **1 - 3** are well explained by the MO calculations on model **a** and **8**. The steric effect between the naphthyl protons at 7- and/or 2-positions and the p-YC$_6$H$_4$ and/or Me groups in type **B** must also be taken into account when the structures are discussed in more detail. Studies on the structures of 8-G-1-(RSe)C$_{10}$H$_6$ are in progress.

Experimental Section

Chemicals were used without further purification unless otherwise noted. Solvents were purified by standard methods. Melting points were uncorrected. ^{1}H, ^{13}C, and ^{77}Se NMR spectra were measured at 400, 100, and 76 MHz, respectively. The ^{1}H, ^{13}C, and ^{77}Se chemical shifts are given in ppm relative to those of internal CHCl$_3$ slightly contaminated in the solution, CDCl$_3$ as the solvent, and external MeSeMe, respectively. Column chromatography was performed on silica gel (Fujisilysia BW-300) and acidic alumina (E. Merck).

1-(Methylselanyl)-8-(p-methoxyphenylselanyl)naphthalene (**2**). Bis[8-(p-methoxyphenylselanyl)naphthyl]-1,1'-diselenide (**9**) was reduced by NaBH$_4$ in an aqueous THF, then allowed to react with methyl iodide gave **2** as a colorless solid, similarly to the case for **1**,[8a] 91 % yield; mp 86.0 - 87.0 ℃. ^{1}H NMR (CDCl$_3$, 400 MHz) 2.38 (s, 3H, J (Se,H) = 13.4 Hz), 3.79 (s, 3H), 6.83 (dd, 2H, J = 8.6 and 2.2 Hz), 7.17 (t, 1H, J = 7.7 Hz), 7.33 (t, 1H, J = 7.7 Hz), 7.45 (dd, 2H, J = 8.1 and 2.2 Hz), 7.45 (dd, 1H, J = 6.8 and 1.1 Hz), 7.64 (dd, 1H, J = 8.1 and 1.0 Hz), 7.70 (dd, 1H, J = 8.0 and 1.1 Hz), 7.79 (dd, 1H, J = 7.3 and 1.1 Hz); ^{13}C NMR (CDCl$_3$,

100 MHz) 13.90 (^1J = 71.2 Hz, ^5J = 15.7 Hz), 55.23, 115.17, 124.73, 125.70, 125.84, 128.26, 128.75, 131.25, 133.10, 133.50, 133.64, 134.94, 135.80, 136.47 (^1J = 11.5 Hz), 159.69; ^{77}Se NMR (CDCl$_3$, 76 MHz) 424.5, 233.1 (^4J(Se,Se) = 341.6 Hz). Anal. Calcd for C$_{18}$H$_{16}$Se$_2$O$_1$: C, 53.22; H, 3.97. Found: C, 53.35; H, 3.90.

1-(Methylselanyl)-8-(*p*-chlorophenylselanyl)naphthalene (3). Following a method similar to that for **2**, **3** was obtained starting from bis[8-(*p*-chlorophenylselanyl)naphthyl]-1,1'-diselenide (**10**) in 87 % yield as a colorless solid, mp 78.5 - 79.5 °C. ^{1}H NMR (CDCl$_3$, 400 MHz) 2.34 (s, 3H, *J* (Se,H) = 13.9 Hz), 7.19 (dd, 2H, *J* = 8.6 and 2.2 Hz), 7.24 (t, 1H, *J* = 7.7 Hz), 7.31 (dd, 2H, *J* = 8.8 and 2.2 Hz), 7.36 (t, 1H, *J* = 7.7 Hz), 7.60 (dd, 1H, *J* = 7.3 and 1.5 Hz), 7.71 (dd, 1H, *J* = 7.1 and 1.2 Hz), 7.73 (dd, 1H, *J* = 6.8 and 1.1 Hz), 7.74 (dd, 1H, *J* = 7.3 and 1.2 Hz); ^{13}C NMR (CDCl$_3$, 100 MHz) 13.43 (^1J = 72.8 Hz, ^5J = 15.7 Hz), 125.96, 125.99, 128.42, 129.49, 130.86, 131.72, 132.67, 133.50, 133.60, 134.49 (^1J = 12.4 Hz), 135.26, 135.59, 135.83; ^{77}Se NMR (CDCl$_3$, 76 MHz) 431.6, 234.7 (^4J(Se,Se) = 316.7 Hz). Anal. Calcd for C$_{17}$H$_{13}$Se$_2$Cl$_1$: C, 49.72; H, 3.19. Found: C, 49.77; H, 3.23.

Bis[8-(*p*-methoxyphenylselanyl)naphthyl]-1,1'-diselenide (9). To a solution of the dianion of naphto[1,8-*c,d*]-1,2-diselenole, which was prepared by reduction of the diselenole with NaBH$_4$ in an aqueous THF, was added *p*-methoxybenzenediazonium chloride at low temperature. After usual workup, the solution was chromatographed on silica gel containing acidic alumina. Recrystallization of the chromatographed product from hexane gave **9** as a yellow solid: 69 % yield; mp 143.5 - 145.0 °C. ^{1}H NMR (CDCl$_3$, 400 MHz) 3.74 (s, 6H), 6.75 (dd, 4H, *J* = 8.9 and 2.6 Hz), 7.18 (t, 2H, *J* = 7.8 Hz), 7.32 (t, 2H, *J* = 7.6 Hz), 7.32 (dd, 4H, *J* = 9.0 and 2.7 Hz), 7.67 (dd, 2H, *J* = 8.0 and 0.9 Hz), 7.79 (dd, 2H, *J* = 8.1 and 1.0 Hz), 7.86 (dd, 2H, *J* = 7.2 and 1.4 Hz), 8.14 (dd, 2H, *J* = 7.5 and 1.0 Hz); ^{13}C NMR (CDCl$_3$, 22.4 MHz) 55.27, 115.06, 125.28, 125.82, 126.52, 128.33, 129.78, 130.25, 130.57, 132.74, 133.42, 135.39, 136.14, 137.39, 159.24; ^{77}Se NMR (CDCl$_3$, 68.68 MHz) 416.2, 541.4 (^4J(Se,Se) = 371.6 Hz). Anal. Calcd for C$_{34}$H$_{26}$O$_2$Se$_4$: C, 52.19; H, 3.35. Found: C, 52.45; H, 3.36.

Bis[8-(*p*-chlorophenylselanyl)naphthyl]-1,1'-diselenide (10). In the similar method for **9**, **10** was given, starting from the dianion of naphto[1,8-*c,d*]-1,2-disenole and *p*-methoxybenzenediazonium chloride, 68 % yield as a yellow solid, mp 185.0 - 186.0 ℃. ^{1}H NMR (CDCl$_3$, 400 MHz) 7.13 (br.s, 8H), 7.16 (t, 2H, *J* = 7.8 Hz), 7.38 (t, 2H, *J* = 7.7 Hz), 7.70 (dd, 2H, *J* = 8.0 and 0.8 Hz), 7.88 (dd, 2H, *J* = 8.2 and 1.1 Hz), 7.94 (dd, 2H, *J* = 7.2 and 1.3 Hz), 8.02 (dd, 2H, *J* = 7.5 and 1.1 Hz); ^{13}C NMR (CDCl$_3$, 22.4 MHz) 125.95, 126.75, 127.26, 128.43, 129.42, 130.19, 131.28, 131.65, 132.48, 132.91, 133.82, 135.62, 136.36, 139.01; ^{77}Se NMR (CDCl$_3$, 68.68 MHz) 429.1, 534.7 (^4J(Se,Se) = 330.1 Hz). Anal. Calcd for C$_{32}$H$_{20}$S$_e$4Cl2: C, 48.58; H, 2.55. Found: C, 48.77; H, 2.56.

X-ray Structural Determination. The intensity data were collected on a Rigaku AFC5R four circle diffractometer with graphite-monochromated Mo Kα radiation ($\lambda = 0.71069$ Å) for **2** and **3**. The structures of **2** and **3** were solved by heavy-atom Patterson methods, PATTY,[24] and expanded using Fourier techniques, DIRDIF94.[25] All the non-hydrogen atoms were refined anisotropically. Hydrogen atoms were included but not refined. The final cycle of full-matrix least-squares refinement was based on 2331 for **2** and on 2754 for **3** observed reflections ($I > 1.50\sigma(I)$) and 191 for **2** and 182 for **3** variable parameters and converged with unweighted and weighted agreement factors of $R = (\Sigma||F_o| - |F_c||)/\Sigma|F_o|$ and $R_\omega = \{\Sigma\omega(|F_o| - |F_c|)^2/\Sigma\omega F_o^2\}^{1/2}$. For least squares, the function minimized was $\Sigma\omega(|F_o|-|F_c|)^2$, where $\omega = (\sigma_c^2|F_o| + p^2|F_o|^2/4)^{-1}$. Crystallographic details are listed in Table 1.

MO Calculations. Ab initio molecular orbital calculations were performed on an Origin computer using the Gaussian 94 program with 6-311++G(3df,2pd) basis sets at the DFT (B3LYP) level on model **a**. The B3LYP/6-311+G(2d,p) method were employed for the calculations of **8**. The molecular orbitals were drawn by a Power Macintosh 8500/180 personal computer using MacSpartan Plus program (Ver. 1.0) with 3-21G$^{(*)}$ basis sets.

References and Notes

(1) (a) Asmus, K.-D. *Acc. Chem. Res.* **1979**, *12*, 436; Musker, W. K. *Acc. Chem. Res.* **1980**, *13*, 200. (b) Bernardi, F.; Csizmadia, I. G.; Mangini, A. (Eds.), *Organic Sulfur Chemistry: Theoretical and Experimental Advances*, Elsevier Scientific, Amsterdam, 1985. (c) Patai, S.; Rappoport, Z. (Eds.), *The Chemistry of organic selenium and tellurium compounds*, John-Wiley and Sons, Vol. 1, New York, 1986. See also refs cited therein.

(2) Fujihara, H.; Saito, R.; Yabe, M.; Furukawa, N. *Chem. Lett.* **1992**, 1437.

(3) (a) Nakanishi, W.; Hayashi, S.; Yamaguchi, H. *Chem. Lett.* **1996**, 947. (b) Hayashi, S.; Nakanishi, W. *J. Org. Chem.* **1999**, *64*, 6688.

(4) Nakanishi, W.; Hayashi, S.; Sakaue, A.; Ono, G.; Kawada, Y. *J. Am. Chem. Soc.* **1998**, *120*, 3635.

(5) (a) Mallory, F. B. *J. Am. Chem. Soc.* **1973**, *95*, 7747. (b) Mallory, F. B.; Mallory, C. W.; Fedarko, M.-C. *J. Am. Chem. Soc.* **1974**, *96*, 3536. (c) Mallory, F. B.; Mallory, C. W.; Ricker, W. M. *J. Am. Chem. Soc.* **1975**, *97*, 4770. Mallory, F. B.; Mallory, C. W.; Ricker, W. M. *J. Org. Chem.* **1985**, *50*, 457. Mallory, F. B.; Mallory, C. W.; Baker, M. B. *J. Am. Chem. Soc.* **1990**, *112*, 2577. (d) Ernst, L.; Ibrom, K. *Angew. Chem. Int. Ed. Engl.* **1995**, *34*, 1881. Ernst, L.; Ibrom, K.; Marat, K.; Mitchell, R. H.; Bodwell, G. J.; Bushnell, G. W. *Chem. Ber.* **1994**, *127*, 1119.

(6) Mallory, F. B.; Luzik, Jr., E. D.; Mallory, C. W.; Carroll, P. J. *J. Org. Chem.* **1992**, *57*, 366. Mallory, F. B.; Mallory, C. W. *J. Am. Chem. Soc.* **1985**, *107*, 4816.

(7) (a) Glass, R. S.; Andruski, S. W.; Broeker, J. L. *Rev. Heteroatom Chem.* **1988**, *1*, 31. Glass, R. S.; Andruski, S. W.; Broeker, J. L.; Firouzabadi, H.; Steffen, L. K.; Wilson, G. S. *J. Am. Chem. Soc.* **1989**, *111*, 4036. Glass, R. S.; Adamowicz, L.; Broeker, J. L. *J. Am. Chem. Soc.* **1991**, *113*, 1065. (b) Fujihara, H.; Ishitani, H.; Takaguchi, Y.; Furukawa, N. *Chem. Lett.* **1995**, 571. (c) Fujihara, H.; Yabe, M.; Chiu, J.-J.; Furukawa, N. *Tetrahedron Lett.* **1991**, *32*, 4345. Furukawa, N.; Fujii, T.; Kimura, T.; Fujihara, H. *Chem. Lett.* **1994**, 1007. (d) Nakanishi, W. *Chem. Lett.* **1993**, 2121.

(8) (a) Nakanishi, W.; Hayashi, S.; Toyota, S. *J. Org. Chem.* **1998**, *63*, 8790. (b) Nakanishi, W.; Hayashi, S.; Toyota, S. *J. Chem. Soc., Chem. Comm.* **1996**, 371.

(9) Regular and inverse substituent effects on $\delta(^1Se)$ via $\delta(^8Se)$ are reported in 1-(MeSe)-8-(p-YC$_6$H$_4$Se)C$_{10}$H$_6$ and 1-[8-(p-YC$_6$H$_4$Se)C$_{10}$H$_6$]SeSe[C$_{10}$H$_6$(SeC$_6$H$_4$Y-p)-8']-1' (Y = H, OMe, Me, Cl, Br, CO$_2$Et, NO$_2$), respectively. See ref. 3.

(10) (a) Pimentel, G. C. *J. Chem. Phys.* **1951**, *19*, 446. Musher, J. I. *Angew. Chem., Int. Ed. Engl.* **1969**, *8*, 54. (b) Chen, M. M. L.; Hoffmann, R. *J. Am. Chem. Soc.* **1976**, *98*, 1647. (c) Cahill, P. A.; Dykstra, C. E.; Martin, J. C. *J. Am. Chem. Soc.* **1985**, *107*, 6359. See also, Hayes, R. A.; Martin, J. C. "*Sulfurane Chemistry*," in "*Organic Sulfur Chemistry: Theoretical and Experimental Advances*," ed by Bernardi, F. Csizmadia, I. G. Mangini, A. Elsevier: Amsterdam, 1985; Chapter 8.

(11) (a) Nakanishi, W.; Hayashi, S.; Kihara, H. *J. Org. Chem.* **1999**, *64*, 2630.

(12) Rosenfield, Jr., R. E.; Parthasarathy, R.; Dunitz, J. D. *J. Am. Chem. Soc.* **1977**, *99*, 4860.

(13) Ramasubbu, N.; Parthasarathy, R. *Phosphorus Sulfur* **1987**, *31*, 221.

(14) *Gaussian 94, Revision D.4*; Frisch, M. J.; Trucks, G. W.; Schlegel, H. B.; Gill, P. M. W.; Johnson, B. G.; Robb, M. A.; Cheeseman, J. R.; Keith, T.; Petersson, G. A.; Montgomery, J. A.; Raghavachari, K.; Al-Laham, M. A.; Zakrzewski, V. G.; Ortiz, J. V.; Foresman, J. B.; Cioslowski, J.; Stefanov, B. B.; Nanayakkara, A.; Challacombe, M.; Peng, C. Y.; Ayala, P. Y.; Chen, W.; Wong, M. W.; Andres, J. L.; Replogle, E. S.; Gomperts, R.; Martin, R. L.; Fox, D. J.; Binkley, J. S.; Defrees, D. J.; Baker, J.; Stewart, J. P.; Head-Gordon, M.; Gonzalez, C.; Pople, J. A. *Gaussian, Inc.*, Pittsburgh, PA, 1995.

(15) These results are essentially the same as those reported in ref 8a. The calculations were performed on a model of **1** with the MP2/6-311++G(3df,2pd) method. The Se---Se distance of the model was fixed at 3.053 Å and the two Se–H$_b$ bonds were placed on the xy-plane and the two Se–H$_a$ bonds were placed on the planes which across the xy-plane with a right angle. The four Se–H

bonds and the two HSeH angles and the two SeSeH angles were optimized. The optimized $\angle$SeSeH values were 72.72° and 157.43°, respectively.

(16) HOMO-n (n = 2 - 5) were also plotted against θ_1. The energy curves are flat or change only monotonically.

(17) MacSpartan Plus Ver. 1.0, Hehre, H.J. *Wavefunction Inc.*

(18) The results of the MO calculations for 1-naphthaleneselenole will be reported elsewhere.

(19) NBO Ver. 3.1, Glendening, E. D.; Reed, A. E.; Carpenter, J. E.; Weinhold, F.

(20) Topson, R. D. *The Nature and Analysis of Substituent Electronic Effects*, in *Progress in Physical Organic Chemistry*, ed by Taft, R. W. John Wiley & Sons, Vol. 12, New York, 1976. See also refs cited therein.

(21) The contribution of the n(Z)---n(Z) π type 2c-4e interaction (type **C** pairing) is important on the structures of 1,8-bis(alkyl(or aryl)chalcogena)naphthalenes, which may be due to the same atoms (usually same groups) substituted at the 1,8-positions.

(22) The interaction between the filled p-type lone pair orbital of the Se atom and the p-type orbital of Y through the π-orbitals of the aryl group must play an important role to determine the structure of **2** and **3**.[23]

(23) Studies on the structures of 1-(*p*-anisylselanyl)naphthalene **(11)** and 1-(*p*-chlorophenylselanyl)naphthalene **(12)**, together with other Y in 1-(*p*-$YC_6H_4Se)C_{10}H_7$, are in progress in our laboratory. The conformations around the Se–C_{An} bond in **2** and the Se–C_{Ar} bond in **3** are close to those in **11** and **12**, respectively. Details on the structures of 1-(*p*-$YC_6H_4Se)C_{10}H_7$ will be reported elsewhere.

(24) Beurskens, P.T.; Admiraal, G.; Beurskens, G.; Bosman, W.P.; Garcia-Granda, S.; Gould, R.O.; Smits, J.M.M.; Smykalla, C. (1992). The DIRDIF program system, Technical Report of the Crystallography Laboratory, University of Nijmegen, The Netherlands.

(25) Beurskens, P.T.; Admiraal, G.; Beurskens, G.; Bosman, W.P.; de Gelder, R.; Israel, R.; Smits, J.M.M. (1994). The DIRDIF-94 program system, Technical Report of the Crystallography Laboratory, University of Nijmegen, The Netherlands.

Chapte 6

Structural Study of Aryl Selenides in Solution Based on the ^{77}Se NMR Chemical Shifts: Application of the GIAO Magnetic Shielding Tensor of ^{77}Se Nucleus

Abstract

The ^{77}Se NMR chemical shifts (δ_{obsd}(Se)) of p-YC$_6$H$_4$SeMe (1: Y = H (a), OMe (b), Me (c), Cl (d), Br (e), COOR (f), and NO$_2$ (g)) and p-YC$_6$H$_4$SePh (2) were determined or redetermined in chloroform-d. The δ_{obsd}(Se) values of 2, p-YC$_6$H$_4$SeR (R = CN (3), Bz (4), H (5), Br (6), Et (7), C$_6$H$_4$Y-p (8), CH=CH$_2$ (9), CH=CHCl-t (10), and CHCH$_2$CCl$_2$-cyclo (11)), 1,1'-[8-(p-YC$_6$H$_4$Se)C$_{10}$H$_6$Se]$_2$ (12), and 1-(MeSe)-8-(p-YC$_6$H$_4$Se)C$_{10}$H$_6$ (13) were plotted against those of 1. The plots were analyzed as two correlations. For example, the points corresponding to a – c make a group (g(m)) and those of d – g belong to another one (g(n)). This must be the reflection of differences in the dihedral angles between the aryl rings and the Se-R bonds, which should result in the different contributions of the inductive and mesomeric effects of the substituents Y on the δ_{obsd}(Se) values.

After reexamination of applicability of the GIAO magnetic shielding tensor for the selenium nucleus (σ(Se)) in selenium compounds of various structures, σ(Se) was calculated for the model compounds, 5, with the B3LYP/6-311+G(d,p) method, to explain the δ_{obsd}(Se) values of 1 – 13 uniformly: δ_{calcd}(Se) was defined as -(σ(Se) – σ(Se)$_{MeSeMe}$). Each selenol was optimized to be the planar structure (14) and the perpendicular one (15), if the calculations were performed assuming the C_s symmetry or the similar geometry. New parameters were devised such as δ_{calcd}(Se:θ_B) = (1 - sinθ_B)•δ_{calcd}(Se)$_{14}$ + sinθ_B•δ_{calcd}(Se)$_{15}$. The δ_{obsd}(Se) values of 1 – 13 correlated well with the new parameters, δ_{calcd}(Se:θ_B), which gave the best-fitted θ_B values. The structures of 1 – 13 in solutions were explained uniformly by the evaluated θ_B values. The observed ratios of the slopes for g(m) versus those of g(n) were also correlated with the θ_B values.

Introduction

Organic selenium compounds are well-known to show versatile reactivities, and they afford many structurally interesting compounds.[1] The ^{77}Se NMR spectroscopy, as well as ^{1}H and ^{13}C NMR spectroscopies, plays an important role in studying organic selenium chemistry.[2] The observed ^{77}Se NMR chemical shifts (δ_{obsd}(Se)) of organic selenium compounds have been interpreted based on the Karplus-Pople equation (equation 1).[3] The ΔE factor, the average excitation energy, could be estimated by the energy difference between HOMO and LUMO of the compound if the 4p atomic orbitals of the selenium atom substantially contribute to both of the orbitals. The $<r^{-3}>$ factor of the 4p orbitals is expected to be proportional to the atomic charge on the Se atom being observed. The quantities Q_i and Q_j represent the elements of the charge density and bond order matrices in the molecular orbital theory of the unperturbed molecule. The ΔE factor, for example, is expected to play an important role in the δ_{obsd}(Se) of diselenides, while the $<r^{-3}>$ factor would be operating in hypervalent compounds or oxides relative to the corresponding selenides.[2] However, the δ_{obsd}(Se) values are not proportional to the ΔE and/or $<r^{-3}>$ factors in some cases, since the values are governed by the complex conjugation of the two factors, together with other factors.

$$\sigma_i^{para} = -\frac{\mu_0\mu_B^2}{2\pi\,\Delta E}\; <r^{-3}>\; [Q_i + \sum_{j \neq i} Q_j] \tag{1}$$

The δ(Se) values are reflected much by the structural change of the selenium compounds. Therefore, it must be very useful not only in the structural study of the selenium compounds but also in the preparation of new compounds, that the calculated ^{77}Se NMR chemical shifts (δ_{calcd}(Se)) explain the δ_{obsd}(Se) values well. Recently, the magnetic shielding tensor is shown to be reliable for some nuclei containing carbon, oxygen, and hydrogen, calculated with the gauge-including atomic orbitals (GIAO) theory.[4] Efforts have also been made to calculate the magnetic shielding tensor for the ^{77}Se nucleus on the theoretical background, and the reliability has been essentially established so far.[5,6]

This encouraged us to interpret uniformly the δ_{obsd}(Se) values of para-substituted phenyl selenides, p-YC$_6$H$_4$SeR (ArSeR: **1** - **13**), in relation to their structures in solutions, based on the δ_{calcd}(Se) values. Before discussion of the δ(Se) values of p-YC$_6$H$_4$SeR, the GIAO magnetic shielding tensor for the ^{77}Se nucleus (σ(Se)) in selenium compounds[7] of versatile structures was calculated and/or recalculated using the Gaussian 94 program[8] with some basis sets. The calculations showed us which method (basis sets and the level) is practically suitable for my purpose to calculate the δ_{calcd}(Se) values of p-YC$_6$H$_4$SeR.

$$Y\!-\!\!\langle\!\!\!\bigcirc\!\!\!\rangle\!\!-\!Se\!-\!R$$
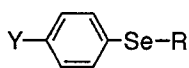
1 (R = Me)	**5** (R = H)	**9** (R = CH=CH$_2$)
2 (R = Ph)	**6** (R = Br)	**10** (R = CH=CHCl-trans)
3 (R = CN)	**7** (R = Et)	**11** (R = CHCH$_2$CCl$_2$-cyclo)
4 (R = Bz)	**8** (R = C$_6$H$_4$Y-p)	

12

13
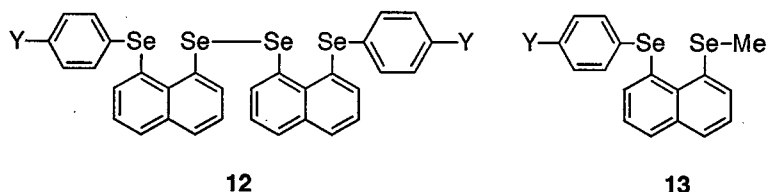
	a	**b**	**c**	**d**	**e**	**f**	**g**	**h**	**i**	**j**	**k**	**l**
Y =	H	OR	Me	Cl	Br	CO$_2$R	NO$_2$	NH$_2$	F	CF$_3$	CHO	CN

The calculations could be performed variously. To learn how the calculations should be carried out for a better interpretation of the δ_{obsd}(Se) values uniformly, the characters of δ_{obsd}(Se) for **1** - **13** were reexamined briefly by plotting the δ_{obsd}(Se) values of **2** - **13** against those of **1**. The results confirmed my calculations of the δ_{calcd}(Se) values for para-substituted benzeneselenols (**5**). Two structures are optimized for each selenol if the calculations are performed assuming the C_s symmetry: one is the planar structure of which Se-H bond is in the aryl plane (**14**) and the other is the perpendicular one where the Se-H bond is perpendicular to the aryl plane (**15**). The σ(Se) values were calculated for **14** and **15** based on the GIAO theory. The electronic effect of Y and R and the steric effect of R in p-YC$_6$H$_4$SeR affect the structure of ArSeR, especially around the Se atom, namely, θ_R in **16**. New parameters (δ_{calcd}(Se:θ)) are devised, of which the θ values are expected to correlate roughly to the angle θ_R. The δ_{obsd}(Se) values are well-explained by the devised parameters, which consequently enables us to understand the electronic and/or steric effects of R on the δ_{obsd}(Se) values.

14   **15**   **16**
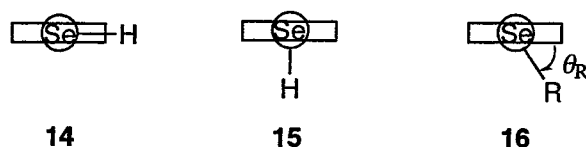
Here I present the results of the calculations for the δ_{calcd}(Se) values based on the GIAO theory, emphasizing how they are useful in explaining the δ_{obsd}(Se) values and understanding the organic selenium chemistry based on ^{77}Se NMR spectroscopy.

Results and Discussion

**GIAO Magnetic Shielding Tensor for ^{77}Se Nucleus of Various Selenium Compounds.**
To know which method of calculations is suitable for explaining the δ_{obsd}(Se) values of p-YC$_6$H$_4$SeR (**1 - 13**), the GIAO magnetic shielding tensor for the ^{77}Se nucleus (σ(Se)) of selenium compounds with various structures is calculated and/or recalculated using the Gaussian 94 program.[8] The employed selenium compounds for the calculations and the optimized symmetry of the compounds are shown in Table 1. The 6-311++G(3df,2pd), 6-311+G(d,p), and 3-21G basis sets were applied at the DFT (B3LYP) level.[9] The HF level was also applied with the 6-311+G(d,p) basis set. Table 1 exhibits the calculated chemical shifts (δ_{calcd}(Se)) relative to dimethyl selenide (δ_{calcd}(Se) = $-(\sigma$(Se) $- \sigma$(Se)$_{MeSeMe}$)), together with the parent σ(Se) values of dimethyl selenide. Natural charges (Qn) calculated by natural population analysis[10,11] and the energy differences ($\Delta\varepsilon$) between the HOMO and the LUMO of the selenium compounds are also given in Table 1, calculated with the 6-311++G(3df,2pd) basis sets at the B3LYP level. Table 1 also contains the δ_{obsd}(Se) values of the selenium compounds.[2]

To begin with, the δ_{obsd}(Se) values are plotted against Qn(Se) and $\Delta\varepsilon$ calculated with the B3LYP/6-311++G(3df,2pd) method. The results are shown in Figures 1 and 2, respectively, which show that those values cannot explain the wide range of δ_{obsd}(Se). However they may be useful for the discussion when applied to a small range of shift values and/or to the selected structures. One must confirm that the p orbitals of the Se atom contribute to both the HOMO and the LUMO of the selenium compound in question when $\Delta\varepsilon$ is applied to the discussion.[3,7]

Table 1. The $\delta_{calcd}(Se)$ and $\delta_{obsd}(Se)$ Values of Selenium Compounds of Various Structures, Together with the $Qn(Se)$ and $\Delta\varepsilon$ Values[a]

compd (no)	structure[b]	$Qn(Se)$[c]	$\Delta\varepsilon$[c,d]	$\delta_{calcd}(Se)$				$\delta_{obsd}(Se)$	solvent
				c	e	f	g		
MeSeMe (i)	C_{2v}	0.2719	0.203	1656.4	1624.4	1942.5	1895.9		
				0.0	0.0	0.0	0.0	0.0	CDCl$_3$
H$_2$Se (ii)	C_{2v}	-0.1695	0.232	-412.6	-412.1	-233.1	-207.1	-344.75[h]	gas phase[i]
MeSeH (iii)	C_s	0.0543	0.208	-187.7	-189.9	-107.2	-93.3	-154.67[j]	gas phase[i]
Me$_3$Se$^+$ (iv)	C_3	1.0229	0.309	220.9	190.0	186.5	140.1	253	H$_2$O
MeSeSeMe (v)	C_2	0.1269	0.179	341.2	375.5	217.8	558.5	281	CDCl$_3$
MeSeCl$_2$Me (vi)	C_{2v}	1.0477	0.193	401.9	377.0	398.0	322.4	448	CH$_2$Cl$_2$
SeF$_6$ (vii)	O_h	2.9570	0.295	632.7	718.9	555.7	533.9	610.3	neat
Me$_2$SeO (viii)	C_s	1.3485	0.221	768.0	757.9	679.9	608.9	812	H$_2$O
F$_2$SeO$_2$ (ix)	C_{2v}	2.7655	0.247	914.6	961.7	1032.1	917.5	948	neat
SeF$_4$ (x)	C_{2v}	2.1805	0.257	1115.0	1244.4	925.1	1029.4	1083	CH$_3$F
F$_2$SeO (xi)	C_s	1.9940	0.252	1353.0	1438.6	1336.0	1270.8	1378.2	neat

[a] The calculated $\sigma(Se)$ values are shown for MeSeMe and those relative to MeSeMe are given for other compounds (see text). [b] Optimized symmetry. [c] B3LYP/6-311++G(3df,2pd). [d] In au. [e] B3LYP/6-311+G(d,p). [f] HF/6-311+G(d,p). [g] B3LYP/3-21G. [h] -288 in D$_2$O. [i] Ref. 5g. [j] -130 in CDCl$_3$.
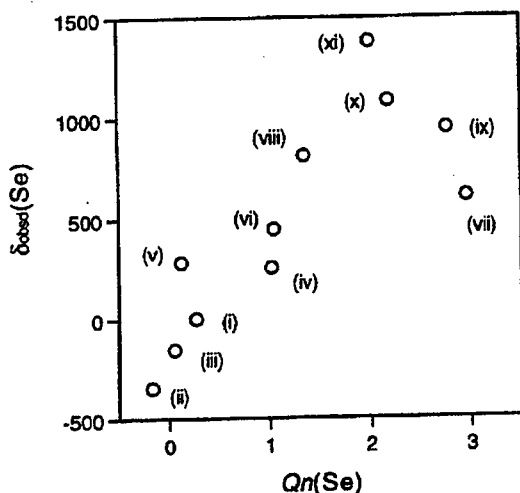
Figure 1. Plot of $\delta_{obsd}(Se)$ versus Qn(Se) calculated with the B3LYP/6-311++G(3df,2pd) method. The numbers shown in the figure correspond to those in Table 1.
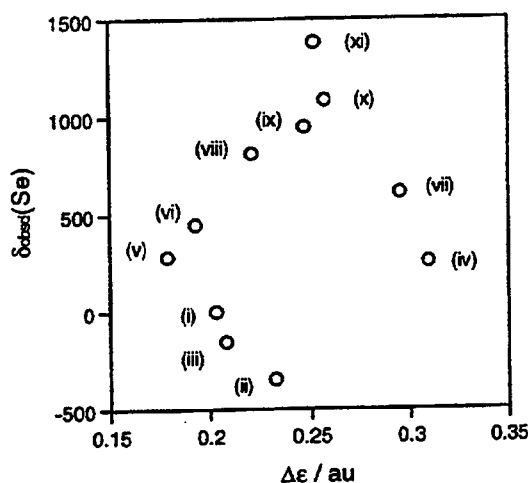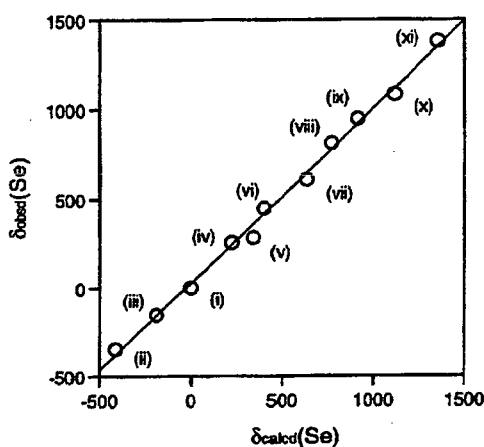

Figure 2. Plot of $\delta_{obsd}(Se)$ versus $\Delta\epsilon$ calculated with the B3LYP/6-311++G(3df,2pd) method. The numbers shown in the figure correspond to those in Table 1.

Figure 3 exhibits the plot of $\delta_{obsd}(Se)$ against $\delta_{calcd}(Se)$ obtained with the B3LYP/6-311++G(3df,2pd) method. Table 2 collects the correlations of $\delta_{obsd}(Se)$ against $\delta_{calcd}(Se)$ obtained with the various methods shown in Table 1. The method with the 6-311++G(3df,2pd) basis set at the B3LYP level is excellent among the results shown in Table 2 ($r = 0.998$).[12] The 6-311+G(d,p) basis set is also recommended for the calculations of the σ(Se) values since the correlation coefficients are also good when the 6-311+G(d,p) basis set is employed at both the B3LYP and the HF levels (Table 2). Those obtained with the B3LYP/3-21G method could not

100

explain well the observed values ($r = 0.971$). Table 2 also contains the constants and the coefficients for the correlations where the point corresponding to MeSeSeMe is omitted from the correlations. The r values were much improved for the B3LYP/3-21G method. The poor accuracy for the optimized structure of MeSeSeMe is mainly responsible for the discrepancy of the calculated values with the 3-21G basis set at the B3LYP level.[13]

Figure 3. Plot of δ_{obsd}(Se) versus δ_{calcd}(Se) calculated with the B3LYP/ 6-311++G(3df,2pd) method. The numbers shown in the figure correspond to those in Table 1.

Table 2. Correlations of δ_{obsd}(Se) versus δ_{calcd}(Se) with Various Methods[a]

method of calculations	a	b	r
versus δ_{calcd}(Se)			
B3LYP/6-311++G(3df,2pd)	0.981	24.3	0.998
B3LYP/6-311+G(d,p)	0.914	29.2	0.993
HF/6-311+G(d,p)	1.066	-0.6	0.990
B3LYP/3-21G	1.092	-21.2	0.971
versus δ_{calcd}(Se) without the point for MeSeSeMe			
B3LYP/6-311++G(3df,2pd)	0.977	33.8	0.999
B3LYP/6-311+G(d,p)	0.911	40.1	0.994
HF/6-311+G(d,p)	1.071	-8.0	0.990
B3LYP/3-21G	1.106	3.2	0.989

[a] δ_{obsd}(Se) = $a \times \delta_{calcd}$(Se) + b, with r (correlation coefficient).

**Table 3.** The δ_{obsd}(Se) Values of Some Aryl Selenides

Y	1[a]	1'	2[a]	3	4	5	6	7	8	9	10	11	12	13
solvent	$CDCl_3$	Neat	$CDCl_3$	$CDCl_3$	$CDCl_3$	Neat	$CDCl_3$	CH_2Cl_2	$CDCl_3$	b	b	b	$CDCl_3$	$CDCl_3$
H	207.8	202.0	423.6	320.8	641.5	145	869.0	327	423.6	395.5	368.6	370.2	429.0	434.3
OMe	197.4	189.5	408.1	308.8	628.9	122	887.7	318	395.6	386.7	361.8	356.8	416.2	424.5
Me	200.6	196.1	415.0	313.0	634.4	128	876.9	323[c]	407.4	390.9	364.6	362.9	422.0	427.7
F		200.0		318.3	634.4	141		324	412.9					
Cl	210.3	203.6	421.9	321.0	637.0	142			419.9	395.4	366.3	370.5	429.1	431.6
Br	210.6		422.3	321.7	637.4				416.5	396.0	366.5	371.5	429.6	432.4
COOR	227.9[d,e]	218.1[f]	433.3[g]	329.4[g]	642.3[g]				436.7[g]				442.5[g]	442.4[g]
NO_2	241.2	233.4	446.3	338.8	645.7		823.0		447.4	404.9	377.0	396.8	456.1	453.9

[a] This work. [b] Not specified. [c] Neat. [d] R = H. [e] Ref. 7. [f] R = Me. [g] R = Et.

Correlations in the $\delta_{obsd}(Se)$ Values of Aryl Selenides. Before I discuss the $\delta_{obsd}(Se)$ values of aryl selenides based on the calculated values, the correlations between the observed values were examined first. The $\delta_{obsd}(Se)$ values of p-YC_6H_4SeMe (**1**: **1a** – **1g**) and p-YC_6H_4SePh (**2**) were determined or redetermined in $CDCl_3$ using an FT NMR spectrometer. The values are given in Table 3. Table 3 also collects the $\delta_{obsd}(Se)$ values of various para-substituted phenyl selenides,[2,14-18] containing those reported for **1** determined in neat liquid by the INDOR ^1H–$\{^{77}Se\}$ technique (shown by **1'**).[14] The $\delta_{obsd}(Se)$ values of **1'** ($\delta_{obsd}(Se)_{1'}$) were plotted against those of **1**. Equation 2 shows the results. The correlation was good irrespective of the different conditions of the measurements. The proportionality constant of 0.939 and the correlation coefficient (r) of 0.995 show that the solvent effect may not work so much in the correlation of the two.

$$\delta_{obsd}(Se)_{1'} = 0.939 \times \delta_{obsd}(Se)_1 + 6.0 \qquad r = 0.995 \qquad (2)$$

$$\delta_{obsd}(Se) \text{ of } ArSeR = a \times \delta_{obsd}(Se)_1 + b \qquad r: \text{correlation coefficient} \qquad (3)$$
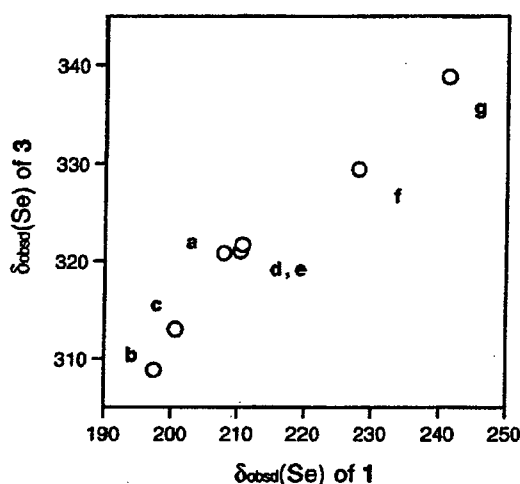
Figure 4. Plot of $\delta_{obsd}(Se)$ of **3** versus those of **1**.

The $\delta_{obsd}(Se)$ values of **2** - **13** were plotted against that of $\delta_{obsd}(Se)_1$. Figure 4 shows the plot for **3**, for example. The plot should be analyzed as two correlations. One of the groups contains the points corresponding to Y = OMe, Me, and H (group **m** (g(**m**))) and another group consists of those of Y = Cl, Br, COOR, and NO_2 (group **n** (g(**n**))). Since the points corresponding to Y = H, Cl, and Br exist at the crossing area of the two groups, there must be other classifications. Another possibility of the classification is as follows. The points corresponding to Y = OMe, Me, Cl, and Br make a group (g(**m'**)) and those with Y = H, COOR, and NO_2 make another (g(**n'**)).

The g(m) and g(n) classifications explains the δ_{obsd}(Se) values better than the g(m') and g(n') groupings. The g(m') and g(n') groupings may be rationalized based on the theoretical background. The Cl and Br atoms donate electrons by the mesomeric mechanism, but H is not an electron donor.[19] The planar structure **14** is calculated to be less stable than the perpendicular structure **15** for g(m'), whereas the former is evaluated to be more stable than the latter for g(n') with the B3LYP/6-311+G(d,p) method (see Table 6). Table 4 collects the results for the g(m) and g(n) classifications.[20] The parameters of the correlations for g(m) and g(n) are given by a_x, b_x, and r_x, where x = m or n, as shown in equation 3. Table 4 also contains correlations similarly treated for δ_{obsd}(Se)$_8$ versus δ_{obsd}(Se)$_2$.

Table 4. Correlations in δ_{obsd}(Se) of Aryl Selenides[a]

correlation	a_m	b_m	r_m	n	a_n	b_n	r_n	n	a_m/a_n
2 versus **1**	1.440	124.7	0.988	3	0.767	260.4	0.994	4	1.88
3 versus **1**	1.142	83.6	0.999	3	0.553	204.8	0.994	4	2.07
4 versus **1**	1.173	398.0	0.989	3	0.279	578.6	0.999	4	4.20
5 versus **1**	2.237	320.0	0.999	3					
6 versus **1**	-1.410	1162.8	0.996	4[b]					
7 versus **1**	0.813	158.5	0.960	3					
8 versus **1**	2.617	-119.7	0.992	3	0.964	215.6	0.993	4	2.71
9 versus **1**	0.811	227.2	0.982	3	0.299	332.7	0.999	3	2.71
10 versus **1**	0.637	236.3	0.993	3	0.345	293.9	1.000	3	1.85
11 versus **1**	1.242	112.5	0.986	3	0.839	194.4	1.000	3	1.48
12 versus **1**	1.187	182.7	0.987	3	0.854	249.4	0.997	4	1.39
13 versus **1**	0.938	239.4	1.000	3	0.696	285.2	0.995	4	1.35
8 versus **2**	1.810	-343.1	1.000	3	1.234	-101.7	0.979	3	1.47

[a] The constants, a_x, b_x, and r_x (x = m and n), are defined by equation 3 and applied for g(m) and g(n), respectively. b Containg **6g**.

Why can the correlations be well-analyzed by the two groups, g(m) and g(n)? The phenomena can be explained by considering the following factors, which contribute to the correlations. (1) The aryl selenides **1** - **13** exist as **16** with θ_R. (2) Since the p-type lone pair of the Se atom in ArSeR is filled with electrons, the interaction between the lone-pair orbital and the orbitals of the Ar and/or R groups will stabilize the compound more effectively, if the electron withdrawing ability of Ar and/or R becomes higher. (3) The electronic and the steric effects of R in ArSeR mainly determine θ_R, which affects the substituent effect of Y on the δ_{obsd}(Se) values. (4) The θ_R value would be larger if the electron-withdrawing ability of R

becomes larger. (5) The θ_R value might depend on Y, but the change is usually not so large. (6) The proportionality constants a_m and a_n would be the reflection not only of the electronic effect of R but also of $\Delta\theta_R$ (= (θ_R of **2 - 13**) – (θ_R of **1**)), which determines the overlap integrals between the p-type lonepair and the π orbital of the Ar group.

The ratio a_m/a_n is expected to be the reflection of θ_R. The torsional angle or "average torsional angle" in ArSeR must change when R in ArSeR is replaced by R'. The change must be the cause for the δ_{obsd}(Se) values of ArSeR analyzed as the two correlations, although it would additionally depend on Y, since Y could affect the torsional angle to some extent. As the "average torsional angle" becomes larger, the ratio a_m/a_n is expected to increase, if the contributions of R on the a_m/a_n ratios are similar for the two selenides. The a_m/a_n values for **2, 3**, and **4** are 1.88, 2.07, and 4.20, respectively, which may show that the torsional angles become larger in the order **1 < 2 ≈ 3 < 4** among the four aryl selenides in solutions.[21] And the a_m/a_n values in Table 4 are all larger than unity, which would be the reflection of the larger θ_R values of **2 - 13** relative to that of **1** in solutions.

After brief examination of the δ_{obsd}(Se) values of aryl selenides, next extension of my investigation is to explain the δ_{obsd}(Se) values of **1 - 13** using the δ_{calcd}(Se) values based on the GIAO theory, in relation to those suggested above discussion.

Structure and δ_{calcd}(Se) for 5a. Ab initio molecular orbital calculations were performed on **5a** as the model compound using the Gaussian 94 program[8] with the 6-311+G(d,p) basis set at the B3LYP level. The structures of **14a** and **15a** were optimized for **5a** when the calculations were performed assuming the C_s symmetry, where the Se-H bond is placed in the phenyl plane and the bond is perpendicular to the phenyl plane as shown in **14** and **15**, respectively. However, one imaginary frequency was predicted for each of the optimized structures in the frequency analysis (-164.3 cm^{-1} for **14a** and -169.7 cm^{-1} for **15a**). The negative frequencies correspond to the motion of the Se-H protons around the Se-C bonds of **14a** and **15a**. The results show that **14a** and **15a** are not the energy minima but correspond to the transition states. The optimized structure with all positive frequencies is obtained at $\theta = 37.30°$.[22] The results are shown in Table 5.

Ab initio MO calculations were also performed on **5a** with the torsional angle C_oC_iSeH (θ_H) fixed at $15t°$ (t = 1, 2, 3, 4, and 5). The results of the calculations are collected in Table 5. The angular dependence of the energy is shown to be very small.[22] The GIAO magnetic shielding tensor for the Se nucleus (σ(Se)) was calculated with the B3LYP/6-311+G(d,p) method for the partially optimized structures of **5a** with θ_H fixed at the given values shown in Table 5, together with the optimized structures of **14a** and **15a**. The results, which are reduced to the δ_{calcd}(Se) values, are also collected in Table 5.

Table 5. Energies and δ(Se) for **5a** Calculated with the B3LYP/6-311+G(d,p) Method

$\theta_H{}^a$ (deg)	E (au)	ΔE^b (kJ•mol^{-1})	$\delta_{calcd}(Se)^c$
0.00^d (14a)	-2633.85503	0.18	81.66
15.00^e	-2633.85505	0.13	74.43
30.00^e	-2633.85507	0.08	59.15
37.30^f	-2633.85510	0.00	51.68
45.00^e	-2633.85506	0.11	45.46
60.00^e	-2633.85505	0.13	38.28
75.00^e	-2633.85501	0.24	38.68
90.00^d (15a)	-2633.85499	0.29	39.99

^{a} The torsional angle of C$_o$C$_i$SeH. ^{b} E (θ_H) - E (θ_H = 37.30°). ^{c} The σ(Se) value for MeSeMe being 1624.36. ^{d} Full-optimized supposing the C_s symmetry. ^{e} Partially optimized with θ_H fixed at a given value. ^{f} Full-optimized supposing the C_1 symmetry starting the partially optimized structure with θ_H fixed at 30.00°.
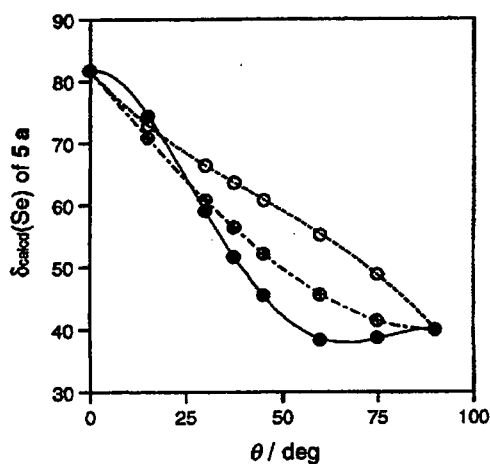
Figure 5. Plots of $\delta_{calcd}(Se)$ of **5a** versus θ: ● stands for $\delta_{calcd}(Se:\theta)$ of **5a**, together with the calibration curve given in eq 4, O for a trial function, $\delta_{calcd}(Se:\theta_A)$, defined by eq 5, and ⊗ for a trial function, $\delta_{calcd}(Se:\theta_B)$, defined by eq 6.

$$\delta_{calcd}(Se:\theta) = -4.246 \times 10^{-6}•\theta^4 + 8.871 \times 10^{-4}•\theta^3 - 5.193 \times 10^{-2}•\theta^2 + 0.1208•\theta + 81.63 \quad (4)$$

$$\delta_{calcd}(Se:\theta_A) = (\delta_{calcd}(Se)_{14}•\cos\theta + \delta_{calcd}(Se)_{15}•\sin\theta)/(\cos\theta + \sin\theta) \quad (5)$$

$$\delta_{calcd}(Se:\theta_B) = \delta_{calcd}(Se)_{14}•(1 - \sin\theta) + \delta_{calcd}(Se)_{15}•\sin\theta \quad (6)$$

Before a discussion of $\delta_{obsd}(Se)$ based on $\delta_{calcd}(Se)$, the angular dependence of $\delta_{calcd}(Se)_{5a}$ in Table 5 was examined. Figure 5 shows the plots of $\delta_{calcd}(Se)_{5a}$ against θ. The solid curve in the figure is drawn according to equation 4: the correlation coefficient for the calibration curve is excellent ($r = 1.000$). The trial functions are devised for the angular dependence of $\delta(Se)$, which are defined by equations 5^{23} and 6. The θ values are shown by θ_A and θ_B, respectively. The $\delta_{calcd}(Se:\theta_A)$ and $\delta_{calcd}(Se:\theta_B)$ curves given by equations 5 and 6 are also drawn in Figure 5. The coincidence of the curves with that of equation 4 is better for $\delta_{calcd}(Se:\theta_B)$ than that for $\delta_{calcd}(Se:\theta_A)$. Equations 4 - 6 will be applied to the $\delta_{obsd}(Se)$ in ArSeR based on the $\delta_{calcd}(Se)$ of **5** in the following section.

Interpretation of $\delta_{obsd}(Se)$ in ArSeR Based on the $\delta_{calcd}(Se)$ of 5. Ab initio molecular orbital calculations were also performed on **5b** - **5l** using the Gaussian 94 program[8] with the B3LYP/6-311+G(d,p) method. The structures of **14** and **15** were optimized for **5** except for **15f** and **15k**, when the C_s symmetry was assumed in the calculations (or the calculations were started from a similar geometry). θ_H is fixed at 90° in the calculations for **15f** and 15k in order to obtain the $\delta_{calcd}(Se)$ values for the structures. Structures **14** and **15** must be recognized as the standard points that give $\delta_{calcd}(Se)$ at $\theta_H = 0°$ and 90°, respectively. Table 6 collects the energies of **14** and **15** bearing various substituents at the para positions. Structure **15** is predicted to be more stable for Y = NH$_2$ **(h)**, OH **(b)**, F **(i)**, Me **(c)**, Cl **(d)**, and Br **(e)** (g(m')), which donate electrons by the mesomeric mechanism. Structure **14** is estimated to be more stable for Y = CN **(l)**, COOH **(f)**, CHO **(k)**, NO$_2$ **(g)**, and CF$_3$ **(j)** (g(n')), which accept electrons through the π framework, except for Y = CF$_3$ **(j)**, an electron-withdrawing group mainly through the σ framework. The g(n') also contains Y = H **(a)**, a nonelectron donor.

The $\sigma(Se)$ values were calculated using the optimized structures of **14** and **15** (partially optimized ones for **15f** and **15k**) with the B3LYP/6-311+G(d,p) method. Table 6 collects the $\delta_{calcd}(Se)$ values for **14** and **15**. Figure 6 shows the plot of $\delta_{calcd}(Se)_{15}$ against $\delta_{calcd}(Se)_{14}$. The plot should be analyzed as the two correlations with g(m') and g(n'), as mentioned above. The correlations are shown in equations 7 and 8, respectively. The point corresponding to Y = CN is omitted in the correlation in equation 8 since the point deviates from the correlation. The point behaves as if it were contained in g(m'). The cyano group might interact with the p-type lone pair at the Se atom of **15**. The omission of the cyano group in the correlation will not affect the following discussion.

Table 6. Energies and δ(Se) for **14** and **15** Calculated with the B3LYP/6-311+G(d,p) Method

Y	E			δ_{calcd}(Se)	
	14[a]	**15**[a]	ΔE[b,c]	**14**	**15**
NH$_2$ (h)	-2689.2290	-2689.2325	9.2	58.6	11.1
OH (b)	-2709.1011	-2709.1027	4.2	69.9	16.9
Me (c)	-2673.1825	-2673.1829	1.1	73.5	25.1
F (i)	-2733.1224	-2733.1232	2.1	81.4	28.2
Cl (d)	-3093.4771	-3093.4773	0.5	84.3	32.4
Br (e)	-5207.3968	-5207.3969	0.3	84.5	33.3
H (a)	-2633.8550	-2633.8550	0.0	81.7	40.0
CF$_3$ (j)	-2971.0044	-2971.0034	-2.6	100.8	49.4
COOH (f)	-2822.4927	-2822.4909[d]	-4.7	104.6	47.8
CHO (k)	-2747.2138	-2747.2117[d]	-5.5	109.5	53.0
CN (l)	-2726.1216	-2726.1200	-4.2	112.3	59.3
NO$_2$ (g)	-2838.4188	-2838.4165	-6.0	119.0	55.3

[a] In au. [b] E(**14**) - E(**15**). [c] In kJ mol^{-1}. [d] The Se-H bond being assumed perpendicular to the phenyl plane.
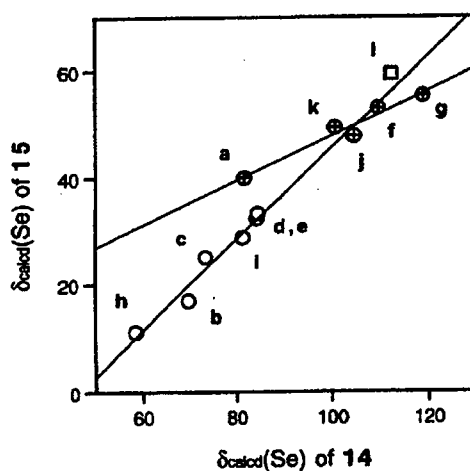
Figure 6. Plots of δ_{calcd}(Se) of **15** versus those of **14** calculated with the B3LYP/6-311+G(d,p) method: O stands for g(m'), ⊗ for g(n'), and □ for Y = CN.

$$\delta_{calcd}(Se)_{15} = 0.860 \times \delta_{calcd}(Se)_{14} - 40.2 \qquad \text{For g(m')} \qquad r = 0.980 \qquad (7)$$

$$\delta_{calcd}(Se)_{15} = 0.416 \times \delta_{calcd}(Se)_{14} + 6.2 \qquad \text{For g(n')} \qquad r = 0.974 \qquad (8)$$

The proportionality constants are less than unity in equations 7 and 8, which exhibits that the interaction between the lone-pair orbital(s) at the Se atom and the orbital(s) at the substituent Y is stronger in **14** than that in **15**. The proportionality constant for g(**m'**) in equation 7 is 2.1 times larger than that for g(**n'**) in equation 8. The results show that the susceptibility of Y on the δ(Se) values is larger in **14** than in **15**, especially for g(**n'**). It must be the reflection of the more effective electron extension of the (p-type) lone pair of the Se atom over Y of the electron withdrawing g(**n'**) than those over electron donating g(**m'**). The mesomeric mechanism must mainly contribute to the interaction in **14**, especially for g(**n'**).

The new parameters, $\delta_{calcd}(Se:\theta_A)$ and $\delta_{calcd}(Se:\theta_B)$ defined by equations 5 and 6, are applied in the plots of the $\delta_{obsd}(Se)$ values of **1 – 13** in Table 3. The predicted θ values must serve as a measure for θ_R in **16**. The results are shown in Table 7:[24] the coefficients of the correlations and the predicted angles are represented by a_X, b_X, r_X, and θ_X where X = A and B (cf. equation 3). The r_B values are very close to those of r_A except for the case of **4**. The r values are larger than 0.99 except r_A for **5, 7,** and **9** and r_B for **4, 5, 7,** and **9**. The insufficient accuracy of the reported chemical shifts would be responsible for the poor correlations for **5** and **7**.[2a] The Se-H group cannot be a good model for the SeCH=CH$_2$ group in **9**: the π-type interaction must be important in the SeCH=CH$_2$ group.

The predicted θ_B values are smaller than θ_A, which must be due to the difference in the function of equations 5 and 6. The θ values, which satisfy equation 4, are also calculated from the θ_A and θ_B values: the values are determined so that $\delta_{calcd}(Se:\theta)$ valuesdefined by equation 4 ($\delta_{calcd}(Se:\theta_{(A)})$ and $\delta_{calcd}(Se:\theta_{(B)})$) give the same values as $\delta_{calcd}(Se:\theta_A)$ and $\delta_{calcd}(Se:\theta_B)$ for **5a**, respectively. The $\theta_{(B)}$ values are substantially the same as the $\theta_{(A)}$ values, which are also collected in Table 7. The $\theta_{(A)}$ (and $\theta_{(B)}$) values are almost linearly correlated with θ_A and θ_B.

While the θ_A values were calculated in the desired range of -1° $\leqq$ θ_A $\leqq$ 90° except 104° for **4**, the range for θ_B examined was -1° $\leqq$ θ_B $\leqq$ 90°. The (θ_A, θ_B) values for **5** are estimated to be (23°, 16°), which are smaller than the calculated θ_H value of 37.30°. The insufficient accuracy of the reported chemical shifts in **5**,[2a] together with the very shallow energy minimum,[22] must be responsible for the difference. The θ_B values of −1° for **1** and 90° for **4** strongly suggest that the structures in the solution are nearly planar and perpendicular, respectively, although the perturbation in the substituent effect on $\delta_{calcd}(Se)$ by R is not considered. The θ_R value of **1a** is reported to be 40°.[25a] The observed value for **1a** is much larger than the calculated θ_B value but ab initio MO calculations on **1a** itself predicted the planar structure with the B3LYP/6-311+G(2d,p) method, even if the calculations are started assuming the C_1 symmetry, although not shown. The θ_R value of 1,4-di(selenocyanato)benzene is reported to be ca. 48°:[25b] the predicted (θ_A, θ_B) for **3** are (43°, 28°). The observed value in the crystal is

Table7. Correlations of $\delta_{obsd}(Se)$ versus $\delta_{calcd}(Se{:}\theta_A)$ and $\delta_{calcd}(Se{:}\theta_B)$, Together with $\theta_{(A)}$ and $\theta_{(B)}$

compd	a_A	b_A	r_A	θ_A	$\theta_{(A)}$	a_B	b_B	r_B	θ_B	$\theta_{(B)}$	n
1	0.899	134.9	1.000	-1	0[a]	0.884	134.9	1.000	-1	0[a]	7
1'	0.755	136.2	0.996	10	14	0.876	134.6	0.996	9	14	7
2	0.578	373.4	0.994	44	28	0.825	374.5	0.994	32	29	7
3	0.458	281.3	0.991	43	28	0.644	281.1	0.991	28	27	8
4	0.633	629.6	0.996	104	90[b]	0.422	623.0	0.984	90	90[b]	8
5	1.144	40.5	0.989	23	20	1.512	38.1	0.988	16	20	5
6	-1.120	966.4	0.997	12	15	-1.321	967.1	0.997	9	14	4
7	0.337	305.8	0.972	71	38	0.444	303.9	0.972	43	36	4
8	1.088	366.0	0.996	80	44	1.256	366.2	0.995	58	44	8
9	0.329	374.5	0.985	69	38	0.426	374.6	0.985	47	37	6
10	0.263	348.8	0.994	62	34	0.358	348.8	0.994	40	34	6
11	0.649	311.9	0.999	24	21	0.857	311.9	0.999	18	21	6
12	0.640	371.2	0.996	20	19	0.818	371.0	0.996	15	19	7
13	0.465	391.0	0.990	25	21	0.617	390.9	0.990	18	21	7

[a] Assumed to be 0°. [b] Assumed to be 90°.

close to θ_A. The crystal packing effect containing the intermolecular interaction and the electronic effect of the cyano group at the other para position in 1,4-bis(selenocyanato)benzene must play an important role in determining the structure of the bis(selenocyanato)benzene in crystals. The (θ_A, θ_B) for **2** and **8** were predicted to be (44°, 32°) and (80°, 58°), respectively. The θ_R value of di-p-tolyl selenide (**8c**)[26a] is reported to be 55°, which is very close to the θ_B value for **8**. The θ_R value of **6a**[26b] is reported to be 68°, which is much larger than the θ_A and θ_B values predicted for **6**. The real angular dependence of δ_{obsd}(Se) must determine the θ_R values of ArSeR. Therefore, the predicted θ values will be close to the observed ones when the calibration curve reproduces the real one for ArSeR in solutions. The above results may show that the real curves for ArSeR in solutions are sometimes different from those calculated for **5a** by equations 5 and 6, although the θ_R values are not measured in solutions.
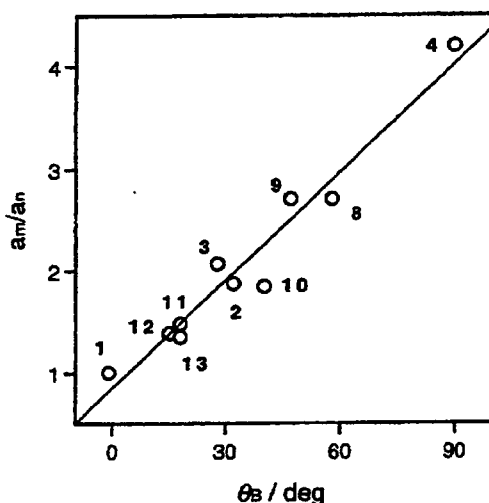

Figure 7. Plot of a_m/a_n versus θ_B.

$$\theta_A = 1.25 \times \theta_B + 4.72 \qquad\qquad r = 0.978 \qquad\qquad (9)$$

$$a_m/a_n = 0.0353 \times \theta_B + 0.85 \qquad\qquad r = 0.975 \qquad\qquad (10)$$

The θ_A values correlated well with the θ_B values. Equation 9 shows the correlation. Therefore, I employ θ_B for the following discussion, although three types of θ values are tabulated. The θ_B values well explain the a_m/a_n values estimated based on δ_{obsd}(Se) of **1** - **13** in solutions, which are expected to correlate with the θ_R values, although they are not directly measured. The ratios of a_m/a_n for **1** − **4** and **8** - **13** are plotted against θ_B. Figure 7 shows the plot,

and the correlation is given in equation 10. It is demonstrated that the a_m/a_n ratio is correlated with θ_B, which suggests that θ_B can be a measure of θ_R in solutions.

17

18 ⇌ **19**
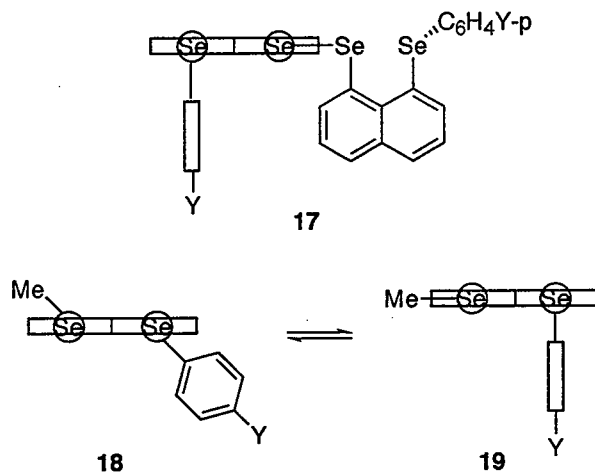
There are mainly three cases in the Y dependence of θ: (a) The θ value is substantially equal for all Y examined. (b) The value changes from Y to Y' but the substantial change is limited only for strong electron-withdrawing Y, such as COOR and/or NO_2 groups. (c) The value explicitly changes from Y to Y'. In case a, the r values in Table 7 must be very good. The coefficients are not as good, but they will be much improved if the points corresponding to the COOR and/or NO_2 groups are omitted in the plots in case b. In case c, the coefficients will not be improved without the points corresponding to the COOR and NO_2 groups in the plots.

The correlations were reexamined for **3**, **9**, and **13**, of which r values were less than 0.992. The points corresponding to Y = OMe, Me, H, Cl, and Br were plotted against $\delta_{calcd}(Se:\theta_B)$ with a single θ_B value. The (θ_B, r_B) values for **3**, **9**, and **13** become (13°, 0.999), (18°, 0.991), and (48°, 0.999), respectively.[27] The θ_B values for the two omitted points are evaluated based on the correlations. The (Y, θ_B) values are (COOR, 23°) and (NO_2, 24°) for **3**, (NO_2, ca. 32°) for **9**, and (COOR, 41°) and (NO_2, 26°) for **13**. The correlations are much improved for **3** and **13**, which shows that **3** and **13** belong to case b. **9** must be case c, since it did not improve. The plot of $\delta_{obsd}(Se)_9$ against $\delta_{calcd}(Se:\theta_B = 47°)$ gives an inversely proportional curve. The point for the methoxyl group actually deviates from the line even when the COOR and NO_2 groups are omitted in the plot.

We would like to discuss the structures of **12** and **13** in more detail. Structures **17**,[28a,b] **18**,[28b] and **19**[28c] are demonstrated in crystals for Y = H. The structure of **12** can be described as **17** with some twisting around the Se-C(C_6H_4Y-p) bonds[29] judging from the (θ_B, r_B) value of (15°, 0.996). How can the structure of **13** in the solution be explained by the treatment? Its correlation is much improved. Our explanation is as follows: **13** is in equilibrium with two conformers, **18** and **19**, in

112

the solution. The molar ratio in **13** is not substantially changed for Y = OMe, Me, H, Cl, and Br, while the ratio of **19** would increase for Y = COOR and NO$_2$. The contribution of **19** must decrease the θ_B value, which is in accordance with the increased θ_B value when the two points are omitted.

These results exhibit that the GIAO method can be a powerful tool to investigate the selenium chemistry containing the structural dependence of the δ(Se) values if one employs the method supporting ^{77}Se NMR spectroscopy. A study containing nonbonded interactions with the method is in progress.

Experimental Section

Chemicals were used without further purification unless otherwise noted. Solvents were purified by standard methods. Melting points were uncorrected. ^{1}H, ^{13}C, and ^{77}Se NMR spectra were measured at 400, 100, and 76 MHz, respectively. The ^{1}H, ^{13}C, and [77]Se chemical shifts are given in ppm relative to those of internal CHCl$_3$ slightly contaminated in the solution, CDCl$_3$ as the solvent, and external MeSeMe, respectively. Column chromatography was performed on silica gel (Fujidebison BW-300), acidic alumina, and basic alumina (E. Merck).

p,p'-Disubstituted diphenyl diselenides,[30] which were prepared according to the method in the literature or the improved method, were reduced by NaBH$_4$ in aqueous THF then allowed to react with methyl iodide, which gave *p*-substituted selenoanisoles (**1a** - **1g**).[2a,16] The NMR spectra of these materials were in good agreement with the literature data.[16] Using a similar method for **1a**, compound **1f** gave 84 % yield as a colorless oil. ^{13}C NMR (CDCl$_3$, 100 MHz) δ 6.43 ([1]*J*(C,Se) = 64.3 Hz), 126.47, 128.61, 130.47, 141.08, 171.85; ^{77}Se NMR (CDCl$_3$, 76 MHz) δ 227.9. Anal. Calcd for C$_8$H$_8$O$_2$Se$_1$: C, 44.67; H, 3.75. Found: C, 44.64; H, 3.77.

The diselenides[30] were reduced by NaBH$_4$ in aqueous THF and the corresponding para-substituted benzene diazonium chlorides were added at a low temperature. After the usual workup, the crude products were chromatographed on silica gel containing acidic and basic alumina. Then the para-substituted phenyl phenyl selenides (**2a** - **2g**)[31] were obtained. In the similar method for **2a**, compound **2f** gave 74 % yield as a colorless oil. ^{77}Se NMR (CDCl$_3$, 76 MHz) δ 433.3. Anal. Calcd for C$_{15}$H$_{14}$O$_2$Se$_1$: C, 59.03; H, 4.62. Found: C, 59.07; H, 4.65. Compound **2g** gave 81 % yield as yellow crystals, mp 58.0 - 58.5 °C. ^{13}C NMR (CDCl$_3$, 100 MHz) δ 123.85, 127.12, 129.29, 129.60, 129.94, 135.77, 143.86, 146.11; ^{77}Se NMR (CDCl$_3$, 76 MHz) δ 446.3. Anal. Calcd for C$_{12}$H$_9$N$_1$O$_2$Se$_1$: C, 51.82; H, 3.26; N, 5.04. Found: C, 51.79; H, 3.29; N, 5.07.

The details for the preparation and the properties of *p,p'*-disubstituted bis[8-

(phenylselanyl)naphthyl]-1,1'-diselenide (**12a** - **12g**) and *p*-substituted 1-(methylselanyl)-8-(phenylselanyl)naphthalenes (**13a** - **13g**) will be reported elsewhere.

MO Calculations. Ab initio molecular orbital calculations were performed on Origin and/or Power Challenge L computers using the Gaussian 94 program[8,9] with 6-311++G(3df,2pd), 6-311+G(d,p), 3-21G, and the LANL2DZ basis sets at the DFT (B3LYP level). The calculations at the HF level were also carried out with the 6-311+G(d,p) basis sets. The calculations of the σ(Se) values based on the GIAO theory were performed by the NMR keyword of the Gaussian 94 program. The natural populations were calculated by the natural population analysis[10] of the program.

References and notes

(1) (a) Baenziger, M. C.; Buckles, R. E.; Maner, R. J.; Simpson, T. D. *J. Am. Chem. Soc.* **1969**, *91*, 5749. (b) *Organic Selenium Compounds: Their Chemistry and Biology*, ed by Klayman, D. L.; Günther,W. H. H. Wiley, New York (1973), Chap. XV. (c) Hayes, R. A.; Martin, J. C. *Sulfurane Chemistry* in *Organic Sulfur Chemistry: Theoretical and Experimental Advances*, Bernardi,F.; Csizmadia, I. G.; Mangini, A., Eds. Elsevier, Amsterdam (1985). See also refs cited therein.

(2) (a) McFarlane, W.; Wood, R. J. *J. Chem. Soc. Dalton Trans.* **1972**, 1397. (b) Iwamura, H.; Nakanishi, W. *J. Syn. Org. Chem. Jpn.* **1981**, *39*, 795; Patai, S.; Rappoport, Z. (eds), *The Chemistry of Organic Selenium and Tellurium Compounds*, Wiley, New York, 1986, Chap. 6 (Vol. 1); Klapötke, T. M.; Broschag, M. *Compilation of Reported* [77]*Se NMR Chemical Shifts*, Wiley, New York, 1996.

(3) Karplus, M.; Pople, J. A. *J. Chem. Phys.* **1963**, *38*, 2803.

(4) Cheeseman, J. R.; Trucks, G. W.; Keith, T. A.; Frisch, M. J. *J. Chem. Phys.* **1996**, *104*, 5497. Pulay, P.; Hinton, J. F. in *Encyclopedia of Nuclear Magnetic Resonance*, Eds. Grant, D. M.; Harris, R. K. John Wiley & Sons, New York, p. 4434 (Vol. 7), 1996. See also, Forsyth, D. A.; Sebag, A. B. *J. Am. Chem. Soc.* **1997**, *119*, 9483; Olah, G. A.; Shamma, T.; Burrichter, A.; Rasul, G.; Prakash, G. K. S. *J. Am. Chem. Soc.* **1997**, *119*, 12923, 12929.

(5) (a) Nakatsuji, H.; Higashioji, T.; Sugimoto, M. *Bull. Chem. Soc. Jpn.* **1993**, *66*, 3235. (b) Magyarfalvi, G.; Pulay, P. *Chem. Phys. Lett.* **1994**, *225*, 280. (c) Bühl, M.; Gauss, J.; Stanton, J. F. *Chem. Phys. Lett.* **1995**, *241*, 248. (d) Bühl, M.; Thiel, W.; Fleischer, U.; Kutzelnigg, W. *J. Phys. Chem.* **1995**, *99*, 4000. (e) Malkin, V. G.; Malkina, O. L.; Casida, M. E.; Salahub, D. R. *J. Am. Chem. Soc.* **1994**, *116*, 5898. (f) Schreckenbach, G.; Ruiz-Morales, Y.; Ziegler, T. *J. Chem.*

Phys. **1996**, 104, 8605. (g) Ellis, P. D.; Odom, J. D.; Lipton, A. S.; Chen, Q.; Gulick, J. M. in *Nuclear Magnetic Shieldings and Molecular Structure*; NATO ASI Series; Tossel, J. A. Ed.; Kluwer Academic Publishers; Dordrecht, 1993, p. 539. See also refs cited therein.

(6) Although the contribution of relativistic terms has been pointed out for heavier atoms, the perturbation is expected to be small for the selenium nucleus. Tanaka, S.; Sugimoto, M.; Takashima, H.; Hada, M.; Nakatsuji, H. *Bull. Chem. Soc. Jpn.* **1996**, 69, 953; Ballard, C. C.; Hada, M.; Kaneko, H.; Nakatsuji, H. *Chem. Phys. Lett.* **1996**, 254, 170; Nakatsuji, H.; Hada, M.; Kaneko, H.; Ballard, C. C. *Chem. Phys. Lett.* **1996**, 255, 195; Hada, M.; Kaneko, H.; Nakatsuji, H. *Chem. Phys. Lett.* **1996**, 261, 7. See also refs cited therein.

(7) Nakanishi, W.; Hayashi, S. *Chem. Lett.* **1998**, 523. The reported δ_{obsd}(Se) value of 222.3 for **1f** should be read to 227.9.

(8) *Gaussian 94, Revision D.4*; Frisch, M. J.; Trucks, G. W.; Schlegel, H. B.; Gill, P. M. W.; Johnson, B. G.; Robb, M. A.; Cheeseman, J. R.; Keith, T.; Petersson, G. A.; Montgomery, J. A.; Raghavachari, K.; Al-Laham, M. A.; Zakrzewski, V. G.; Ortiz, J. V.; Foresman, J. B.; Cioslowski, J.; Stefanov, B. B.; Nanayakkara, A.; Challacombe, M.; Peng, C. Y.; Ayala, P. Y.; Chen, W.; Wong, M. W.; Andres, J. L.; Replogle, E. S.; Gomperts, R.; Martin, R. L.; Fox, D. J.; Binkley, J. S.; Defrees, D. J.; Baker, J.; Stewart, J. P.; Head-Gordon, M.; Gonzalez, C.; Pople, J. A. *Gaussian, Inc.*, Pittsburgh, PA, 1995.

(9) The basis sets including effective core potentials such as LANL2DZ were not suitable for the calculations. The correlation was very poor.

(10) NBO Ver. 3.1, Glendening, E. D. Reed, A. E.; Carpenter, J. E.; Weinhold, F.; Gaussian Link 607.

(11) Reed, A. E.; Curtiss, L. A.; Weinhold, F. *Chem. Rev.* **1988**, 88, 899.

(12) The δ_{calcd}(Se) value for a MeSe$^-$ ion obtained with the B3LYP/6-311++G(3df,2pd) method and the δ_{obsd}(Se) value for MeSeNa in water were –207.9 and –330, respectively. The interaction with the counterion, as well as the solvation, must affect the δ_{obsd}(Se) value for MeSeNa. A similar discrepancy for H_2Se (and MeSeH) became smaller when the δ_{obsd}(Se) value for the gas phase was employed.[5g]

(13) Although the correlation coefficient was not improved in the calculations with the B3LYP/6-311+G(d,p) method on the structures obtained with the B3LYP/3-21G method (r = 0.976), the results of the calculations on the σ(Se) values with the 3-21G basis sets at the B3LYP level on the structures obtained with the B3LYP/6-311+G(d,p) method gave a better r value of 0.980.

(14) Kalabin, G. A.; Kushnarev, D. F.; Bzesovsky, V. M.; Tschmutova, G. A. *J. Org. Mag. Res.* **1979**, 12, 598.

(15) Mullen, G. P.; Luthra, N. P.; Dunlap, R. B.; Odom, J. D. *J. Org. Chem.* **1985**, *50*, 811.

(16) Gronowitz, S.; Konar, A.; Hörnfeldt, A.-B. *Org. Mag. Res.* **1977**, *9*, 213.

(17) Kalabin, G. A.; Kushnarev, D. F.; Mannafov, T. G. *Zh. Org. Khim.* **1980**, *16*, 505.

(18) Nakanishi, W.; Hayashi, S.; Yamaguchi, H. *Chem. Lett.* **1996**, 947.

(19) Topson, R. D.*The Nature and Analysis of Substituent Electronic Effects*, in *Progress in Physical Organic Chemistry*, Taft, R. W., Ed. John Wiley & Sons, Vol. 12, New York, 1976. See also refs cited therein.

(20) The substituent effect of **6** on the δ_{obsd}(Se) values was inversely correlated with those of **1**. Therefore, it must be careful to discuss in detail those for **6**.

(21) The a_m, a_n and a_m/a_n values were 1.81, 1.23, and 1.47, respectively, for the plot of δ_{obsd}(Se)$_8$ against δ_{obsd}(Se)$_2$. Since **8** bears two substituents at both *para* positions whereas **2** has only one, the substituent effect on δ_{obsd}(Se)$_8$ is expected to be twice of δ_{obsd}(Se)$_2$. Indeed the a_m value of 1.81 is close to that expected but the a_n value of 1.23 would be too small from the expectation, which may be explained by the saturating effect of the second substituents on δ_{obsd}(Se) operating especially for g(n').

(22) Indeed, the structure **16** with $\theta_H = 37.30°$ is optimized for **5a** with the B3LYP/6-311+G(d,p) method when the calculations are started at the partially optimized structure, with θ_H being fixed at 30.00°, but the calculations are stopped at $\theta_H = 18.48°$ when they are started at the partially optimized structure, with θ_H being fixed at 15.00°.

(23) The parameters are devised on the basis that the atomic overlap integral S between carbon 2p π_a and 2p π_b orbitals of the ethylene-type π orbital, where the two atomic orbitals are crossing with θ, is proportional to $\cos\theta$, $S = \langle \chi_a | \chi_b \rangle = \langle 2p\pi_a | \cos\theta \cdot 2p\pi_b + \sin\theta \cdot 2p\pi_b' \rangle = \cos\theta \langle 2p\pi_a | 2p\pi_b \rangle = \cos\theta \cdot S_0$ (2pπ_b' being orthogonal to 2pπ_b).
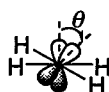
(24) Best-fitted correlations were obtained by the following steps. The δ_{calcd}(Se:θ') values were calculated for every 5 to 10°. A θ' value was looked for which gives the largest r value among the δ_{calcd}(Se:θ') values. Then the best-fitted θ value was determined, as it gave the largest r values among the δ_{calcd}(Se:θ) calculated every 1° near the θ' value.

(25) (a) Zaripov, N. M.; Golubinskii, A. V.; Chmutova, G. A.; Vilkov, L. V. *Zh. Strukt. Khim.* **1978**, *19*, 894. (b) McDonald, W. S.; Pettit, L. D. *J. Chem. Soc. A.* **1970**, 2044.

(26) (a) Blackmore, W. R.; Abrahams, S. C. *Acta Crysallogr.* **1955**, *8*, 323. (b) Zaripov, N. M.; Golubinskii, A. V.; Popic, M. V.; Vilkov, L. V.; Mannafov, T. G. *Zh. Strukt. Khim.* **1980**, *21*, (2), 37.

(27) The (a_B, b_B, r_B, θ_B, n) values for **3**, **9**, and **13** are (0.835, 260.5, 0.999, 13, 6), (0.563, 357.1, 0.991, 18, 5), and (0.488, 409.5, 0.999, 48, 5), respectively.

(28) (a) Nakanishi, W.; Hayashi, S.; Toyota, S. *J. Chem. Soc., Chem. Commun.* **1996**, 371. (b) Nakanishi, W.; Hayashi, S.; Toyota, S. *J. Org. Chem.* **1998**, *63*, 8790. (c) Nakanishi, W.; Hayashi, S. *J. Org. Chem.* **1999**, *64*, 6688.

(29) The correlations were similarly reexamined for **3**, **9**, and **13** with θ_A. The evaluated (a_A, b_A, r_A, θ_A, n) values for **3**, **9**, and **13** are (0.666, 261.0, 0.999, 17, 6), (0.426, 357.1, 0.991, 24, 5), and (0.384, 409.5, 0.999, 71, 5), respectively. The (θ_B, r_B) values for **3**, **9**, and **13** become (17°, 0.999), (24°, 0.991), and (71°, 0.999), respectively. The (Y, θ_A) values for the omitted points were estimated to be (COOR, 51°) and (NO_2, 52°) for **3**, (NO_2, ca. 57°) for **9**, and (COOR, 66°) and (NO_2, 54°) for **13**.

(30) Kalabin, G. A.; Kushnarev, D. F.; Kataeva, L. M.; Kashurnikova, L. V.; Vinokurova, R. I. *Zh. Org. Khim.* **1978**, *14*, 2478.

(31) Greenberg, B.; Gould, E. S.; Burlant, W. M. *J. Am. Chem. Soc.* **1956**, *78*, 4028.

Chapter 7

Novel Substituent Effect on ^{77}Se NMR Chemical Shifts Caused by 4c-6e versus 2c-4e and 3c-4e in Naphthalene Peri Positions: Spectroscopic and Theoretical Study

Abstract

$\delta(^8Se)$ values for $1\text{-}[8\text{-}(p\text{-}YC_6H_4Se)C_{10}H_6]SeSe[C_{10}H_6(SeC_6H_4Y\text{-}p)\text{-}8']\text{-}1'$ (**1** : Y = H, OMe, Me, Cl, Br, COOEt, and NO_2) showed a good correlation with those of $1\text{-}(MeSe)\text{-}8\text{-}(p\text{-}YC_6H_4Se)C_{10}H_6$ (**2**). While the $\delta(^1Se)$ values correlated well with $\delta(^8Se)$ in **2** with a positive proportionality constant of 0.252 (regular correlation), a similar correlation for **1** gave a negative proportionality constant of –0.282 (inverse correlation). To clarify the mechanism associated with the inverse correlation in **1**, together with the regular correlation in **2**, ab initio MO calculations, containing the GIAO magnetic shielding tensor for the Se nucleus ($\sigma(Se)$), were performed on $p\text{-}YC_6H_4{}^ASeH\text{---}{}^BSeH\text{--}{}^BSeH\text{---}H^ASeC_6H_4Y\text{-}p$ (**3**: model of Se_4 4c-6e for **1**) and on $p\text{-}YC_6H_4{}^ASeH\text{---}{}^BSeH_2$ (**4** and **5**: models of Se_2 π type 2c-4e and $^ASe\text{---}{}^BSe\text{--}H$ 3c-4e for **2**, respectively) with the 6-311+G(2d,p) basis sets at B3LYP and/or HF levels. The characteristic nature of the substituent effects on atomic charges and $\delta(Se)$ values in **3** is demonstrated to be $Y^{\delta-}\leftarrow C_6H_4\text{-}Se^{\delta+}\text{---}Se^{\delta+}\text{--}Se^{\delta+}\text{---}Se^{\delta+}\text{-}C_6H_4\rightarrow Y^{\delta-}$ and $Y^{\delta-}\leftarrow C_6H_4\text{-}Se^{down}\text{---}Se^{up}\text{--}Se^{up}\text{---}Se^{down}\text{-}C_6H_4\rightarrow Y^{\delta-}$, respectively, (Y = electron-withdrawing) and in **5** is $Y^{\delta-}\leftarrow C_6H_4\text{-}Se^{\delta+}\text{---}Se^{\delta-}\text{-}H^{\delta+}$ and $Y^{\delta-}\leftarrow C_6H_4\text{-}Se^{down}\text{---}Se^{down}\text{-}H^{down}$, respectively. In the case of **4**, a substantial contribution through the naphthylidene group is suggested. These results indicate that the nature of the interaction between the linear four Se atoms in **1** is of the 4c-6e type and that between the two Se atoms in **2** is π type 2c-4e and/or 3c-4e according to the conformations around the Se atoms. The observed NMR parameters are well explained by model calculations on **3** - **5**. Plots of $^4J(^1Se,^8Se)$ versus $\delta(^8Se)$ of **1** and **2** gave good correlations with negative proportionality constants, which indicates that the J values become larger as the electron density on the ^8Se atoms increases.

Introduction

In my previous chapter,[1] I reported the linear alignment of the four selenium atoms in bis[8-(phenylselanyl)naphthyl] diselenide (**1a**), revealed by the X-ray crystallographic analysis. This alignment is the results of an energy lowering effect due to the construction of the four center-six electron bond (4c-6e) with four selenium 4p atomic orbitals as indicated by MO calculations.[1]

The character of the charge transfer in the formation of the 4c-6e is that from the p-type lone pairs of the outside two selenium atoms to the central σ^*(Se–Se) orbital. The Se–Se distance in the diselenide moiety of a model compound of **1a**, H_2Se---HSe–SeH---Se_2H, is calculated to be longer than that calculated for free H_2Se_2.

1a

2a

2d
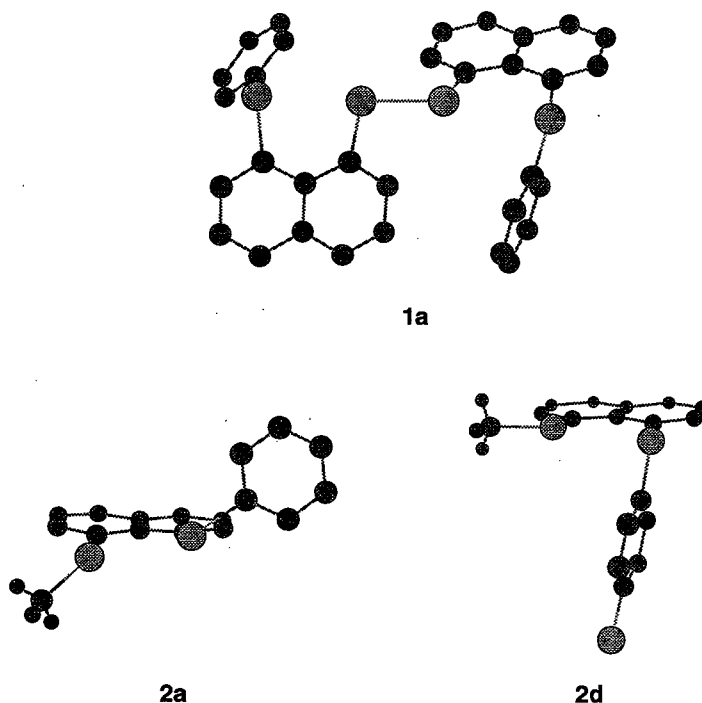
Scheme 1. Structures 1a, 2a, and 2d

On the other hand, X-ray crystallographic analysis of 1-(methylselanyl)-8-(phenylselanyl)naphthalene (**2a**) showed that the two Se–C bonds of the methylselanyl and phenylselanyl groups declined about 50° and 40°, respectively, from the naphthyl plane.[1] The structure **2a** in the vicinity of the Se–C bonds is reproduced by MO calculations performed on a model compound of **2a**, H_2Se---SeH_2. The interaction of two p-type lone pairs of the Se atoms in **2a** forms two new π-type molecular orbitals, which assume an orientation that avoids the exchange repulsion. The bent structure of **2a** must lower the energy of the filled π- and π^*-orbitals of the adduct as much as possible. The nonbonded interactions in **2a** can be represented by the π-type two-center four-electron interaction (2c-4e).[1] However, I found another type of structure,[2] very recently, in which the n(Se)---σ^*(Se–C) 3c-4e interaction is observed in 1-

(methylselanyl)-8-(*p*-anisylselanyl)naphthalene   (**2b**)   and   1-(methylselanyl)-8-(*p*-chlorophenylselanyl)naphthalene (**2d**). Structures **1a**, **2a**, and **2d** are shown in Scheme 1 and the corresponding orbital interactions are outlined in Scheme 2, for convenience of discussion.

Lone pair-lone pair interactions have been demonstrated to play an important role in the nonbonded spin–spin couplings between selenium–selenium,[3,4] selenium–fluorine,[5] fluorine–fluorine,[6] and fluorine–nitrogen[7] atoms. The values of ^4J(Se,Se) of **1a**,[1] **2a**,[1] 1-(acetoxymethylselanyl)-8-(methylselanyl)naphthalene,[4b] and 1-(methylseleninyl)-8-(methylselanyl)naphthalene[4b] are reported to be 341.4, 322.4, 310, and 203 Hz, respectively. The values of ^4J(F,Se) and ^4J(F,F) in 8-fluoro-1-(*p*-anisylselanyl)naphthalene,[5] 8-fluoro-1-(methylselanyl)naphthalene,[5] and 1,8-difluoronaphthalene[6b] are observed to be 285.0, 276.7, and 58.8 Hz, respectively. Orientation of the lone pairs at the Se atoms and/or electron densities of the orbitals must play an important role in determining the *J* values. The structure of **2a** is very close to that of 1,8-bis(methylsulfanyl)naphthalene[8] and of 1,8-bis(phenyltelluro)naphthalene,[9] especially in the vicinity of the heteroatoms. Influence of the lone pair-lone pair interactions on the NMR chemical shifts is also of interest.[5,10]
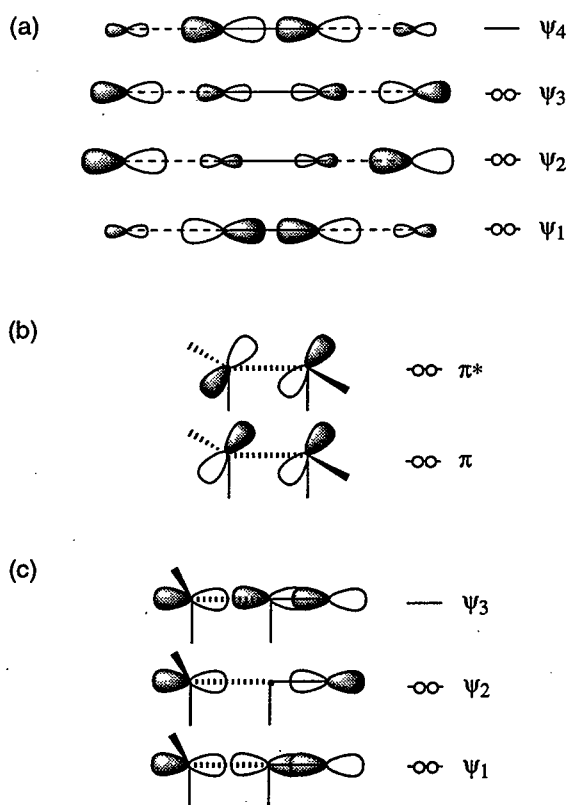
Scheme 2.   Interactions between Lone Pairs of Se Atoms: (a) Linear 4c-6e Constructed
by Four Se Atoms, (b) π Type Se---Se 2c-4e, and (c) Linear Se---Se–C 3c-4e

As an extension of my study, I looked for novel properties that arose from the 4c-6e type interaction constructed by the linearly aligned four Se atoms in **1a**. The properties of the π type

2c-4e in **2a** and the linear 3c-4e in **2d** were also of interest. It was desirable that the ^{77}Se NMR chemical shifts were predicted precisely from theoretical considerations. Magnetic shielding tensors have recently been calculated based on the gauge including atomic orbitals (GIAO) theory for some nuclei of the first- and second-row elements.[11,12] The contribution of relativistic terms has been pointed out for the heavier atoms in such calculations,[13] however, the contribution to the Se nucleus is expected to be small. The method is satisfactorily applied on organoselenium compounds,[14] containing para-substituted phenyl selenides.[15]

Ab initio MO calculations, containing the GIAO magnetic shielding tensor of the selenium nucleus (σ(Se)), were performed on the model adducts of the diselenides and the bis-selenides to elucidate the nature of the nonbonded interactions characteristic of the 4c-6e, 2c-4e, and 3c-4e types. Here, I would like to present the results of investigations exhibiting the characteristic substituent effect on the Se atoms in 4c-6e in **1**, in contrast to that of 2c-4e and/or 3c-4e in **2**. The interpretation of the nonbonded interactions in **1a**, **2a**, and their derivatives based on the MO calculations is further examined.

Results and Discussion

Substituent Effect on ^{77}Se NMR Chemical Shifts and Coupling Constants. Di[(para-substituted phenylselanyl)naphthyl] diselenides $(1-[8-(p-YC_6H_4Se)C_{10}H_6]Se-Se[C_{10}H_6(SeC_6H_4Y-p)-8']-1'$ (**1**: **1a** - **1g** for Y = H, OMe, Me, Cl, Br, COOEt, NO$_2$, respectively)) were prepared by the reaction of the dianion of naphto[1,8-c,d]-1,2-diselenole with 2 equiv or more of para-substituted benzenediazonium chloride at low temperature. 1-(Methylselanyl)-8-(para-substituted phenylselanyl)naphthalenes **2** (**2a** - **2g**) were prepared by the addition of methyl iodide to aqueous THF solutions of the corresponding 8-(p-substituted phenylselanyl)-1-naphthaleneselenates, which were obtained in the reaction of **1a** - **1g** with sodium borohydride, respectively.
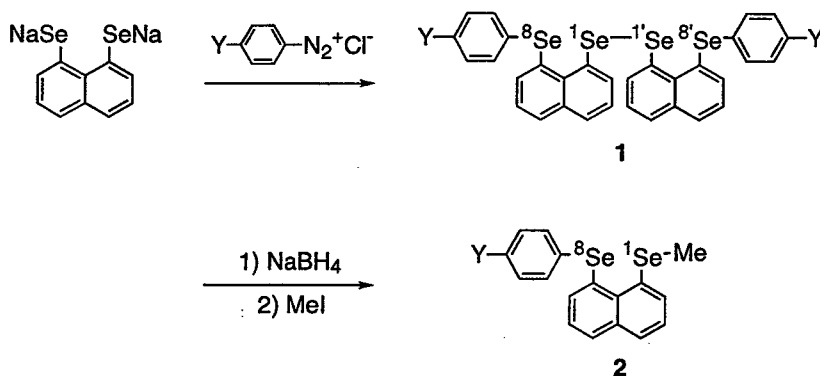

	a	**b**	**c**	**d**	**e**	**f**	**g**
Y :	H	OMe	Me	Cl	Br	CO$_2$Et	NO$_2$

Table 1. ^{77}Se NMR Chemical Shifts and Coupling Constants of 1 and 2, Together with the Selected [13]C Chemical Shifts and Coupling Constants[a]

Y	1				2[b]				
	$\delta(^8Se)$	$\delta(^1Se)$	$^4J(^8Se,^1Se)$	$^5J(^8Se,^1Se)$	$\delta(^8Se)$	$\delta(^1Se)$	$^4J(^8Se,^1Se)$	$\delta(C_{Me})$	$^1J(^1Se,C_{Me})$
OMe	416.2	541.4	371.6	12.4	424.5	233.1	341.6	13.9	71.2
Me	422.0	537.4	354.4	11.9	427.7	234.5	330.9	13.7	72.8
H	429.0	534.2	341.4	13.6	434.3	235.4	322.4	13.4	72.8
Cl	429.1	534.7	330.1	14.0	431.6	234.7	316.7	13.5	72.8
Br	429.6	534.0	327.1	c	432.4	235.2	313.9	13.4	72.7
COOEt	442.5	530.2	311.4	13.7	442.4	239.2	294.7	12.9	74.5
NO$_2$	456.1	529.6	294.1	13.5	453.9	240.1	272.5	12.5	76.1

[a] The values of $\delta(Se)$ and $\delta(C)$ are from external MeSeMe and CDCl$_3$, respectively, and coupling constants are in Hz. [b] Values of $^5J(^8Se,C_{Me})$ were observed to be 15.0 - 16.1 Hz. [c] Not observed due to low solubility and low sensitivity.

The ^{77}Se NMR spectra of **1** and **2** are measured, along with the ^{1}H and ^{13}C NMR spectra for the compounds. Table 1 summarizes the ^{77}Se NMR chemical shifts and coupling constants of **1** and **2** together with selected ^{13}C chemical shifts. The Se atoms of arylselanyl groups at the 8,8'- and 8-positions in **1** and **2** are numbered as ^{8}Se (or $^{8'}$Se) and other Se atoms in **1** and **2** as ^{1}Se (or $^{1'}$Se).
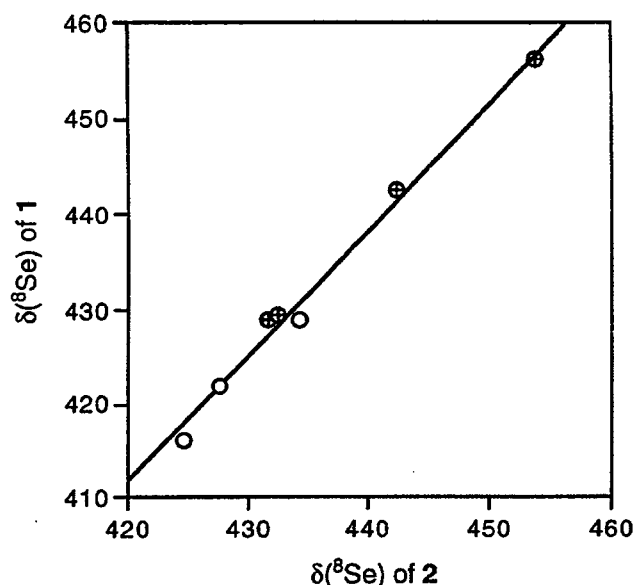
Figure 1. Plot of $\delta(^8$Se) of **1** versus $\delta(^8$Se) of **2**: ○ and ⊕ stand for g(m) and g(n), respectively. See also ref 20.

The $\delta(^8$Se) values of **1** show a good correlation with those of **2**. Figure 1 shows the results, and the correlation is shown in eq 1.[16,17] The substituent effect on $\delta(^8$Se) of **1** is 1.33 times larger than that of **2**. The selanyl groups at the 1-positions in **1** and **2** must affect the magnitude of the substituent effect on the $\delta(^8$Se) values relative to those of 1-(arylselanyl)naphthalenes. Therefore, the larger substituent effect for **1** may be due to the greater electron-accepting ability of the naphthyl group bearing an Se–Se bond with a low-lying σ^*(Se–Se) orbital in **1** relative to the 8-(methylselanyl)naphthyl group in **2**. The conformational effect of the ArSe group must also play an important role for the magnitude of the substituent effect. The substituent effect on the δ(Se) values in p-YC$_6$H$_4$SeR is larger for the Se–C$_R$ bond being in the aryl plane than for the bond perpendicular to the plane.[18,19] The structures **1a** and **2a** correspond the planar and the perpendicular ones, respectively.[20]

The $\delta(^1$Se) values of **1** and **2** were plotted versus $\delta(^8$Se) of **1** and **2**, respectively. Figure 2 shows the plot of $\delta(^1$Se) versus $\delta(^8$Se) of **1** and the correlations for **1** and **2** are shown in eqs 2 and 3, respectively. Figures 3 and 4 exhibit the plots of $^4J(^8$Se,^{1}Se) (= $^4J(^{8'}$Se,$^{1'}$Se)) versus $\delta(^8$Se) in **1** and **2**, respectively. Each plot was better analyzed as the two correlations depending on the two groups of substituents, g(m) and g(n): g(m) consists of the points corresponding to Y =

OMe, Me, H and the points of Y = Cl, Br, COOEt, and NO_2 belong to g(n). The correlations for g(m) and g(n) are given in eqs 4m, 4n and 5m, 5n for **1** and **2**, respectively. Figure 5 shows the plot of $^4J(^8Se,^1Se)$ of **1** versus those of **2**. The plot is also analyzed with g(m) and g(n), of which correlations are given in eqs 6m and 6n, respectively.
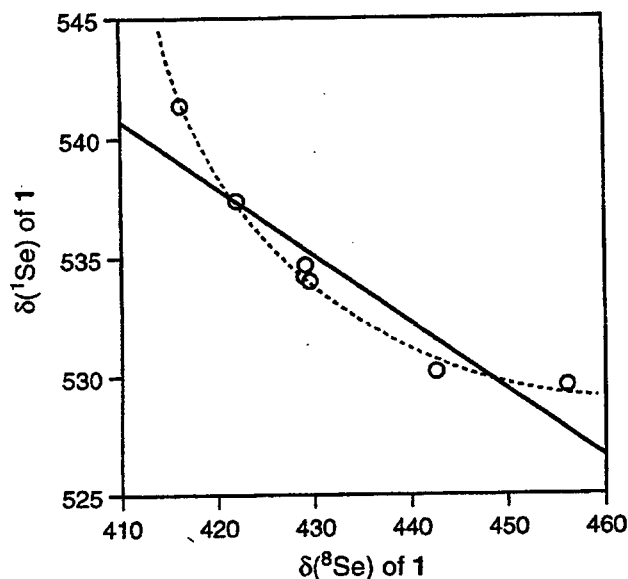

Figure 2. Plot of $\delta(^1Se)$ versus $\delta(^8Se)$ of **1**. Deviation from linearity is emphasized by a dotted line.

|		
$\delta(^8Se)$ of **1** = 1.33 × $\delta(^8Se)$ of **2** − 147.1	(r = 0.994)	(1)
$\delta(^1Se)$ of **1** = −0.282 × $\delta(^8Se)$ of **1** + 656.2	(r = 0.924)	(2)
$\delta(^1Se)$ of **2** = 0.252 × $\delta(^8Se)$ of **2** + 126.5	(r = 0.965)	(3)
$^4J(^8Se,^1Se)$ of **1** = −2.34 × $\delta(^8Se)$ of **1** + 1345.2	(r = 0.991 for g(m))	(4m)
$^4J(^8Se,^1Se)$ of **1** = −1.29 × $\delta(^8Se)$ of **1** + 883.5	(r = 0.998 for g(n))	(4n)
$^4J(^8Se,^1Se)$ of **2** = −1.86 × $\delta(^8Se)$ of **2** + 1128.7	(r = 0.965 for g(m))	(5m)
$^4J(^8Se,^1Se)$ of **2** = −1.96 × $\delta(^8Se)$ of **2** + 1161.0	(r = 1.000 for g(n))	(5n)
$^4J(^8Se,^1Se)$ of **1** = 1.57 × $^4J(^8Se,^1Se)$ of **2** − 166.3	(r = 1.000 for g(m))	(6m)
$^4J(^8Se,^1Se)$ of **1** = 0.809 × $^4J(^8Se,^1Se)$ of **2** + 73.4	(r = 1.000 for g(n))	(6n)

Now, I would like to discuss the substituent effect on $\delta(^1Se)$, resulting from the nonbonded Se---Se interactions in **1** and **2**. As shown in Figure 2 and eq 2, the plot of $\delta(^1Se)$ versus $\delta(^8Se)$ in **1** gave a rather poor correlation with a negative proportionality constant (inverse correlation) or the plots had better be analyzed as inversely proportional shown by a dotted line in the Figure.
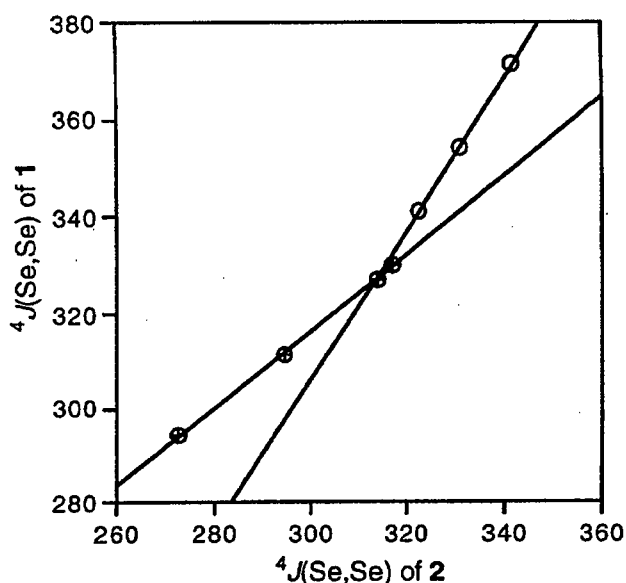
On the other hand, a better correlation was held with a positive proportionality constant for **2** (regular correlation: see eq 3).
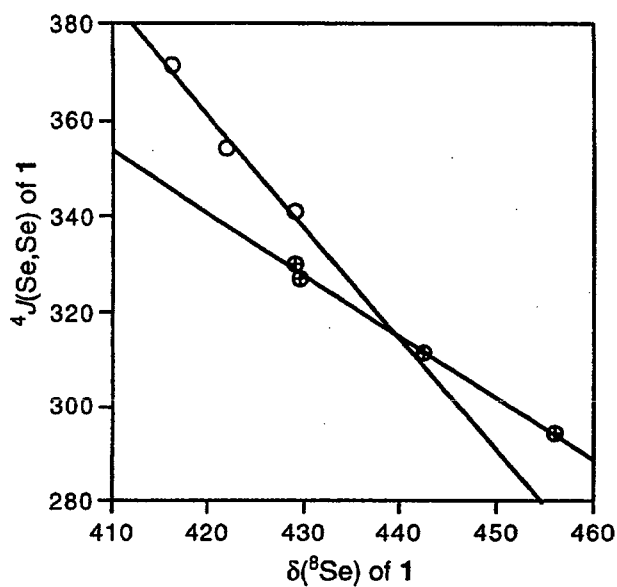
Figure 3. Plot of $^4J(\text{Se,Se})$ versus $\delta(^8\text{Se})$ of **1**: $\bigcirc$ and $\oplus$ stand for g(m) and g(n), respectively.
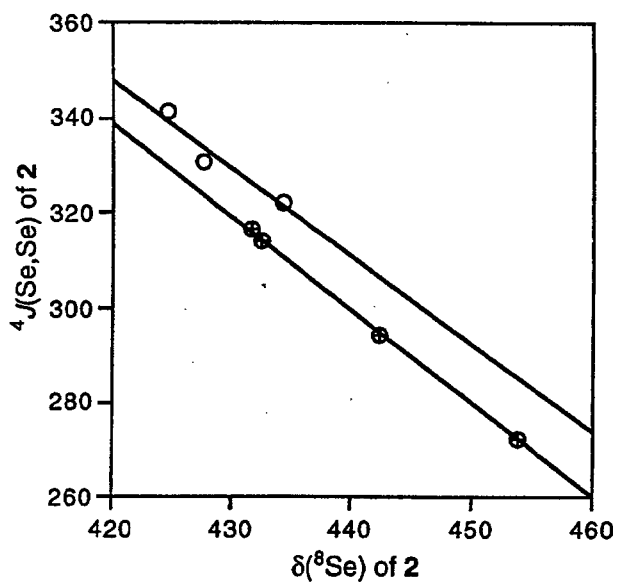
Figure 4. Plot of $^4J(\text{Se,Se})$ versus $\delta(^8\text{Se})$ of **2**: $\bigcirc$ and $\oplus$ stand for g(m) and g(n), respectively.

Figure 5. Plot of ^4J(Se,Se) of **1** versus ^4J(Se,Se) of **2**: ○ and ⊕ stand for g(**m**) and g(**n**), respectively.

Regular correlation in **2** could be explained by assuming that the electron density on the ^{1}Se atom decreased as that on the ^{8}Se atom became smaller, if the $\delta(^8$Se) and $\delta(^1$Se) values are mainly governed by the charges on the atoms. However, there are other explanations for the regular correlation. One of mechanisms is to consider the ^{1}Se–C_{Me} bond polarization induced by the charge on the ^{8}Se atom. Since the electron density near the two Se atoms in **2** should be very high due to the very close location of the two Se atoms, the electrons on the Se atoms must be expelled to the adjacent atoms or the Se–C bonds. The expelled electrons from the ^{1}Se atom may return to the atom, if the electron density on the ^{8}Se atom decreased, which must result in the increase of the electron density at the ^{1}Se atom. The observed regular correlation in **2** can be achieved only when the $\delta(^8$Se) and $\delta(^1$Se) values shift downfield and upfield, respectively, as the charges at the Se atoms become larger, in this explanation. The contribution of the through-bond interaction must also be considered, since the π type 2c-4e orientation of the p-type lone pairs enables them to interact easily with the π-orbitals of the naphthalene ring of **2**.

The mechanism operating in the inverse correlation in **1** must be different from that of the regular correlation in **2**. It is reasonable to assume that the σ^*-orbital of the inside Se–Se bond can accept electrons of the ^{8}Se atoms more easily when the electron density of the ^{8}Se atoms increases. The electron density at the ^{1}Se atom will be effectively increased, as the density at the ^{8}Se atoms becomes larger, in this case. The NMR signals of both ^{8}Se and ^{1}Se atoms in **1** would shift in the same direction, if the chemical shifts are mainly determined by the charges on the atoms. However, the observations are just the opposite of what is expected. Therefore, the $\delta(^1$Se)

126

values must be negatively proportional to the charges in this case. Ab initio MO calculations, containing the $\sigma(Se)$ values calculated based on the GIAO theory, will reveal the details, which will be discussed in the next section.

After establishment of the inverse correlation of $\delta(^1Se)$ versus $\delta(^8Se)$ in **1** experimentally, together with the regular correlation in **2**, next extension of my study is to examine the nonbonded interaction by means of coupling constants in connection with $\delta(^8Se)$ in **1** and **2**. The plot of $^4J(Se,Se)$ versus $\delta(^8Se)$ in **1** was analyzed as two correlations as shown in Figure 3 and eqs 4m and 4n. The plot in **2** was similarly analyzed as the two correlations (Figure 4 and eqs 5m and 5n). The analysis by the two correlation methods show the importance of the substituent dependence on structures. All of the proportionality constants in eqs 4 and 5 were negative, which implies that as the value for $^4J(^8Se,^1Se)$ in **1** and **2** becomes smaller, then the $\delta(^8Se)$ experiences a down field shift. The results are explained well by assuming that the J-values became larger as the electron density of the ^8Se atoms increases. The observation of the long range $^5J(^8Se,^1Se)$ (and $^5J(^1Se,^8Se)$) couplings of 12 - 14 Hz in **1** further support the effective orbital interaction between the ^8Se atom with the $\sigma^*(Se-Se)$ orbital in **1**.

$$\delta(C_{Me})\ \text{of}\ \mathbf{2} = -0.048 \times \delta(^8Se)\ \text{of}\ \mathbf{2} + 34.1 \qquad (r = 0.993) \qquad (7)$$

$$^1J(^1Se,C_{Me})\ \text{of}\ \mathbf{2} = 0.154 \times \delta(^8Se)\ \text{of}\ \mathbf{2} + 6.5 \qquad (r = 0.973) \qquad (8)$$

The $\delta(C_{Me})$ and $^1J(^1Se,C_{Me})$ values were plotted versus those of $\delta(^8Se)$ in **2**, of which correlations were given in eqs 7 and 8, respectively. Good correlations were obtained for these plots, which demonstrated that the influence of the substituents at the phenyl p-positions was transmitted even to the $\delta(C_{Me})$ and $^1J(^1Se,C_{Me})$ values. These results can be explained by assuming that the fairly large interaction is operating between the lone pairs of the ^8Se atom and the $\sigma^*(^1Se-C_{Me})$ orbital. The $^8Se\text{---}^1Se-C_{Me}$ interaction can be accounted for by the contribution of the unsymmetrical 3c-4e model,[21] as was observed in the F---Se-C interaction.[5] Ab initio MO calculations were performed on appropriate models of **1** and **2** which reveal the nature of the nonbonded interactions of 4c-6e type in **1** and π type 2c-4e and/or n(Se)---σ^*(Se-C) 3c-4e in **2**.

Nature of the Nonbonded Se---Se Interactions Revealed by MO Calculations. Scheme 3 shows some adducts, p-YC$_6$H$_4{}^A$SeH---^{B}SeH–^{B}SeH---^{A}HSeC$_6$H$_4$Y-p (**3**: model of **1**) and p-YC$_6$H$_4{}^A$SeH---^{B}SeH$_2$ (**4** and **5**: model of **2**), where the napthtylidene and methyl groups in **1** and **2** are replaced by hydrogens in the models. The structures **3** - **5** around the Se atoms are deformed but remained close to those of **1a**, **2a**, and **2d**, respectively. Ab initio molecular orbital calculations on **3** - **5** were performed with the 6-311+G(2d,p) basis sets of the Gaussian 94 program[22] at the B3LYP level. Similar calculations were also performed on p-YC$_6$H$_4$SeH (**6**$_{pl}$ and

6_{pd}),[23] where the Se–H bond is in the aryl plane in 6_{pl} and it is perpendicular to the plane in 6_{pd}. Ab initio MO calculations of 3 - 6 were carried out for Y = H, OH, Me, Cl, Br, COOH, and NO_2. The GIAO magnetic shielding tensor[11,12] for the Se nucleus ($\sigma(Se)$) and the natural charges (Qn) were also obtained using the natural population analysis.[24]
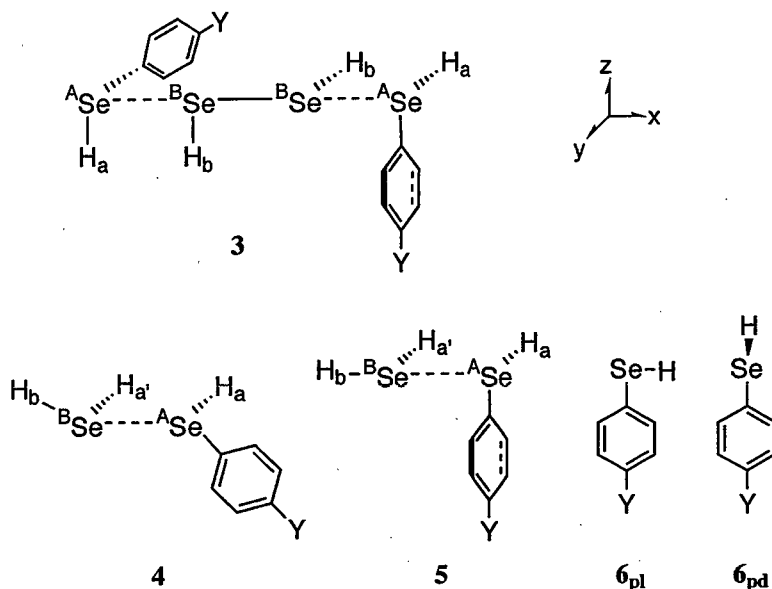
Scheme 3.   Structures of Models 3 - 6, Together with the Axes

Optimized structure of 6_{pl} was employed in 3 and 5 and 6_{pd} in 4 without further optimization, except for $r(Se–C)$, $r(Se–H)$, and $\angle CSeH$ which were reoptimized in the models. As shown in Scheme 3, the four Se atoms in 3 were placed on the x axis. Se–C bonds were on the y or z direction. The aryl plane was on the yz plane. Nonbonded Se---Se distances, $r(^ASe–^BSe)$, were fixed at the observed value of 3.053 Å in 1a. The two $^BSe–H_b$ bonds of the central H_2Se_2 component were placed on the xz and xy planes. The $r(Se–H)$, $r(Se–C)$, $r(^BSe–^BSe)$, $\angle C^ASeH_a$, and $\angle ^BSe^BSeH_b$ were optimized. The arylselanyl group and the ^BSe and H_b atoms in 4 were placed on the xz plane. The $\angle C^ASe^BSe$ and $\angle ^ASe^BSeH_b$ were fixed at the observed values of 157.0° and 144.4°, respectively, and the nonbonded Se---Se distance ($r(^ASe–^BSe)$) was fixed at the observed value of 3.070 Å in 2a. Two other Se–H bonds were in the plane perpendicular to the xz plane and the $r(Se–H)$, $r(Se–C)$, $\angle CSeH$, and $\angle HSeH$ were optimized. The components of 5, p-YC_6H_4SeH and HSeH, were located in the yz and xy planes, respectively, with the C–Se and Se---Se–H bonds on the z and x axes. The nonbonded Se---Se distance ($r(^ASe–^BSe)$) was also fixed at 3.070 Å. The $r(Se–H)$, $r(C–Se)$, $\angle CSeH$, and $\angle HSeH$ were optimized.

Structures 3 were optimized in the limited conditions with the B3LYP/6-311+G(2d,p) method. The natural population analysis could not be achieved with the method due to "strongly delocalized NBO set" in the calculations, therefore natural charges were obtained with the

B3LYP/3-21G* method, using the structures obtained by the B3LYP/6-311+G(2d,p) method. The σ(Se) value of **3f** was not obtained by the B3LYP/6-311+G(2d,p) method due to "consistency failure" in the calculations. Thus, the σ(Se) values of **3** were calculated with the 6-311+G(2d,p) basis sets at the Hartree-Fock (HF) level. Table 2 exhibits the results of MO calculations for **3** where the σ(Se) values are given by the calculated δ(Se) values which are defined as $-(\sigma(Se) - \sigma(Se)_{MeSeMe})$. Structures **4** and **5** were also optimized in the limited conditions with the B3LYP/6-311+G(2d,p) method. While the Qn and σ(Se) values for **5** were obtained with the method, the σ(Se) values for **4f** and **4g** could not be obtained by the method. Therefore, the σ(Se) values of **4** were recalculated with the HF/6-311+G(2d,p) method. Table 3 summarizes the results obtained for **4** and **5**. Correlations between the calculated values in **3 – 5** are summarized in Table 4.

Table 2. Results of ab Initio MO Calculations on 3 with the 6-311+G(2d,p) Basis Sets[a,b]

Y	$Qn(^{A}Se)_{B}{}^{c}$	$Qn(^{B}Se)_{B}{}^{c}$	$\delta(^{A}Se)_{B}{}^{d}$	$\delta(^{B}Se)_{B}{}^{d}$	$\delta(^{A}Se)_{H}{}^{e}$	$\delta(^{B}Se)_{H}{}^{e}$
OH	0.2075	-0.1686	108.26	-28.99	132.15	2.32
Me	0.2107	-0.1670	112.13	-28.71	137.11	1.98
H	0.2137	-0.1665	120.26	-28.77	145.92	1.41
Cl	0.2239	-0.1657	120.50	-28.07	148.59	1.08
Br	0.2231	-0.1657	120.50	-28.06	149.79	0.89
COOH	0.2315	-0.1640	f	f	165.60	-1.54
NO$_2$	0.2460	-0.1620	149.10	-24.46	175.21	-2.09

[a] The σ(Se) values for MeSeMe are 1645.53 and 1915.42 with B3LYP/6-311+G(2d,p) and HF/6-311+G(2d,p)//B3LYP/6-311+G(2d,p) methods, respectively. [b] Subscripts B and H show B3LYP and HF levels, respectively. [c] Calculated with the B3LYP/3-21G*//B3LYP/6-311+G(2d,p) method. [d] Calculated with the B3LYP/6-311+G(2d,p) method. [e] Calculated with the HF/6-311+G(2d,p)//B3LYP/6-311+G(2d,p) method. [f] Not obtained due to "Consistency failure" in the calculations.

Table 3. **Results of ab initio MO Calculations on 4 and 5 with the B3LYP/6-311+G(2d,p) Method^{a,b}**

Y	4									5					
	$Qn(^ASe)$	$Qn(^BSe)$	$Qn(H_b)$	$\delta(^ASe)$	$\delta(^BSe)$	$\delta(H_b)$	$\delta(^ASe)^c$	$\delta(^BSe)^c$	$\delta(H_b)^c$	$Qn(^ASe)$	$Qn(^BSe)$	$Qn(H_b)$	$\delta(^ASe)$	$\delta(^BSe)$	$\delta(H_b)$
OH	0.0882	-0.1669	0.0816	30.56	-400.01	1.769	77.59	-239.53	2.103	0.1704	-0.2022	0.0572	104.79	-389.24	2.055
Me	0.0855	-0.1669	0.0814	37.59	-399.56	1.783	83.20	-239.09	2.109	0.1731	-0.2013	0.0573	108.48	-389.23	2.044
H	0.0861	-0.1668	0.0821	49.99	-398.76	1.801	92.75	-238.71	2.130	0.1776	-0.2019	0.0586	115.35	-387.28	2.071
Cl	0.0923	-0.1671	0.0844	39.47	-398.34	1.809	88.36	-238.78	2.153	0.1857	-0.2037	0.0615	118.21	-386.56	2.092
Br	0.0926	-0.1671	0.0845	39.70	-397.96	1.812	89.28	-238.47	2.157	0.1869	-0.2038	0.0618	117.89	-386.18	2.095
COOH	0.0924	-0.1669	0.0850	d	d	d	99.30	-238.04	2.180	0.1998	-0.2045	0.0639	137.43	-385.84	2.094
NO$_2$	0.0994	-0.1672	0.0881	d	d	d	102.05	-239.38	2.227	0.2154	-0.2065	0.0683	150.20	-384.20	2.130

^{a} The σ(Se) values for MeSeMe are 1645.53 and 1915.42 with B3LYP/6-311+G(2d,p) and HF/6-311+G(2d,p)//B3LYP/6-311+G(2d,p) methods, respectively. ^{b} The σ(H) values for TMS are 31.945 and 32.198 with B3LYP/6-311+G(2d,p) and HF/6-311+G(2d,p)//B3LYP/6-311+G(2d,p) methods, respectively. ^{c} Calculated with the HF/6-311+G(2d,p)//B3LYP/6-311+G(2d,p) method. ^{d} Not obtained due to "consistency failure" in the calculations.
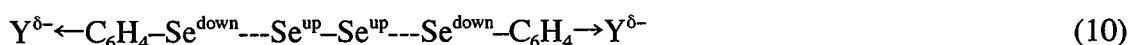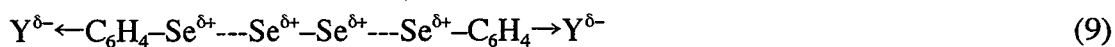
Table 4. Correlations between Calculated Values for 3 - 5[a,b]

no	Y	X	a	b	r	n
1	$Qn(^BSe)_B$ of **3**	$Qn(^ASe)_B$ of **3**	0.156	-0.2004	0.981	7
2	$\delta(^ASe)_B$ of **3**	$Qn(^ASe)_B$ of **3**	990.2	-96.85	0.967	6[c]
3	$\delta(^BSe)_B$ of **3**	$Qn(^BSe)_B$ of **3**	733.5	93.85	0.948	6[c]
4	$\delta(^BSe)_B$ of **3**	$\delta(^ASe)_B$ of **3**	0.115	-41.86	0.970	6[c]
5	$\delta(^ASe)_H$ of **3**	$Qn(^ASe)_B$ of **3**	1102.2	-94.45	0.974	7
6	$\delta(^BSe)_H$ of **3**	$Qn(^BSe)_B$ of **3**	-769.8	-126.93	0.957	7
7	$\delta(^BSe)_H$ of **3**	$\delta(^ASe)_H$ of **3**	-0.111	17.35	0.985	7
8	$Qn(^BSe)_B$ of **4**	$Qn(^ASe)_B$ of **4**	-0.026	-0.1646	0.860	7
9	$Qn(H_b)_B$ of **4**	$Qn(^ASe)_B$ of **4**	0.486	0.0397	0.978	7
10	$\delta(^ASe)_H$ of **4**	$Qn(^ASe)_B$ of **4**	1223.2	-20.87	0.686	7
11	$\delta(^BSe)_H$ of **4**	$Qn(^BSe)_B$ of **4**	612.2	-136.62	0.172	7
12	$\delta(H_b)_H$ of **4**	$Qn(H_b)_B$ of **4**	17.79	0.659	0.985	7
13	$\delta(^BSe)_H$ of **4**	$\delta(^ASe)_H$ of **4**	0.025	-241.15	0.419	7
14	$\delta(H_b)_H$ of **4**	$\delta(^ASe)_H$ of **4**	0.0045	1.742	0.901	7
15	$Qn(^BSe)_B$ of **5**	$Qn(^ASe)_B$ of **5**	-0.108	-0.1833	0.963	7
16	$Qn(H_b)_B$ of **5**	$Qn(^ASe)_B$ of **5**	0.249	0.0147	0.993	7
17	$\delta(^ASe)_B$ of **5**	$Qn(^ASe)_B$ of **5**	1006.9	-66.52	0.988	7
18	$\delta(^BSe)_B$ of **5**	$Qn(^BSe)_B$ of **5**	-949.5	-580.07	0.928	7
19	$\delta(H_b)_B$ of **5**	$Qn(H_b)_B$ of **5**	6.968	1.656	0.965	7
20	$\delta(^BSe)_B$ of **5**	$\delta(^ASe)_B$ of **5**	0.102	-399.40	0.910	7
21	$\delta(H_b)_B$ of **5**	$\delta(^ASe)_B$ of **5**	0.0016	1.891	0.889	7

[a] $Y = aX + b$ (r: correlation coefficient). [b] Subscripts B and H show B3LYP and HF levels, respectively. [c] Without the point for Y = COOH.

Let me discuss the characteristics of the interaction of 4c-6e in **3** first, based on results of ab initio MO calculations shown in Table 4 (No 1 - 7). The $Qn(^BSe)_B$ values correlate well with those of $Qn(^ASe)_B$, where the subscript B stands for the B3LYP level. The results further show that the magnitude of the charge transfer from ^ASe to ^BSe in **3** becomes greater as the electron density on ^ASe increases, which must be a reflection of the $n(^ASe)---\sigma^*(^BSe-^BSe)---n(^ASe)$ type interaction of the bond. While $\delta(^BSe)_B$ correlated with $\delta(^ASe)_B$ accompanied by a positive proportionality constant of 0.115, the proportionality constant was -0.111 in the correlation between $\delta(^BSe)_H$ and $\delta(^ASe)_H$, where the subscript H means the HF level. Computation at the B3LYP level could not explain the observed values. This discrepancy arises from the positive proportionality constant in the correlation of $\delta(^BSe)_B$ versus $Qn(^BSe)_B$ (No 3). The value is negative in the correlation of $\delta(^BSe)_H$ with $Qn(^BSe)_B$ (No 6). The calculations at the B3LYP level

usually explain the observed values better than those at the HF level.[14,15] However, the results at the HF level reproduced the observed substituent effect on $\delta(^BSe)_B$ but those at the B3LYP level did not, in this case. The superior nature of the calculations at the DFT (B3LYP) level come from inclusion of the electron correlation effect in the calculations, but the method sometimes overestimates this effect.[14] This overestimation of the electron correlation effect at the B3LYP level might lead to failure. The characters in the substituent effect on the atomic charges and the $\delta(Se)$ values of **3** are shown in eqs 9 and 10, respectively, assuming Y is electron withdrawing. The superscript up (or down) in eq 10 shows upfield (or downfield) shifts in the $\delta(Se)$ values.

$$Y^{\delta-}\leftarrow C_6H_4-Se^{\delta+}---Se^{\delta+}-Se^{\delta+}---Se^{\delta+}-C_6H_4\rightarrow Y^{\delta-} \qquad (9)$$

$$Y^{\delta-}\leftarrow C_6H_4-Se^{down}---Se^{up}-Se^{up}---Se^{down}-C_6H_4\rightarrow Y^{\delta-} \qquad (10)$$

The correlations in **4** are shown in Table 4 (No 8 - 14), which are mainly the results of the HF level. The p-type lone pairs of the Se atoms in **2a** can interact through π orbitals of the naphthalene ring, as was shown in the sulfur analog. The mechanism of the substituent effect on $\delta(^BSe)$ in **2** would be through-bond by way of the naphthylidene π-system, if the structures **2** are very close to that of **2a**. The results of the calculations on **4** are in accordance of the expectation. Nevertheless the $^BSe-H_b$ polarization mechanism is predicted to operate in **4**.

$$Y^{\delta-}\leftarrow C_6H_4-Se^{\delta+}---Se^{\delta-}-H_b^{\delta+} \qquad (11)$$

$$Y^{\delta-}\leftarrow C_6H_4-Se^{down}---Se^{down}-H_b^{down} \qquad (12)$$

Correlations with **5** exhibit the typical characters expected for the $^ASe---^BSe-H_b$ 3c-4e type interaction (Table 4: No 15 - 21). The observed $\delta(Se)$ values in **2** can be well explained by the results of the calculations on **5** at least in a qualitative sense. The proportionality constant of No 20 in Table 4 (0.102) is smaller than that of eq 3 (0.252), which may be due to the contribution of the mechanism other than **5** such as through-bond one discussed above. We believe that the mechanism shown for **5** is substantially the same as that operating in **2d** - **2g**. This mechanism may also be operating in **2a** - **2c**, as well as a through-bond mechanism. The nature of the substituent effect on the atomic charges and the $\delta(Se)$ values are shown in eqs 11 and 12, respectively, exemplified by the electron-withdrawing group of Y. The $\delta(C_{Me})$ values in **2** go upfield when Y = electron-withdrawing which is just the opposite of that predicted for H_b shown in eq 12. The discrepancy may arise from the difference between H in **5** and CH_3 in **2**: the C–H bond in **2** can also be polarized.

Glass and his co-workers have shown that the p-type lone pairs of sulfur atoms in naphtho[1,8-*b,c*]-1,5-dithiocin (**7**) lie in the naphthyl plane and interact directly with each other whereas those in 1,8-bis(methylthio)naphthalene (**8**) mainly interact with the π-orbitals of the naphthalene ring.[8] The orientation of the lone pairs of Se atoms in PhSe groups of **1** is close to that in the S atoms of the former, whereas that of the Se atoms in **2** is very similar to that in S atoms of the latter. The role of the π-framework must be important in the transmittance of the substituent effect in **2** as discussed in **4**.

7   8
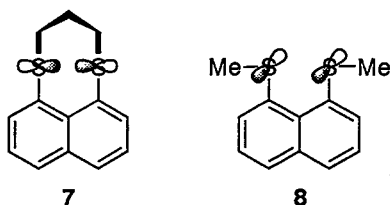
The Correlation of Observed and Calculated Values. The observed NMR parameters are plotted versus the calculated ones. The correlations of $\delta(^8Se)$ of **1** versus $\delta(^ASe)_B$ and $\delta(^ASe)_H$ in **3** are shown in eqs 13 and 14, respectively. The *a* and *r* values in eq 13 are very close to 1.0, which suggests that **3** can be a good model of **1**, as a first approximation. The $\delta(^1Se)$ values of **1** are plotted versus $\delta(^BSe)_H$ of **3**. The plot is shown in Figure 6 and is analyzed as two correlations with g(**m**) and g(**n**), which are shown in eqs 15m and 15n, respectively. The necessity of needing two correlations may be due to the conformational effects of the phenyl group in **1** (see also Scheme 1). A plot of $\delta(^8Se)$ of **2** versus $\delta(^ASe)_B$ of **5** is similarly analyzed by the two correlation methods, which are shown in eqs 16m and 16n, respectively. The results suggest the contribution of mechanism **5** for the transmittance of substituent effects in **2**.

$\delta(^8Se)$ of **1** = 0.953 × $\delta(^ASe)_B$ of **3** + 314.2   ($r = 0.999$)   (13)

$\delta(^8Se)$ of **1** = 0.869 × $\delta(^ASe)_H$ of **3** + 301.2   ($r = 0.990$)   (14)

$\delta(^1Se)$ of **1** = 7.675 × $\delta(^BSe)_H$ of **3** + 523.1   ($r = 0.978$ for g(**m**))   (15m)

$\delta(^1Se)$ of **1** = 1.585 × $\delta(^BSe)_H$ of **3** + 532.8   ($r = 0.997$ for g(**n**))   (15n)

$\delta(^8Se)$ of **2** = 0.932 × $\delta(^ASe)_B$ of **5** + 326.7   ($r = 1.000$ for g(**m**))   (16m)

$\delta(^8Se)$ of **2** = 0.657 × $\delta(^ASe)_B$ of **5** + 354.1   ($r = 0.991$ for g(**n**))   (16n)

$^4J(^8Se,^1Se)$ of **1** = -1877 × $Qn(^ASe)_B$ of **3** + 750.2   ($r = 0.969$)   (17)

$^4J(^8Se,^1Se)$ of **2** = -1439 × $Qn(^ASe)_B$ of **5** + 582.4   ($r = 0.993$)   (18)

We would like to comment on the $^4J(^8Se,^1Se)$ values of **1** and **2** next, although the *J*-values were not calculated. The $^4J(^8Se,^1Se)$ values of **1** and **2** are plotted versus $Qn(^ASe)_B$ of **3** and **5**, respectively, of which correlations are given in eqs 17 and 18. The negative proportionality

constants in eqs 17 and 18 clearly show that the J-values become larger if the electron density on the ^{A}Se atoms increases, as suggested in the previous section. The correlation coefficient of eq 17 is smaller than that of eq 18.
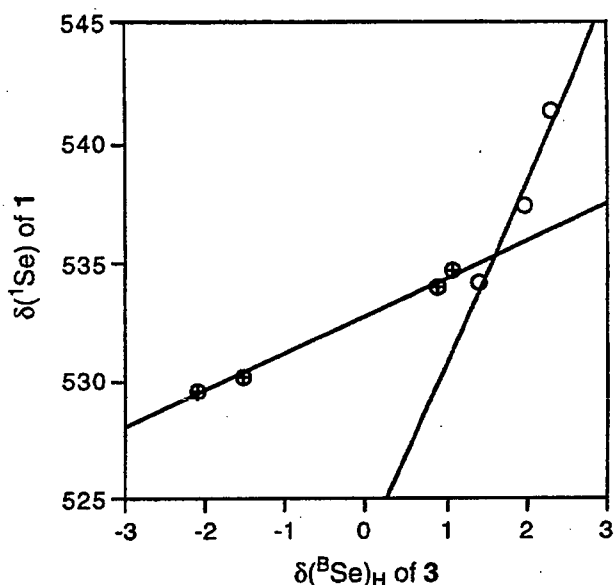
Figure 6. Plot of $\delta(^1\text{Se})$ of **1** versus $\delta(^B\text{Se})_H$ of **3**:
$\bigcirc$ and $\oplus$ stand for g(m) and g(n), respectively.

Although there are some common terms in the equations for the $\delta(\text{Se})^{25}$ and $J(\text{Se,Se})^{26}$ values, one must be careful when the mechanism of the nuclear couplings is considered in relation to the chemical shifts. The contribution of the 4s-orbitals of the Se atoms to $J(\text{Se,Se})^{27,28}$ is the striking contrast to the significant contribution of the 4p atomic orbitals to the diamagnetic term of the $\delta(\text{Se})$ values. A through-space mechanism must be operating for the nonbonded Se---Se nuclear spin-spin couplings, even if the substituent effect on the remote atomic charges is effectively transmitted through the π-framework as expected in **2** and which is missing in **4** and **5**.[29] The correlations of the Qn, $\delta(\text{Se})$, with the J-values for **1** show that this effect is transmitted by a through-space mechanism in contrast to the situation in **2**. The mechanism for **2** would change from mainly **4** for g(**m**) to mainly **5** for g(**n**). Analysis of the two correlations for the plot of $^4J(^8\text{Se},^1\text{Se})$ of **1** versus those of **2** (eqs 6m and 6n) may shed light on the situation discussed above.

Further study on the nonbonded interactions containing the Se atom(s) is currently in progress.

Experimental Section

Chemicals were used without further purification unless otherwise noted. Solvents were purified by standard methods. Melting points were uncorrected. ^{1}H, ^{13}C, and ^{77}Se NMR spectra were measured at 400, 100, and 76 MHz, respectively, with a JEOL JNM-LA 400 spectrometer. The ^{1}H, ^{13}C, and ^{77}Se chemical shifts are given in ppm relative to those of internal CHCl$_3$ slightly contaminated in the solution, CDCl$_3$ as the solvent, and external MeSeMe, respectively. Column chromatography was performed on silica gel (Fuji Silysia BW-300), acidic alumina and basic alumina (E. Merk).

Preparation. The diselenide **1a**[1] and the bis-selenide **2a**[1] were prepared by the same method as shown in the previous chapter. The selenides p-YC$_6$H$_4$SePh (**9**) were prepared similarly to the method shown in the literature.[15b,30,31] The reaction of p-iodonitrobenzene with sodium benzeneselenate in ethanol was more effective to prepare **9g**.

1a: mp 162 - 163 °C. (Lit:[1] mp 161 - 163 °C.), **2a**: mp 101.5 - 102.5 °C. (Lit:[1] mp 101.5 - 102.5 °C.), **9b**: mp 45 - 46 °C (Lit:[30] mp 45 - 46 °C), **9c**: colorless oil; bp 100 - 101 °C/1mmHg (Lit:[30] bp 100 °C/1mmHg), **9d**: colorless oil; bp 148 - 149 °C/1mmHg (Lit:[30] bp 145 - 150 °C/1mmHg), **9e**: mp 32 - 33 °C (Lit:[30] mp 32 °C), **9f**: colorless oil[15b], **9g**: mp 58 - 59 °C (Lit:[15b,31] mp 58 °C).

Bis[8-(p-methoxyphenylselanyl)naphthyl]-1,1'-diselenide (1b). To a solution of the dianion of naphto[1,8-c,d]-1,2-diselenole, which was prepared by reduction of the diselenole with NaBH$_4$ in an aqueous THF, was added p-methoxybenzenediazonium chloride at low temperature. After usual workup, the solution was chromatographed on silica gel containing acidic and basic alumina. Recrystallization of the chromatographed product from hexane gave **1b** as a yellow solid: 69 % yield, mp 143.5 - 145.0 °C. ^{1}H NMR (CDCl$_3$, 400 MHz) 3.74 (s, 6H), 6.75 (dd, 4H, J = 8.9 and 2.6 Hz), 7.18 (t, 2H, J = 7.8 Hz), 7.32 (t, 2H, J = 7.6 Hz), 7.32 (dd, 4H, J = 9.0 and 2.7 Hz), 7.67 (dd, 2H, J = 8.0 and 0.9 Hz), 7.79 (dd, 2H, J = 8.1 and 1.0 Hz), 7.86 (dd, 2H, J = 7.2 and 1.4 Hz), 8.14 (dd, 2H, J = 7.5 and 1.0 Hz); ^{13}C NMR (CDCl$_3$, 100 MHz) 55.27, 115.06, 125.28, 125.82, 126.52, 128.33, 129.78, 130.25, 130.57, 132.74, 133.42, 135.39, 136.14, 137.39, 159.24; ^{77}Se NMR (CDCl3, 76 MHz) 416.2, 541.4 (^4J(^{8}Se,^{1}Se) = 371.6 Hz). Anal. Calcd for C$_{34}$H$_{26}$O$_2$Se$_4$: C, 52.19; H, 3.35. Found: C, 52.45; H, 3.36.

Bis[8-(p-methylphenylselanyl)naphthyl]-1,1'-diselenide (1c). In the similar method for **1b**, **1c** gave 72 % yield as a yellow solid, mp 165.5 -166.5 °C. ^{1}H NMR (CDCl$_3$, 400 MHz) 2.27 (s, 6H), 7.00 (dd, 4H, J = 8.3 and 2.5 Hz), 7.16 (t, 2H, J = 7.8 Hz), 7.20 (dd, 4H, J = 8.2 and 2.5 Hz), 7.34 (t, 2H, J = 7.9 Hz), 7.67 (dd, 2H, J = 8.1 and 0.8 Hz), 7.83 (dd, 2H, J = 8.2 and 1.2 Hz), 7.92 (dd, 2H, J = 7.2 and 1.3 Hz), 8.11 (dd, 2H, J = 7.5 and 1.0 Hz); ^{13}C NMR (CDCl$_3$, 100 MHz) 21.06, 125.84, 126.57, 128.16, 128.40, 130.09, 130.49, 130.66, 130.86, 131.68, 132.32,

135.62, 136.15, 136.79, 138.37; ^{77}Se NMR (CDCl$_3$, 76 MHz) 422.0, 537.4 ($^4J(^8$Se,^{1}Se) = 354.4 Hz). Anal. Calcd for C$_{34}$H$_{26}$Se$_4$: C, 54.42; H, 3.49. Found: C, 54.71; H, 3.57.

Bis[8-(*p*-chlorophenylselanyl)naphthyl]-1,1'-diselenide (1d). In the similar method for **1b**, **1d** gave 68 % yield as a yellow solid, mp 185.0 - 186.0 °C. ^{1}H NMR (CDCl$_3$, 400 MHz) 7.13 (br.s, 8H), 7.16 (t, 2H, *J* = 7.8 Hz), 7.38 (t, 2H, *J* = 7.7 Hz), 7.70 (dd, 2H, *J* = 8.0 and 0.8 Hz), 7.88 (dd, 2H, *J* = 8.2 and 1.1 Hz), 7.94 (dd, 2H, *J* = 7.2 and 1.3 Hz), 8.02 (dd, 2H, *J* = 7.5 and 1.1 Hz); ^{13}C NMR (CDCl$_3$, 100 MHz) 125.95, 126.75, 127.26, 128.43, 129.42, 130.19, 131.28, 131.65, 132.48, 132.91, 133.82, 135.62, 136.36, 139.01; ^{77}Se NMR (CDCl$_3$, 76 MHz) 429.1, 534.7 ($^4J(^8$Se,^{1}Se) = 330.1 Hz). Anal. Calcd for C$_{32}$H$_{20}$Se$_4$Cl$_2$: C, 48.58; H, 2.55. Found: C, 48.77; H, 2.56.

Bis[8-(*p*-bromophenylselanyl)naphthyl]-1,1'-diselenide (1e). In the similar method for **1b**, **1e** gave 72 % yield as a yellow solid, mp 203.0 - 205.0 °C. ^{1}H NMR (CDCl$_3$, 400 MHz) 7.06 (dd, 4H, *J* = 6.6 and 2.2 Hz), 7.16 (t, 2H, *J* = 7.8 Hz), 7.27 (dd, 4H, *J* = 8.6 and 2.2 Hz), 7.38 (t, 2H, *J* = 7.6 Hz), 7.70 (dd, 2H, *J* = 8.1 and 0.9 Hz), 7.89 (dd, 2H, *J* = 8.2 and 1.2 Hz), 7.95 (dd, 2H, *J* = 7.1 and 1.3 Hz), 8.01 (dd, 2H, *J* = 7.5 and 1.1 Hz); ^{13}C NMR (CDCl$_3$, 100 MHz) 120.77, 125.95, 126.78, 126.85, 128.40, 130.02, 131.38, 131.71, 132.28, 132.29, 134.56, 135.54, 136.32, 139.19; ^{77}Se NMR (CDCl$_3$, 76 MHz) 429.6, 534.0 ($^4J(^8$Se,^{1}Se) = 327.1 Hz). Anal. Calcd for C$_{32}$H$_{20}$Se$_4$Br$_2$: C, 43.67; H, 2.29. Found: C, 43.84; H, 2.25.

Bis{8-[*p*-(ethoxycarbonyl)phenylselanyl]naphthyl}-1,1'-diselenide (1f). In the similar method for **1b**, **1f** gave 58 % yield as a yellow solid, mp 167.0 - 169.5°C. ^{1}H NMR (CDCl$_3$, 400 MHz) 1.34 (t, 6H, *J* = 7.1 Hz), 4.32 (q, 4H, *J* = 7.1 Hz),7.12 (t, 2H, *J* = 7.8 Hz), 7.15 (dd, 2H, *J* = 8.7 and 1.9 Hz), 7.39 (t, 2H, *J* = 7.6 Hz), 7.67 (dd, 2H, *J* = 8.0 and 0.9 Hz), 7.81 (dd, 4H, *J* = 8.6 and 1.9 Hz), 7.90 (dd, 2H, *J* = 8.2 and 1.1 Hz), 7.97 (dd, 2H, *J* = 7.6 and 1.2 Hz), 7.98 (dd, 2H, *J* = 7.1 and 1.4 Hz); ^{13}C NMR (CDCl$_3$, 100 MHz) 14.28, 60.83, 125.64, 125.93, 126.79, 128.27, 128.34, 128.78, 129.90, 130.13, 131.71, 132.07, 135.70, 136.36, 139.80, 142.50, 166.17; ^{77}Se NMR (CDCl$_3$, 76 MHz) 442.5, 530.2 ($^4J(^8$Se,^{1}Se) = 311.4 Hz). Anal. Calcd for C$_{38}$H$_{30}$Se$_4$O$_4$: C, 52.67; H, 3.49. Found: C, 52.84; H, 3.50.

Bis[8-(*p*-nitrophenylselanyl)naphthyl]-1,1'-diselenide (1g). In the similar method for **1b**, **1g** gave 56 % yield as a yellow solid, mp 230.0 - 233.5 °C. ^{1}H NMR (CDCl$_3$, 400 MHz) 7.14 (t, 2H, *J* = 7.8 Hz), 7.16 (dd, 2H, *J* = 9.0 and 2.5 Hz), 7.46 (t, 2H, *J* = 7.7 Hz), 7.73 (dd, 2H, *J* = 8.1 and 1.0 Hz), 7.91 (dd, 2H, *J* = 7.6 and 1.1 Hz), 7.97 (dd, 4H, *J* = 9.0 and 2.2 Hz), 7.99 (dd, 2H, *J* = 7.9 and 1.3 Hz), 8.02 (dd, 2H, *J* = 7.1 and 1.4 Hz); ^{13}C NMR (CDCl$_3$, 100 MHz) 124.10, 124.42, 126.22, 126.97, 128.66, 128.84, 129.45, 132.11, 132.48, 135.55, 136.56, 140.34, 146.00, 146.15; ^{77}Se NMR (CDCl$_3$, 76 MHz) 456.1, 529.6 ($^4J(^8$Se,^{1}Se) = 294.1 Hz). Anal. Calcd for C$_{32}$H$_{20}$Se$_4$N$_2$O$_4$: C, 47.31; H, 2.48; N, 3.45. Found: C, 47.52; H, 2.58; N, 3.35.

1-(Methylselanyl)-8-(*p*-methoxyphenylselanyl)naphthalene (2b). The diselenide **1a** was reduced by NaBH$_4$ in an aqueous THF then allowed to react with methyl iodide gave **2b** as a white solid, 91 % yield, mp 86.0 - 87.0 °C. ^{1}H NMR (CDCl$_3$, 400 MHz) 2.38 (s, 3H, *J* (Se,H) = 13.4 Hz), 3.79 (s, 3H), 6.83 (dd, 2H, *J* = 8.6 and 2.2 Hz), 7.17 (t, 1H, *J* = 7.7 Hz), 7.33 (t, 1H, *J* = 7.7 Hz), 7.45 (dd, 2H, *J* = 8.1 and 2.2 Hz), 7.45 (dd, 1H, *J* = 6.8 and 1.1 Hz), 7.64 (dd, 1H, *J* = 8.1 and 1.0 Hz), 7.70 (dd, 1H, *J* = 8.0 and 1.1 Hz), 7.79 (dd, 1H, *J* = 7.3 and 1.1 Hz); ^{13}C NMR (CDCl$_3$, 100 MHz) 13.90 (^1J = 71.2 Hz, ^5J = 15.7 Hz), 55.23, 115.17, 124.73, 125.70, 125.84, 128.26, 128.75, 131.25, 133.10, 133.50, 133.64, 134.94, 135.80, 136.47 (^1J = 11.5 Hz), 159.69; ^{77}Se NMR (CDCl$_3$, 76 MHz) 424.5, 233.1 (^4J(^{8}Se,^{1}Se) = 341.6 Hz). Anal. Calcd for C$_{18}$H$_{16}$Se$_2$O$_1$: C, 53.22; H, 3.97. Found: C, 53.35; H, 3.90.

1-(Methylselanyl)-8-(*p*-methylphenylselanyl)naphthalene (2c). In the similar method for **2b**, **2c** gave 89 % yield as a white solid, mp 78.5 - 79.5 °C. ^{1}H NMR (CDCl$_3$, 400 MHz) 2.32 (s, 3H), 2.36 (s, 3H, *J* (Se,H) = 13.9 Hz), 7.08 (dd, 2H, *J* = 7.8 and 2.2 Hz), 7.20 (t, 1H, *J* = 7.7 Hz), 7.34 (t, 1H, *J* = 7.8 Hz), 7.36 (dd, 2H, *J* = 8.0 and 2.2 Hz), 7.58(dd, 1H, *J* = 7.5 and 1.3 Hz), 7.69 (dd, 1H, *J* = 8.2 and 1.1 Hz), 7.71 (dd, 1H, *J* = 8.4 and 1.1 Hz), 7.76 (dd, 1H, *J* = 7.4 and 1.3 Hz); ^{13}C NMR (CDCl$_3$, 100 MHz) 13.65 (^1J = 72.8 Hz, ^5J = 16.6 Hz), 21.27, 125.77, 125.88, 128.46, 128.77, 130.22, 131.24, 131.74, 132.22, 132.79, 133.86 (^1J = 11.6 Hz), 134.52, 135.17, 135.78, 137.53; ^{77}Se NMR (CDCl$_3$, 76 MHz) 427.7, 234.5 (^4J(^{8}Se,^{1}Se) = 330.9 Hz). Anal. Calcd for C$_{18}$H$_{16}$Se$_2$: C, 55.40; H, 4.13. Found: C, 55.52; H, 4.19.

1-(Methylselanyl)-8-(*p*-chlorophenylselanyl)naphthalene (2d). In the similar method for **2b**, **2d** gave 87 % yield as a white solid, mp 78.5 - 79.5 °C. ^{1}H NMR (CDCl$_3$, 400 MHz) 2.34 (s, 3H, *J* (Se,H) = 13.9 Hz), 7.19 (dd, 2H, *J* = 8.6 and 2.2 Hz), 7.24 (t, 1H, *J* = 7.7 Hz), 7.31 (dd, 2H, *J* = 8.8 and 2.2 Hz), 7.36 (t, 1H, *J* = 7.7 Hz), 7.60 (dd, 1H, *J* = 7.3 and 1.5 Hz), 7.71 (dd, 1H, *J* = 7.1 and 1.2 Hz), 7.73 (dd, 1H, *J* = 6.8 and 1.1 Hz), 7.74 (dd, 1H, *J* = 7.3 and 1.2 Hz); ^{13}C NMR (CDCl$_3$, 100 MHz) 13.43 (^1J = 72.8 Hz, ^5J = 15.7 Hz), 125.96, 125.99, 128.42, 129.49, 130.86, 131.72, 132.67, 133.50, 133.60, 134.49 (^1J = 12.4 Hz), 135.26, 135.59, 135.83; ^{77}Se NMR (CDCl$_3$, 76 MHz) 431.6, 234.7 (^4J(^{8}Se,^{1}Se) = 316.7 Hz). Anal. Calcd for C$_{17}$H$_{13}$Se$_2$Cl$_1$: C, 49.72; H, 3.19. Found: C, 49.77; H, 3.23.

1-(Methylselanyl)-8-(*p*-bromophenylselanyl)naphthalene (2e). In the similar method for **2b**, **2e** gave 88 % yield as a white solid, mp 90.0 - 91.0 °C. ^{1}H NMR (CDCl$_3$, 400 MHz) 2.34 (s, 3H, *J* (Se,H) = 13.9 Hz), 7.23 (dd, 2H, *J* = 8.6 and 2.2 Hz), 7.25 (t, 1H, *J* = 7.8 Hz), 7.34 (dd, 2H, *J* = 8.6 and 2.2 Hz), 7.37 (t, 1H, *J* = 7.7 Hz), 7.62 (dd, 1H, *J* = 7.4 and 1.2 Hz), 7.72 (dd, 1H, *J* = 7.5 and 1.2 Hz), 7.74 (dd, 1H, *J* = 7.6 and 1.2 Hz), 7.74 (dd, 1H, *J* = 7.6 and 1.3 Hz); ^{13}C NMR (CDCl$_3$, 100 MHz) 13.40 (^1J = 72.7 Hz, ^5J = 15.7 Hz), 121.57, 125.98, 126.01, 128.40, 129.57, 130.63, 131.77, 132.40 (^1J = 10.7 Hz), 132.58, 134.38, 134.50 (^1J = 11.6 Hz), 135.29, 135.79,

135.84; ^{77}Se NMR (CDCl$_3$, 76 MHz) 432.4, 235.2 ($^4J(^8$Se,^{1}Se) = 313.9 Hz). Anal. Calcd for C$_{17}$H$_{13}$Se$_2$Br$_1$: C, 44.87; H, 2.88. Found: C, 44.89; H, 2.90.

1-(Methylselanyl)-8-[*p*-(ethoxycarbonyl)phenylselany]naphthalene (2f). In the similar method for **2b**, **2f** gave 84 % yield as a white solid, mp 83.5 - 84.0 °C. ^{1}H NMR (CDCl$_3$, 400 MHz) 1.33 (t, 3H, *J* = 7.1 Hz), 2.30 (s, 3H, *J* (Se,H) = 14.6 Hz), 4.31 (q, 2H, *J* = 7.1 Hz), 7.27 (dd, 2H, *J* = 8.6 and 2.2 Hz), 7.29 (t, 1H, *J* = 7.7 Hz), 7.37 (t, 1H, *J* = 7.7 Hz), 7.62 (dd, 2H, *J* = 7.4 and 1.2 Hz), 7.72 (dd, 1H, *J* = 8.0 and 1.0 Hz), 7.76 (dd, 1H, *J* = 7.3 and 1.2 Hz), 7.81 (dd, 1H, *J* = 8.0 and 1.4 Hz), 7.82 (dd, 1H, *J* = 8.3 and 2.2 Hz); ^{13}C NMR (CDCl$_3$, 100 MHz) 12.85 (^1J = 74.5 Hz, ^5J = 15.7 Hz), 14.29, 60.89, 126.03, 126.13, 127.99, 128.63, 130.14, 130.47, 130.80 (^1J = 12.5 Hz), 131.34, 132.37, 135.52, 135.91, 137.77, 142.80, 166.31; ^{77}Se NMR (CDCl$_3$, 76 MHz) 442.4, 239.2 ($^4J(^8$Se,^{1}Se) = 294.7 Hz). Anal. Calcd for C$_{20}$H$_{18}$Se$_2$ O$_2$: C, 53.59; H, 4.05. Found: C, 53.61; H, 4.09.

1-(Methylselanyl)-8-(*p*-nitrophenylselanyl)naphthalene (2g). In the similar method for **2b**, **2g** gave 81 % yield as a white solid, mp 140.0 - 141.0 °C. ^{1}H NMR (CDCl$_3$, 400 MHz) 2.29 (s, 3H, *J* (Se,H) = 13.9 Hz), 7.23 (dd, 2H, *J* = 9.0 and 2.4 Hz), 7.37 (t, 1H, *J* = 7.7 Hz), 7.40 (t, 1H, *J* = 7.7 Hz), 7.63 (dd, 1H, *J* = 7.4 and 1.0 Hz), 7.74 (dd, 1H, *J* = 8.2 and 1.0 Hz), 7.86 (dd, 1H, *J* = 7.3 and 1.4 Hz), 7.90 (dd, 1H, *J* = 8.1 and 1.2 Hz), 7.97 (dd, 2H, *J* = 9.0 and 2.4 Hz); ^{13}C NMR (CDCl$_3$, 100 MHz) 12.47 (^1J = 76.1 Hz, ^5J = 14.8 Hz), 123.92, 126.11, 126.37, 126.65, 127.81, 130.02 (^1J = 13.2 Hz), 130.67, 131.47, 132.42, 135.40, 136.00, 139.04 (^1J = 9.9 Hz), 146.11, 146.74; ^{77}Se NMR (CDCl$_3$, 76 MHz) 453.9, 240.1 ($^4J(^8$Se,^{1}Se) = 272.5 Hz). Anal. Calcd for C$_{17}$H$_{13}$Se$_2$N$_1$O$_2$: C, 48.48; H, 3.11; N, 3.33. Found: C, 48.66; H, 3.10; N, 3.27.

MO Calculations. Ab initio molecular orbital calculations were performed on an Origin computer using the Gaussian 94 program with 6-311+G(d,p) basis sets at B3LYP and/or HF levels.[22] The σ values for H, C, and Se nuclei were calculated using the NMR key word of the program and the natural charges (*Qn*) were calculated by the natural population analysis.[24]

References

(1) Nakanishi, W.; Hayashi, S.; Toyota, S. *J. Org. Chem.* **1998**, *63*, 8790. See also Nakanishi, W.; Hayashi, S.; Toyota, S. *J. Chem. Soc., Chem. Commun.* **1996**, 371.

(2) Nakanishi, W.; Hayashi, S. unpublished results.

(3) Nakanishi, W.; Hayashi, S.; Yamaguchi, H. *Chem. Lett.* **1996**, 947.

(4) (a) Johannsen, I.; Eggert, H. *J. Am. Chem. Soc.* **1984**, *106*, 1240. Johannsen, I.; Eggert, H.; Gronowitz, S.; Hörnfeldt, A.-B. *Chem. Scr.* **1987**, *27*, 359. Fujihara, H.; Mima, H.; Erata, T.; Furukawa, N. *J. Am. Chem. Soc.* **1992**, *114*, 3117. (b) Fujihara, H.; Saito, R.; Yabe, M.; Furukawa, N. *Chem. Lett.* **1992**, 1437.

(5) Nakanishi, W.; Hayashi, S.; Sakaue, A.; Ono, G.; Kawada, Y. *J. Am. Chem. Soc.* **1998**, *120*, 3635.

(6) (a) Mallory, F. B. *J. Am. Chem. Soc.* **1973**, *95*, 7747. (b) Mallory, F. B.; Mallory, C. W.; Fedarko, M.-C. *J. Am. Chem. Soc.* **1974**, *96*, 3536. (c) Mallory, F. B.; Mallory, C. W.; Ricker, W. M. *J. Am. Chem. Soc.* **1975**, *97*, 4770. Mallory, F. B.; Mallory, C. W.; Ricker, W. M. *J. Org. Chem.* **1985**, *50*, 457. Mallory, F. B.; Mallory, C. W.; Baker, M. B. *J. Am. Chem. Soc.* **1990**, *112*, 2577. (d) Ernst, L.; Ibrom, K. *Angew. Chem. Int. Ed. Engl.* **1995**, *34*, 1881. Ernst, L.; Ibrom, K.; Marat, K.; Mitchell, R. H.; Bodwell, G. J.; Bushnell, G. W. *Chem. Ber.* **1994**, *127*, 1119.

(7) Mallory, F. B.; Luzik, Jr., E. D.; Mallory, C. W.; Carroll, P. J. *J. Org. Chem.* **1992**, *57*, 366. Mallory, F. B.; Mallory, C. W. *J. Am. Chem. Soc.* **1985**, *107*, 4816.

(8) (a) Glass, R. S.; Andruski, S. W.; Broeker, J. L. *Rev. Heteroatom Chem.* **1988**, *1*, 31. Glass, R. S.; Andruski, S. W.; Broeker, J. L.; Firouzabadi, H.; Steffen, L. K.; Wilson, G. S. *J. Am. Chem. Soc.* **1989**, *111*, 4036. (b) Glass, R. S.; Adamowicz, L.; Broeker, J. L. *J. Am. Chem. Soc.* **1991**, *113*, 1065.

(9) Fujihara, H.; Ishitani, H.; Takaguchi, Y.; Furukawa, N. *Chem. Lett.* **1995**, 571.

(10) (a) Goldstein, B. M.; Kennedy, S. D.; Hennen, W. J. *J. Am. Chem. Soc.* **1990**, *112*, 8265. (b) Barton, D. H. R.; Hall, M. B.; Lin, Z.; Parekh, S. I.; Reibenspies, J. *J. Am. Chem. Soc.* **1993**, *115*, 5056.

(11) Cheeseman, J. R.; Trucks, G. W.; Keith, T. A.; Frisch, M. J. *J. Chem. Phys.* **1996**, *104*, 5497.

(12) (a) Forsyth, D. A.; Sebag, A. B. *J. Am. Chem. Soc.* **1997**, *119*, 9483; (b) Olah, G. A.; Shamma, T.; Burrichter, A.; Rasul, G.; Prakash, G. K. S. *J. Am. Chem. Soc.* **1997**, *119*, 12923; Olah, G. A.; Shamma, T.; Burrichter, A.; Rasul, G.; Hachoumy, M.; Prakash, G. K. S. *J. Am. Chem. Soc.* **1997**, *119*, 12929.

(13) Tanaka, S.; Sugimoto, M.; Takashima, H.; Hada, M.; Nakatuji, H. *Bull. Chem. Soc., Jpn.* **1966**, *69*, 953; Ballard, C. C.; Hada, M.; Kaneko, H.; Nakastuji, H. *Chem. Phys. Lett.* **1996**, *254*, 170; Nakastuji, H.; Hada, M.; Kaneko, H.; Nakajima, T. *Chem. Phys. Lett.* **1996**, *255*, 429; Hada, M.; Kaneko, H.; Nakastuji, H. *Chem. Phys. Lett.* **1996**, *261*, 7; Nakastuji, H.; Hu, Z.-M.; Nakajima, T. *Chem. Phys. Lett.* **1997**, *275*, 429. See also refs cited therein.

(14) (a) Nakatsuji, H.; Higashioji, T.; Sugimoto, M. *Bull. Chem. Soc. Jpn.* **1993**, *66*, 3235. (b) Magyarfalvi, G.; Pulay, P. *Chem. Phys. Lett.* **1994**, *225*, 280. (c) Bühl, M.; Gauss, J.; Stanton,

J. F. *Chem. Phys. Lett.* **1995**, *241*, 248. (d) Bühl, M.; Thiel, W.; Fleischer, U.; Kutzelnigg, W. *J. Phys. Chem.* **1995**, *99*, 4000. (e) Malkin, V. G.; Malkina, O. L.; Casida, M. E.; Salahub, D. R. *J. Am. Chem. Soc.* **1994**, *116*, 5898. (f) Schreckenbach, G.; Ruiz-Morales, Y.; Ziegler, T. *J. Chem. Phys.* **1996**, 104, 8605. (g) Ellis, P. D.; Odom, J. D.; Lipton, A. S.; Chen, Q.; Gulick, J. M. in *Nuclear Magnetic Shieldings and Molecular Structure*; NATO ASI Series; Tossel, J. A. Ed.; Kluwer Academic Publishers; Dordrecht, 1993, p. 539. See also refs cited therein.

(15) (a) Nakanishi, W.; Hayashi, S. *Chem. Lett.* **1998**, 523. (b) Nakanishi, W.; Hayashi, S. *J. Phys. Chem.* **1999**, *64*, 6688.

(16) The $\delta(^8Se)$ values of **1** and **2** were plotted versus $\delta(Se)$ of $p\text{-}YC_6H_4SePh$ (**9**) and the correlations are given in eqs a and b, respectively. As shown in eqs 1, a, and b, the $\delta(^8Se)$ in **1** and **2** and $\delta(Se)$ in **9** are well correlated with each other, which means that the effect of the substituents on $\delta(Se)$ of the $p\text{-}YC_6H_4Se$ groups would be essentially the same for the three selenides, although the magnitudes of the effect are different. A slight deviation was observed for the point corresponding to Y = OMe in eq b.

$\delta(^8Se)$ of **1** = 1.07 × $\delta(Se)$ of **9** - 21.4 $\qquad$ ($r = 0.996$) $\qquad$ (a)

$\delta(^8Se)$ of **2** = 0.794 × $\delta(Se)$ of **9** + 98.2 $\qquad$ ($r = 0.991$) $\qquad$ (b)

(17) The $\delta(^8Se)$ values of **1** and **2** were also plotted versus $\delta(Se)$ of 1-(p-substituted phenylselanyl)naphthalenes (**10**) and the correlations are given in eqs c and d, respectively. However, the correlation for **1** (eq c) is poorer than that of eq a in ref 16. It must be due to the characteristic structures of **10**. Details will be reported elsewhere.

$\delta(^8Se)$ of **1** = 1.51 × $\delta(Se)$ of **10** - 116.0 $\qquad$ ($r = 0.987$) $\qquad$ (c)

$\delta(^8Se)$ of **2** = 1.14 × $\delta(Se)$ of **10** + 22.0 $\qquad$ ($r = 0.997$) $\qquad$ (d)

(18) The details of the substituent effect on $\delta(Se)$ in $p\text{-}YC_6H_4SeR$ (R = Me, Ph, CN, $CH=CH_2$ etc.), together with **1** and **2**, are discussed in ref 15. The $\delta(^8Se)$ values of **1** and **2** can be discussed as a class of p-substituted phenyl selenides.

(19) Details of the substituent effect on $\delta(^8Se)$ and $\delta(C_i)$ are discussed in the supporting informations.

(20) The results show that the substituent dependence of the structures **1** and **2** would also be considered for the detail discussion, since the plot gives better correlations if it is analyzes as the two correlations with g(**m**) ($a = 1.27$ and $r = 0.990$) and g(**n**) ($a = 1.22$ and $r = 1.00$) as will be discussed in the plots of $^4J(^8Se,^1Se)$ ($= {}^4J(^{8'}Se,^{1'}Se)$) versus $\delta(^8Se)$ in **1** and **2** in the text.

(21) (a) Pimentel, G. C. *J. Chem. Phys.* **1951**, *19*, 446. Musher, J. I. *Angew. Chem., Int. Ed. Engl.* **1969**, *8*, 54. (b) Chen, M. M. L.; Hoffmann, R. *J. Am. Chem. Soc.* **1976**, *98*, 1647. (c) Cahill, P. A.; Dykstra, C. E.; Martin, J. C. *J. Am. Chem. Soc.* **1985**, *107*, 6359. See also, Hayes, R. A.; Martin, J. C. "Sulfurane Chemistry," in "Organic Sulfur Chemistry: Theoretical and

Experimental Advances," ed by Bernardi, F. Csizmadia, I. G. Mangini, A. Elsevier: Amsterdam, 1985; Chapter 8.

(22) *Gaussian 94, Revision D.4*; Frisch, M. J.; Trucks, G. W.; Schlegel, H. B.; Gill, P. M. W.; Johnson, B. G.; Robb, M. A.; Cheeseman, J. R.; Keith, T.; Petersson, G. A.; Montgomery, J. A.; Raghavachari, K.; Al-Laham, M. A.; Zakrzewski, V. G.; Ortiz, J. V.; Foresman, J. B.; Cioslowski, J.; Stefanov, B. B.; Nanayakkara, A.; Challacombe, M.; Peng, C. Y.; Ayala, P. Y.; Chen, W.; Wong, M. W.; Andres, J. L.; Replogle, E. S.; Gomperts, R.; Martin, R. L.; Fox, D. J.; Binkley, J. S.; Defrees, D. J.; Baker, J.; Stewart, J. P.; Head-Gordon, M.; Gonzalez, C.; Pople, J. A. Gaussian, Inc., Pittsburgh PA, 1995.

(23) The structures 6_{pl} and 6_{pd} (a - g for Y = H, OH, Me, Cl, Br, COOH, and NO_2, respectively) were full optimized with the 6-311+G(2d,p) basis sets at the B3LYP level except for 6_{pd} with Y = COOH. Calculations for 6_{pd} with Y = COOH were achieved with the torsional angle between the Se–H bond and the phenyl plane fixed to be perpendicular. The structures 6_{pl} and 6_{pd} would not be the energy minima but the transition states.[15b]

(24) NBO Ver. 3.1, Glendening, E. D.; Reed, A. E.; Carpenter, J. E.; Weinhold, F.

(25) Karplus, M.; Pople, J. A. *J. Chem. Phys.* **1963**, *38*, 2803.

(26) McConnell, H. M., *J. Chem. Phys.* **1956**, *24*, 460.

(27) Reich, H. J.; Trend, J. E. *J. Chem. Soc., Chem. Commun.* **1976**, 310.

(28) Nakanishi, W.; Ikeda, Y. *Bull. Chem. Soc. Jpn.* **1983**, *56*, 1161.

(29) The contribution of the through-bond mechanism is estimated to be very small for $^4J(F,F)$ in 1,8-di(fluoro)naphthalene.[6b]

(30) Greenberg, B.; Gold, E. S.; Burlant, WM. *J. Am. Chem. Soc.* **1956**, *78*, 4028.

(31) Chem. Abstr. **1955**, *49*, 2349g.

List of Publications

1   W. Nakanishi, S. Hayashi and S. Toyota, Structure of bis[8-(phenylselanyl)naphthyl] diselenide: first linear alignment of four Se atoms as a four-center six-electron bond, *Chem. Commun.*, **1996**, pp. 371-372 (1996).

2   W. Nakanishi, S. Hayashi, and H. Yamaguchi, Inverse Substituent Effect on ^{77}Se NMR Chemical Shifts in Naphthalene Systems with Linear 4c-6e Se4 Bond: 1-[8-(p-YC$_6$H$_4$Se)-C$_{10}$H$_6$]SeSe[C$_{10}$H$_6$(SeC$_6$H$_4$-Y-p)-8']-1' versus 1-(MeSe)-8-(p-YC$_6$H$_4$Se)C$_{10}$H$_6$, *Chem. Lett.*, **1996**, pp. 947-948 (1996).

3   W. Nakanishi, S. Hayashi, A. Sakaue, G. Ono, and Y. Kawada, Attractive Interaction Caused by the Linear F---Se-C Alignment in Naphthalene Peri Positions, *J. Am. Chem. Soc.* **120**, pp. 3635-3640 (1998).

4   W. Nakanishi and S. Hayashi, On the Factors to Determine ^{77}Se NMR Chemical Shifts of Organic Selenium Compounds: Application of GIAO Magnetic Shielding Tensor to ^{77}Se NMR Spectroscopy, *Chem. Lett.*, **1998**, pp. 523-524 (1998).

5   W. Nakanishi, S. Hayashi, and S. Toyota, Four-Center Six-Electron Interaction versus Lone Pair-Lone Pair Interaction between Selenium Atoms in Naphthalene Peri Positions, *J. Org. Chem.*, **63**, pp. 8790-8800 (1998).

6   W. Nakanishi, S. Hayashi, and H. Kihara, On the Stability and the Bonding Model of n→σ* Type Molecular Complexes, R$_2$Z-X-X: Proposal of 3c-4e Description for Z-X-X in the Adducts, *J. Org. Chem.*, **64**, pp. 2300-2307 (1999).

7   W. Nakanishi and S. Hayashi, Structural Study of Aryl Selenides in Solution Based on the ^{77}Se NMR Chemical Shifts: Application of the GIAO Magnetic Shielding Tensor of ^{77}Se Nucleus, *J. Phys. Chem. A*, **103**, pp. 6074-6081 (1999).

8   S. Hayashi and W. Nakanishi, Novel Substituent Effect on ^{77}Se NMR Chemical Shifts Caused by 4c-6e versus 2c-4e and 3c-4e in Naphthalene Peri Positions: Spectroscopic and Theoretical Study, *J. Org. Chem.*, **64**, pp. 6688-6696 (1999).

9   W. Nakanishi, S. Hayashi, and T. Uehara, Successive Change in Conformation Caused by p-Y Groups in 1-(MeSe)-8-(p-YC$_6$H$_4$Se)C$_{10}$H$_6$: Role of Linear Se---Se-C 3c-4e versus n(Se)---n(Se) 2c-4e Nonbonded Interactions, *J. Phys. Chem. A*, **103**, pp. 9906-9912 (1999).

Other Publications

1. W. Nakanishi, S. Hayashi, H. Tsukada and H. Iwamura, Structural Studies of Halogen Adducts of Diorganyl Chalcogenides in Solutions by ^{1}H, ^{13}C, ^{77}Se and ^{125}Te NMR, *J. Org. Chem.*, **3**, pp. 358-368 (1990).

2. W. Nakanishi, Y. Yamamoto, S. Hayashi, H. Tsukada and H. Iwamura, Structural Studies of Halogen Adducts of Some Cyclic Selenides and Tellurides by ^{1}H, ^{13}C, ^{77}Se and ^{125}Te NMR. Evidence for the Formation of Molecular Complexes of Selenoxanthone and Selenanthrene with Bromine, *J. Phys. Org. Chem.*, **3**, pp. 369-374 (1990).

3. W. Nakanishi, Y. Okumura and S. Hayashi, Structural Studies of Bromine Adducts of 1,2- and 1,4-Bis(phenylseleno)benzenes. Evidence for the (TB, MC) Structure of 1,2-$(PhSeBr_2)_2C_6H_4$, *J. Phys. Org. Chem.*, **4**, pp. 523-525 (1991).

4. W. Nakanishi, K. Sakamoto, K. Isaka, and S. Hayashi, Molecular Complex Formation of Diphenyl Selenides with Bromine: Electronic and Steric Effects, *Phosphorus, Sulfur and Silicon and The Related Elements*, **67**, pp. 79-82 (1992).

5. W. Nakanishi, S. Hayashi, Y. Nakamura, and H. Iwamura, Molecular Complex Formation of Diphenyl Selenides with Bromine: Electronic and Steric Requirements, *Chem. Lett.*, **1992**, pp. 735-738 (1992).

6. W. Nakanishi and S. Hayashi, Evidence for the Equilibrium and Estimation of the Equilibrium Constants between Molecular Complexes and Trigonal Bipyramidal Adducts of Diaryl Selenide Dibromides in Solution, *Chem. Lett.*, **1995**, pp. 75-76 (1995).

7. W. Nakanishi, S. Hayashi, Y. Kusuyama, T. Negoro, S. Masuda, and H. Mutoh, Why Selenoxanthone Gives an MC with Bromine: An Examination of Electronic States of Xanthones and Xanthenes by Electron Spectroscopy and ab initio MO Calculations, *J. Org. Chem.*, **63**, 8373-8379 (1998).

8. K. Tomioka, H. Hujieda, S. Hayashi, M. A. Hussein, T. Kambara, Y. Nomura, M. Kanai, and K. Koga, Catalytic Asymmetric Reaction of Lithium Ester Enolates with Imines, *Chem. Commun.*, **1999**, pp. 715-716 (1999).

9. Warô Nakanishi and Satoko Hayashi, Inter-element Linkage in 1,2- and 1,4-Bis(Arylseranyl)benzenes with Halogens, *J. Organomet. Chem.*, in press.

Acknowledgment

I would like to express grateful acknowledgements to Professor Waro Nakanishi of Wakayama University for his valuable and helpful suggestions, discussion, and encouragement during this work.
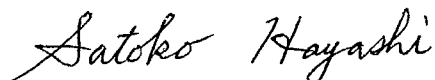
Grateful acknowledgments are made to Professor Masaji Oda of Osaka University for helpful discussions and suggestions.

Last but not least, I thank my parents, Mr. Kunizo Hayashi and Mrs. Utako Hayashi for their affectionate encouragement.

August   2000

Satoko Hayashi

Satoko Hayashi

Department of Material Science and Chemistry
Faculty of Systems Engineering
Wakayama University